GEOLOGICA ULTRAIECTINA

Mededelingen van de
Faculteit Geowetenschappen
Universiteit Utrecht

No. 248

Sedimentary development, seismic stratigraphy and burial compaction of the Chalk Group in the Netherlands North Sea area

Allard van der Molen

The research for this thesis was carried out at:

Faculty of Geosciences
Utrecht University
Budapestlaan 4
3584 CD Utrecht
The Netherlands

www.geo.uu.nl

ISBN 90-5744-110-1
© Copyright 2004, A.S. van der Molen

Typeset with LaTeX 2$_\varepsilon$ open source

Cover illustration: Base Upper Cretaceous (Base Chalk Group) 3D-seismic horizon from the Dutch Central Graben (Fig. 3.7, Page 155)

Sedimentary development, seismic stratigraphy and burial compaction of the Chalk Group in the Netherlands North Sea area

Sedimentaire ontwikkeling, seismische stratigrafie
en begravingscompactie van de Chalk Groep
in het Nederlandse Noordzeegebied

PROEFSCHRIFT

Ter verkrijging van de graad van doctor aan de Universiteit Utrecht
op gezag van de Rector Magnificus, Prof. Dr. W.H. Gispen,
ingevolge het besluit van het College van Promoties in het openbaar te verdedigen
op maandag 15 november 2004 des middags te 14.30 uur

door

Allard Sytse van der Molen

Geboren op 12 november 1972 te Drachten

Promotores: Prof. Dr. Th.E. Wong
Prof. Dr. J.E. Meulenkamp

Faculty of Geosciences
Utrecht University

It's easy to get buried in the past
(when you try to make a good thing last)

Neil Young

This study was funded by the **Netherlands Institute of Applied Geoscience TNO - *National Geological Survey*** (TNO-NITG) in Utrecht. The research was carried out at this institute and at the Faculty of Geosciences, Utrecht University. TNO-NITG supplied most material and allowed publication of the results. Petro-Canada B.V. (The Hague) provided additional funding and material and also allowed publication of results. Schlumberger N.V. (The Hague) provided the GeoFrame software package.

Contents

1 Introduction **1**
1.1 General introduction 1
1.2 Aim and outline of this thesis 6
1.3 Geological setting 7
1.4 Composition, sedimentation and diagenesis of chalk 10

2 Improved subdivision of the Chalk Group in the Netherlands North Sea area through mapping and facies analysis of seismic sequences **17**
2.1 Introduction 18
2.2 Dataset and methods 20
2.2.1 Seismic reflection data 20
2.2.2 Well data 20
2.2.3 Seismic interpretation techniques 20
2.2.4 Integration of the seismic and well database 21
2.3 Description of the seismic sequences 22
2.3.1 Base Chalk Group seismic horizon (Base Cenomanian) 22
2.3.2 Seismic sequence CK1, Texel Formation (Cenomanian) 23
2.3.3 Seismic sequence CK2 (Turonian to Coniacian) 23
2.3.4 Seismic sequence CK3 (Coniacian) 28
2.3.5 Seismic sequence CK4 (Santonian) 28
2.3.6 Seismic sequence CK5 (lower Campanian) 29
2.3.7 Seismic sequence CK6 (lower Campanian) 29
2.3.8 Seismic sequence CK7 (middle to upper Campanian) 34
2.3.9 Seismic sequence CK8 (lower Maastrichtian) 34
2.3.10 Seismic sequence CK9 (lower to upper Maastrichtian) 34
2.3.11 Seismic sequence CK10 (upper Maastrichtian to lower Danian) 35
2.3.12 Seismic sequence CK11 (Danian) 40
2.3.13 Top Chalk Group seismic horizon 40

2.4 Discussion 41
2.4.1 Seismic interpretation 41
2.4.2 Biostratigraphy 50
2.5 Conclusions 53

3 Cenomanian to Danian tectono-sedimentary evolution of the Netherlands North Sea area 55
3.1 Introduction 56
3.2 Structural elements and basin architecture 57
3.2.1 Province A (West Netherlands Basin–Winterton High–London-Brabant Massif) 59
3.2.2 Province B (Broad Fourteens Basin) 60
3.2.3 Province C (Texel-IJsselmeer High–Noord Holland Platform) 61
3.2.4 Province D (Cleaver Bank High) 63
3.2.5 Province E (Terschelling Basin–Vlieland High & Basin) . . . 63
3.2.6 Province F (Dutch Central Graben) 64
3.2.7 Province G (Step Graben) 65
3.2.8 Province H (Elbow Split High–Outer Rough Basin) 65
3.2.9 Province I (Schill Grund High–Ameland Block) 65
3.3 Cenomanian to Danian evolution of the Netherlands North Sea area 66
3.4 Inversion tectonics and chalk (re)deposition in the Dutch Central Graben 70
3.5 Discussion 74
3.6 Conclusions 77

4 Metre-scale cyclicity in well logs of the Chalk Group, Netherlands North Sea area 79
4.1 Introduction 80
4.2 Milankovitch cycles in the Chalk 81
4.3 Database & Methods 85
4.4 Results 87
4.4.1 Well-log correlation 88
4.4.2 Spectral log facies 90
4.4.3 Metre-scale cyclicity 90
4.4.4 Identification of Milankovitch cycles 95
4.5 Discussion 98
4.5.1 Spectral log facies 98
4.5.2 Metre-scale cyclicity 99

4.5.3 Identification of Milankovitch cyclicity and inferred net accumulation rates . . . 102
4.6 Conclusions . . . 105

5 Acoustic velocity and burial history analysis of the Chalk Group, Netherlands North Sea area 109
5.1 Introduction . . . 110
5.2 Published compaction trends for the Chalk . . . 111
5.3 Database and Methods . . . 114
5.3.1 Seismic horizons . . . 114
5.3.2 Stratigraphic boundary depth data . . . 114
5.3.3 Sonics logs . . . 116
5.3.4 Interval velocity (V_{int}) from TVD-data and seismic horizons . . . 116
5.3.5 Mean sonic velocity (V_μ), V_0 and k from sonic logs . . . 118
5.3.6 Velocity and burial anomalies . . . 119
5.4 Results . . . 120
5.4.1 Interval velocity (V_{int}) from TVD-data and seismic horizons . . . 120
5.4.2 Mean velocity (V_μ) from sonic logs . . . 123
5.4.3 $k_{\,log}$, $V_{0\,log}$ and $R^2{}_{log}$ . . . 126
5.4.4 Velocity and burial anomalies . . . 130
5.5 Discussion . . . 131
5.5.1 Acoustic velocity of the Chalk . . . 131
5.5.2 Compaction of the Chalk . . . 134
5.5.3 Variation in chalk compaction . . . 136
5.6 Conclusions . . . 137

6 Synthesis 139

References 145

Appendix - Colour plates 153

Samenvatting 167

Dankwoord 173

Curriculum vitae 175

Chapter 1

Introduction

1.1 General introduction

The Chalk Group accumulated during a 40 million-year episode of the Earth's history (100–61 Ma BP) during which intense volcanic activity at oceanic spreading ridges coincided with globally high sea levels, high sea-surface temperatures and a peak in the production of organic matter. Larson (1991a; 1991b) postulated that massive upwelling of magma from the core/mantle boundary to the surface of the Earth, which he labelled the mid-Cretaceous 'superplume', brought about these extraordinary circumstances (Fig. 1.1). The elevated newly formed ocean crust resulted in a sea level rise (Hays & Pitman, 1973). Furthermore, the augmented release of CO_2 raised atmospheric CO_2-levels to about four times higher than at present, causing warming of the Earth's atmosphere and subsequent additional sea level rise (Huber et al., 2002). The high eustatic sea level resulted in the inundation of large areas of land, reducing the influx of erosional detritus into the oceans. The ensuing clear water conditions, in combination with the warm climate, resulted in the proliferation of calcareous nannoplankton, the skeletal remains of which formed thick layers of calcitic ooze on the sea floor (Håkansson et al., 1974; Hancock, 1975).

At the end of the Cretaceous period, a cataclysmic event took place that led to the disappearance of many fossil groups including dinosaurs, ammonites, belemnites, inoceramid and rudistid bivalves and many of the chalk forming calcareous nannoplankton (Smit, 1990). Increased levels of cosmogenic iridium and glass spherules in sediments from the Cretaceous–Tertiary transition (KTB) suggested that a meteorite impact resulted in this mass-extinction event (Alvarez et al., 1980; Smit & Hertogen, 1980). The discovery of a large impact crater dating from the KTB in the Yucatan Peninsula, Mexico, confirmed this hypothesis. Very recently, the 'Silverpit

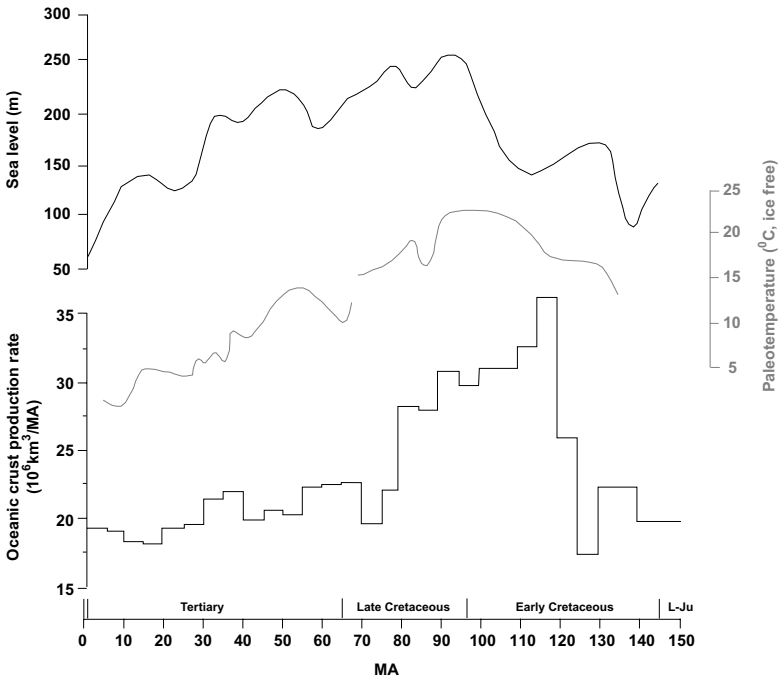

Figure 1.1: Combined plot of world oceanic crust production, high-latitude sea-surface temperatures and long-term eustatic sea level (after: Larson, 1991).

Crater', a smaller impact crater of the same age has been identified on 3D-seismic data from the UK sector of the North Sea (Stewart & Allen, 2002; Stewart, 2003; Underhill, 2004). In NW-Europe, the period of chalk deposition ended with the surfacing of landmasses during the Alpine continental convergence, at the beginning of the Tertiary, because influx of erosional detritus effectively ended the clear water conditions that had favoured the coccolithoporids, and deposition of siliciclastic sediments took over (Ziegler, 1990).

In the North Sea Basin, the present-day thickness of the Chalk exceeds 2500 m in the Central Graben (Fig. 1.2) and maximum burial depth is more than 3000 m in the centre of the basin (Fig. 1.3; Ziegler, 1990). The autochthonous chalk was reworked to a large extent by bottom currents (Scholle, 1998). In areas where chalk deposition was accompanied by sufficient tectonic activity, such as the Central Graben that was tectonically inverted during the Late Cretaceous and early Paleocene, redeposition in the form of turbidites, slumps and debris flow deposits took place (Watts et al., 1980; Hatton, 1986; Kennedy, 1987).

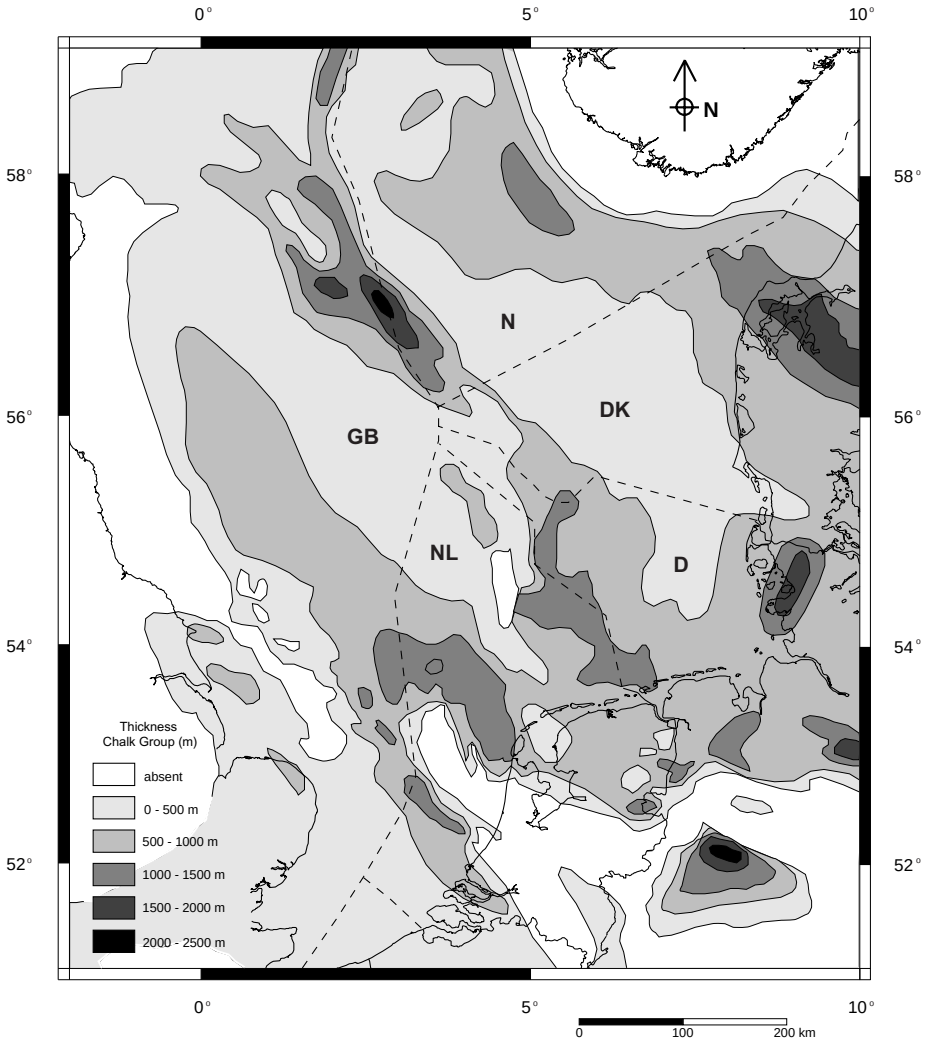

Figure 1.2: Thickness of the Chalk Group in the central and southern North Sea (after: Ziegler, 1990). The North Sea offshore sectors are outlined by dashed lines. NL: Netherlands, D: Germany, DK: Denmark, N: Norway, GB: Great Britain.

The Chalk has long formed an important hydrocarbon reservoir in the Norwegian (over 14 billion barrels STOIIP) and Danish (over 8 billion barrels STOIIP) sections of the Central Graben (Fig. 1.4). The Norwegian fields are the largest, with highest porosity and permeability, and allochthonous chalk forming the main reservoir facies.

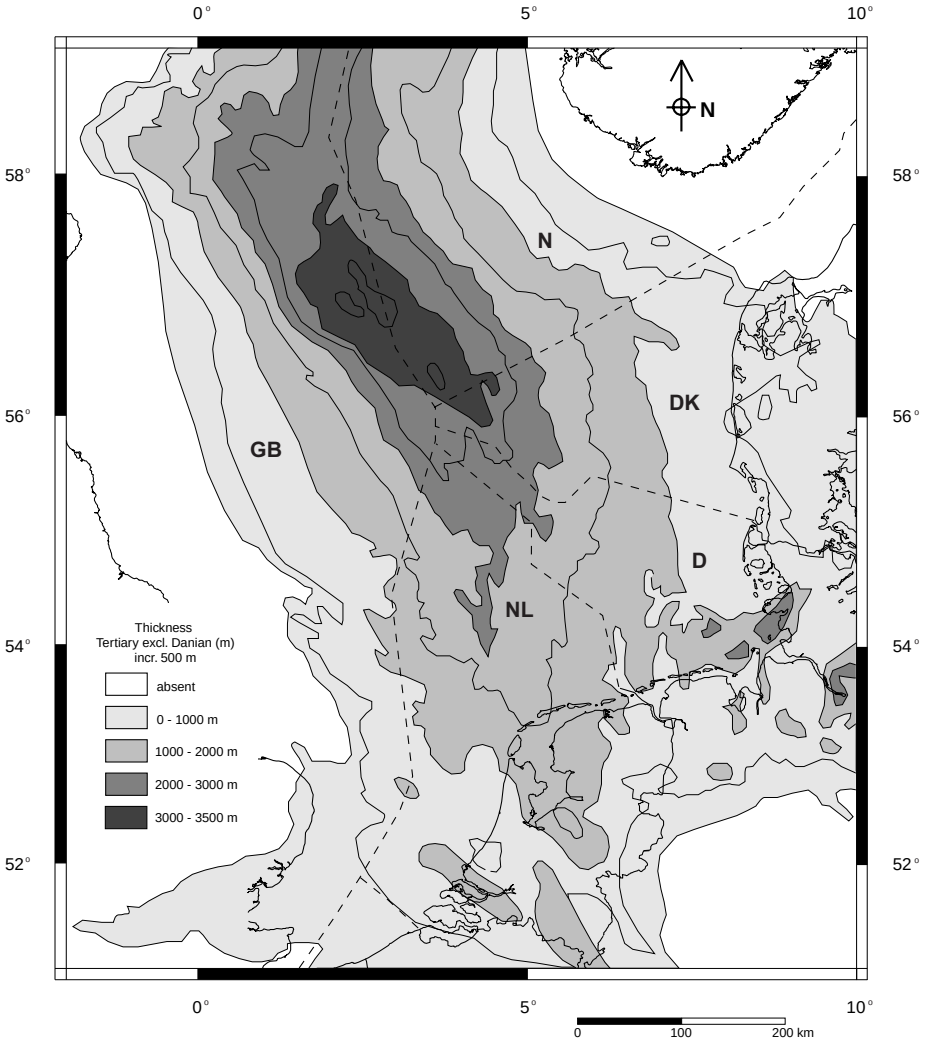

Figure 1.3: Thickness of the post-Chalk Group succession in the central and southern North Sea (after: Ziegler, 1990).

As this area is most deeply buried, overpressures are highest here (Fig. 1.3). In the shallower Danish fields, autochthonous chalks also form hydrocarbon reservoirs because low but producable porosities and permeabilities are preserved at these burial depths when hydrocarbons enter the sediment early. Additional isolated chalk fields are present in the British part of the Central Graben. In the Dutch Central

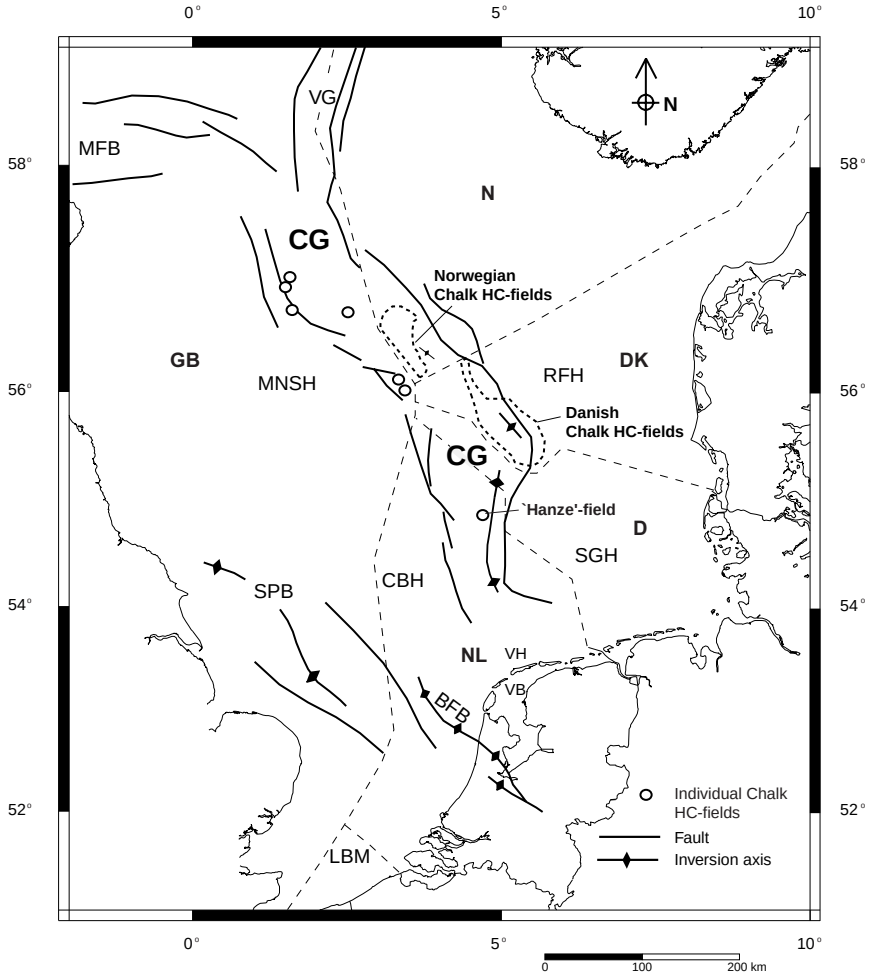

Figure 1.4: Cretaceous tectonic elements of the central and southern North Sea with major Chalk hydrocarbon (HC) fields indicated. MFB = Moray Firth Basin, VG = Viking Graben, CG = Central Graben, MNSH = Mid North Sea High, RFH = Rynkøbing Fyn High, SPB = Sole Pit Basin, CBH = Cleaver Bank High, SGH = Schill Grund High, VH = Vlieland High, VB = Vlieland Basin, BFB = Broad Fourteens Basin, LBM = London Brabant Massif (after: Ziegler, 1990; Megson & Hardman, 2001).

Graben, the 'Hanze Field' is the only oil field in the Chalk to date (Megson, 1992; Oakman & Partington, 1998; Bramwell et al., 1999; Megson & Hardman, 2001; Hofmann, 2002; Surlyk et al., 2003).

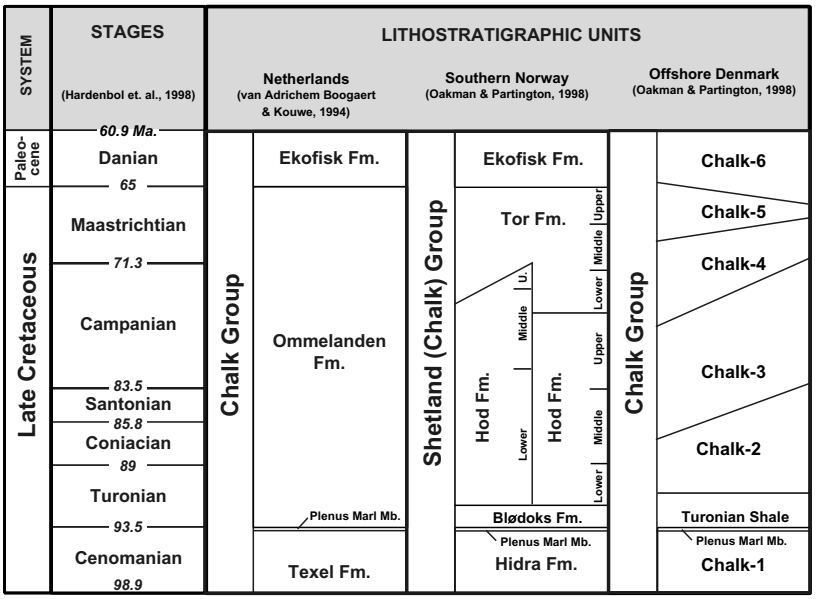

Figure 1.5: Lithostratigraphic subdivision of the Chalk Group in the Netherlands, Danish and Norwegian sectors of the North Sea.

1.2 Aim and outline of this thesis

In the Netherlands offshore sector, available data and knowledge of the Chalk Group are limited due to its hitherto restricted significance as a hydrocarbon reservoir. For example, the stratigraphic subdivision of the Chalk in this area comprises only three formations, i.e. the Cenomanian *Texel Formation* (CKTX), the Turonian to Maastrichtian *Ommelanden Formation* (CKGR) and the Danian *Ekofisk Formation* (CKEK), contrary to more detailed subdivisions used in sectors where the Chalk does form an important hydrocarbon-producing interval (Fig. 1.5; Van Adrichem Boogaert & Kouwe, 1994; Oakman & Partington, 1998). The first aim of this thesis is, therefore, to present a more detailed subdivision of the Chalk Group in the Dutch North Sea sector. Due to the scarcity of cored intervals and biostratigraphical data, this subdivision is largely based on the interpretation of geophysical data.

The chalks of the North Sea area show a great variety of lithofacies resulting from a broad spectrum of depositional mechanisms and physical and chemical compaction processes. Chalk was originally formed by settling of calcareous nannoplankton remains from suspension in the water column (Hancock, 1975). However, in areas that underwent significant tectonic activity, slope instability processes resulted in resed-

imentation of the autochthonous chalk (Watts et al., 1980; Hatton, 1986; Kennedy, 1987). Investigation of these sedimentary processes, as well as their controls and products, not only yields additional information on the sedimentology and diagenesis of the Chalk Group, but also on the paleoenvironmental and basinal evolution of the study area during the Late Cretaceous and early Paleocene. Therefore, the second aim of this thesis is to reconstruct the sedimentary development of the Chalk Group in the Dutch sector of the North Sea.

Although the Chalk Group is characterised by a remarkably uniform lithology, marked lateral variations in acoustic velocity are present throughout the North Sea basin. These acoustic velocity variations are primarily the result of variations in compaction, which in turn are caused by spatial differences in burial history (Scholle, 1977; Japsen, 1998; Mallon & Swarbrick, 2002). A better understanding of the spatial variation of seismic velocity therefore yields information about the compaction of the Chalk, the burial history of the sediment and helps to improve time-depth conversions through this interval. The third aim of this thesis is, therefore, to explain the regional variations in seismic velocity of the Chalk.

The sedimentary development and seismostratigraphy of the Chalk were studied by seismic interpretation and well log correlation of this interval throughout the Dutch offshore area. The results are described in Chapter 2, *Improved subdivision of the Chalk Group in the Netherlands North Sea area through mapping and facies analysis of seismic sequences*. By integrating the results of Chapter 2, the regional tectono-sedimentary evolution of the Netherlands North Sea sector during the Late Cretaceous to early Paleocene was reconstructed, as described in Chapter 3, *Cenomanian to Danian tectono-sedimentary evolution of the Netherlands North Sea area*. Cyclicities in well log response, inferring sedimentary processes (pelagic vs. reworking) and sedimentation rates are discussed in Chapter 4, *Metre-scale cyclicity in well logs of the Chalk Group, Netherlands North Sea area*. The burial history of the Chalk Group, as studied by investigating acoustic velocities, is described in Chapter 5, *Acoustic velocity and burial history analysis of the Chalk Group, Netherlands North Sea area*. Chapter 6, *Synthesis*, summarises the results.

1.3 Geological setting

The tectonic framework of the North Sea Basin consists of a complex configuration of intra-basinal lows and highs, resulting from multiple tectonic phases during the late Paleozoic to early Tertiary. The North Sea Basin at the onset of chalk deposition was the product of several rifting pulses during the Triassic and Jurassic. Post-rift thermal relaxation and subsidence, together with a steady eustatic sea level rise,

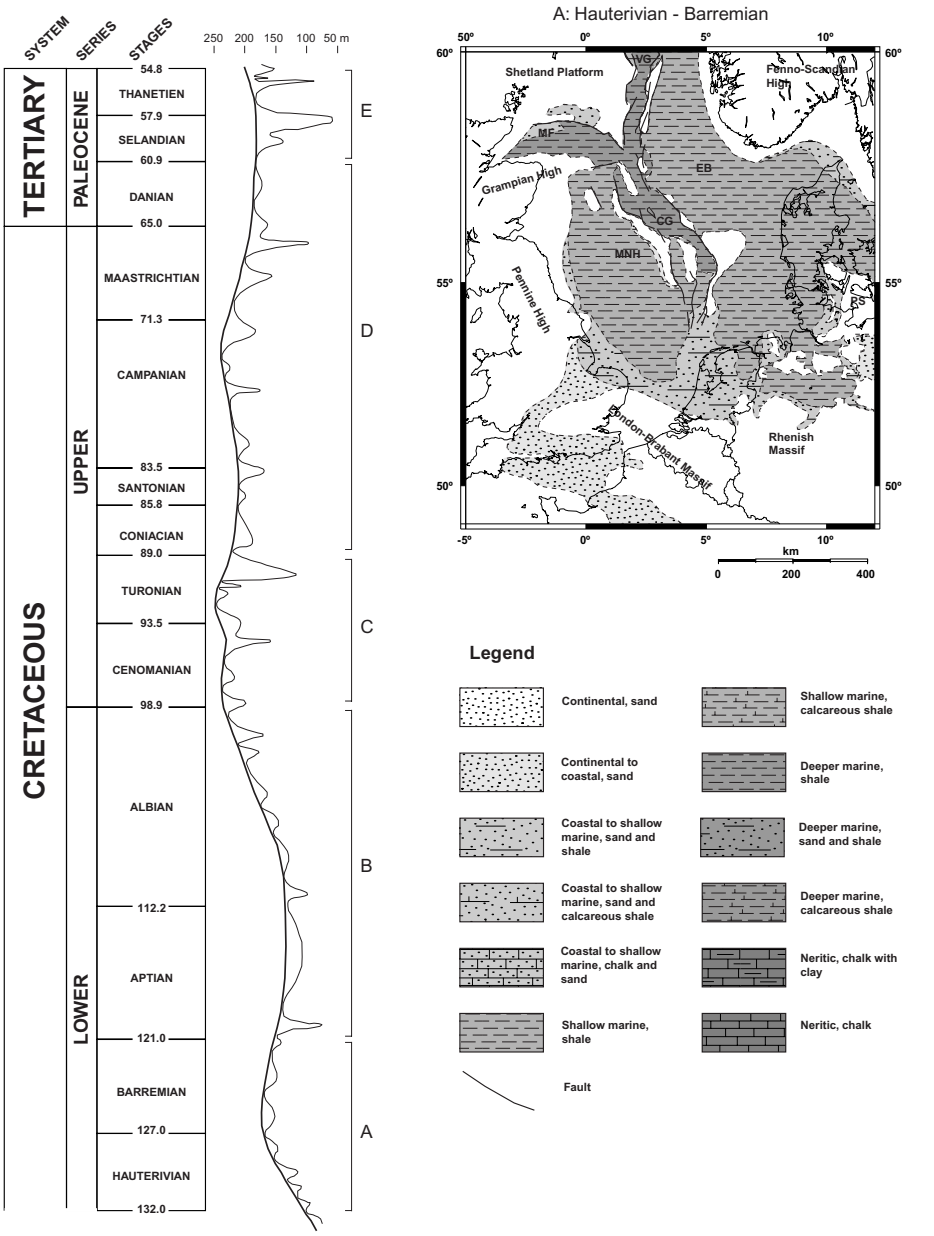

Figure 1.6: (left) Lower Cretaceous to lower Paleocene long-term and short-term eustatic sea level curve. Ranges A–E refer to the paleogeographical maps of Fig. 1.6 & Fig. 1.7. Upper right: Hauterivian–Barremian NW-European paleogeography (A) (after: Ziegler, 1990; Hardenbol et al., 1998).

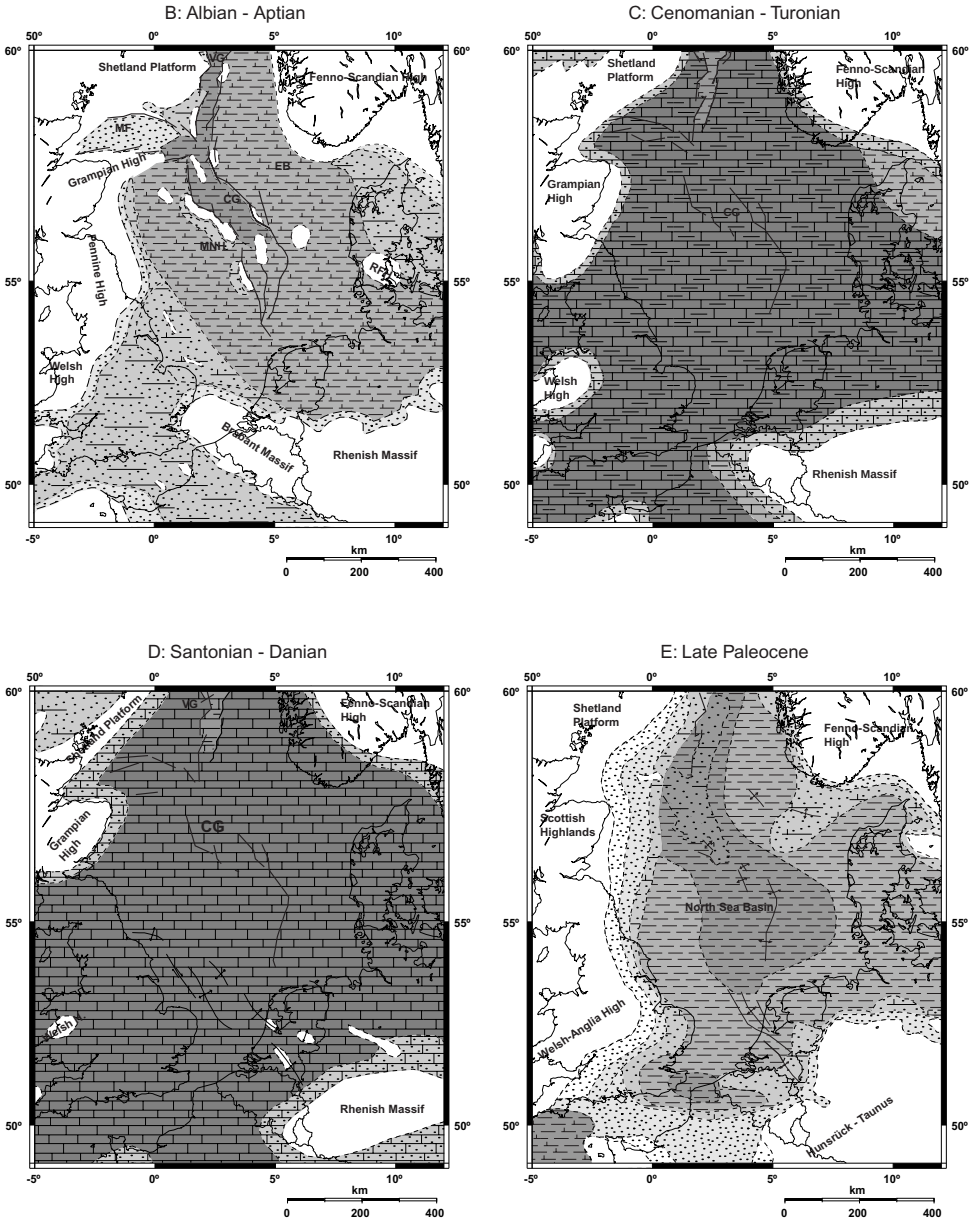

Figure 1.7: (continued from Fig. 1.6) Albian–Aptian (B), Cenomanian–Turonian (C), Santonian–Danian (D), late Paleocene (E) NW-European paleogeography (after: Ziegler, 1990).

resulted in the overstepping of basin margins during the Early Cretaceous (Fig. 1.6 & Fig. 1.7; Olsen, 1987; Ziegler, 1990; Glennie, 1992). At the end of the Early Cretaceous (Latest Albian), sea levels exceeded present-day levels by 100–300 m. With the transgression much of the Early Cretaceous landmasses were flooded, and deposition of chalk began (Ziegler, 1990).

The global climate developed from a 'warm greenhouse phase' in the Albian to middle Cenomanian to a 'hot greenhouse phase' in the latest Cenomanian to early Campanian, the peak of the transgression occurring during the late Santonian and subsequently cooled to a 'cool greenhouse phase' during the middle Campanian to Maastrichtian (Huber et al., 2002). However, marked temperature fluctuations occurred throughout this period (Li & Keller, 1999). At the hottest period, sea-surface temperatures exceeded present-day values by 4–7 °C, with up to 250 m higher sea levels (Hardenbol et al., 1998; Norris et al., 2002).

Worldwide excessive organic carbon burial during transgression led to global 'Oceanic Anoxic Events' during the Cretaceous (Jenkyns, 1980; Larson, 1991a). The second of these anoxic events occured at the Cenomanian–Turonian boundary, probably lasted for about 320 ky and led to the formation of the clay-rich Plenus Marl Member (Fig. 1.5; Van Adrichem Boogaert & Kouwe, 1994; Paul et al., 1999; Prokoph et al., 2001).

Throughout the Cretaceous and Paleogene, a number of compressional phases, related to the Tethys closure and the opening of the Northern Atlantic Ocean, followed the early Mesozoic rifting. The most important of these compressional phases occurred at the early to middle Turonian, during the early Campanian and late Campanian to early Maastrichtian (jointly referred to as the 'Sub-Hercynian' phase) and at the start of the Tertiary, during the 'Laramide' phase (Ziegler, 1990; Huyghe & Mugnier, 1994). During these phases, a number of intra-basinal lows were tectonically inverted, whereby chalk fills were deeply eroded. In the Netherlands North Sea area, these compressional phases resulted in the inversion of the Broad Fourteens Basin and the Dutch Central Graben (Fig. 1.8; Van Wijhe, 1987; Dronkers & Mrozek, 1991).

1.4 Composition, sedimentation and diagenesis of chalk

North Sea chalk consists for 96–99 % of calcite ($CaCO_3$), almost exclusively from coccoliths and coccolith fragments. Coccoliths are intricately adorned round shell-platelets produced by green-brown algae of the phylum Haptophyta (or coccolithophorids). These coccolithophorids inhabited open-marine, pelagic habitats. Coc-

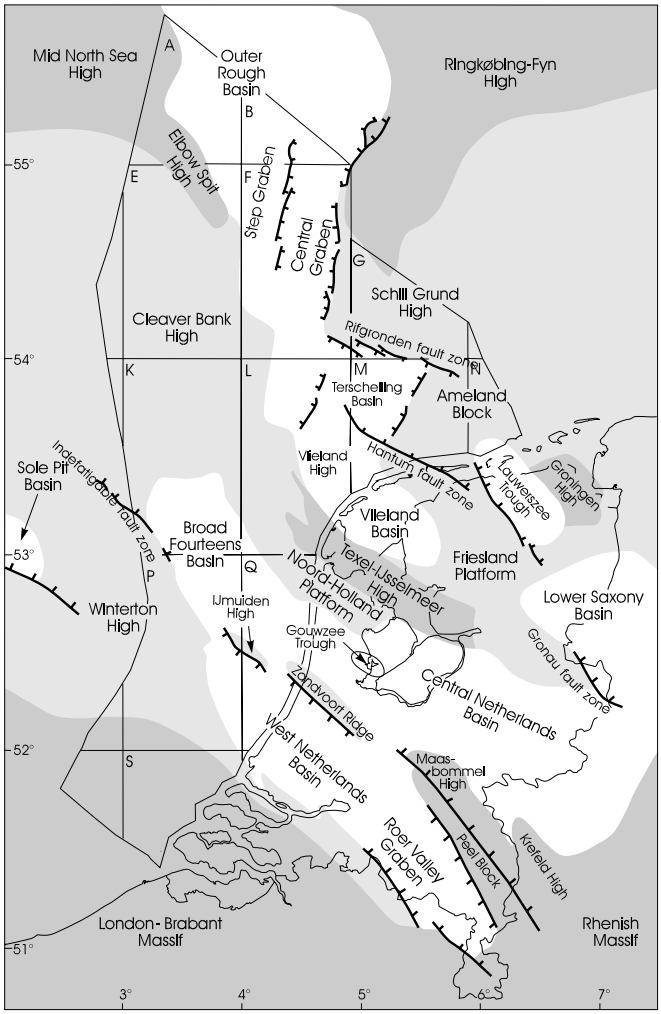

Figure 1.8: Jurassic - Cretaceous tectonic elements of the Netherlands (map: TNO-NITG). The Netherlands North Sea sector is subdivided into quadrants A–S.

coliths are about 0.5–20 μ in diameter and are built up of individual plates. Apart from coccoliths, biogenic carbonate constituents of typical North Sea chalk include a variety of planktonic foraminifera. Non-carbonate biogenic particles include radiolarians, diatoms and sponge spicules. The most important non-biogenic, non-carbonate constituents are small amounts (usually less then 1 %) of clay minerals, reflecting

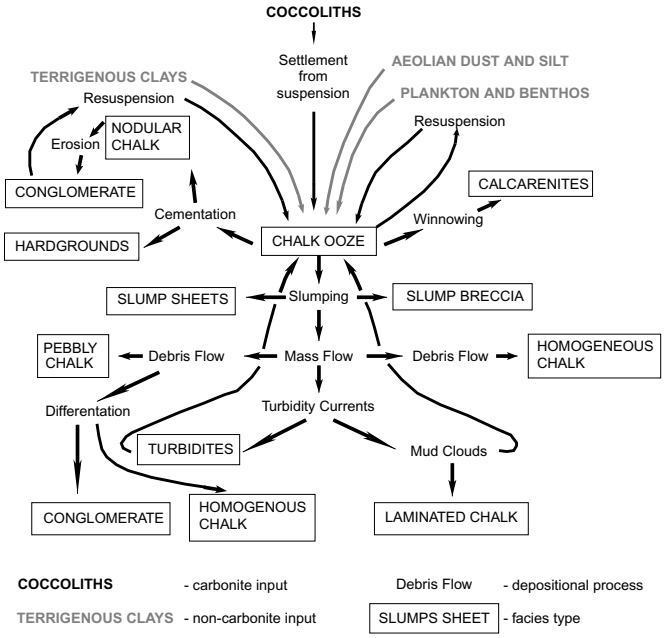

Figure 1.9: Overview of the depositional processes and resulting facies types (after Kennedy, 1987).

the influx of erosional detritus (Table 1.1; Håkansson et al., 1974; Hancock, 1975; Jorgensen, 1986; Kennedy, 1987).

The primary sedimentation mechanism of chalk was the settlement of coccoliths from suspension in the water column (Fig. 1.9). In recent analogues it has been shown that nannofossil debris only settles as part of faecal pellets because individual tests are too light to reach the seabed. Plankton feeders such as Copepods therefore probably play an important role in the deposition. Larger and heavier planktonic foraminifera and radiolarians may have settled as individual grains. Chalk has most likely been deposited in a wide range of water depths, but faunal analysis on this matter provides ambiguous information. However, values of a hundred to a few hundred metres water depth for shelf-sea chalk and up to a thousand metres for deep sea chalk such as that of the North Sea Central Graben seem to be most likely. As coccolithophorids inhabited the photic zone, i.e. the top 40 m of the water column, and climate was warm at high latitudes, the high sea level ensured deposition over large areas (Håkansson et al., 1974; Hancock, 1975; Kennedy, 1987; Tucker & Wright, 1990; Zijlstra, 1994, 1995; Surlyk, 1997).

	Avg. %	**Max. %**	**Min. %**
SiO_2	0.63	2.12	0.15
Al_2O_3	0.33	1.01	0.08
Fe_2O_2	0.08	0.13	0.01
MnO	0.04	0.06	0.02
MgO	0.30	0.36	0.22
CaO	54.90	55.54	54.08
Na_2O	0.05	0.16	0.01
K_2O	0.03	0.05	0.01
P_2O_5	0.08	0.14	0.05
Co_2	43.54	43.85	42.86
sum	99.98		
$CaCO_3$	98.17	99.09	96.77

Table 1.1: Chemical composition of chalk, UK mainland (Hancock, 1990).

Chalk formed by primary, i.e. pelagic, sedimentation is also known as 'autochthonous' chalk, and is described as the bioturbated periodite facies. Within autochthonous chalk a conspicuous, decimetre to metre scale, rhythmic stratification is commonly present that is often interpreted as Milankovitch-style variations in sedimentation rate, early diagenetic processes, siliciclastic influx, water temperature etc. In outcrop, this stratification is characterised by regularly spaced flint layers, indistinct colour bands, variations in clay content and degree of bioturbation (Barron et al., 1985; Hart, 1987; Ditchfield & Marshall, 1989; Herrington et al., 1991; Mettraux et al., 1995). In the subsurface, cyclic variations in clay content and porosity are made apparent by frequency analysis of well logs, representing cyclicities in terms of wavelength in the depth domain (Niebuhr & Prokoph, 1997; Stage, 1999; 2001).

Autochthonous chalk can be subject to redeposition by various mass-movement mechanisms (Fig. 1.9 & Fig. 1.10). Chalk can be transported by turbidity currents that form metre-scale beds with features similar to their siliciclastic counterparts and are easily confused with periodite sequences. Redeposition in the form of slumps or slump folds involves the plastic deformation of sediment. Slump dimensions are of the order of decimetres to tens of metres. Lithified chalk is often subject to mass-movements by debris flows, in which chalk clasts are often reshaped or broken up during transport. Large masses of (partly) lithified chalk can move downslope while remaining internally intact. Such masses form slide sheets that can be several kilometres long (Watts et al., 1980; Hatton, 1986; Bromley & Ekdale, 1987; Kennedy,

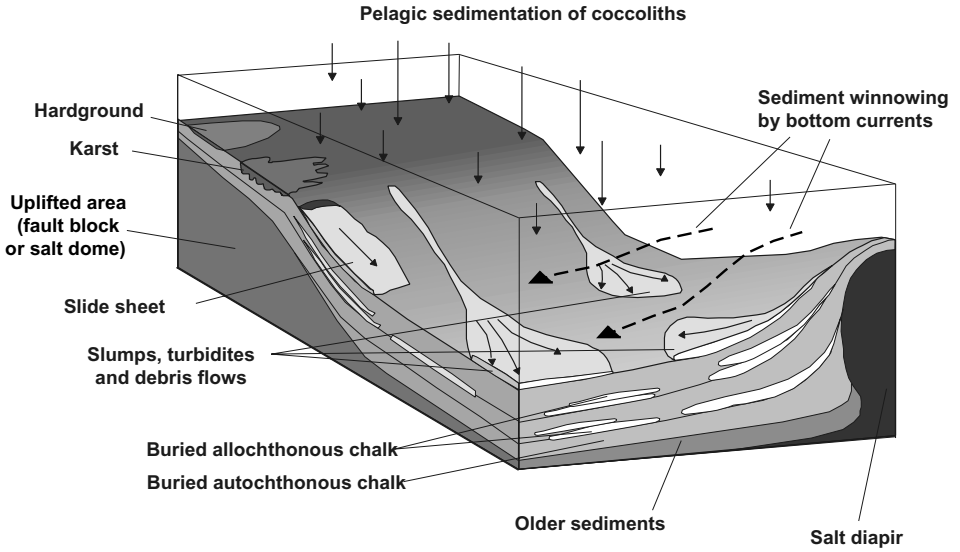

Figure 1.10: Overview of various depositionary processes recognised in the Chalk (after: Kennedy, 1987; Taylor & Lapré, 1987).

1987).

With ongoing sedimentation, newly deposited sediment went through a succession of shallow zones within the uppermost metre of the seabed, where the transition from a fluid suspension to a solid-phase coccolith ooze occurred (Fig. 1.11). Upon deposition the sediment started out as a suspension layer, consisting for 80–90 % of water. Such suspension layers were probably often (re) moved by bottom currents, which formed nepheloid currents responsible for significant syn-sedimentary redistribution of chalk along the sea floor. Directly underneath the suspension layer, the intensely bioturbated 'mixed layer' formed the first solid phase layer and was about 5 to 8 cm deep. Here, bioturbation commonly removed all sedimentary structures, homogenising the material completely and reducing porosity to 75–80 %. Down to a depth of about 30 cm, bioturbation by deeper burrowing animals further reduced porosity to 70–75 %, in what is known as the 'transition zone'. Few burrowing animals reached as deep as 1 metre, Thalassionides being the most important. In the Anoxic Bacterial Zone (30–100 m), activity of sulphite-reducing bacteria led to the formation of H_2S and carbonate ions. The H_2S escaped into the overlying aerobic

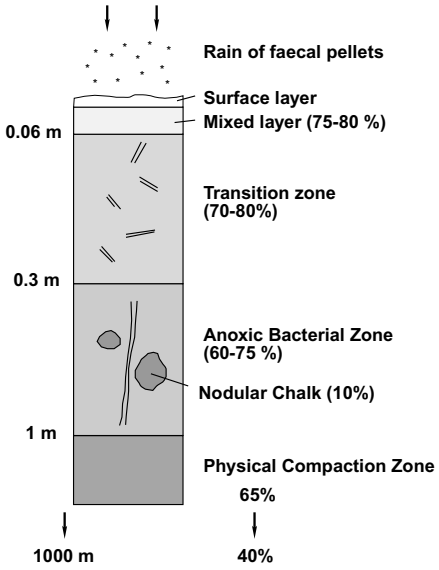

Figure 1.11: Shallow burial depth compaction zones of chalk. Porosity is reduced to about 65% within the first metre of burial (after: Hancock, 1990).

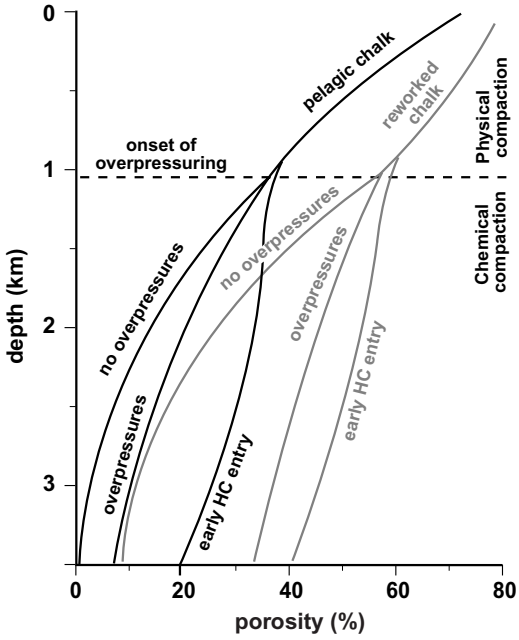

Figure 1.12: Deep burial diagenesis pathways of Norwegian Central Graben chalk. The porosity contrast between pelagic and reworked chalk is increased during the physical compaction stage. Porosity reduction during the subsequent chemical compaction stage depends on the occurrence of overpressures and/or hydrocarbons (after: Brasher & Vagle, 1996).

zone to be reoxidised, the new carbonate ions combined again with calcium to precipitate as new calcite crystals. As a result, hardened patches or nodules of chalk were formed, which could ultimately transform into hardgrounds (Håkansson et al., 1974; Scholle, 1974, 1977; Hancock, 1990; Zijlstra, 1994, 1995; Molenaar & Zijlstra, 1997).

The material consolidated by physical compaction from chalk ooze to soft chalk reducing porosities from more than 80 % to about 40 %, during burial down to about one kilometre (Fig. 1.12). Below this depth, compaction was mostly chemical and was controlled by calcite crystal size, pore fluid composition, pore fluid (over-) pressure, sedimentary process (i.e. autochthonous or allochthonous) and the possible migration of hydrocarbons. The main chemical compaction processes were stylolitisation, intergranular pressure solution, cementation and spot welding (Scholle, 1974, 1977; Taylor & Lapré, 1987; Maliva & Dickson, 1992; Brasher & Vagle, 1996).

Chapter 2

Improved subdivision of the Chalk Group in the Netherlands North Sea area through mapping and facies analysis of seismic sequences

A seismostratigraphic analysis was carried out to arrive at an improved lithostratigraphic subdivision of the Upper Cretaceous to lower Paleocene Chalk Group in the Dutch sector of the North Sea. Based on the mapping and correlation of unconformities, the Chalk was subdivided into eleven seismostratigraphic sequences. These represent the Cenomanian (CK1), Turonian (CK2), Coniacian (CK3), Santonian (CK4), lower Campanian (CK5; CK6), middle to upper Campanian (CK7), lower Maastrichtian (CK8), lower to upper Maastrichtian (CK9), upper Maastrichtian to lower Danian (CK10) and Danian (CK11). The seismic sequences generally show parallel and continuous seismic reflections reflecting autochthonous chalk or subseismic scale resedimentation. Indications for large scale reworking are found in the Central Graben area. Here, the seismic response of the Chalk is characterised by discontinuous to chaotic reflections. Reflection strength varies both vertically and laterally, and is controlled by decametre-scale variations in density.

2.1 Introduction

In the North Sea region, the Upper Cretaceous to Paleogene Chalk Group forms an almost pure calcitic succession, reaching a maximum thickness of over 2500 m in the Norwegian and British sectors of the Central Graben (Fig. 1.2; Hancock, 1975; Ziegler, 1990). The Chalk represents a period of time when a high eustatic sea level, coinciding with a low detrital influx, permitted pelagic sedimentation on the continental shelves (Fig. 1.6 & Fig. 1.7; Ziegler, 1990; Hardenbol et al. 1998). Primary mechanism in the deposition of the Chalk was the settlement of calcareous ooze (almost entirely consisting of coccoliths) from suspension in the water column (Fig. 1.10; Hancock, 1975; Kennedy, 1987).

Due to its hitherto limited significance as a hydrocarbon reservoir in the Dutch offshore, the Chalk is one of the least studied stratigraphic intervals in this area. Consequently, both cored sections and biostratigraphical data are scarce, leaving a rather crude subdivision of the Dutch offshore Chalk Group into three lithostratigraphical units, the Cenomanian Texel Formation, the Turonian to Maastrichtian Ommelanden Formation and the Danian Ekofisk Formation (Fig. 1.5; Van Adrichem Boogaert & Kouwe, 1994).

In seismic data, a chronostratigraphic subdivision of a rock interval is reconstructed by identifying and tracing unconformities (Mitchum et al., 1977a). Based on 2D-seismic data, the Chalk has been subdivided into eight seismic sequences (Andersen et al., 1990) in the Danish offshore and six in the Norwegian offshore (Bramwell et al., 1999). Furthermore, sedimentation, diagenesis and deformation of an interval can be studied through analysis of seismic facies characteristics like reflection configuration, amplitude, frequency and continuity (Mitchum et al., 1977b). Pelagic limestones, such as autochthonous chalks, are characterised by low-amplitude, parallel and continuous seismic reflections (Nygaard et al., 1990; Macurda, 1997; Gras & Geluk, 1999). In contrast, the seismic facies of allochthonous chalk often show discontinuous, chaotic or 'hummocky' seismic reflections (Johnson, 1987; Nygaard et al., 1990; Andersen et al., 1990; Skirius et al., 1999; Britze et al. 2000).

Based on the mapping of unconformities and subsequent dating of the sequences, a (seismic) stratigraphical subdivision of the Chalk Group in the Netherlands offshore was devised. This subdivision supports the existing regional partitioning of the Texel Formation and Ekofisk Formation while improving the subdivision of the Ommelanden Formation. Furthermore, it allows for a better understanding of the sedimentary development of the Chalk and timing of regional tectonic events in the study area. In this chapter, a workflow is adapted that integrates several datasets, i.e. seismic data, well logs and biostratigraphic data, to improve the quality of the subdivision (Nygaard et al., 1990; Kristensen et al., 1995).

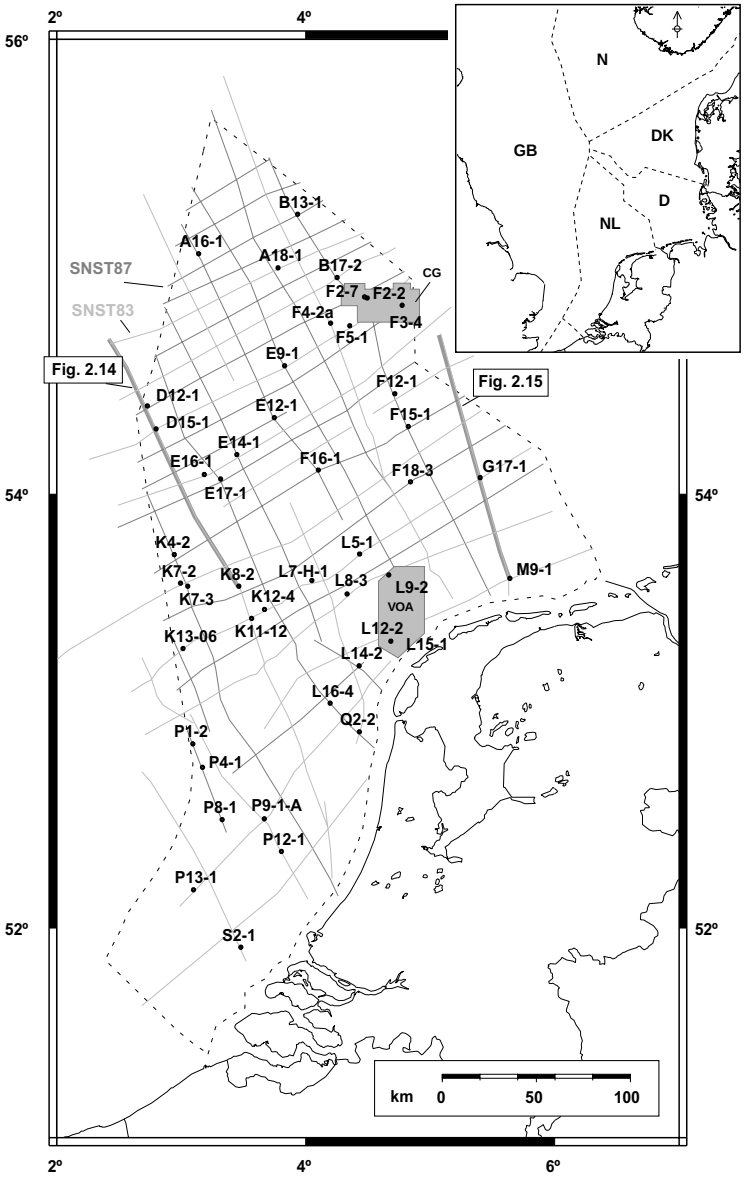

Figure 2.1: Map of the study area, indicating the 2D-seismic surveys (SNST83: light grey, SNST87: dark grey), 3D-seismic surveys (CG = Central Graben, VOA = Vlieland offshore area) and wells used. Also indicated are the locations of a seismic profile on the Cleaver Bank High (Fig. 2.14) and Schill Grund High–Ameland Block (Fig. 2.15). The small map indicates the position of the study area (NL) and the surrounding offshore sectors. GB = British, N = Norwegian, DK = Danish and D = German sectors.

2.2 Dataset and methods

2.2.1 Seismic reflection data

The seismic data used in this study consist of digital 2D and 3D surveys. The backbone of the dataset is formed by the *NOPEC* SNST83 (acquired in 1983) and SNST87 (acquired in 1987) 2D-surveys (Fig. 2.1). Together, these surveys cover the entire Netherlands offshore area with a spacing of about 20 to 40 kilometres between consecutive lines. The shot point (SP) interval of the SNST83-survey varies between 18 m and 28 m (avg. 25 m), with the exception of line SNST83-7 (SP interval: 50 m). In the SNST87-survey, the SP interval is a constant 25 m.

In the Dutch Central Graben, two 3D-seismic surveys with a combined area of 550 km^2 (Fig. 2.1; CG) were studied. The area covers the offshore blocks F2 and F3. The F2-survey was acquired in 1994 as part of the exploration effort for the 'Hanze Field', which is the only hydrocarbon producing reservoir in the Chalk of the Dutch offshore to date (Hofmann, 2002). This survey is about 100 km^2 in size, with a common depth point (CDP) spacing of both inlines and crosslines (or 'bin size') of 12.5 meters. It partly overlaps the adjacent F3-survey, which was acquired in 1989, covers 500 km^2 and has a bin size of 25 m. The Vlieland offshore research area consists of a 1000 km^2 3D-seismic survey, located just north of the Wadden Sea island of Vlieland. The area covers the offshore blocks L9, L12 and L15 (Fig. 2.1; VOA). This survey was acquired in 1989 and bin size is also 25 m.

2.2.2 Well data

The seismic dataset has been complemented with digital logs of 45 boreholes from the study area. The well log dataset consists of gamma-ray and sonic logs in all wells, supplemented with density and resistivity logs where available. Industrial reports of micropaleontological dating, based on benthic foraminifera taken from ditch cutting samples, were available for 15 wells. These reports were used to date the interpreted seismic sequences.

2.2.3 Seismic interpretation techniques

The method employed for the mapping and seismic facies analysis of the Chalk interval closely followed standard seismic stratigraphy interpretation techniques (Mitchum et al., 1977c; Brown, 1991). All seismic interpretations, as well as subsequent well log analyses, were carried out on a UNIX seismic workstation using the GeoFrame software package of Schlumberger. In the seismic surveys, reflection terminations were identified first. Wherever these reflection terminations were found to follow

surfaces within the rock interval, indicative of stratigraphic unconformities, these were mapped throughout the seismic grid. Subsequently, the reflection configurations along the unconformities were noted to study the nature of the unconformity, i.e. onlap or erosional truncation. Following this procedure, older seismic sequences were separated from younger, resulting in the subdivision of the studied interval into seismic sequences.

The identified seismic sequences were subsequently classified according to seismic facies characteristics such as reflection configuration, amplitude, frequency and continuity (Mitchum et al., 1977b). Seismic facies was predominantly used to distinguish autochthonous chalk, characterised by parallel and continuous reflections (Fontaine et al., 1987; Nygaard et al., 1990; Andersen et al., 1990; Macurda, 1997; Gras & Geluk, 1999; Britze et al. 2000), from allochthonous sediment, characterised by chaotic ('hummocky') reflections (Johnson, 1987; Nygaard et al., 1990; Andersen et al., 1990; Britze et al., 2000). High amplitudes (i.e. strong seismic reflections) may indicate higher porosities (Britze et al., 2000) or the presence of hard-grounds in the Chalk (Gras & Geluk, 1999).

2.2.4 Integration of the seismic and well database

Seismic-to-well ties were made using synthetic seismograms. These were constructed by calculating an impedance curve from a sonic log, which was calibrated first with checkshot data to improve depth-time conversion. Where available, a density log was used as well. The impedance curve in turn was convoluted with a theoretical seismic wavelet to form a synthetic seismogram. Comparing the synthetic seismogram to an original seismic section, the seismic sequence boundaries were identified in the well logs. This procedure was carried out using the 'synthetic'-module in GeoFrame (Henry, 2000; Box & Lowrey, 2003).

After tying the seismic sequence boundaries to the well logs, characteristic responses of well logs such as gamma-ray logs, which indicate clay content (Rider, 1996) and sonic and density logs, which in chalks measure primarily porosity (Campbell & Gravdal, 1995; Anderson, 1999), were identified for each sequence. Since well logs have a high resolution, i.e. tens of centimetres compared to several tens of meters in seismic data (Kearey & Brooks, 1991; Rider, 1996), the petrophysical properties of the sequences could be studied in more detail. Using synthetic seismograms, possible controls of sub-seismic petrophysical properties on seismic response were also studied.

The age of the seismic sequences was determined using the results of existing industrial micropaleontological analyses performed on samples of some of the wells that were tied to the seismic dataset. Since most of the micropaleontological analy-

ses date from the 1970s and 1980s, the biozonations had to be actualised using recent biozonations of the Chalk interval (Hardenbol et al., 1998b; Bergen & Sikora, 1999). Older biozonations were used in some exceptional cases (Koch, 1977; King, 1989; King et al., 1989). To ensure optimal usage of the available biostratigraphical information, only the data of those wells was used that are positioned in an area where the seismic sequences are clearly developed and of which good synthetic seismograms could be constructed to tie the well database to the seismic data. Only last occurrence depths (LOD) of index foraminifera were used for age determination, to rule out the possible effects of caving.

2.3 Description of the seismic sequences

2.3.1 Base Chalk Group seismic horizon (Base Cenomanian)

The lower boundary of the Chalk succession is formed by the Base Chalk Group seismic horizon (Fig. 2.2). In the largest part of the study area, this boundary forms a strong positive seismic reflector (Fig. 2.14 & Fig. 2.15), because of the marked impedance contrast between the high velocity Chalk Group and the underlying Lower Cretaceous sediments. In the sonic and density logs, this is indicated by a strong shift towards higher densities (Fig. 2.18 & Fig. 2.19). Where the lower boundary is more subtly developed, i.e. by a gradual upward increase in carbonate content in the underlying Lower Cretaceous Holland Formation (Van Adrichem Boogaert & Kouwe, 1994), the transition with the Chalk needs to be identified on well logs.

In well logs the Chalk Group is generally characterised by conspicuously low gamma-ray readings, which are a result of very small amounts of clay, as well as high density and low sonic log values, compared to the enveloping siliciclastic sediments. The lower boundary surface of the Chalk Group is clearly deformed by short wavelength (i.e. several kilometres in dimension) deformations in the northeastern and central parts of the Netherlands offshore area (quadrants D through N, quadrant B), as a result of diapirism of underlying Zechstein salt. Although undetected in this study, it is important to note that many more salt structures are probably present throughout the area. The Base Chalk Group seismic horizon is shallowest in the south of the study area (southeastern part of the K-quadrant, area around the P-quadrant) and is deepest in parts of the centre (northern part of quadrants K and L, southern F and G) and towards the northern part of the study area (quadrants A and B). The Chalk is absent in parts of the F-quadrant (southern Dutch Central Graben, Fig. 1.8) and parts of the P, Q and K quadrants (Broad Fourteens Basin, Fig. 1.8).

2.3.2 Seismic sequence CK1, Texel Formation (Cenomanian)

The basal seismic sequence of the Chalk succession represents the Cenomanian Texel Formation (Fig. 1.5; Van Adrichem Boogaert & Kouwe, 1994). The areal extent of the sequence is outlined on the Base Chalk Group reflector map (Fig. 2.2). In the large area in the west, containing parts of quadrants D, E, F, J, K and L, sequence CK1 is developed as a single or double, parallel and continuous, weak reflection (Fig. 2.14). A similar facies is encountered in most of the eastern section of the study area, in quadrants G, M and N (Fig. 2.15), and in the southernmost part (quadrant P and surroundings). In the northeast (southern part of quadrant B and northern parts of quadrants F and G), extensive deformation by salt doming and faulting resulted in a much less clearly developed CK1, consisting of a weak and discontinuous single reflection wiggle. In the south of quadrant L, CK1 is found to fill into WNW–ESE trending channels about 1–2 km wide and over 10 km long. The present areal extent of CK1 is almost exclusively the result of erosion, with the exception of parts of quadrants G and L, where the sequence is observed to onlap onto previously existing topographic highs. The Cenomanian age of CK1 is suggested by the presence of the benthic foraminifera *Gavelinella intermedia* and *Gavelinella cenomanica*, as well as the planktonic foraminifera *Rotalipora cushmani* and *Praeglobotruncana sp.* (Fig. 2.20).

2.3.3 Seismic sequence CK2 (Turonian to Coniacian)

The conspicuous Plenus Marl Member (Fig. 1.5; Van Adrichem Boogaert & Kouwe, 1994) forms the base of sequence CK2 (Fig. 2.3). In well logs, the Plenus Marl Member forms a distinct spike in gamma-ray, sonic and density logs (Fig. 2.18 & Fig. 2.19). The present areal extent of this sequence is roughly similar to that of CK1 and is controlled by erosional truncation by overlying sequences. Where CK2 is developed most clearly, it consists of a set of, usually three, very high-amplitude seismic reflection couplets. This occurs in the western part of the study area (Quadrants D, E, F, J, K and L, Fig. 2.14), as well as in quadrant M and parts of G (Fig. 2.15). In these areas CK2 is up to 125 ms thick. Synthetic seismograms (Fig. 2.16 & Fig. 2.17) show that the high-amplitude seismic reflections are caused by strong, 5 to 10 m scale, porosity variations that result in characteristic serrated sonic and density log responses (Fig. 2.18 & Fig. 2.19). In the northeastern part of the study area, CK2 is less clearly developed and consists of low-amplitude, parallel and discontinuous to chaotic reflections (southern part of quadrant B, northern F and western G-quadrants). In the southernmost area of the Dutch offshore (P-quadrant), this sequence shows low-amplitude, but continuous, parallel reflections.

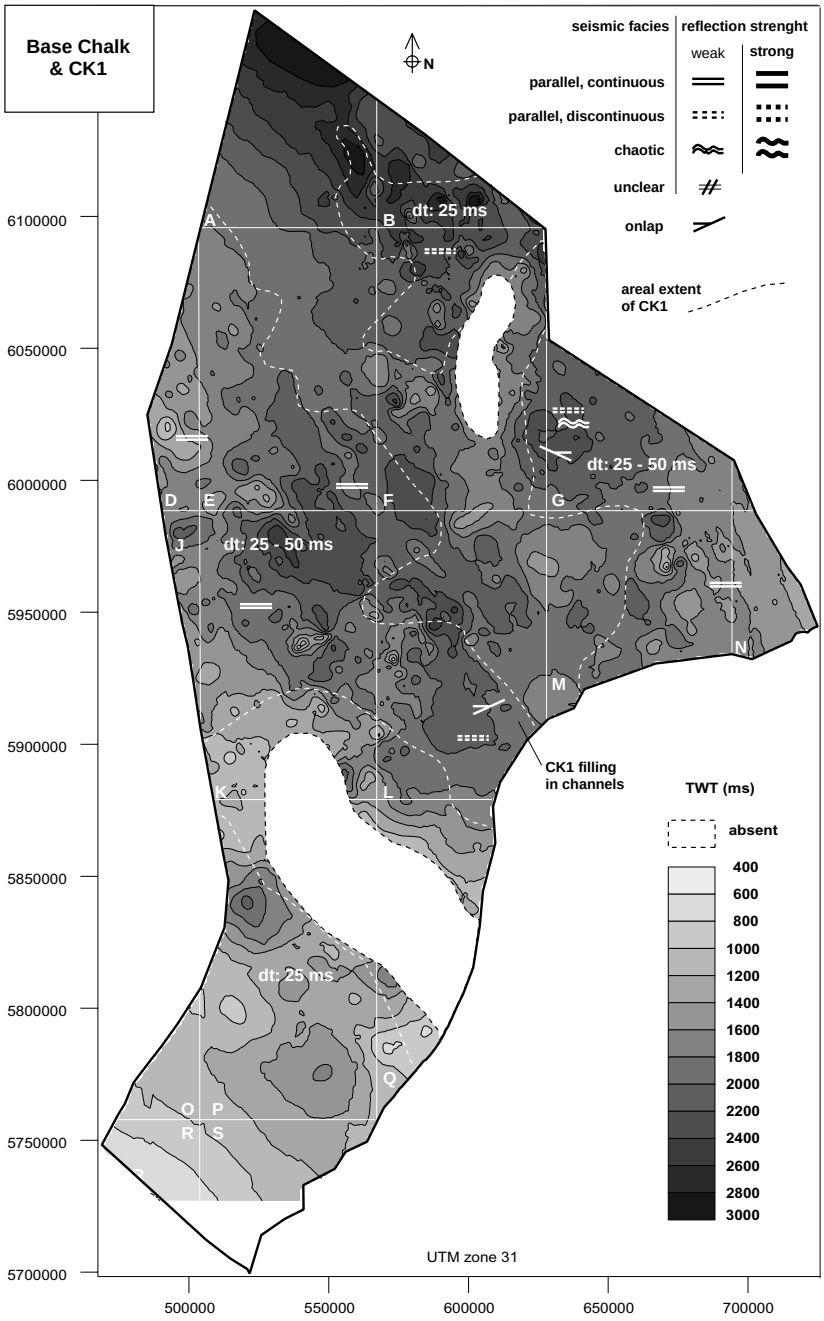

Figure 2.2: TWT-map of the Base Chalk Group (Base Cenomanian) seismic horizon indicating the subcrop outline (dashed line) and seismic facies of sequence CK1 (Cenomanian).

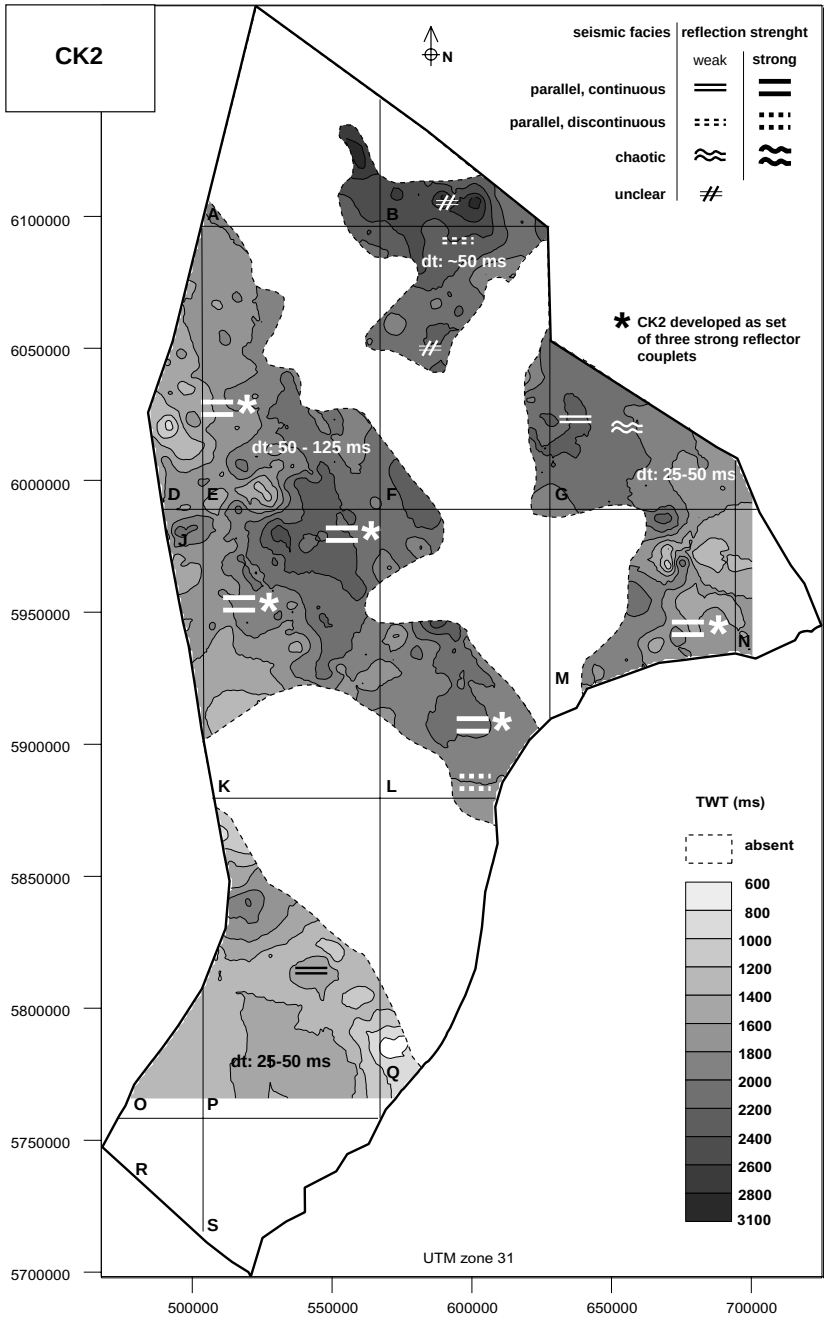

Figure 2.3: TWT and seismic facies map of the base of seismic sequence CK2 (Turonian).

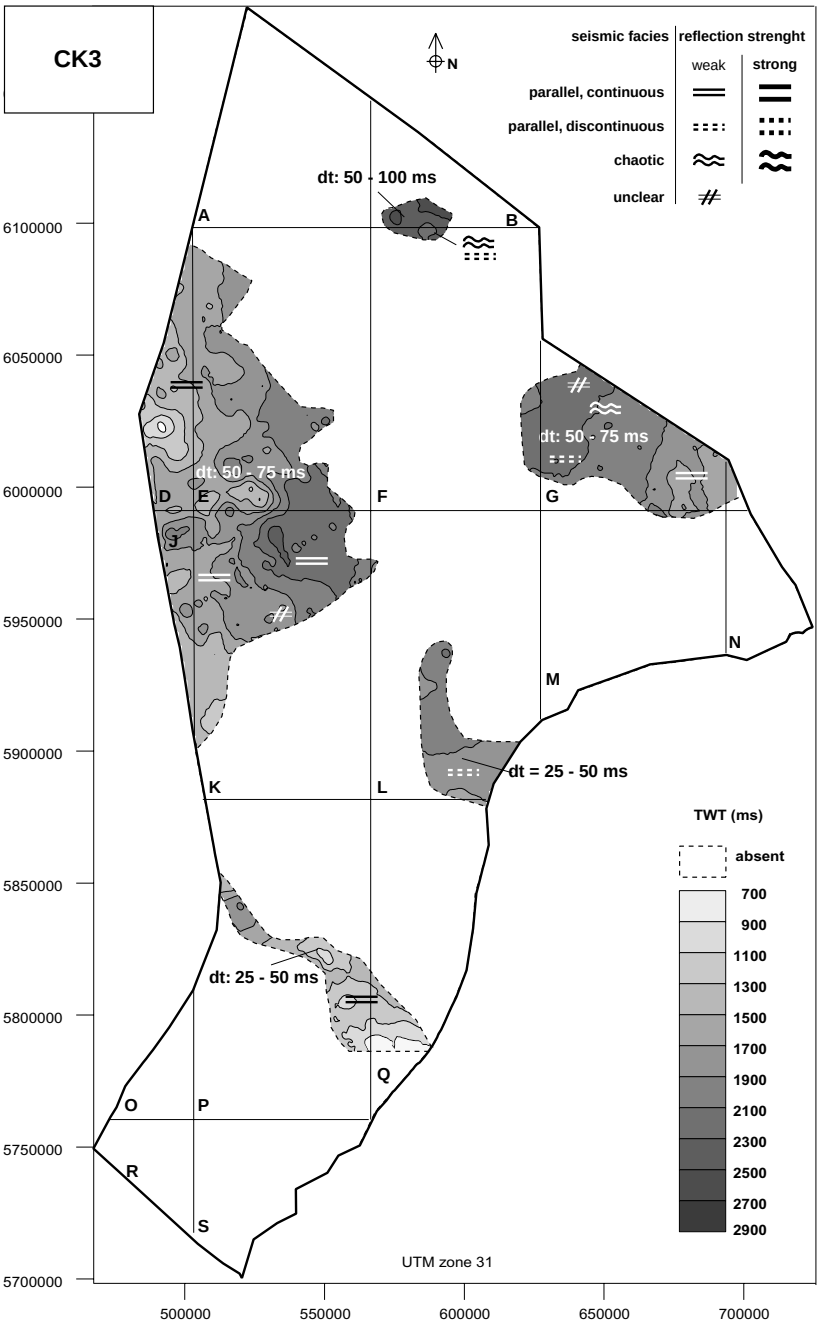

Figure 2.4: TWT and seismic facies map of the base of seismic sequence CK3 (Coniacian).

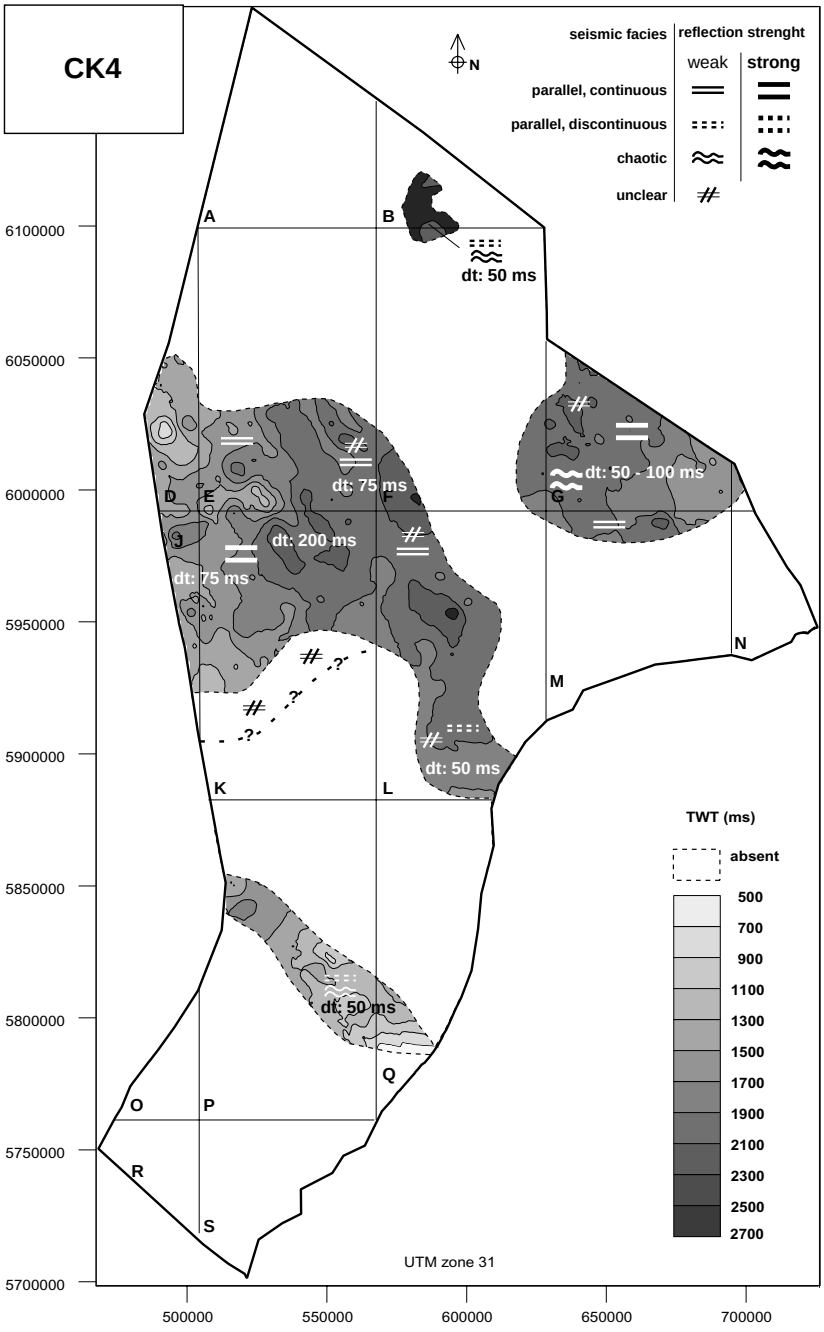

Figure 2.5: TWT and seismic facies map of the base of seismic sequence CK4 (Santonian).

Seismic sequence CK2 is probably of Turonian age, including early occurrences of the benthic foraminifera *Stensioina granulata spp.*, *Stensioina granulata granulata*, and *Gavelinella tourainensis* (Fig. 2.20).

2.3.4 Seismic sequence CK3 (Coniacian)

Seismic sequence CK3 (Fig. 2.4) has the smallest remaining areal extent of all intra-Chalk sequences of the Dutch offshore. The sequence is present only in larger areas in the west (quadrants D, E, J and K) and east (quadrant G), as well as in smaller patches in the northern (B-quadrant), central (L) and southern (P and Q quadrants) parts of the study area. If present at all, CK3 was eroded in the remaining area. This is evident from the type of reflection terminations observed along the CK3 subcrop boundaries, which indicate truncation. In the western part of the study area, as well as in the southern G-quadrant, CK3 is usually 50–75 ms thick and characterised by low-amplitude, continuous parallel reflections (Fig. 2.14). In the northern G-quadrant, as well the small patch in quadrant B, the sequence shows discontinuous to chaotic reflections (Fig. 2.15). Furthermore, unfavourable seismic quality often renders the internal reflection configuration unclear in this region. The small subcrops in the central and southern parts of the study area display continuous to discontinuous, low-amplitude reflections in this sequence. CK3 shows fairly constant sonic and density log readings throughout the study area, with the exception of the upper part of CK3 in G17-1. Here, very strong porosity variations are visible that locally cause high amplitude reflections and extend into the overlying sequence CK4 (Fig. 2.16). A Coniacian age of CK3 is inferred from the stratigraphic position of this sequence above and below dated sequences.

2.3.5 Seismic sequence CK4 (Santonian)

Sequence CK4 (Fig. 2.5) oversteps the preceding sequence in most of the study area, with the exception of the northern part of quadrants D and E, where the sequence is missing. Throughout most of the Netherlands offshore, in the area encompassing D, E, F, J, K, and L-quadrants (Fig. 2.14), as well as the G-quadrant (Fig. 2.15), CK4 shows continuous parallel reflections, with high amplitudes in quadrants K and G. In these areas, strong decametre-scale density (porosity) variations can be observed in CK4 in the well logs. Good examples are the sonic logs of L5-1, K7-3, B17-2, G17-1 and F15-1 (Fig. 2.16 & Fig. 2.17). As a contrast, chaotic reflections make up the sequence in quadrants B, western quadrant G and in the south of the study area, in quadrants P and Q. In some parts of the study area low seismic quality makes an adequate seismic qualification impossible. In quadrant K, for instance, sequence CK4, as well as a number of younger sequences, is most probably present

but cannot be identified. Reflection configurations along subcrop boundaries hint to erosional truncation by younger sequences. The thickness of CK4 varies strongly (dt: 25–200 ms) throughout the area. Sequence CK4 is probably of Santonian age, as suggested by the early occurrences of *Stensioina exsculpta spp.* and *Stensioina exsculpta gracilis*.

2.3.6 Seismic sequence CK5 (lower Campanian)

The present areal extent of seismic sequence CK5 (Fig. 2.6) roughly equals that of the preceding sequence in the area around quadrant G, as well as the narrow strip in quadrants P and Q. In the area around the southern E-quadrant, the (southward) progressive areal reduction of subsequent sequences is continued, and CK5 is missing in this area. The seismic facies is characterised by generally low-amplitude, low frequency parallel and continuous reflections. In well logs (sonic and density), CK5 shows a varied log response, but usually with minor high-frequency variations (Fig. 2.18 & Fig. 2.19). In parts of quadrant K, low seismic quality makes identification and seismic facies characterisation of the sequence impossible. In the southern part of quadrants M and N, sequence CK5 directly overlies the Texel Formation. Here, CK5 is made up of discontinuous/parallel to chaotic reflections. Throughout the study area, the thickness of CK5 varies strongly (dt: 25–150 ms). The age of CK5 is probably early Campanian, which is suggested by the occurrence of *Stensioina exsculpta ssp.* in P12-1 and the stratigraphic position of the sequence.

2.3.7 Seismic sequence CK6 (lower Campanian)

Sequence CK6 (Fig. 2.7) is only found in the area of quadrants G, L and M (Fig. 2.15), where it is 50–75 ms thick, as well as a smaller area in the north-western part of the P-quadrant where CK6 reaches a thickness of about 100 ms. The sequence is generally made up of low-amplitude, parallel and continuous reflections (Fig. 2.15), and shows a regular high frequency response in sonic and density logs, locally with a generally downward increasing density trend. In the P-quadrant, however, chaotic seismic reflections are dominant. Seismic sequence CK6 is probably of early Campanian age, as is suggested by the occurrence of *Stensioina exsculpta spp.* in M9-1 and *Stensioina exsculpta gracilis* in P8-1, and the stratigraphic position of the sequence.

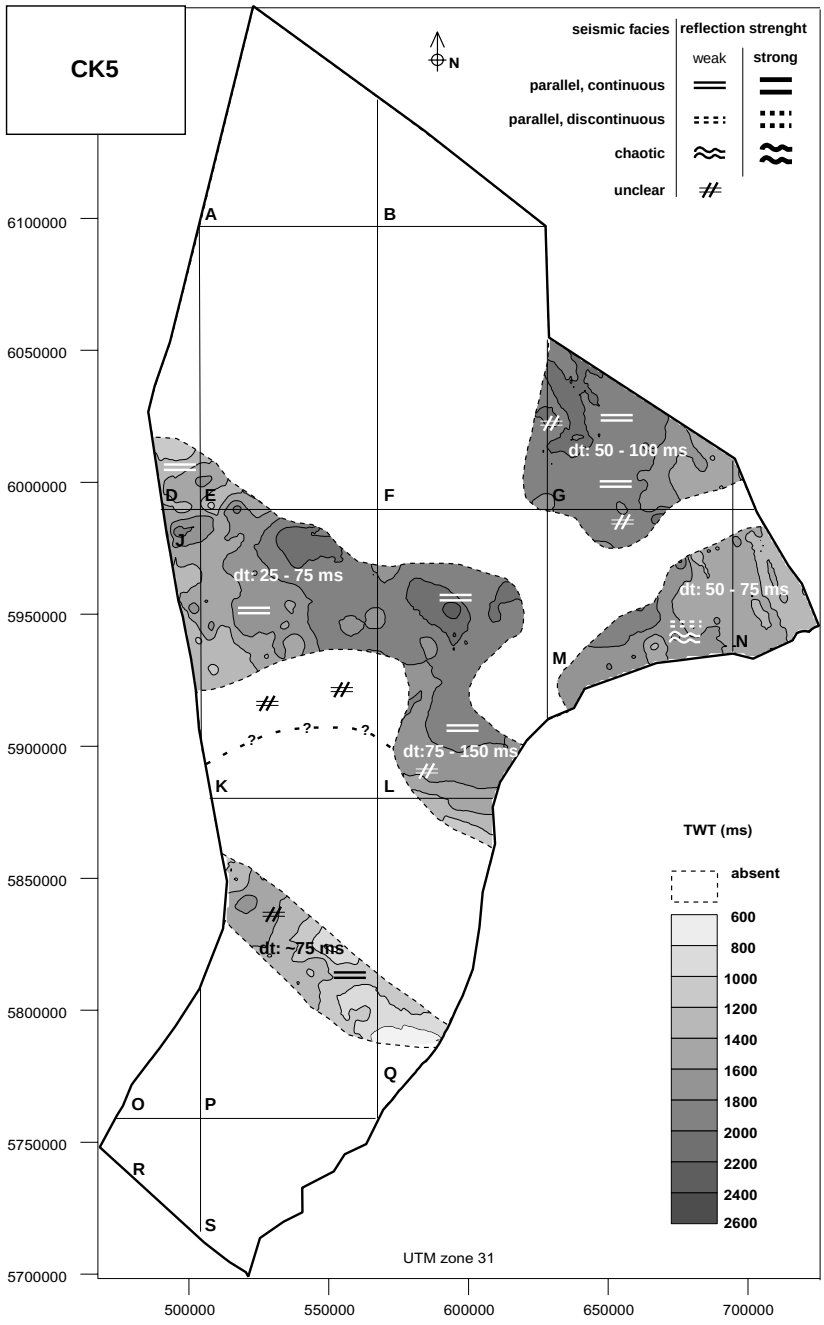

Figure 2.6: TWT and seismic facies map of the base of seismic sequence CK5 (lower Campanian).

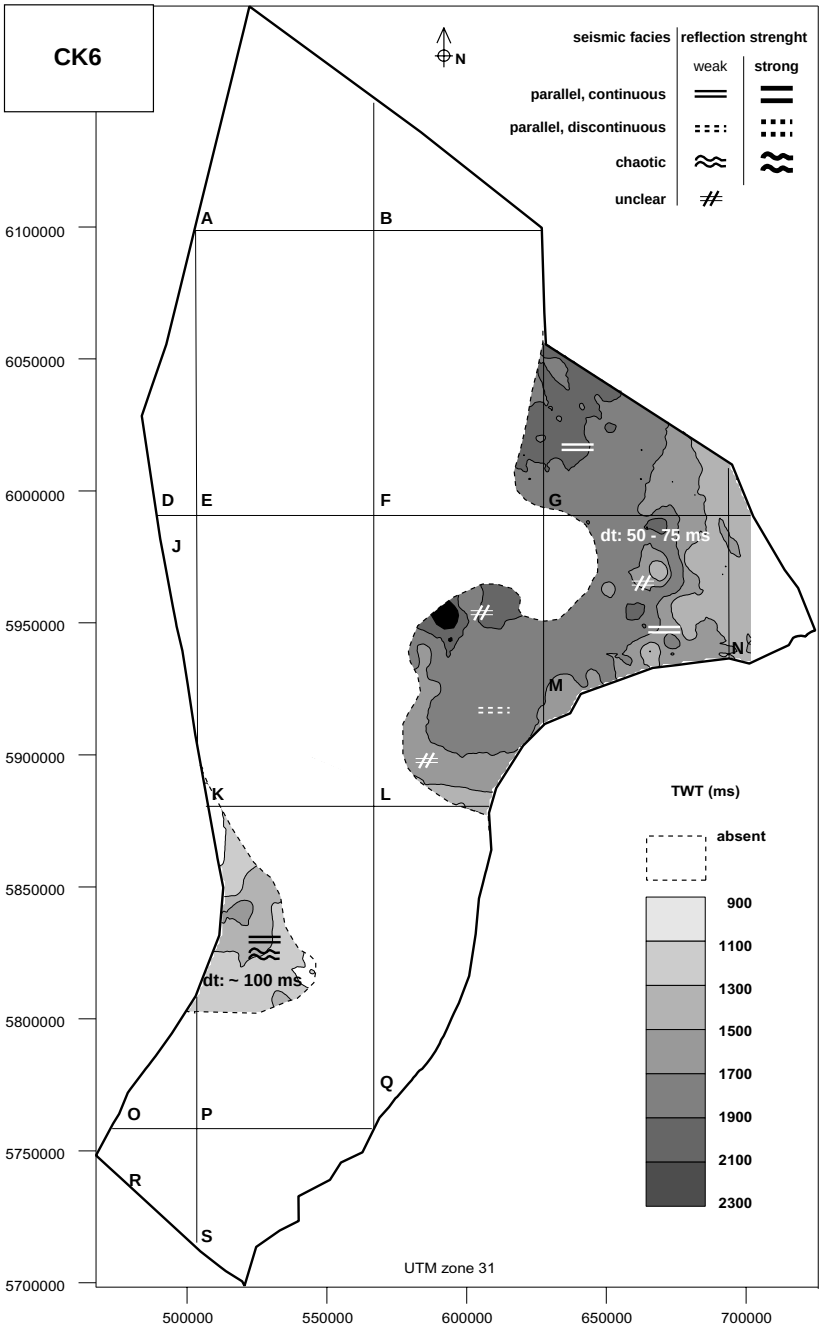

Figure 2.7: TWT and seismic facies map of the base of seismic sequence CK6 (lower Campanian).

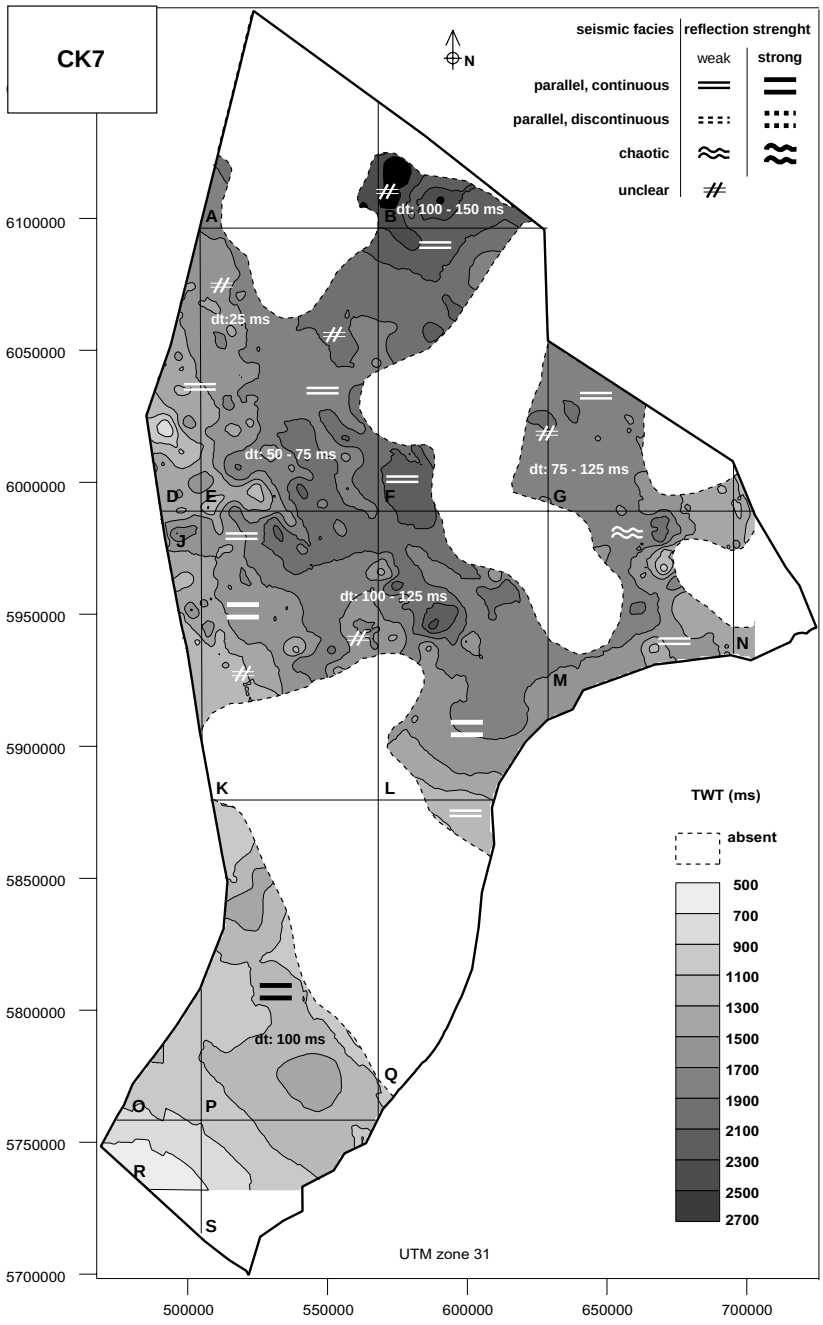

Figure 2.8: TWT and seismic facies map of the base of seismic sequence CK7 (middle to upper Campanian).

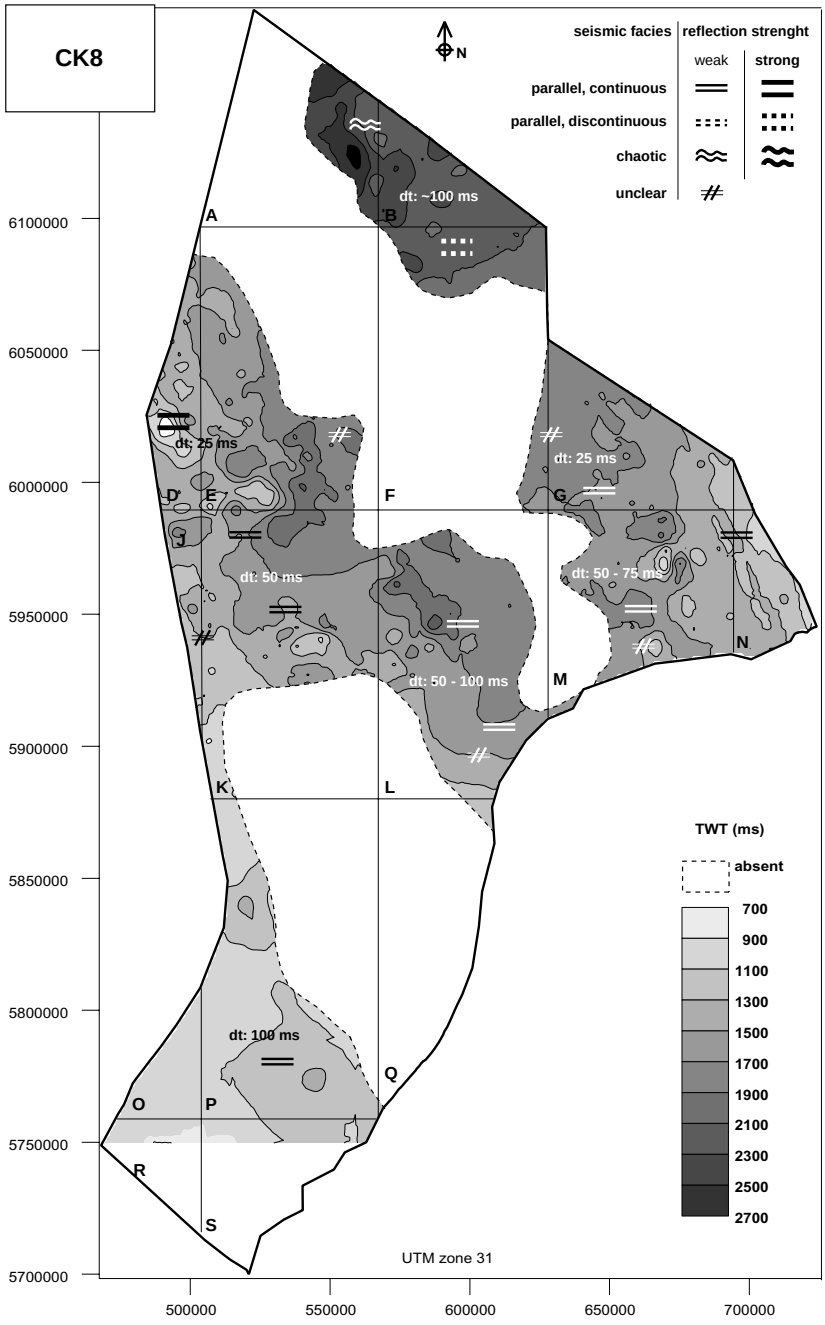

Figure 2.9: TWT and seismic facies map of the base of seismic sequence CK8 (lower Maastrichtian).

2.3.8 Seismic sequence CK7 (middle to upper Campanian)

Seismic sequence CK7 (Fig. 2.8) forms the base of a seismic mega-sequence that encompasses CK7 to CK11, and has a much greater areal extent than the underlying mega-sequence consisting of CK1 to CK6. CK7 is found throughout the study area, and its base forms a marked angular unconformity. This sequence locally overlies sequences as old as CK2. The sequence is around 50–150 ms thick, and consists of continuous parallel reflections of low amplitude throughout most of the Netherlands offshore. Exceptions to this are encountered in the area of the K, L and P-quadrants, where amplitudes are high. Furthermore, in the northern part of quadrant M chaotic seismic reflections are encountered. Seismic image quality is usually less clear along the boundaries of the CK7 subcrop, where the sequence is rapidly thinned by erosion. In sonic and density logs, CK7 generally shows a fairly constant high frequency log response, with a strong general downward increasing density (decreasing porosity) trend. Deposition of CK7 most likely took place during the middle and late Campanian, which is suggested by the presence of *Gavelinella clementiana* in P8-1 and the stratigraphic position of the sequence (Fig. 2.20).

2.3.9 Seismic sequence CK8 (lower Maastrichtian)

The present areal extent of sequence CK8 (Fig. 2.9) roughly equals that of CK7, with the exception of the northern E-quadrant, where CK8 is absent. The easternmost part of the Netherlands offshore is entirely covered by CK8, which oversteps CK7 in parts of western G and N-quadrant (Fig. 2.15). Moreover, CK8 oversteps CK7 in the northernmost part of the study area, extending into the eastern A-quadrant. In this northern subcrop, chaotic and discontinuous parallel seismic reflections, often with high amplitudes, dominate the seismic facies. It is typically about 100 ms thick. Throughout most of the study area, the seismic facies is similar to CK7, with high amplitudes only encountered in quadrant D. The thickness varies from 25–125 ms. In the south (quadrant P), the sequence is about 100 ms thick. In sonic and density logs, CK8, like most sequences, shows modest high frequency variations. However, marked regional variation exists in large-scale trends (Fig. 2.18 & Fig. 2.19). The micropaleontological evidence points to an early Maastrichtian age, including last occurrences of *Bolivinoides draco miliaris* in B17-2, *Gavelinella montelerensis* in E12-1 and *Bolivinoides laevigatus* in P8-1.

2.3.10 Seismic sequence CK9 (lower to upper Maastrichtian)

Sequence CK9 (Fig. 2.10) has the widest areal extent of all intra-Chalk sequences and shows marked variation in both seismic facies and amplitude strength. Throughout

the north (A and B-quadrants), west (D, E and J; Fig. 2.14) and east (eastern part of quadrant G; Fig. 2.15), amplitudes are strong. In the A and B quadrants the seismic facies of CK9 consists partly of discontinuous reflections. In the northwestern part (southern quadrant A, northern E), throughout the central part (southeastern E, as well as L, M, N and eastern part of G), and in the south of the study area (P and Q quadrants) amplitudes are usually low. Throughout the study area, small zones of chaotic reflections are encountered. In the eastern section of the Dutch offshore, however, these chaotic reflections are found along a prominent NNW–SSE trending facies belt. This facies belt probably outlines a large channel, which cuts into older sequences. Sequence CK9 is up to 200 ms thick here. In well logs (sonic and density), CK9 shows a variable response in seismic-scale variations, as well as in larger scale trends and absolute values (Fig. 2.18 & Fig. 2.19). As with the previous sequence, an unambiguous age determination cannot be made with the available biostratigraphical data. An early Maastrichtian age for this sequence is suggested in the east and south of the study area (wells F18-3, G17-1, M9-1 and P8-1), by the last occurrences of *Bolivinoides laevigatus*, *Bolivinoides draco miliaris*, *Gavelinella pertusa*, *Gavelinella voltziana*. In the west and north of the study area, however, wells D15-1, A18-1 and B17-2 suggest a late Maastrichtian age for this sequence, as suggested by the (last) occurrence of *Bolivinoides draco draco*.

2.3.11 Seismic sequence CK10 (upper Maastrichtian to lower Danian)

Like the previous sequences, CK10 covers most of the study area (Fig. 2.11). It is absent, however, in the southernmost part of the study area (southern P-quadrants), in parts in the east (M and N quadrants), and two smaller areas in the north. The seismic facies of CK10 is less variable than that of CK9, consisting almost exclusively of continuous parallel reflections. Throughout most of the east (quadrants B, F, G, and northern part of M) and in the southernmost part (quadrant P) of the study area, amplitude strength is generally high, compared to low amplitudes in the remaining area. As is the case with most of the older sequences, the exact boundary of the CK10 subcrop in the southern K and southwestern L-quadrants is inconclusive due to low seismic quality. Indications of small channels are found in the northern K-quadrant and in quadrant A. Sonic and density log character is variable, with very strong decametre scale variations occurring in areas where seismic amplitudes are high (Fig. 2.18 & Fig. 2.19). In the eastern and southern part of the study area, as well as in E12-1, a late Maastrichtian age is suggested by the last occurrences of the planktonic foraminifera *Racemiguembelina fructicosa* and *Pseudotextularia elegans*, and the benthic foraminifera *Bolivinoides draco draco*.

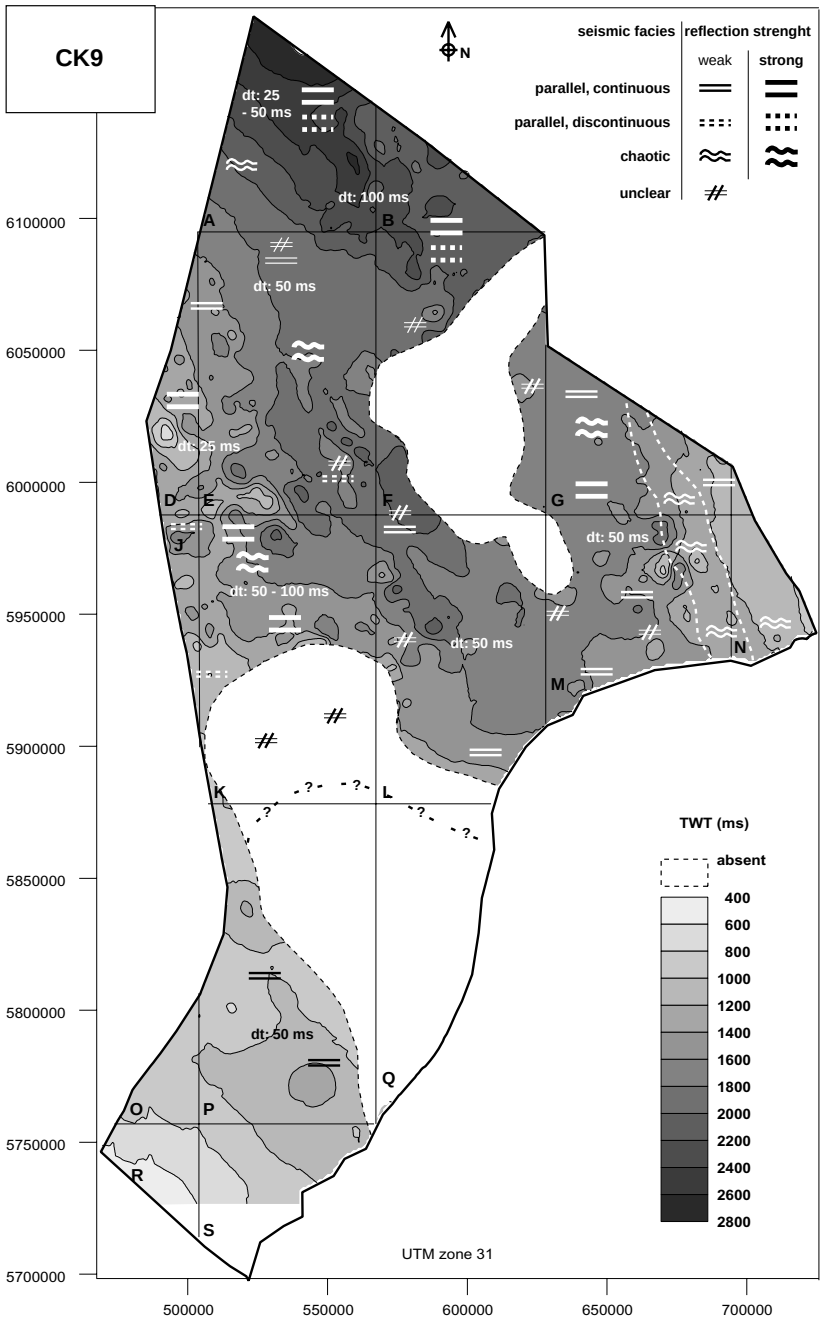

Figure 2.10: TWT and seismic facies map of the base of seismic sequence CK9 (lower to upper Maastrichtian).

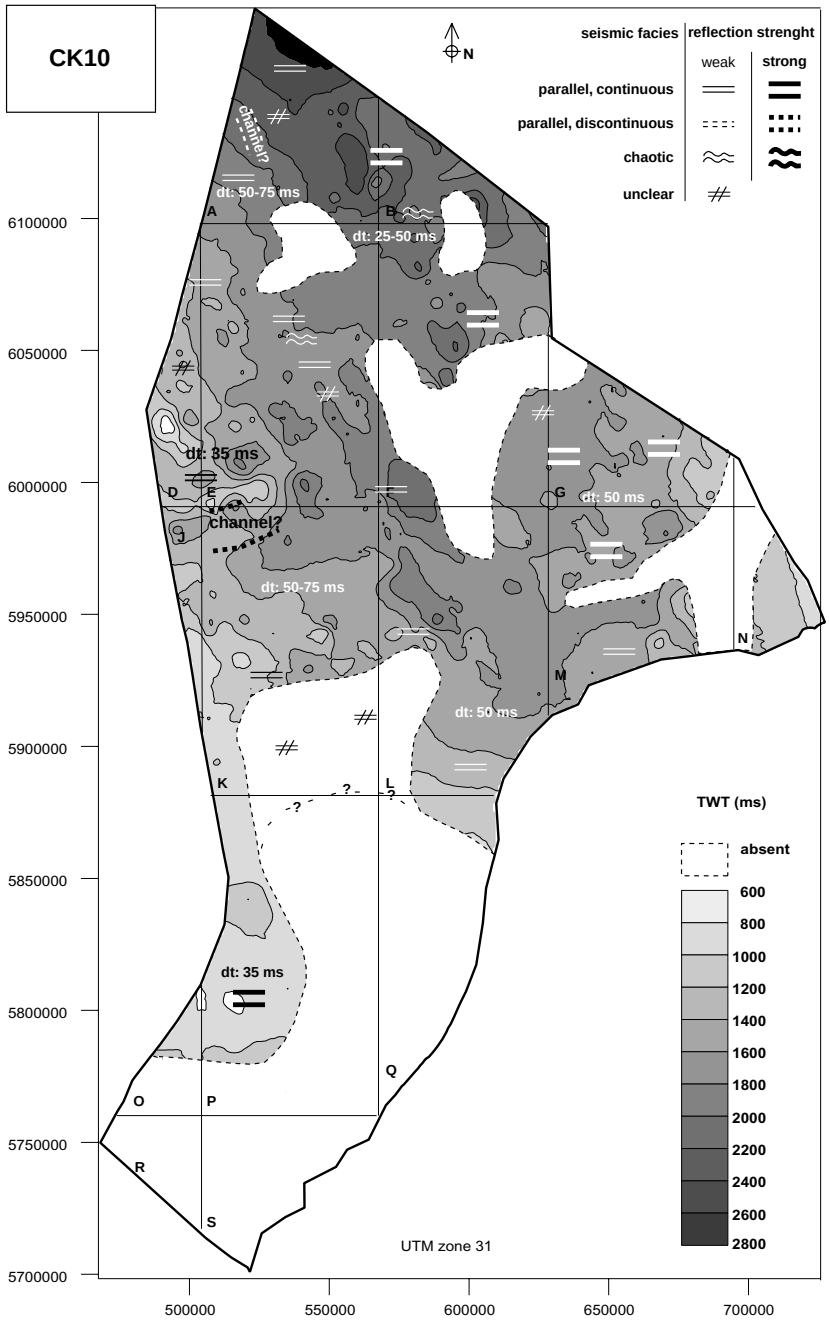

Figure 2.11: TWT and seismic facies map of the base of seismic sequence CK10 (upper Maastrichtian to lower Danian).

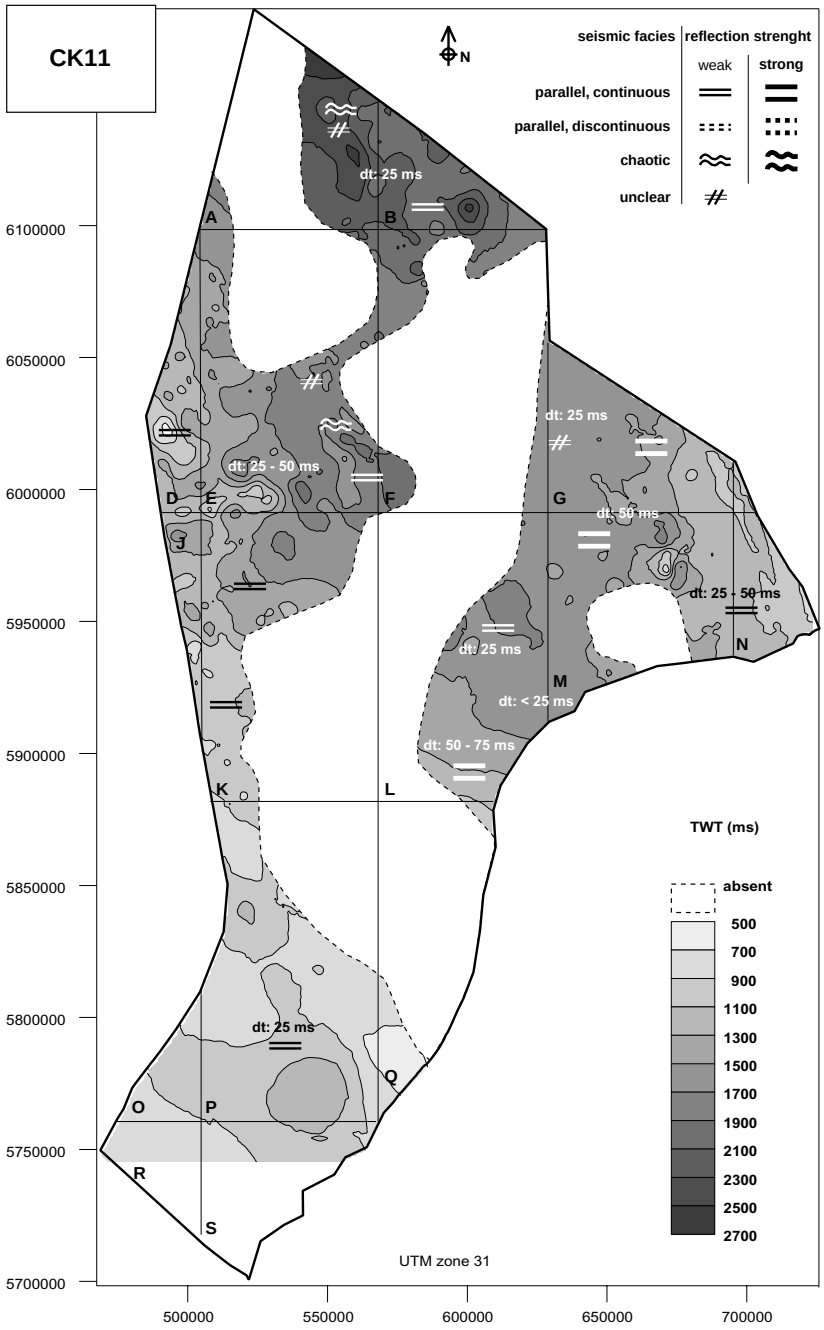

Figure 2.12: TWT and seismic facies map of the base of seismic sequence CK11 (Danian).

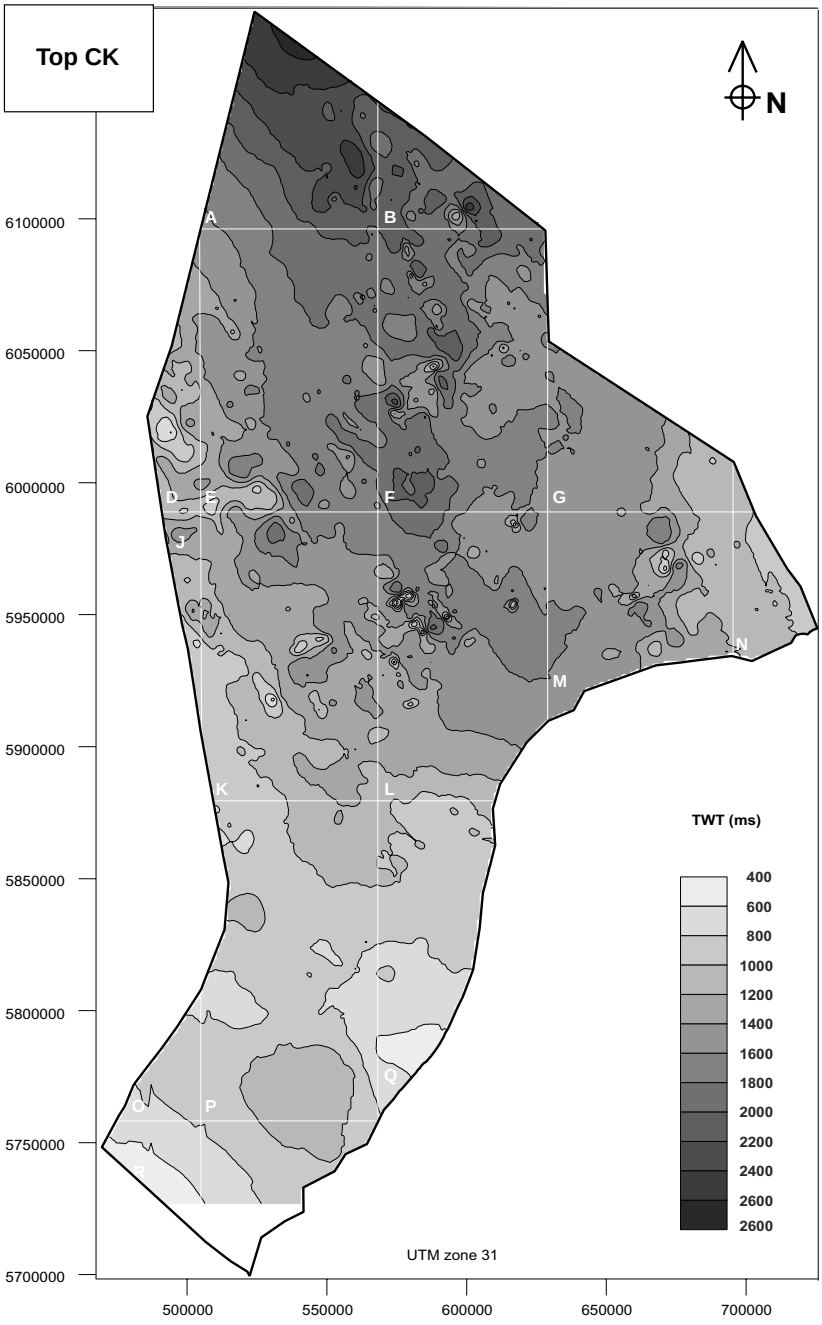

Figure 2.13: TWT-map of the Top Chalk seismic horizon.

In the north of the study area, however, an early Danian age is indicated by *Globoconusa daubjergensis* (A18-1 and B17-2).

2.3.12 Seismic sequence CK11 (Danian)

The areal extent of seismic sequence CK11 is smaller than that of the previous sequences throughout most of the study area (Fig. 2.12). The sequence is absent in two large, roughly N–S trending zones in the central part of the study area, as well as in a smaller area in the east (quadrant M). In the north of the study area (quadrants A and B), CK11 is thin (about 25 ms) and consists of chaotic seismic reflections in the north, and weak parallel and continuous reflections in the south. In the west (quadrants D, E, J and K; Fig. 2.14), this sequence varies in thickness between 25 and 50 ms, and generally shows low amplitude, parallel, continuous reflections. In the south (quadrants O, P and Q), seismic facies is similar and thickness around 25 ms. In contrast, in most of the large subcrop in the eastern part of the Netherlands offshore (quadrants L, M, G and N; Fig. 2.15), the seismic facies of CK11 is characterised by very strong, parallel and continuous reflections. Here, the sequence is up to 75 ms thick (southern L-quadrant). In the sonic and density logs, CK11 shows very strong, high frequency (meter-scale), variations (Fig. 2.18 & Fig. 2.19). In most of the wells, a Danian age is suggested for CK11, including last occurrences of *Globorotalia pseudobulloides*, *Globoconusa daubjergensis* and associated species (Fig. 2.20). However, it is unclear when the onset of the CK11 depositionary phase took place exactly.

2.3.13 Top Chalk Group seismic horizon

The upper boundary of the Chalk succession is formed by the Top Chalk Group seismic horizon (Fig. 2.13). This seismic horizon marks the transition from chalk, generally with a high acoustic velocity, and the overlying post-Danian siliciclastic sediments, which have a lower acoustic velocity. The resulting acoustic impedance contrast makes for an exceptionally strong seismic reflector, which makes the Top Chalk horizon one of the most clearly developed in the Netherlands offshore (Fig. 2.14 & Fig. 2.15). In well logs, the top of the Chalk Group is easily recognisable by the very strong and almost instantaneous downward increase in gamma-ray values in the overlying siliciclastics of the North Sea Supergroup (Van Adrichem Boogaert & Kouwe, 1994). The sonic and density values show a very strong downward shift towards lower densities (i.e. higher sonic) values (Fig. 2.18 & Fig. 2.19). The Top Chalk is deepest in the north (2600 ms TWT), and gradually becomes shallower towards the south (400 ms TWT). As the acoustic velocity of the overlying Tertiary sediments is about 2000 ms (Japsen, 1999), the TWT-values can be viewed

as depth values (in meters). Short wavelength (i.e. several kilometres wide) deformations are visible throughout the northern half of the study area. Like the short wavelength deformations in the Base Chalk reflector, these are expressions of salt diapirs. The apparent deformation lineaments are an artefact, resulting from the sampling interval, i.e. the location of the seismic lines.

2.4 Discussion

2.4.1 Seismic interpretation

The eleven seismic sequences mapped in the Chalk Group in the Netherlands offshore area following the definition of Vail et al. (1977b) and Emery & Myers (1996), are stratigraphic units deposited during a certain time interval that are separated by (erosional) unconformities from other stratigraphic units that were formed during earlier and later stages. These unconformities represent basinwide fluctuations of the relative sea level, possibly caused by short pulses of uplift (Cloetingh, 1985; 1986). The seismic sequences were classified in terms of seismic facies characteristics, such as reflection configuration, continuity and amplitude strength, following the 'classic' seismic interpretation methodology of Vail (1977b). An important characteristic of the application of this method in deep-water chalks is that no shifts in depositional facies belts, in coastal settings indicative of relative sea level variations, can be recognised here (Vail et al., 1977a; Surlyk, 1997). Therefore, the observation of Bramwell et al. (1999), that a subdivision as presented in their paper is not a 'classical' sequence stratigraphic subdivision but rather a more basic 'allostratigraphical' subdivision, is followed in the present study.

Comparing the subcrop maps of each seismic sequence (Fig. 2.2 to Fig. 2.12), it is clear that two 'mega-sequences' of Chalk deposition in the study area can be identified. The Chalk deposits of CK1 to CK6 (Cenomanian to lower Campanian), appear to have been removed by a large erosional phase that preceded the deposition of sequence CK7. This erosion phase affected sediment as deep as CK2. This sequence is absent in large areas of the Netherlands offshore, while the underlying sequences CK1 and CK2 (Cenomanian to Turonian) each have a much wider areal extent.

The second tectono-sedimentary mega-sequence encompasses seismic sequences CK7 through CK11 (middle Campanian to Danian), which covers most of the Netherlands offshore area, with the exception of the Dutch Central Graben and Broad Fourteens Basin. A smaller erosion phase affected CK11 and to a lesser extent CK10. A detailed overview of smaller-scale vertical movements is provided in Chapter 3.

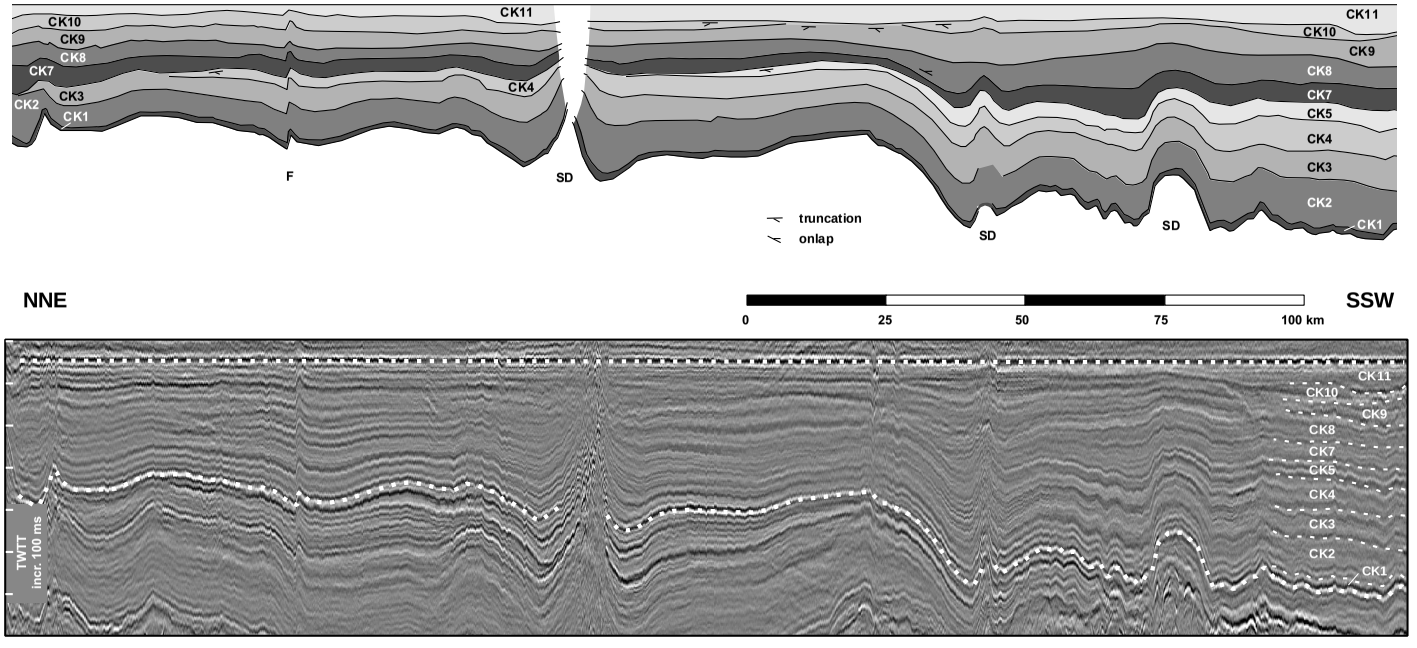

Figure 2.14: Seismic profile showing the seismic character of the Chalk Group on the Cleaver Bank High (F = fault, SD = salt diapir). Profile is flattened at the Top Chalk horizon.

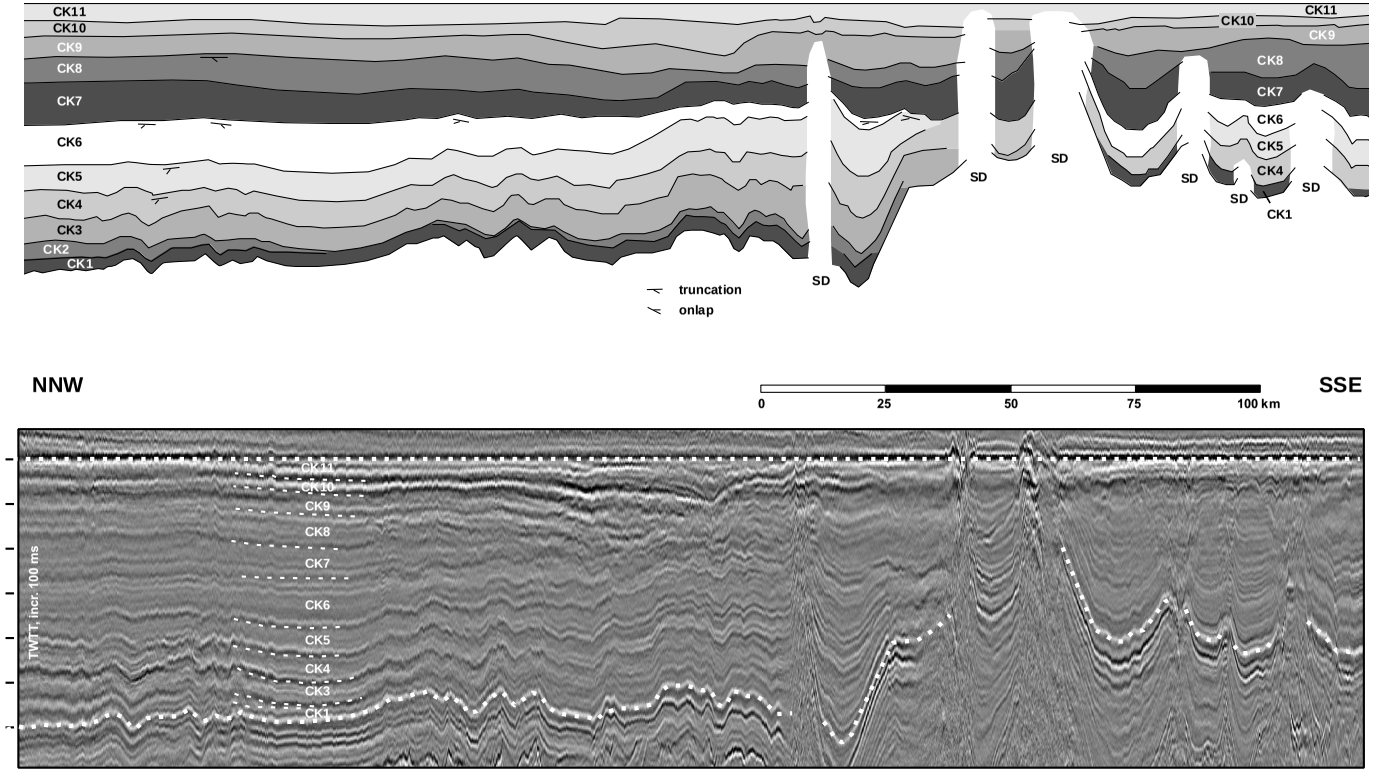

Figure 2.15: Seismic profile showing the seismic character of the Chalk Group on the Schill Grund High and Ameland Block (F = fault, SD = salt diapir). Profile is flattened at the Top Chalk horizon.

The unconformities separating the intra-Chalk sequences are indicated by seismic reflection terminations. In most cases, however, sequence boundaries form distinct seismic reflectors as well (Fig. 2.14) & Fig. 2.15). From the synthetic seismograms (Fig. 2.16 & Fig. 2.17) it is evident that these reflections are caused by small shifts in density values at sequence boundaries. In most cases, moving upward trough the logs, the lower boundary of a sequence is marked by a sudden increase in density (or decrease in porosity). Examples of this are marked * in the well logs of Fig. 2.16 & Fig. 2.17. As sequence boundaries represent a break in sedimentation, it is conceivable that these sudden density increases (and thus: seismic reflections) represent cementation surfaces (i.e. tight zones or hardgrounds) because these are a common indicator to low or halted sedimentation in chalks (Håkansson et al., 1974; Hancock, 1975; Zijlstra, 1994, 1995; Molenaar & Zijlstra, 1997). A sudden downward decrease in density is also observed. Good examples are found at the base of CK8 in B17-2 and the base of CK8 in G17-1 (both are marked ** in Fig. 2.16). In the case of B17-2, this probably represents an uplift and erosion phase, after which older (and therefore more compacted) sediment is overlain by younger (less compacted) chalk. The density contrast in G17-1 indicates the opposite, here denser chalk overlies more porous sediment. This may indicate a drop in sedimentation rate, as such a decrease results in more vigorous bioturbation, and hence compaction, of sediment (Hancock & Scholle, 1975).

Scrutiny of density shifts in well logs, as discussed above, reveals the likely presence of many more smaller sequences in the Chalk than can be observed in the seismic data. Likewise, the subcrops presented in Fig. 2.2 to Fig. 2.12 possibly vary because thin layers of chalk may be present that cannot be distinguished on the seismic data.

Throughout the Netherlands offshore the seismic response of the Chalk is predominantly characterised by parallel and continuous reflections with varying amplitude strength. This indicates that sediment accumulated at equal rates throughout the area and was not originating from, or growing into, a certain direction because this would have resulted in prograding seismic reflections (Macurda, 1997). This parallel configuration is also described in the Chalk of the Danish Central Graben (Nygaard et al. 1990; Andersen et al., 1990; Britze et al., 2000), Norwegian Central Graben (Bramwell et al, 1999) and the southern Netherlands (Gras & Geluk, 1999) confirming that settlement from suspension was the primary sedimentation process (Fontaine et al., 1987; Macurda, 1997). Locally, the parallel reflections are found to be discontinuous, possibly indicating low porosities (Britze et al., 2000).

Areas showing irregular or chaotic reflections are present near the inversion zones, especially along the Dutch Central Graben (in quadrants G and B). Chaotic reflections most probably indicate mass reworking of sediment. The geometry of such

disturbances does not resemble a classic slump or slide sheet, but might in fact be a stack of slumps as described by various authors (Watts et al., 1980; Hatton, 1986; Kennedy, 1987; Andersen et al., 1990). Chaotic reflections outline a large NNW–SSE trending channel, approximately 100 km long (inside the study area) and about 10–20 km wide, in lower Maastrichtian strata (sequence CK9) of the Schill Grund High–Ameland Block area (Fig 1.8). Similar channels, although much smaller, are found in the upper Maastrichtian sediments (sequence CK10) of the Cleaver Bank High (northern part of quadrant K) and Elbow Split High.

Reflection strength, or 'reflectivity', is another seismic facies criterium with which the Chalk can be classified. Reflectivity is found to be in most cases controlled by geological factors rather than seismic processing, and zones of high and low reflectivity in the Chalk often follow stratigraphical boundaries (Fig. 2.2 to Fig. 2.12). For example, strong amplitudes make up seismic sequence CK2 (Fig. 2.3), as well as the three upper sequences, CK9, CK10 and CK11 (Fig. 2.10, Fig. 2.11 and Fig. 2.12), throughout the study area. In most areas, the middle sequences show low reflectivity. Reflection strength also appears to follow geographical boundaries. In both the Schill Grund High–Ameland Block area (eastern part of quadrants G and M, quadrant N) and Cleaver Bank High (quadrants D, J and western part of quadrants K and E), the entire Chalk Group shows strong parallel and continuous reflections. In these areas the Chalk is very thick (more than 1000 m, Fig. 1.2) and the different seismic sequences are most clearly developed.

In the Chalk, reflection strength is primarily controlled by the magnitude of decametre scale porosity variations. Such porosity variations are visible in sonic and density logs where they give rise to a conspicuously 'serrated' log response. In the sonic log of G17-1 (Fig. 2.16), interval 'A' (encompassing CK3, CK4) shows very strong, 10–20 meter-scale, variations in acoustic slowness. The synthetic seismogram of this interval shows high-amplitude reflections that match those observed in the seismic reference section. Similar petrophysical characteristics are observed in sequences CK3 and CK4 in the well logs of, for instance, B17-2 and L5-1 ('A', Fig. 2.16), as well as F15-1 and K7-3 (Fig. 2.18 & Fig. 2.19). In contrast, interval 'B' in the sonic log of B17-2 (Fig. 2.16) shows only minor acoustic slowness variations throughout. The very low amplitudes of the reflections in the resulting synthetic seismogram mirror the low reflectivity facies of the seismic reference section.

Throughout the Netherlands offshore, abundant examples can be found of the relationship between porosity variations and reflectivity (Fig. 2.16). In most of the study area, the upper sequences of the Chalk, CK10 and CK11, are characterised by severe porosity variations (Fig. 2.18 & Fig. 2.19). Reflections are generally strong in these sequences (Fig. 2.11 & Fig. 2.12) and the synthetic seismograms indicate that these strong reflections are genuine, not multiples of the Top Chalk reflection.

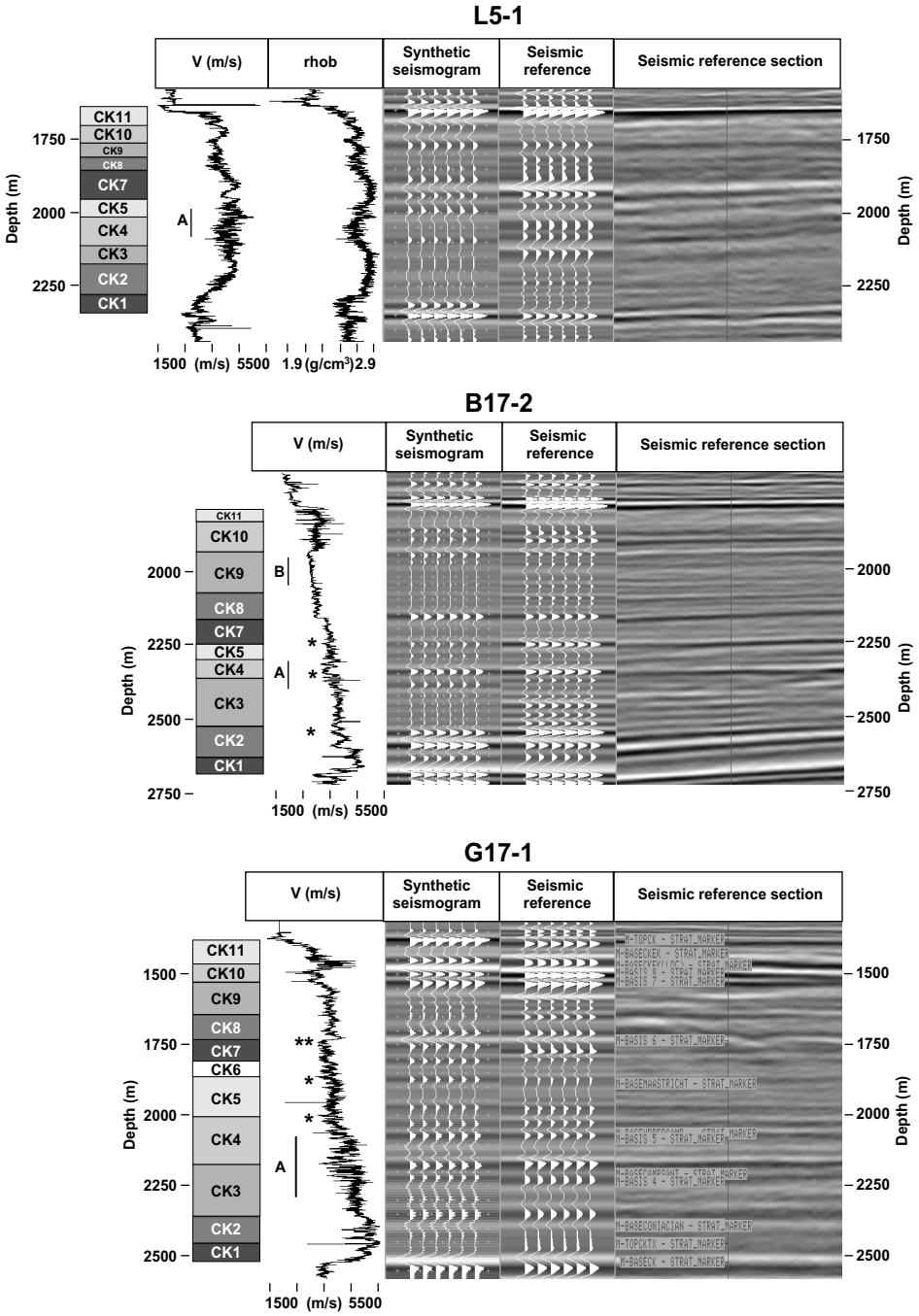
L5-1
V (m/s)
rhob
Synthetic seismogram
Seismic reference
Seismic reference section
CK11
CK10
CK9
CK8
CK7
CK5
CK4
CK3
CK2
CK1
A
Depth (m)
1750
2000
2250
1500 (m/s) 5500
1.9 (g/cm³) 2.9
B17-2
V (m/s)
Synthetic seismogram
Seismic reference
Seismic reference section
CK11
CK10
CK9
CK8
CK7
CK5
CK4
CK3
CK2
CK1
B
A
2000
2250
2500
2750
Depth (m)
1500 (m/s) 5500
G17-1
V (m/s)
Synthetic seismogram
Seismic reference
Seismic reference section
CK11
CK10
CK9
CK8
CK7
CK6
CK5
CK4
CK3
CK2
CK1
A
1500
1750
2000
2250
2500
Depth (m)
1500 (m/s) 5500
M-TOPCK - STRAT_MARKER
M-BASECKEK - STRAT_MARKER
M-BASECKVVIOC - STRAT_MARKER
M-BASIS 7 - STRAT_MARKER
M-BASIS 6 - STRAT_MARKER
M-BASEMAASTRICHT - STRAT_MARKER
M-BASIS 5 - STRAT_MARKER
M-BASIS 4 - STRAT_MARKER
M-BASECONTACTAN - STRAT_MARKER
M-TOPCKTX - STRAT_MARKER
M-BASECK - STRAT_MARKER

Figure 2.16 ***(facing page)*:** Synthetic seismograms of wells L5-1, B17-2 and G17-1. At these well locations the Chalk interval typically shows high amplitude, parallel and continuous reflections.

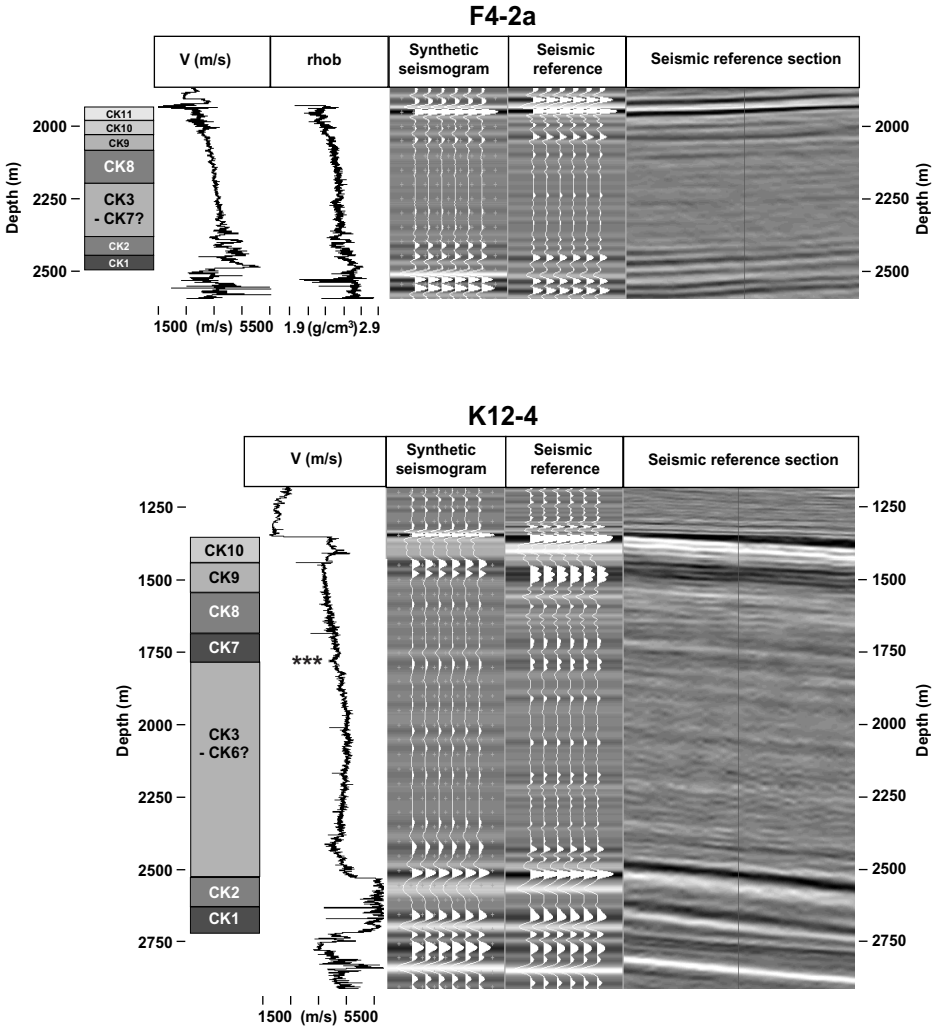

Figure 2.17: Synthetic seismograms of wells F4-2A and K12-4. Here the Chalk interval typically shows a low-amplitude, 'transparent' seismic facies, with the exception of the lower and upper two sequences.

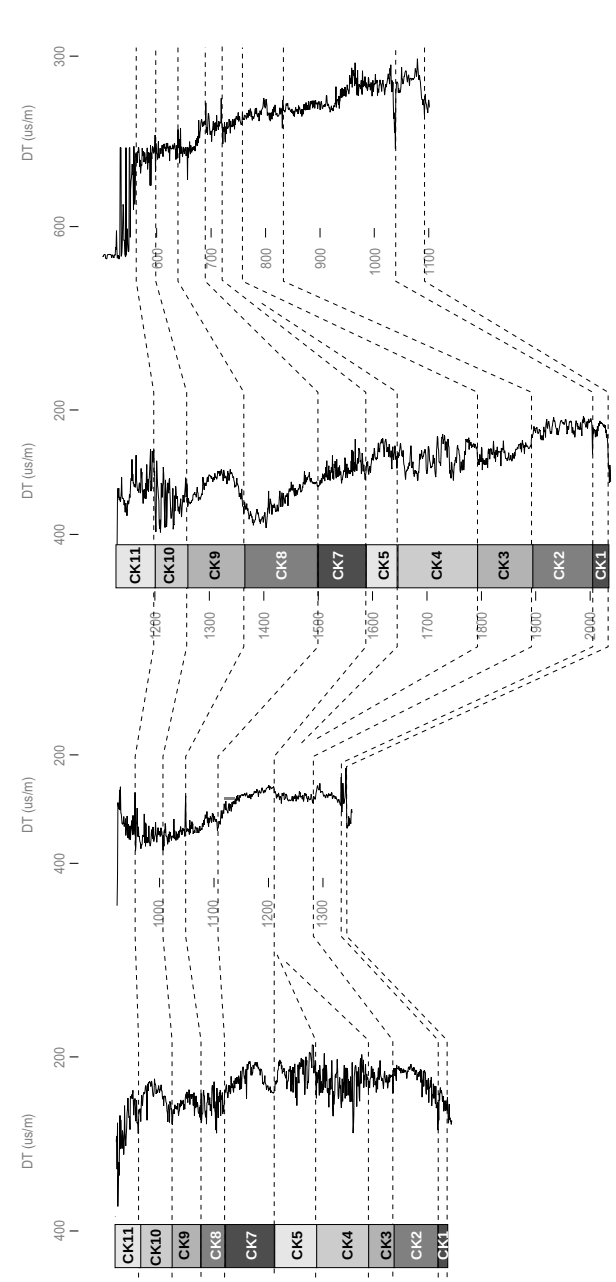

Figure 2.18: Sonic log profile of wells L5-1, P13-1, K7-3 and D15-1 (Fig. 2.1) indicating the eleven intra-Chalk seismic sequences as these have been tied to the well-database using synthetic seismograms.

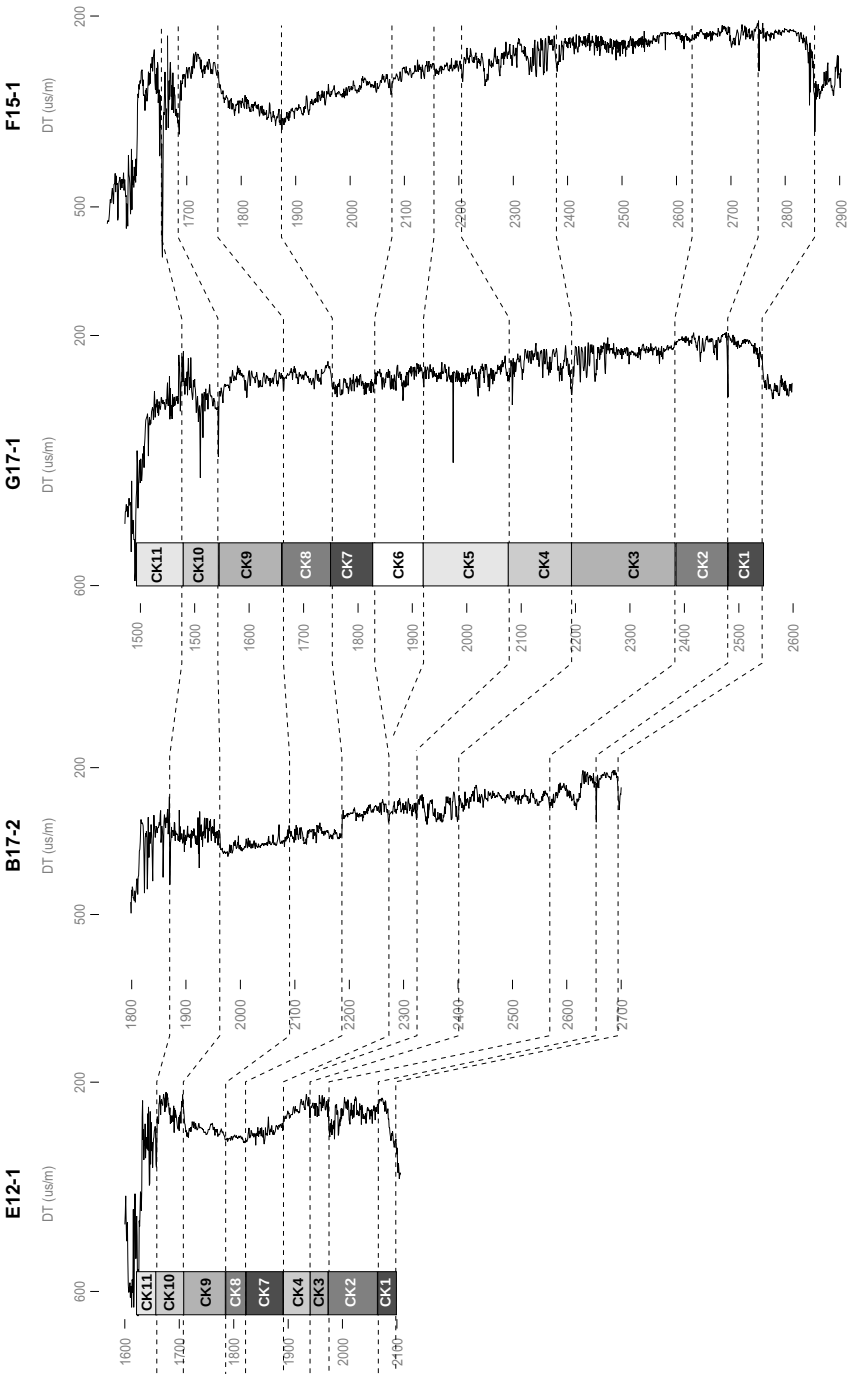

Figure 2.19: (Continued from Fig. 2.18) sonic log profile of wells E12-1, B17-2, G17-1 and F15-1 (Fig. 2.1).

A similar relation can be found between the log character of CK2 and the high-amplitude seismic facies of this sequence. In contrast, the middle sequences (CK3 through CK9) of, among others, wells F4-2A and K12-4 (Fig. 2.17) show small metre-scale variation in porosity, displaying instead very gentle porosity increases and decreases over hundreds of meters depth. The corresponding seismic sections show a transparent seismic facies. The quality of the synthetic seismograms in these logs is demonstrated by the fact that subtle changes in density, such as at level *** in K12-4, result in an equally subtle reflection in the seismic data.

The observed relation between the magnitude of porosity (density) variations and seismic reflection strength rules out the possibility that variations in reflectivity might represent seismic processing artefacts. However, it is important to note that in areas where strong lateral acoustic velocity variations occur over short distances, the image quality of post-stack migrated seismic data does deteriorate (Yilmaz, 1987). This effect accounts for the unclear (designated # in the seismic facies maps) seismic facies often encountered in the vicinity of salt diapirs. Britze et al. (2000) state that a direct relation exists in chalk between the amplitude and continuity of a reflection and the porosity of the rock, rather than the degree of porosity variations. This relation is such that high-amplitude, parallel and continuous reflections in seismic data are caused by porous chalk, while tight chalk is represented by low-amplitude, discontinuous reflections. However, such a relation cannot be identified in the present dataset. For instance, the high-amplitude interval 'A' of B17-2 (Fig. 2.16) has a lower average porosity (i.e. higher velocity) than the low-amplitude interval 'B' of the same log. Alternatively, Gras & Geluk (1999) suggested that high amplitudes observed in the top section of the Chalk in the southern Netherlands are caused by 'emerging surfaces', but lacked sufficient well log data to confirm this hypothesis.

2.4.2 Biostratigraphy

In the Danish offshore, where the Chalk Group forms an important reservoir rock and consequently a large biostratigraphical database is at hand, significant problems were described when dating seismic sequences (Andersen et al., 1990; Vejbæk & Andersen, 2002). Similar problems are also described by Herngreen et al. (1996). The two most important processes that have a detrimental effect on adequate age determinations such as used in this study are resedimentation and 'caving'. Resedimentation, which is a common feature of the Chalk in (syn-depositional) tectonically active areas such as the Central Graben (Scholle, 1977; Hatton, 1986; Kennedy, 1987), has the effect of introducing older sediment into younger layers, leading to an overestimation of the age of the sediment. Resedimentation, however, is difficult to prove. Only in wells in which consistently older ages are determined for each seismic sequence,

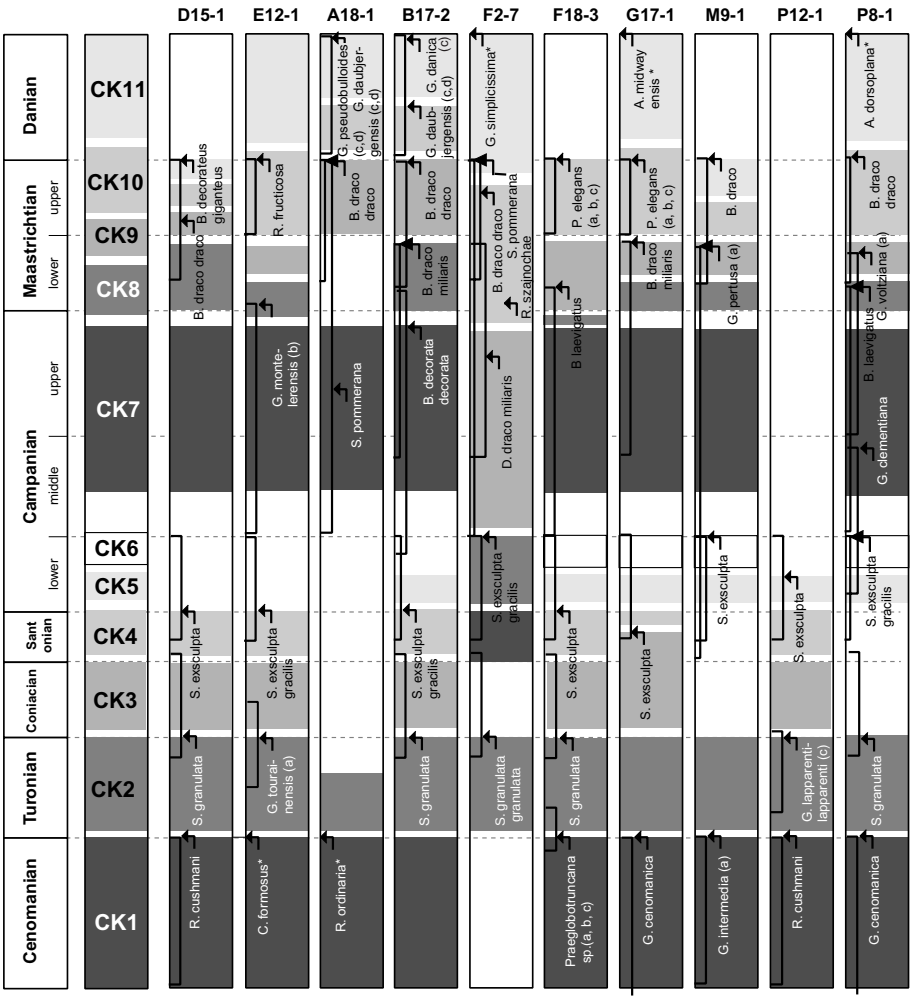

Figure 2.20: Overview of the biostratigraphical database used for age determination of seismic sequences in the present study. Age ranges were predominantly compiled from Hardenbol et al. (1998b) for Upper Cretaceous to lower Paleocene index species, as well as King et al. (1989; species marked 'a'), Sikora & Bergen (1999; species marked 'b') for Upper Cretaceous, Koch (1977; species marked 'c') for Upper Cretaceous to lower Paleocene and King (1989; species marked 'd') for lower Paleocene species. Of species marked ('*') the ages from the original biostratigraphic analysis were copied.

compared to other wells, can resedimentation be assumed. In the biostratigraphical dataset of the present study, F2-7 shows older ages for most of the seismic sequences (Fig. 2.20). As this well is located in the Dutch Central Graben, in an area where chaotic seismic reflections indicate massive sediment reworking, resedimentation offers the best explanation for these higher ages. Caving has the reverse effect and includes falling of rock material from shallower depths (and in the present case: younger ages) into the borehole during drilling, after which the caved rocks are brought up to the surfaces together with the older material. To mitigate the effect of caving, only last occurrences of the key foraminifera species were noted.

In Fig. 2.20, an overview is given of the foraminifera database on which the ages of the seismic sequences is based. In this overview, an arrow indicates the relative stratigraphic position of the last occurrence depth (LOD) of an index species within the seismic sequence in that well. Since the observed LOD in the well does not necessarily represent the regional LOD of a species, the entire age range was considered. Subsequent correlation was carried out under the assumption that the seismic sequences represent regional synchronous phases of chalk sedimentation, notwithstanding regional variations in the exact age of the oldest and youngest sediment within the sequence. Sequences without any LOD were correlated based on their stratigraphic position. In Fig. 2.20, sequence ages were preferably fitted to stratigraphic ages for simplicity, and unconformities separating subsequent sequences were assumed to represent short periods in time. Comparing Fig. 2.20 to the seismic maps and profiles, it is clear that the inferred periods of deposition of most sequences are often much longer than expected from their thickness, if a constant accumulation rate is assumed. It should be noted, therefore, that these periods represent ranges during which shorter periods of chalk deposition took place, as well as phases of non-deposition or erosion.

Following the definition of Van Adrichem Boogaert & Kouwe (1994), the top of the Cenomanian sequence CK1 is placed at the well log spike that represents the Plenus Marl Member (Fig. 2.18 & Fig. 2.19). Bergen & Sikora (1999) note that *Rotalipora cushmani*, which indicates the Cenomanian according to Koch (1977) and King et al. (1989), is very rare. However, this species is found in both wells P12-1 and D15-1, demonstrating its usefulness in identifying the Texel Formation in the study area. *Praeglobotruncana sp.* extends into the Turonian (Koch, 1977; King et al., 1989; Bergen & Sikora, 1999), but is thought to represent the Cenomanian in F18-3 based on the position of the Plenus Marl well log marker. This marker was also used to determine the age of CK1 in B17-2, where no key species were found. In wells D15-1, B17-2, F18-3 and P8-1, *Stensioina granulata* is not specified (i.e. *S. g. granulata*, *S. g. polonica* or other). It is important to note that the LOD of *S. granulata* in these wells may represent an age ranging from late Turonian

(*S. g. humilis*) to early Santonian (*S. g. granulata*; Kock, 1977; King et al., 1989; Bergen & Sikora, 1999). Furthermore, *S. g. polonica*, of early to middle Santonian age according to Koch (1977) and King et al. (1989), is specifically identified as a 'misleading index' by Sikora & Bergen (1999), based on its diachronity even within the Valhall study area. This may also explain the relatively high age of the top of CK3 in F18-3. Similarly, *Stensioina exsculpta* is not specified (i.e. *S. e. exsculpta* or *S. e. gracilis*) in wells D15-1, F18-3, G17-1, M9-1 and P12-1. However, Sikora & Bergen (1999) state that these subspecies are commonly associated and both extend into the middle Campanian.

The onset of CK7 post-dates the last occurrence of the benthic foraminifera *S. exsculpta spp.* and *S. exsculpta gracilis* (the latest occurrence is at the top of CK6 in M9-1 and P8-1). As the onset of CK7 also post-dates the strongest uplift and erosion phase in the study area, it is presumable that deposition did not start until the middle Campanian. The occurrence of *Stensioina pommerana* in the lower section of CK7 in well A18-1, suggests that this represents an early occurrence of this early Campanian to late Maastrichtian benthic foraminifera (Hardenbol et al., 1998b). In F2-7, the occurrence of *Bolivinoides draco miliaris* is probably not younger than late Campanian because of the shallower LDO of *Reussella szajnochae*, which indicates the end of the Campanian (Hardenbol et al., 1998b). In M9-1, at the top of CK1, *Bolivinoides draco* remains unspecified (i.e. *B. d. draco* or *B. d. miliaris*) but its stratigraphic position suggests that this represents the late Maastrichtian (*B. d. draco*; Hardenbol et al., 1998b).

2.5 Conclusions

- Based on the identification and mapping of unconformities throughout a regional seismic grid, the Upper Cretaceous to lower Paleocene Chalk Group of the Netherlands offshore was subdivided into eleven seismic sequences.

- The seismic sequences represent the Cenomanian (CK1), Turonian (CK2), Coniacian (CK3), Santonian (CK4), lower Campanian (CK5; CK6), middle to upper Campanian (CK7), lower Maastrichtian (CK8), lower to upper Maastrichtian (CK9), upper Maastrichtian to lower Danian (CK10) and Danian (CK11).

- With a few exceptions, the present areal extent of all seismic sequences of the Chalk is controlled by erosion by overlying sequences.

- The seismic facies of the Chalk is characterised by parallel and continuous reflections, of varying amplitudes. Locally, chaotic reflections are encountered

which indicate massive reworking of sediment.

- Reflection strength is controlled by the magnitude of decametre-scale variations in density (i.e. porosity).
- Two mega-sequences can be recognised in the study area, the first includes sequences CK1 to CK6, it is separated from the second mega-sequence (including CK7 to CK11) by a large uplift and erosion phase that predates the deposition of CK7.

Chapter 3

Cenomanian to Danian tectono-sedimentary evolution of the Netherlands North Sea area

The sediments of the Chalk Group in the Netherlands offshore were deposited on a sea floor that consisted of several intra-basinal 'highs' and 'lows' of early Mesozoic age. Following rifting in the Jurassic, the area subsided at the beginning of the Late Cretaceous. The coinciding sea level rise resulted in the inundation of large landmasses and cessation of detrital influx. The clear-water conditions that followed favoured the growth of calcareous algae, leading to the accumulation of chalk on the sea floor. Most of the study area subsided rapidly during the early stages of Chalk deposition, leading to thick accumulations of sediment. At the beginning of the middle Campanian, prior to the deposition of sequence CK7, compression led to uplift of most of the early Mesozoic lows, initiating the inversion of the Broad Fourteens Basin and Dutch Central Graben. Several uplift phases took place in the Campanian to Danian, giving rise to reworking of chalk. A final uplift phase after the Danian concluded the deposition of the Chalk Group.

3.1 Introduction

At the onset of Chalk deposition, the sea floor of the North Sea area was made up of an amalgamation of intra-basinal highs and lows. These structural elements possessed a dominant NW–SE orientation that stemmed from the old Caledonian and Variscan lineaments. The disintegration of Pangea was accompanied by rifting pulses during the Triassic ('Hardegsen' and 'Early Kimmerian' phases), the Jurassic ('Mid Kimmerian' phase) and the 'Late Kimmerian' phase at the Jurassic–Cretaceous transition. During the latter phase rifting accelerated, predominantly affecting the Central and Viking Graben, but gradually diminished afterwards. As a result, Variscan faults were reactivated as dextral wrench faults and NW–SE oriented wrench basins were formed. Rifting ceased during the Early Cretaceous and the area started to subside regionally (Fig. 1.4; Van Hoorn, 1987; Van Wijhe, 1987; Vejbæk & Andersen, 1987, 2002; Ziegler, 1990; Dronkers & Mrozek, 1991). At the same time, a eustatic sea-level rise started, which flooded large areas of land and strongly reducing the influx of detritus to the basin (Ziegler, 1990). Calcareous algae flourished due to the ensuing clear-water conditions, leaving thick layers of calcitic remains on the sea floor (Hancock, 1975; Kennedy, 1987).

The deposition of the Chalk Group coincided with the convergence of the African and Eurasian plates, as well as the opening of the Northern Atlantic Ocean. This led to northward compression in the North Sea area by which movement along early Mesozoic faults was reversed and intra-basinal lows were inverted (Van Hoorn, 1987; Van Wijhe, 1987; Vejbæk & Andersen, 1987, 2002; Ziegler, 1990; Dronkers & Mrozek, 1991). The most important of these compressional phases occurred during the early to middle Turonian, during the early Campanian and late Campanian to early Maastrichtian (jointly referred to as the 'Sub-Hercynian' phase) and at the start of the Tertiary, during the 'Laramide' phase (Ziegler, 1990; Huyghe & Mugnier, 1994; De Jager, 2003). In the inverted areas, the Chalk succession was deeply eroded or was entirely removed. Locally, the sediment became subject to reworking in the form of turbidites, slumps, slide sheets and debris-flow deposits (Hancock, 1975; Watts et al., 1980; Schatzinger et al., 1985; Kennedy, 1987; Farmer & Barkved, 1999). An important feature often observed along inverted structures are 'marginal throughs', which form by subsidence of former graben shoulders. In these marginal throughs thick successions of syn-tectonic sediments accumulate, often provided by the inverting basin in the form of allochthonous chalk (Voigt, 1962; Kockel, 2003).

Throughout the North Sea Basin, the presence of Upper Permian (Zechstein) salt resulted, passively and actively, in the local modification of the tectonic configuration. Passively, salt absorbs stresses reducing the magnitude of faulting in the overburden. Actively, the salt reacts to overburden by diapirism, often triggered by

the activity of basement faults. This results in the formation of salt diapirs and salt swells, usually with associated rim synclines (Dronkers & Mrozek, 1991; Koyi & Petersen, 1993; Remmelts, 1995; Buchanan et al., 1996; Davison et al., 2000a; 2000b; Scheck et al., 2003).

In the Netherlands offshore area, all Mesozoic basins were inverted to some extent. The Broad Fourteens Basin and Dutch Central Graben (Fig. 3.1), where uplift locally resulted in the removal of the entire Chalk succession, were the most important of these (Van Wijhe, 1987; Dronkers & Mrozek, 1991; De Jager, 2003). The magnitude of inversion was largest in the Broad Fourteens Basin. Uplift in this area has been estimated to be as high as 3500 m in the central part of the basin (Dronkers & Mrozek, 1991; Hooper et al., 1995). Recently, however, De Jager (2003) reduced this estimate to 1500 to 2000 m. Basin inversion of the Dutch Central Graben was less because of the presence of a thick sequence of Zechstein salt, which accommodated uplift partly by plastic deformation. As a result, around 700 m of uplift occurred as broad, gently folding anticlines, severely thinning and removing the Chalk (Heybroek, 1987; Dronkers & Mrozek, 1991; Buchanan et al., 1996; De Jager, 2003). In the Netherlands mainland area, the Central and West Netherlands Basins and Roer Valley Graben were inverted (Fig. 1.8; Heybroek, 1974; Gras, 1995).

The exact timing and mechanisms of uplift phases, as part of the Late Cretaceous to Paleogene geodynamic evolution of the North Sea, remains the subject of ongoing investigations (Van Hoorn, 1987; Vejbæk & Andersen, 1987, 2002; Huyghe & Mugnier, 1994; Clausen & Hansen, 2000; De Jager, 2003). As a practical implication, such investigations help to understand the velocity/depth relationships needed for time-depth conversion of seismic surveys, the timing of hydrocarbon generation and migration, and the mechanisms controlling the formation of reservoirs and traps (Dronkers & Mrozek, 1991). The seismic sequences of the Chalk Group were mapped and classified to improve the stratigraphic subdivision of this interval in the Dutch offshore (Chapter 2). The results also enable the study of timing and extent of vertical movements during the Late Cretaceous to Early Paleocene, as well as the interplay of tectonism and sedimentation. Therefore, this chapter describes and discusses the tectono-sedimentary development of the Chalk Group based on the results of the regional seismic interpretation outlined in Chapter 2.

3.2 Structural elements and basin architecture

Figure 3.1 shows the Base Chalk Group reflection, flattened at the top of the Chalk, viewed downwards from the southeast, indicating the present day thickness of the Chalk Group in the study area. Furthermore, the map outlines the total amount of syn and post-depositional vertical movement; with the Chalk being thickest in

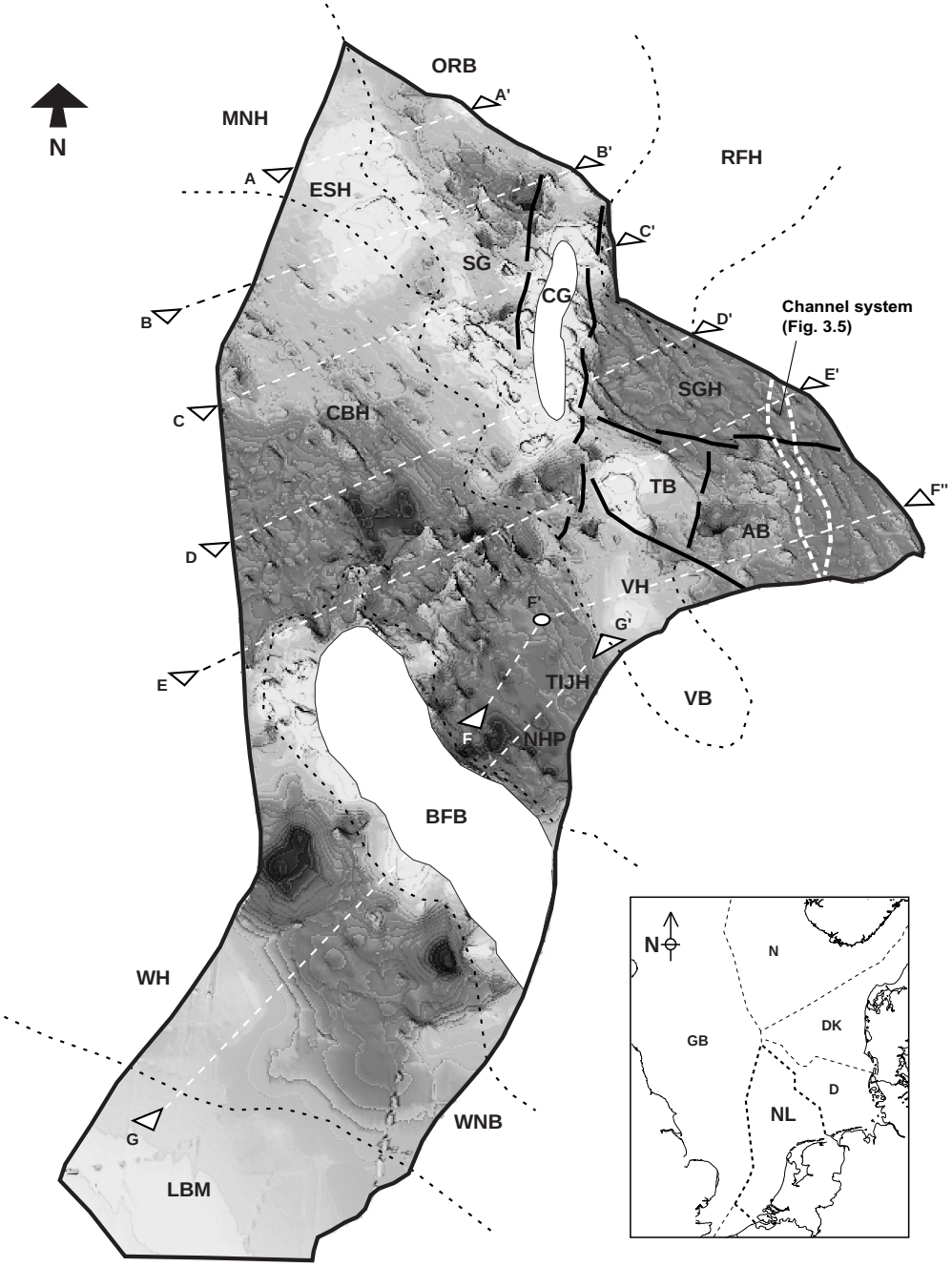
N
ORB
MNH
RFH
ESH
SG
CG
CBH
SGH
TB
AB
VH
TIJH
VB
NHP
BFB
WH
WNB
LBM
A
A'
B
B'
C
C'
D
D'
E
E'
F
F'
F''
G
G'
Channel system
(Fig. 3.5)
N
N
GB
DK
D
NL

subsided areas and thinnest where uplift took place (Fig. 3.2). Salt diapirs can be seen throughout the area. The internal configuration of the Chalk interval is represented by profiles A through G (Fig. 3.3 & Fig. 3.4), all of which are also flattened at Top Chalk level to designate syn-depositionary vertical movements.

In Fig. 3.1 and Fig. 3.4, the early Mesozoic structural elements (Fig. 1.8) are indicated. The names of these structures are derived from their original geometry during the Late Triassic to Early Cretaceous. The extent to which the compressional tectonic regime overturned these structures is made evident by the thickness distribution of the Chalk, with the Chalk being thickest on former highs and thinnest on former basins. Based on thickness distribution, a regional subdivision into several, roughly NW–SE trending, Chalk provinces can be made (Fig. 3.1 & 3.2). These Chalk provinces are made up of one or more Mesozoic structural elements, and are discussed from south to north in the sections below.

3.2.1 Province A (West Netherlands Basin–Winterton High–London-Brabant Massif)

The southernmost part of the study area lies south of the Broad Fourteens Basin (BFB) and encompasses the westernmost part of the West Netherlands Basin (WNB), the eastern tip of the Winterton High (WH), as well as the northern flank of the London-Brabant Massif (LBM, Fig. 3.1). The London-Brabant Massif was subareally exposed at the onset of Chalk deposition (Ziegler, 1990; Fig. 1.7). The data used in the present study shows onlap of Cenomanian to Santonian strata to the northern flank of the London-Brabant Massif, which was overstepped in the early Campanian by sequence CK6 (Fig. 3.4).

Figure 3.1 ***(facing page)*****:** Base Chalk surface flattened at Top Chalk level (i.e. TWT isopach of the Chalk Group), viewed from the south. Indicated by white dashed lines are the locations of profiles A–A' to G–G' of Fig. 3.4. The geometry of this surface outlines the vertical movement that occurred during deposition of the Chalk Group. Compression during the Late Cretaceous and Paleogene inverted the older structures, leading to uplift of former basins such as the Central Graben (CG) and Broad Fourteens Basin (BFB), and subsidence of former highs such as the southern Cleaver Bank High (CBH), Texel-IJsselmeer High (TIJH), North Holland Platform (NHP) and Schill Grund High (SGH). Other structural elements include the London-Brabant Massif (LBM), Winterton High (WH), West Netherlands Basin (WNB), Vlieland Basin (VB), Vlieland High (VH), Terschelling Basin (TB), Ameland Block (AB), Rynkøbing-Fyn High (RFH), Step Graben (SG), Outer Rough Basin (ORB), Elbow Split High (ESH), and Mid North Sea High (MNH). **See Fig. 3.1 (page 154) in Appendix - Colour plates for a colour version of this figure.**

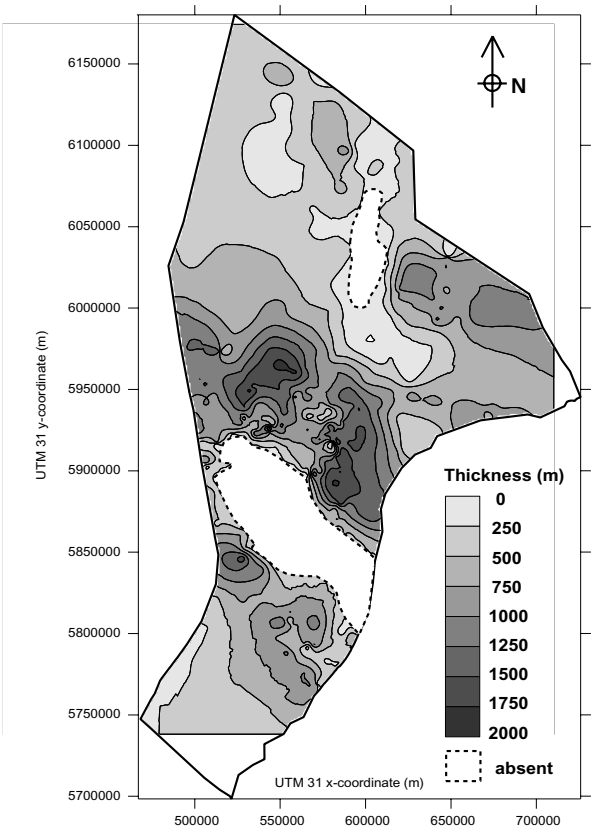

Figure 3.2: Thickness of the Chalk Group in the Netherlands offshore. This map was compiled from true vertical depth (TVD) data of the upper and lower boundary of the Chalk Group of 869 released wells from the database of TNO-NITG (Section 5.3.2)

A broad south-westwardly tilted marginal through, consisting largely of Cenomanian to lower Campanian sediment (sequences CK1 to CK6), forms the transition with the Broad Fourteens Basin in the north. The Chalk succession was most likely very thick in this marginal through, prior to the uplift of the Broad Fourteens Basin. The geometry of this area is testament to the amount of uplift this basin experienced during the Maastrichtian and Danian. Nevertheless, no evidence for seismic-scale reworking is present in the P, Q and S-quadrants.

3.2.2 Province B (Broad Fourteens Basin)

The Broad Fourteens Basin (BFB, Fig. 3.1) developed during the middle Triassic and was inverted in the Late Cretaceous and Paleogene (Van Wijhe, 1987; Ziegler, 1990; Hooper et al., 1995; De Jager, 2003). The amount of uplift of this area is the highest

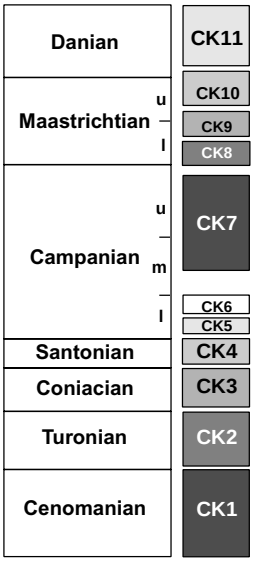

Figure 3.3: Overview of seismic sequences mapped in the Chalk Group in the Netherlands North Sea area (Chapter 2)

of all inverted basins in the study area. The absence of a thick succession of Zechstein salt in the southern part of the basin, which in the Central Graben accommodated much of the compression, partly led to this dramatic uplift (Dronkers & Mrozek, 1991). Uplift of the central part of the Broad Fourteens Basin started in the Albian. Inversion of the basin margins probably began later, during the early Maastrichtian (Hooper et al., 1995). Since the Chalk is missing in most of the Broad Fourteens Basin this area does not play an important role in the present study. Furthermore, the internal reflection configuration of the Chalk pockets along the basin boundaries could not be studied due to low seismic quality.

3.2.3 Province C (Texel-IJsselmeer High–Noord Holland Platform)

This Chalk province forms the eastern part of the northern marginal through of the Broad Fourteens Basin and encompasses the northwestern sections of the Texel-IJsselmeer High (TIJH), the Noord Holland Platform (NHP) and the northwesterly connection to the Cleaver Bank High (CBH, Fig. 3.1). The Texel-IJsselmeer High came into being in the middle Jurassic, but was only slightly affected by inversion tectonics during the Late Cretaceous and Paleogene (Van Wijhe, 1987). The transition to the Vlieland Basin in the east is gradual, whilst the Broad Fourteens Basin to the east is separated by large normal faults. To the west, a shallow zone separates

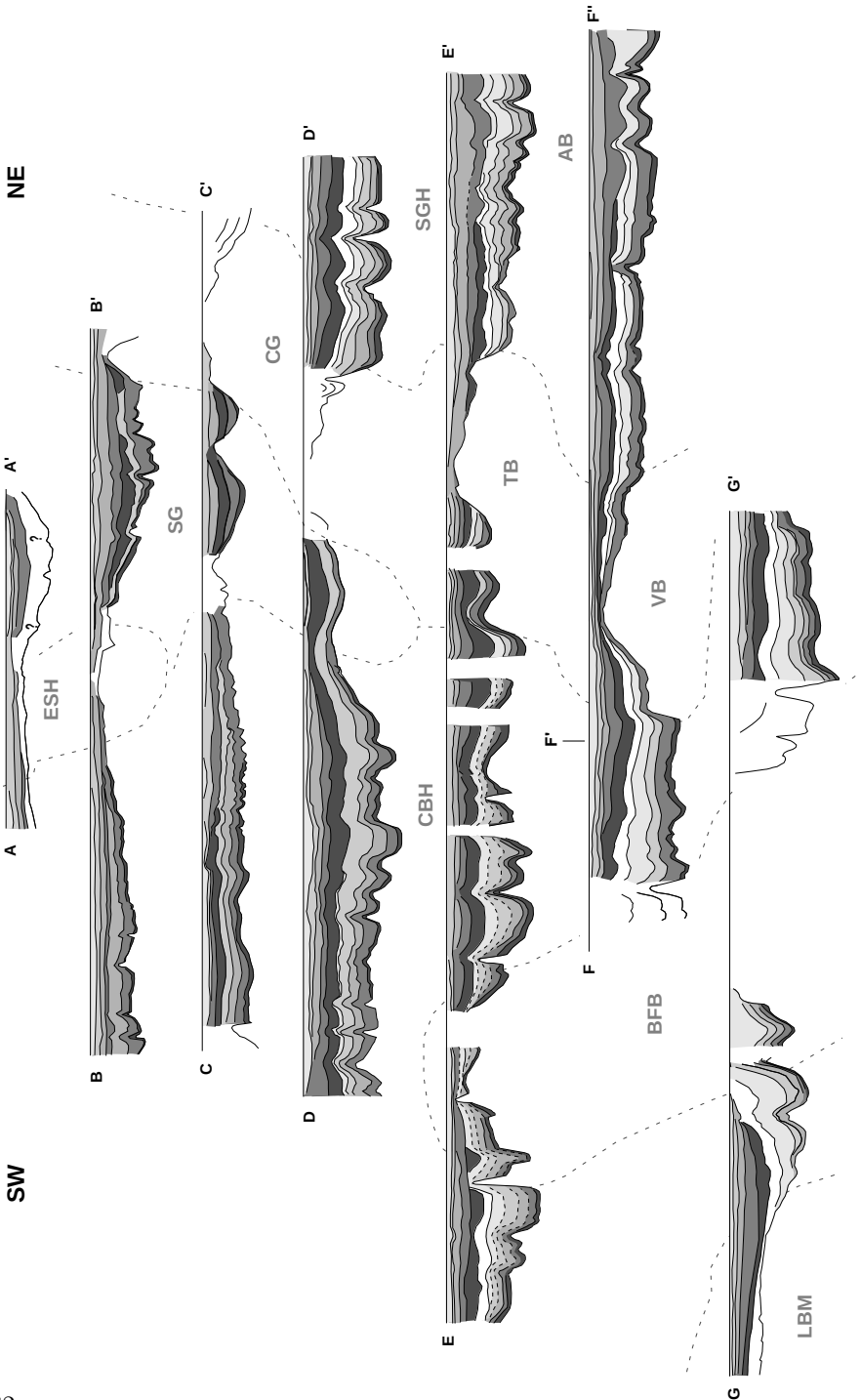
NE
SW
A
A'
B
B'
C
C'
D
D'
E
E'
F
F'
F''
G
G'
ESH
SG
CG
SGH
CBH
TB
AB
VB
BFB
LBM
?
?

the southern Cleaver Bank High. The Chalk is thick in this area, and resembles the Cleaver Bank High and Schill Grund High in seismic facies character.

3.2.4 Province D (Cleaver Bank High)

The Cleaver Bank High (CBH, Fig. 3.1) occupies the western Dutch offshore (E, K and western L-quadrants) and extends westward into the British sector. The Cleaver Bank High was deeply eroded during the Late Jurassic–Early Cretaceous. When the eustatic sea level rose during the Hauterivian–Barremian, the area was gradually inundated and deposition of siliciclastic sediment began. The area gradually subsided throughout the Cretaceous (Ziegler, 1990; Oudmayer & De Jager, 1993).

Presently, the Chalk succession is thickest (Fig. 3.2) in the south of the Cleaver Bank High (K-quadrant), thinning northwards. This area probably represents the western part of the northern Broad Fourteens Basin marginal through. The area subsided rapidly in Coniacian to early Campanian times, during deposition of CK3 and CK4 (Fig. 3.4). Furthermore, a broad SSE-wards tilting of the entire Cleaver Bank High took place during the early Campanian just before the deposition of sequence CK7 (Fig. 2.14; Fig. 3.4). During the early Maastrichtian, the southern part of the Cleaver Bank High again subsided rapidly, resulting in the increased thickness of sequences CK8 and CK9 and onlap onto the 'hinge' zone. This hinge zone underwent a last short uplift phase at the beginning of the Danian, prior to the deposition of CK11, (Fig. 2.14). The Chalk sequence in the Cleaver Bank High is autochthonous without any evidence of seismic-scale sediment reworking.

3.2.5 Province E (Terschelling Basin–Vlieland High & Basin)

The Terschelling Basin (TB), Vlieland High (VH), Vlieland Basin (VB, Fig. 3.1) and Lauwerszee Trough (outside study area) form the en-echelon connection between the Central Graben in the north-west, Lower Saxony Basin in the south-east, and line up along the Variscan trend (Herngreen et al., 1991). As the Central Graben and Lower Saxony Basins, both Terschelling Basin and Vlieland Basin were inverted

Figure 3.4 ***(facing page)*****:** Profiles A–A' to G–G' of the Chalk Group, flattened at top Chalk level. The Mesozoic structural elements are indicated in grey. Compression during deposition of the Chalk led to uplift of previous basins, most markedly the Broad Fourteens Basin and Central Graben. Subsidence and accumulation of a thick Chalk interval occurred in former highs, such as the southern Cleaver Bank High and Schill Grund High. See Fig. 3.1 for location of the profiles and explanation of the used abbreviations and Fig. 3.2 for greyscale code of the seismic sequences.

during deposition of the Chalk (Fig. 3.1).

The Terschelling Basin moved upwards sometime before the early Campanian, prior to the deposition of CK7. The thickness of the Chalk Group on top of the inverted basin is about 200 m. The Terschelling Basin shows an asymmetrical E–W profile that is similar to the southernmost part of Central Graben and features a discrete normal fault zone to the east, while to the west a more gradual, ramp-like, transition zone is present (Fig. 3.4). The Rifgronden Fault Zone that also separates the Schill Grund High and Ameland Block bound the basin to the north. The north-eastern section of the Hantum Fault Zone in the south separates the Terschelling Basin from the Vlieland Basin/High.

The Vlieland Basin displays a more gentle dome-shaped E–W profile and experienced intermittent uplift during the Coniacian to early Maastrichtian. The slow and continuous nature of the uplift is underlined by the parallel and continuous seismic reflections, which indicate exclusively pelagic sedimentation over the Vlieland Basin. On the western flank of the structure, the earliest sequence of the Chalk Group (CK1, Cenomanian) was found to have filled up pre-existing WNW–ESE trending channels that are about 1–2 km wide and over 10 km long.

3.2.6 Province F (Dutch Central Graben)

The NS-trending Dutch Central Graben (CG, Fig. 3.1) forms the southern part of the North Sea rift system that originated in the Early Triassic. The graben subsided rapidly during Triassic and Jurassic times, leading to the accumulation of a thick siliciclastic sequence (Heybroek, 1975; Van Wijhe, 1987; Ziegler, 1990). Tectonic inversion during the Late Cretaceous and Paleogene resulted in the removal of 750 m of sediment (Dronkers & Mrozek, 1991).

The Chalk succession is usually thin throughout the Dutch Central Graben, but modification of the basin floor geometry by salt diapirs locally resulted in an interval as thick as 450 m. The Chalk is absent in the southern part of the graben, in an area along the inversion axis (Fig. 3.1). A zone of discontinuous, very pronounced, normal faults bounds the Dutch Central Graben to the east. The western boundary is more subtle. Small normal faults separate the Dutch Central Graben from the Step Graben in the north. In the south, a westward dipping ramp-like transition zone forms the boundary between these areas (Fig. 2). The Central Graben boundary faults often served as triggers for diapirism of Zechstein salt (Remmelts, 1995). The marked vertical movements of the Dutch Central Graben during deposition of the Chalk Group led to massive reworking. The complex interplay of tectonism and sedimentation is discussed in more detail in Section 4.

3.2.7 Province G (Step Graben)

The Step Graben (SG, Fig. 3.1) forms a transition zone in which the maximum subsidence of the Central Graben to the west was accompanied by intermediate fault blocks, stepping down from the Cleaver Bank High in the east (Heybroek, 1975).

The Chalk succession is thickest in the centre of the Step Graben (about 800 m in the north-western part of the F-quadrant), thinning towards the edges. An uplift phase at the beginning of the Maastrichtian, prior to the deposition of CK8, resulted in the southward tilting of the area and erosion of older sediment in the north (A and B-quadrants). Subsequently, the central part of the Step Graben subsided rapidly and the area became partly filled with reworked sediment from the Central Graben. The south (south-western F-quadrant) was uplifted at a much later stage, during or after the Danian. Large normal faults form the boundary with the Dutch Central Graben to the west. To the east, the southeastward extension of the Elbow Split High, mentioned in the previous section, forms the transition with the Cleaver Bank High.

3.2.8 Province H (Elbow Split High–Outer Rough Basin)

The northward thinning of the Chalk interval in the Cleaver Bank High is continued into the northernmost area of the Dutch offshore, in the area encompassing the Elbow Split High (ESH) and the southern part of the Outer Rough Basin (ORB, Fig. 3.1). Here, the Chalk interval is 250–500 m thick (Fig. 3.2). Most of the Chalk succession is of Maastrichtian to Danian age (CK9–CK11), with a thin older layer of undetermined age below an angular unconformity (Fig. 3.4). The extension of the Elbow Split High towards the southeast forms the separating ridge between the Cleaver Bank High to the west and Step Graben to the east. This ridge was uplifted during several stages in the Maastrichtian and Danian. However, no seismic scale reworking of chalk occurred in this area.

3.2.9 Province I (Schill Grund High–Ameland Block)

Like the Cleaver Bank High, the Schill Grund High (SGH) and Ameland Block (AB, Fig. 3.1) formed emergent platforms throughout the Jurassic and earliest Cretaceous. The areas were flooded during the Early Cretaceous and subsequent gradual subsidence enabled the deposition of a thick succession of Chalk (Heybroek, 1975; Van Wijhe, 1987; Ziegler, 1990).

The Schill Grund High and Ameland Block are separated by the NW–SE trending Rifgronden Fault Zone (Fig. 3.1). Movement along this fault zone resulted in

the marked uplift of the Ameland Block during the early Campanian, prior to the deposition of CK7. The Chalk Group is up to 1200 m thick in the Schill Grund High and the absence of thickness variations of seismic sequences indicate a constant subsidence of this area. The Schill Grund High and Ameland Block subsided at the same rate from middle Campanian times on. However, the southeast (eastern part of quadrant M, quadrant N) was shortly uplifted during the late Campanian, prior to the deposition of sequence CK8. This uplift pulse was followed by rapid subsidence in the Maastrichtian. Like in the Cleaver Bank High, the Chalk sequence in the Schill Grund High and Ameland Block province is autochthonous with no evidence of seismic-scale sediment reworking.

As a unique feature in the study area, a large N–S trending channel system was active in the eastern part of the Ameland Block during the late Maastrichtian and possibly also the Danian. This system consists of at least two separate channels that are about 500 m wide and 100 m deep (Fig. 3.5). Each of these structures in turn appear to consist of several channel fills stacked on top of each other, suggesting migration of the channel path through time. The channels seem to be controlled by faults in some cases. Furthermore, the often chaotic seismic reflection configuration indicates extensive sediment reworking, possibly of the channel levees.

3.3 Cenomanian to Danian evolution of the Netherlands North Sea area

A schematic overview of the Cenomanian to Danian evolution of the Netherlands is given in Fig. 3.6. The deposition of chalk in the area started in the Cenomanian, following a renewed eustatic sea level rise in the Albian. The London-Brabant Massif still stood above water during this period. Pelagic sedimentation of sequence CK 1 filled in sea floor topography lows, lapping onto the emergent areas. At the end of the Cenomanian, anoxic bottom conditions led to the deposition of the organic material-rich Plenus Marl (Van Adrichem Boogaert & Kouwe, 1994).

Ongoing sea level rise during the Turonian, accompanying the deposition of CK2, resulted in the flooding of the Vlieland High and Terschelling Basin. The southern coast of the Chalk sea moved further towards the south as the gently dipping northern flank of the London Brabant Massif was steadily flooded. The southern Ameland Block subsided rapidly, as did the northern and southern Broad Fourteens Basin marginal throughs. The northern Step Graben, possibly in conjunction with the adjacent Dutch Central Graben, witnessed similar subsidence rates. Subsidence continued during the Coniacian and Santonian, allowing the formation of sequences CK3 and CK4. During this period, the Vlieland Basin and Terschelling Basin, as

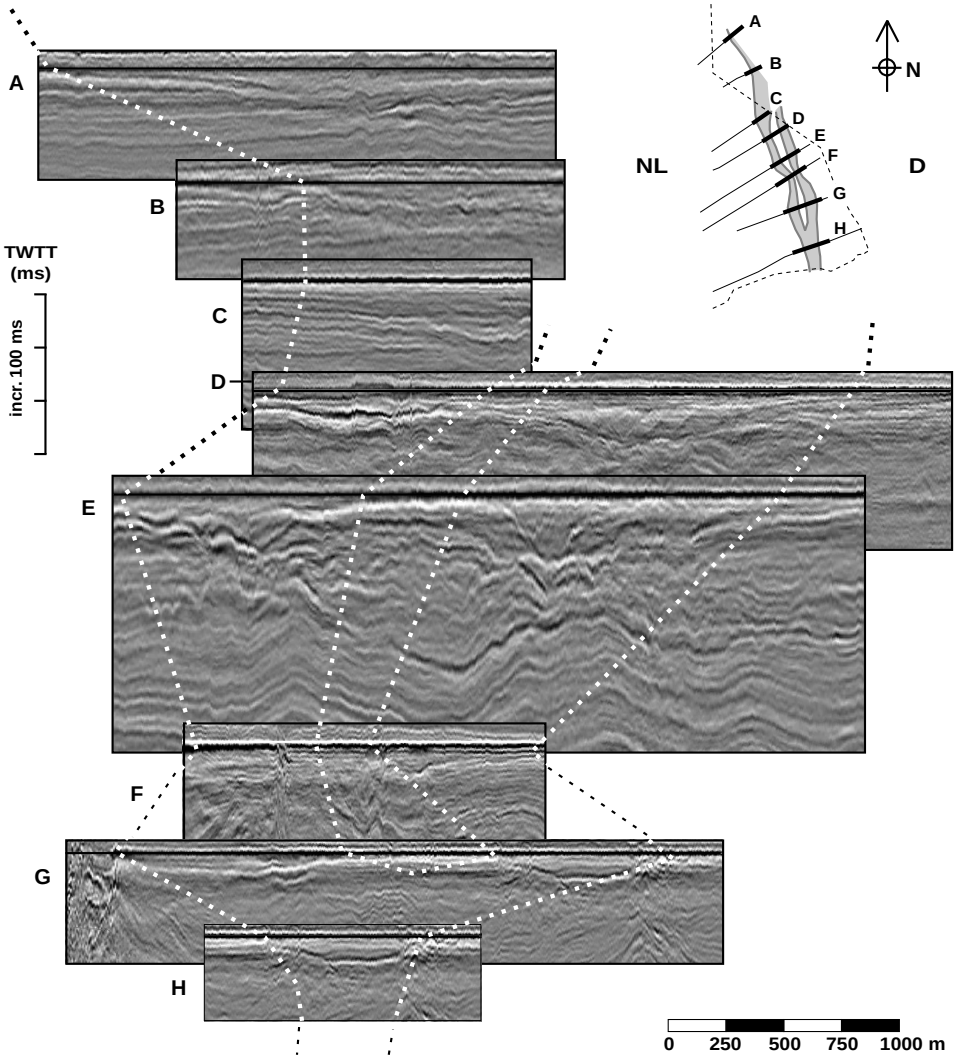

Figure 3.5: Fence diagram of the N–S trending channel system in the Maastrichtian and Danian chalk of the Schill Grund High and Ameland Block, in the westernmost part of the study area. Seismic section are flattened at the top Chalk level.

well as the southern parts of the adjacent Dutch Central Graben and Step Graben, already witnessed uplift.

In early Campanian times, during deposition of sequences CK5 and CK6, the entire southern and eastern part of the Netherlands North Sea area subsided rapidly. This included the southern Cleaver Bank High, Schill Grund High and Ameland Block. The Vlieland High, Terschelling Basin and southern Step Graben rose during this period. The northern flank of the London-Brabant Massif was finally overstepped at the end of the early Campanian.

At the onset of the middle Campanian, prior to deposition of sequence CK7, an important uplift and erosion phase took place that affected most of the study area. During this phase, The Cleaver Bank High tilted to the south (Fig. 2.14) and the Ameland Block suddenly rose with movement along the Rifgronden Fault Zone (Fig. 2.15). The Broad Fourteens Basin started rising during this period. In the north of the study area, the Central Graben, Step Graben and Elbow Split High were uplifted.

At the end of the Campanian, prior to deposition of sequence CK8, uplift continued in most of the Netherlands North Sea. The Central Graben continued to move upwards, as did the Step Graben, Elbow Split High and northern Cleaver Bank High. Upwarping of the Broad Fourteens Basin increased in intensity. The eastern part of the Ameland Block was subject to a short and very pronounced uplift pulse.

In the Maastrichtian, during deposition of CK8 and CK9, the Ameland Block subsided rapidly. At the beginning of this period the inverted Terschelling Basin was overstepped. A N–S oriented channel system developed in the Schill Grund High and Ameland Block area during this period. The Maastrichtian period, including deposition of CK10, was a relatively stable period in most of the study area. The Broad Fourteens Basin and Central Graben continued to move up. Minor uplift occurs in the Vlieland and Elbow Split High.

The final stage of Chalk deposition in the study area (sequence CK11) was accompanied by renewed inversion of the Broad Fourteens Basin as well as the Dutch Central Graben. As a result, large allochthonous bodies developed in Maastrichtian sediment in this area. The Elbow Split High, Terschelling Basin, parts of the Cleaver Bank High and the Ameland Block were uplifted to a lesser extent. Compression in the North Sea area ended after the Danian. Thermal relaxation during this period resulted in the rapid subsidence of the North Sea area and accumulation of siliciclastic sediments (Clarke, 1973; Clausen & Huuse, 1999; Huuse, 1999).

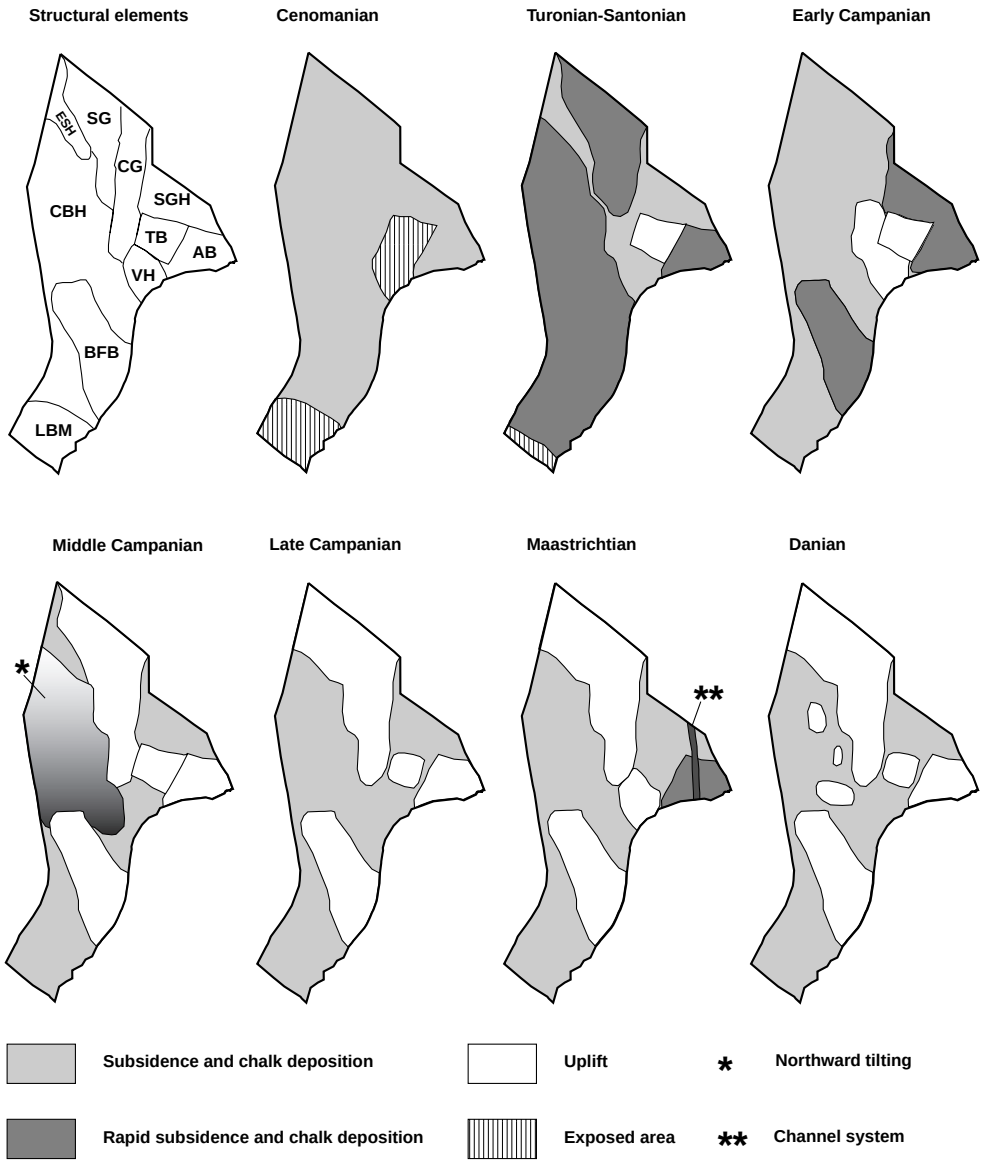

Figure 3.6: Schematic overview of the tectono-sedimentary evolution of the Netherlands offshore area during the Late Cretaceous to Paleogene. Subsidence predominated in the area during the Cenomanian to early Campanian. From the middle Campanian onwards, many of the Early Mesozoic basins experienced uplift.

3.4 Inversion tectonics and chalk (re)deposition in the Dutch Central Graben

The shape of the Base Chalk reflector (Fig. 3.7) illustrates the complex syn-depositionary tectonic evolution of the Dutch Central Graben. Uplift of the graben took place along reactivated, N–S and NE–SW trending, normal faults and resulted in a dome-shaped central inversion zone. To the east, the graben is bounded by a very pronounced normal fault zone. The transition to the Step Graben in the west is more subtle (Section 3.2.6). The thickness of the Chalk is about 400 m in the rim syncline of the western salt diapirs, decreasing to zero in the southern part of the inversion zone (Fig. 3.8).

Salt diapirs form a prominent structural feature that are mostly found along the boundary faults of the graben (Remmelts, 1995; Buchanan et al., 1996; Davison et al., 2000a). The 'Hanze' salt diapir in the western part of the survey is the location of the only intra-Chalk oil field in the Dutch offshore. The NW–SE orientation of the south-eastern salt wall (A) and northern part of the boundary fault (B) confirm that the Dutch Central Graben is bounded by a chain of en-echelon aligned normal faults. The orientation of these faults illustrates the dextral transpressional movement the Graben underwent during the compressional phases in the Late Cretaceous to Paleogene (Van Wijhe, 1987; Ziegler, 1990; Clausen & Hansen, 2000).

A wide variety of seismic facies types can be recognised in the Chalk succession of the Dutch Central Graben 3D-seismic area, (Fig. 3.9). In general, the seismic facies is characterised by parallel and continuous to discontinuous reflections. Chaotic intervals, indicating reworking, occur on the flanks of the inversion zone, on top of

Figure 3.7 ***(facing page)*****:** Base Chalk TWT map of the Dutch Central Graben survey. The geometry of this horizon clearly illustrates the dramatic tectonic events that shaped the Chalk in this area. During the Late Cretaceous and Paleogene, the Dutch Central Graben was inverted, whereby movement along existing boundary faults (F) was reversed. As a result, the Chalk Group is thickest outside the inverted graben, decreasing to zero in the southernmost part of the inversion zone. Reactivated NS (A) and WSW-ENE (B) trending normal fault systems accommodated the uplift of the inversion zone. The upward movement of Zechstein salt, usually along the graben boundary faults, formed salt diapirs (SD). These salt diapirs have deformed the Chalk into highly fractured 4-way structural closures that are important hydrocarbon exploration targets in the Chalk in the North Sea (Oakman & Partington, 1998; Bramwell et al., 1999; Davison et al., 2000b). The 'Hanze' field is presently the only example of such a field in the Dutch offshore (Hofmann et al., 2002). **See Fig. 3.7 (page 155) in Appendix - Colour plates for a colour version of this figure.**

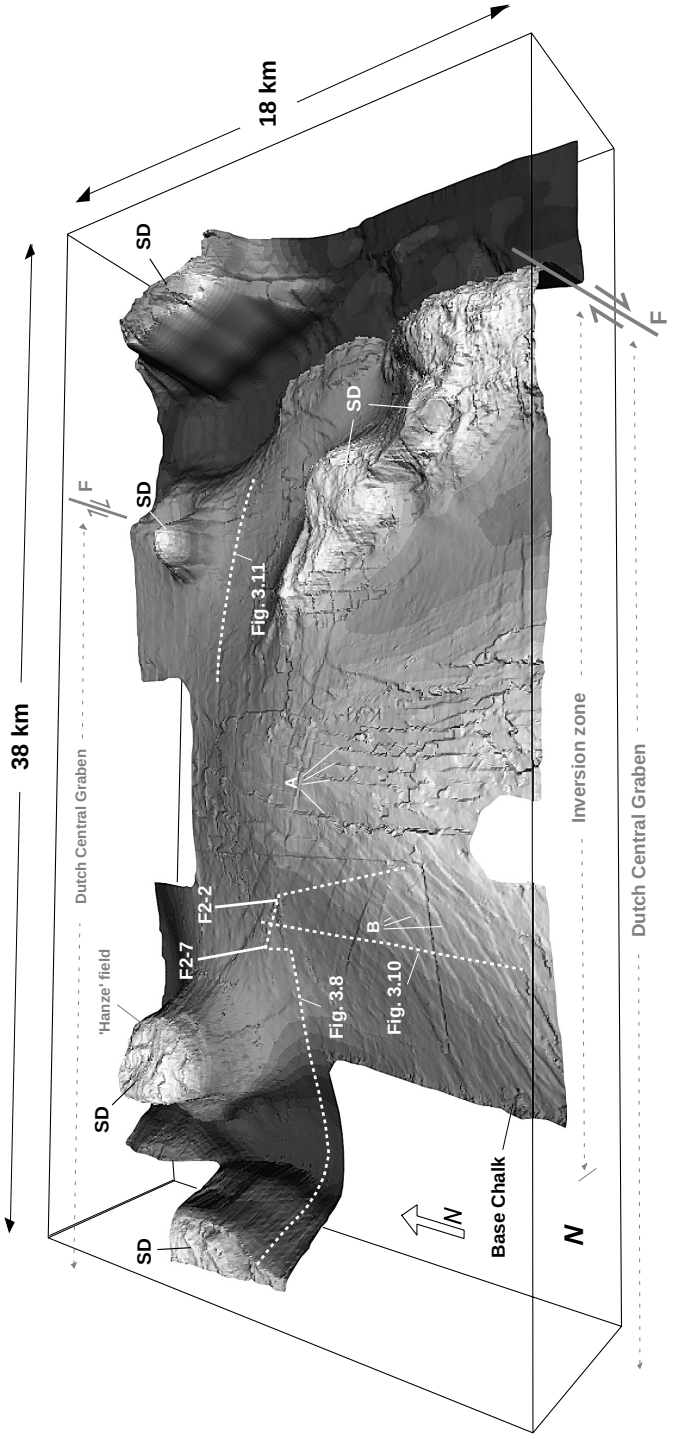
18 km
38 km
SD
SD
SD
SD
SD
F
F
Fig. 3.11
A
B
F2-2
F2-7
Fig. 3.8
Fig. 3.10
'Hanze' field
Dutch Central Graben
Inversion zone
Dutch Central Graben
Base Chalk
N
N

the salt diapirs and just east of the Dutch Central Graben. As seismic image quality on the crests and flanks of the salt diapirs is generally low, chalk reworking can best be studied away from these structures.

Along the northern and eastern flank of the central inversion zone, a large structure showing chaotic seismic reflections is present (Fig. 3.9). This sediment body is several kilometres wide, has a maximum thickness of about 200 m (100 ms TWT) and encompasses sequences CK1, CK2 and CK7 (Fig. 3.10). The location of this sediment body suggests that it is the result of a massive slope failure and moved towards the north and east, off the rising inversion dome. The geometry of this structure, as well as its disturbed internal configuration, indicates that this is a slump. Formation must have occurred in the Campanian, prior to the deposition of sequence CK8. Movement along normal faults at a much later stage altered the geometry of the slump.

Above the slump, a single strong positive reflection is visible that has a random appearance. This reflection is also encountered on the western flank of the inversion dome, as well as east of the Graben, in the easternmost part of the 3D-seismic survey (Fig. 3.8). The reflection forms an irregular surface that cross-cuts as well as follows sedimentary bedding, and also appears to be linked to faults. The nature of the process that caused this structure is undetermined.

A striking example of a slide sheet is present in the Maastrichtian to Danian chalk (CK9 to CK11) on the west flank of the inversion zone (Fig. 3.8). The structure is about 5 km long and 100 m (50 ms TWT) thick, and characterised by listric faults at the top and compressional structures at the base of the structure (Fig. 3.11). Reflection geometries suggest that this allochthonous body remained fairly coherent internally and was transported over a short distance. This particular slope failure must have occurred at the end of the Danian, just before the deposition of the first post-Chalk siliciclastic sediments as these form the first undisturbed reflections above the slide sheet.

The Upper Maastrichtian and Danian chalk in the eastern part of the study area often shows discontinuous to chaotic seismic reflections (Fig. 3.9). This seismic facies probably represents reworking on a smaller scale than the allochthonous sediment bodies described in the previous section, with sediment being supplied from the continuously rising salt diapirs.

Figure 3.8 ***(facing page)*:** Seismic section of the Dutch Central Graben area. Seismic facies is characterised by fairly parallel and continuous to discontinuous reflections in the rim syncline (W), changing to more irregular reflection patterns on the inversion dome, towards the SE.

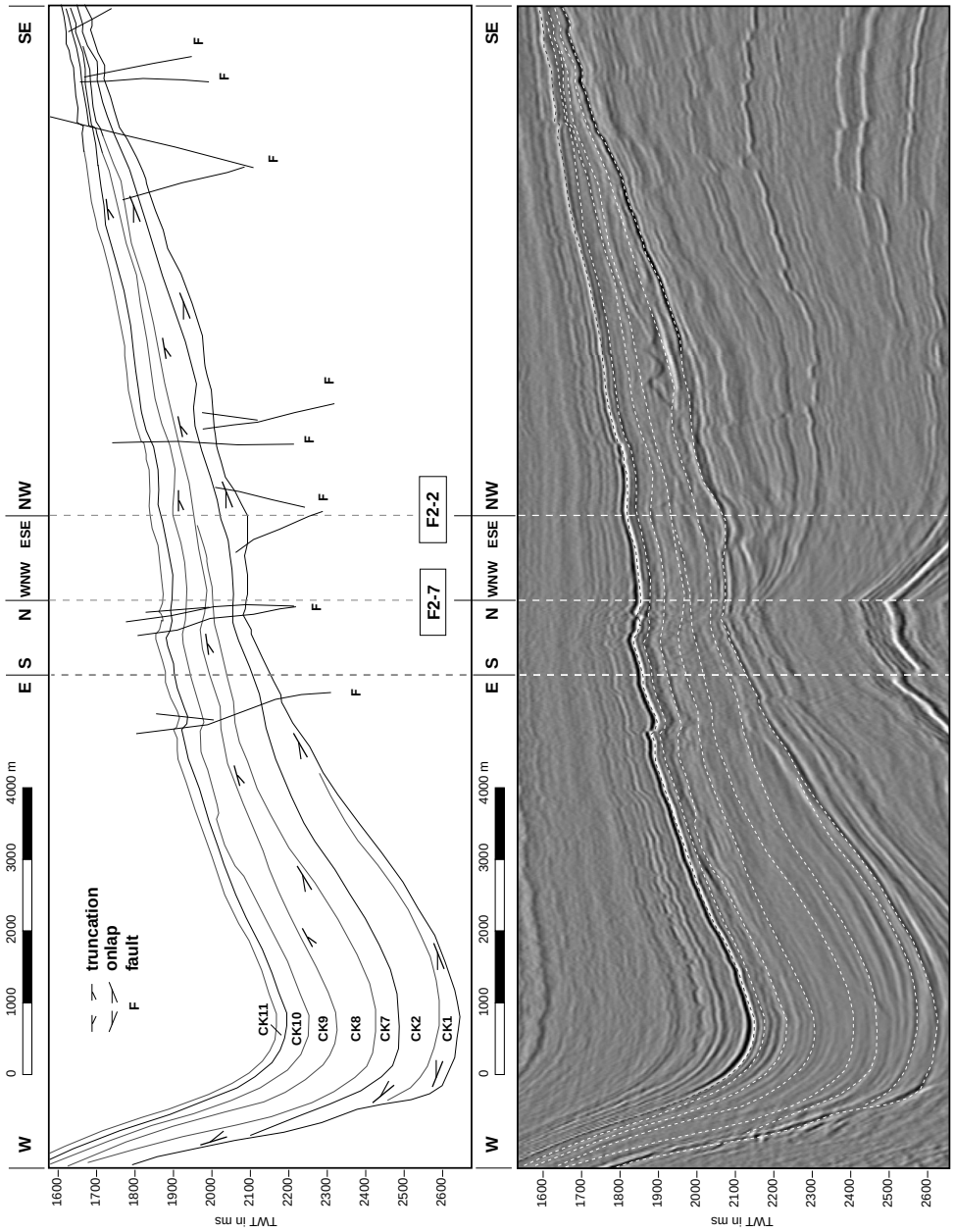
W
E
S
N
WNW
ESE
NW
SE
0
1000
2000
3000
4000 m
truncation
onlap
fault
F
CK11
CK10
CK9
CK8
CK7
CK2
CK1
F2-7
F2-2
TWT in ms
1600
1700
1800
1900
2000
2100
2200
2300
2400
2500
2600

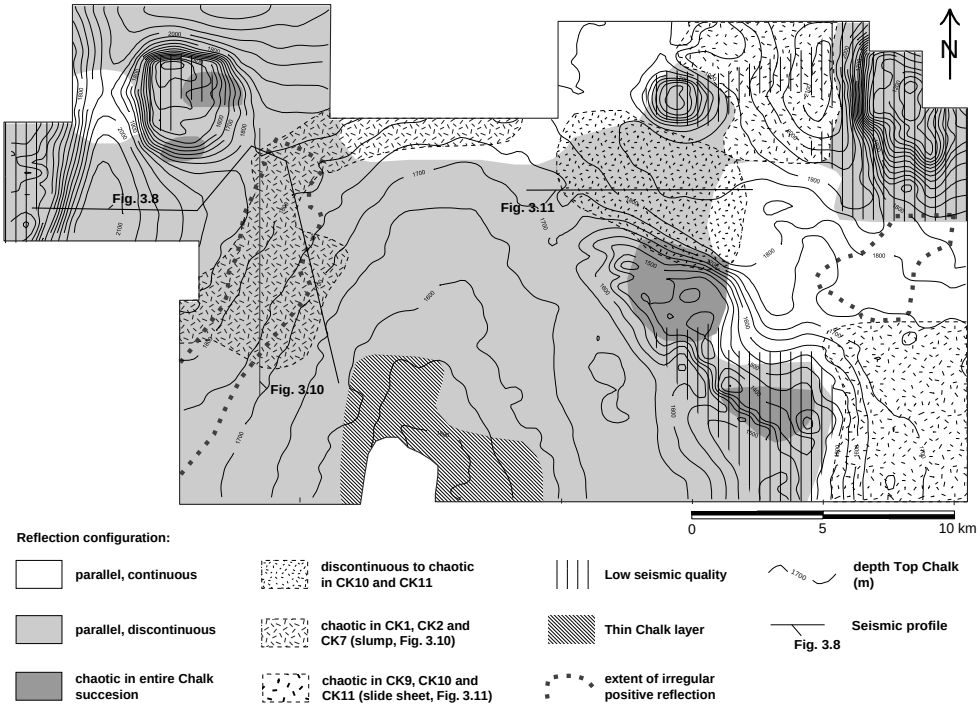

Figure 3.9: Seismic facies map of the Chalk in the Dutch Central Graben survey. The area shows a wide range of seismic facies, indicating different depositional processes controlling the formation of the Chalk in this area. In general, the seismic facies is characterised by parallel and continuous to discontinuous reflections. On the flanks of the inversion dome, on top of the salt diapirs and just east of the Dutch Central Graben, chaotic intervals occur that indicate sediment reworking.

3.5 Discussion

The Cenomanian to Danian tectono-sedimentary evolution of the Netherlands offshore area was reconstructed from the distribution and thickness of intra-Chalk seismic sequences. The distinction of these sequences points to regionally synchronous periods of chalk deposition, separated by periods of non-deposition and/or erosion.

As the sequence boundaries are in most cases expressed in the form of angular truncations, synchronous tectonic activity is most likely to have controlled the sedimentary development of the Chalk. However, the possible effects of eustatic sea level fluctuations cannot be ignored. In stable areas, for instance, seismic sequence boundaries are often developed as parallel reflections, with no indication of tilting.

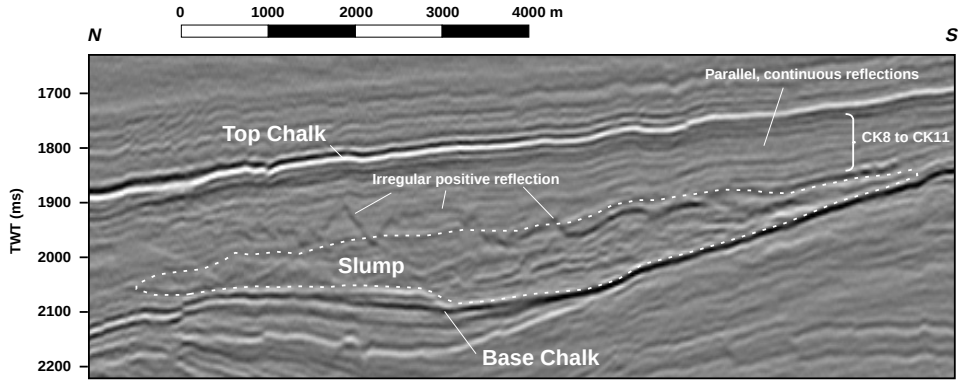

Figure 3.10: Interval of irregular seismic reflections in the basal section of the Chalk interval, indicating slumping off the western flank of the inversion dome. Above the slump a chaotic positive reflection is visible, the nature of which is undetermined.

Examples of this can be seen in the Cleaver Bank High (Fig. 2.14) and Schill Grund High (Fig. 2.15). The high seismic amplitude of these parallel sequence boundaries indicates that deposition was interrupted and sediment was allowed to compact to some extent before sedimentation resumed. This does indicate the possible importance of non-tectonic controls on the deposition of the Chalk as well.

Based on the thickness of sequences CK1 to CK6, high subsidence and sediment accumulation rates during several stages in the Cenomanian to the early Campanian are inferred in large portions of the Netherlands offshore. These areas include the Broad Fourteens Basin, the Cleaver Bank High, the Step Graben, the Dutch Central Graben, the Schill Grund High and the Ameland Block (Fig. 3.4 & Fig. 3.6). However, it is important to note that variations in magnitude of uplift and erosion influence this interpretation. For instance, the possibility that a thick section of early Campanian chalk accumulated in the northern Cleaver Bank High, prior to the southward tilting of this area, cannot be excluded.

The Late Cretaceous and Paleogene compressional phases that resulted in the inversion of the Broad Fourteens Basin and Dutch Central Graben are traditionally grouped in the late Santonian to Campanian 'Sub-Hercynian' Phase and early Paleocene 'Laramide' Phase (Van Wijhe, 1987; Ziegler, 1990; Dronkers & Mrozek, 1991). The present study confirms that uplift occurred throughout the Campanian to Maastrichtian, with peaks during the middle Campanian (prior to the deposition of CK7) and in the late Campanian (prior to CK8). The Broad Fourteens Basin experienced most of its uplift during this period, as is illustrated by the geometry of

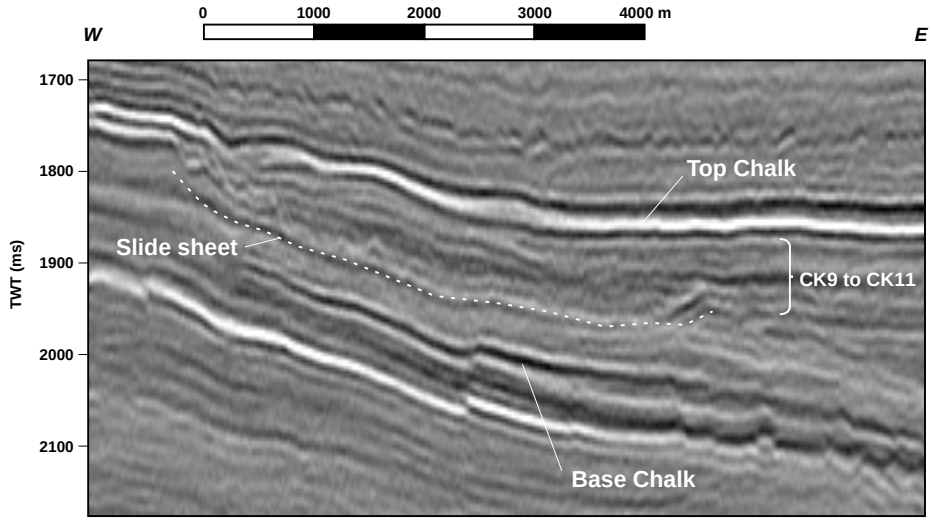

Figure 3.11: Slide sheet in upper section of the Chalk interval, on the eastern flank of the inversion dome. The slide sheet is about 5 km in length and is characterised by listric faults at the top and compressional structures at the base of the structure. Reflection geometries suggest that this allochthonous body remained fairly coherent internally, contrary to the large slump of Fig. 3.10, and was transported over a short distance.

the seismic units to the south of this structure (Fig. 3.4). However, inversion of the central part of the Broad Fourteens Basin probably already started in the Albian (Hooper et al., 1995). This was accompanied by rapid subsidence of the marginal throughs, as indicated by the thick sequences of Cenomanian to early Campanian sediment in these structures. The extent of uplift prior to the deposition of CK7 in the Dutch Central Graben is evidenced by the removal of the Coniacian to lower Campanian succession on the inversion dome (Fig. 3.9). The inversion dome clearly continued to rise throughout the Campanian and Maastrichtian, and with a final pulse after the Danian.

The dominant seismic facies of parallel and continuous reflections suggests that the Chalk Group in the study area is largely autochthonous (Chapter 2). Large scale reworking of chalk occurred on the flanks of the Central Graben inversion dome (Fig. 3.10 & Fig. 3.11). It is important to note reworking is also likely to be present in the vicinity of the salt diapirs (Hancock, 1975; Watts et al., 1980; Schatzinger et al., 1985; Kennedy, 1987; Farmer & Barkved, 1999; Davison et al., 2000b). However, the high acoustic velocity of salt leads to complications in seismic data processing, in turn resulting in low image quality. Furthermore, seismic resolu-

tion, being controlled by the wavelength, sonic velocity and reflection depth, cannot be expected to be better then several tens of meters both vertically and laterally here (Kearey & Brooks, 1991). This means that meter-scale allochthonous bodies including turbidites, debris-flow deposits and slumps are not visible in seismic data. It should therefore be stressed that the terms 'autochthonous' and 'allochthonous' are used as descriptive terms to aid seismic interpretation in this setting. Therefore, autochthonous chalks, following our definition, include true pelagic chalks as well as sub-seismic resedimentation structures and allochthonous chalks are all super-seismic scale resedimentation structures.

3.6 Conclusions

- Based on thickness distribution of the Chalk interval, a regional subdivision into nine, roughly NW–SE trending, Chalk provinces was made. These chalk provinces are made up of one or more early Mesozoic structural elements.
- The thickness of the Chalk Group is controlled by Late Cretaceous to Paleogene inversion tectonics. The Chalk is generally thick on the Early Mesozoic 'highs', which experienced gradual syn-depositional subsidence. In contrast, the Chalk is thin or missing in former grabens, which were inverted during several phases in the Late Cretaceous to Paleogene.
- Subsidence prevailed in the Dutch offshore during the Cenomanian to early Campanian, leading to the formation of thick successions of chalk, particularly in the marginal throughs north and south of the inverted Broad Fourteens Basin and in the Schill Grund High—Ameland Block province.
- During the Turonian to Santonian, the Vlieland Basin and Terschelling Basin were uplifted. Inversion of the Central Graben and the whole Broad Fourteens Basin started in the middle Campanian.
- Chalk was reworked in the form of massive slumps and slide sheets in tectonically active areas. Good examples of such sediment bodies are found in the Dutch Central Graben.
- In the Maastrichtian to Danian chalk of the Schill Grund High and Ameland Block, a large channel system is present that suggests marked bottom current activity or even sub-areal exposure during this period.

Chapter 4

Metre-scale cyclicity in well logs of the Chalk Group, Netherlands North Sea area

Rhythmic bedding forms one of the most characteristic features of the Chalk. For over a century, these bedding cycles have been interpreted to represent climate variations controlled by cyclic variations in the Earth's orbit. A great variety of bedding cycles, from centimetre to metre-scale, have been described in outcrops and cores. However, exploration geophysical well logs are rarely used for this purpose, although these allow the study of thick successions of chalk at decimetre-scale resolution and are widely available in the North Sea area. Therefore, a frequency analysis was carried out of the Chalk interval in well logs of 43 boreholes from the Netherlands North Sea sector. The interval contains cyclic intervals in most of the areas that underwent gradual subsidence during deposition of the Chalk. In contrast, predominantly chaotic ('a-periodic') log responses are encountered in the Dutch Central Graben and the areas around the Broad Fourteens Basin. Based on the calculated frequency spectra, a selection of logs showing pronounced cyclicity was made and used, where possible, to identify the mode of astronomical periodicity represented in the sediments (i.e. eccentricity, obliquity or precession cycles). Most often, the Chalk interval contains 5–7 m and 2–3 m cycles, that are interpreted to represent 100 ky eccentricity and 40 ky obliquity 'Milankovitch' cycles. A gradual decrease of cycle wavelength can be traced along the Campanian–Maastrichtian interval of several wells that probably reflects a regional decrease in primary carbonate production during this period.

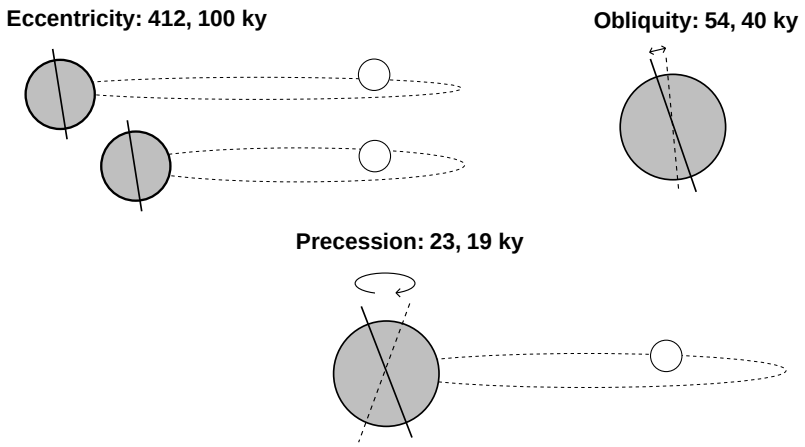

Figure 4.1: Overview of the different modes of cyclic variations in the Earth's orbit occurring within the Milankovitch range.

4.1 Introduction

Rhythmic bedding forms one of the most characteristic features of the sediments of the Chalk Group. The origin of this rhythmicity has long been debated but is generally attributed to cyclic variations in the Earth's orbit, also known as 'Milankovitch' cycles (Fig. 4.1; e.g. Gilbert, 1895; Barron et al., 1985; Herbert & Fischer, 1986; R.O.C.C. Group, 1986; De Boer, 1991). Cyclicity in chalk is typically manifested as variations in porosity, cementation, carbon and oxygen isotope ratios and clay content, as well as by periodic development of marl layers, (nodular) chert layers and hardgrounds (Hancock, 1975; Hart, 1987; Zijlstra, 1994, 1995; Molenaar & Zijlstra, 1997). Such cyclicity is thought to result from cyclic variations in carbonate productivity, terrigenous dilution, redox conditions and bottom current activity (Barron et al., 1985; R.O.C.C. Group, 1986). Astronomical cycles recognised in chalk deposits include 412 ky eccentricity (E2), 100 ky eccentricity (E1), 50 ky obliquity (O2), 40 ky obliquity (O1) and the 23 ky (P2) and 19 ky (P1) precession cycles (Hart, 1987; Cottle, 1989; Ditchfield & Marshall, 1989; Gale, 1989; Herbert & D'Hondt, 1990; Herrington et al., 1991).

Frequency analysis of cyclic bedded intervals enables the identification and study of the periodic climate variations. It also enables high-resolution stratigraphic correlation and relative age definition of the sediment and provides an indication of the sedimentation rates during the Late Cretaceous and early Paleocene (e.g. Gale, 1989; Gale et al., 1999; Prokoph et al., 2001). Although the bulk of cyclicity studies

in the Chalk have focussed on outcrops, geophysical borehole logs provide an important advantage for this task, as usually longer stratigraphic intervals can be studied at ample locations (over 1000 boreholes have been drilled in the Dutch offshore area alone. Furthermore, the ordered fashion in which digital oil industry logging data are stored enables a more straightforward frequency analysis of bedding thicknesses.

In this chapter, the results are presented of a frequency analysis performed on gamma-ray, sonic, density and resistivity logs of 43 boreholes in the Netherlands offshore area (Fig. 4.2). Based on these results, different spectral log facies types were distinguished allowing for the identification of log intervals showing strong periodicity, most likely representing autochthonous chalks, and chaotic intervals that most likely indicate reworking. This sedimentological characterisation refines the one based on seismic facies (Chapter 2) because of the higher resolution of well logs. The periodic log intervals were found to contain several simultaneously occurring cyclic log response variations, with different frequencies. Assuming these to be orbitally forced, an attempt was made to identify Milankovitch cycles by comparing wavelength ratios of the different cyclicities.

4.2 Milankovitch cycles in the Chalk

Most studies of cyclicity in the Chalk have focussed on outcrops or cores (Table 4.1). In the Cenomanian to Campanian Chalk of southeastern England, 40 ky obliquity (O1) and 23 ky precession (P2) cycles were described by Hart (1987). The 23 ky precession cycles here, and in the Cenomanian successions in the Anglo-Paris Basin (France) and the Crimea (Ukraine), are developed as approximately 50 cm thick alternations of marl (darker grey argillaceous micrite) and pure chalk (Hart, 1987; Ditchfield & Marshall, 1989; Gale, 1989; Gale et al., 1999). Cyclic oxygen and carbon stable isotope composition variations follow this lithological alternation and indicate paleotemperature fluctuations of up to 4.5 °C (Ditchfield & Marshall, 1989; Scholle et al. 1998). Variations in dinoflagellate cyst abundance illustrate the paleoenvironmental effect of such temperature fluctuations (Wendler et al., 2002). Spectral analysis of greyscale reflectance data from rock samples confirms that the marl-chalk alternations are 23 ky precessional cycles, bundled into sets of five that represent a 100 ky eccentricity (E1) cycle. A composite cyclostratigraphy for the Cenomanian interval in the Anglo-Paris basin shows that this stage consists of forty-four 100 ky E1 cycles, equalling 4.4 Ma (Gale, 1989; Gale et al., 1999). In the Turonian of southeast England, foraminifera abundance shows strong cyclic variations at the scale of 8.25 m (412 ky E2), 2.1 m (100 ky E1) and many smaller scales, including 48 cm (23 ky P2) cycles. These cycles are interpreted to be orbitally induced climatic cycles as well (Cottle, 1989).

λ (m)	Stage	Location	Reference
2 (E1); 0.6 (P2)	Maas	Dan Field	Stage (1999; 2001b)
27–29 (E2); 6–8 (E1)	Camp	North German Basin	Niebuhr & Prokoph (1997)
1 (O2); 0.5 (P2); 0.25–0.05 (?)	Tur–Camp	Dan Field	Herrington et al. (1991)
8.25 (E2); 2.1 (E1)	Tur	UK	Cottle (1989)
1.1–1.2 (O1); 0.6–0.7 (P2)	U.Con–Camp	UK	Hart (1987)
0.8–0.9 (O1); 0.4–0.5 (P2)	Cen–L.Con	UK	Hart (1987)
3.3–3.8 (E1)	Cen–Tur	Lower Saxony Basin	Niebuhr et al. (2001)
0.5 (P2)	Cen	UK	Ditchfield & Marshall (1989)
2 (E1); 0.4 (P2)	Cen	UK, F, Ukraine	Gale (1989)

Table 4.1: Overview of cyclicities described in Chalk intervals. Cyclicity types: E2 = 412 ky eccentricity, E1 = 100 ky eccentricity, O2 = 50 ky obliquity, O1 = 40 ky obliquity, P2 = 23 ky precession and P1 = 19 ky precession. Stages: Cen (Cenomanian), Tur (Turonian), Con (Coniacian), Camp (Campanian) and Maas (Maastrichtian). Locations: UK (British onshore), F (French onshore).

Herrington et al. (1991) described decimetre-scale alternations of clay-rich and clay-poor chalk in the Campanian part of the Hod Formation, in cores from the 'Eldfisk' oil field, located in the Norwegian Central Graben (Fig. 1.4 & Fig. 1.5). Thicknesses of clay-poor/clay-rich chalk couplets vary but are mostly about 100 cm, 50 cm and 25 cm thick. Alternations like these are similar to the lithological alternations described from outcrops throughout Europe and occur where the sediment is free of oil traces. The authors interpreted the decimetre scale alternation as the result of 'tens of thousands of years' Milankovitch cyclicity, without elaborating further on the astronomical cycle mode.

Cores of Maastrichtian chalks of the 'Dan' oil field, located in the Danish Central Graben (Fig. 1.4), contain lithologic cycles that vary in thickness from 2 m to 30 cm (Scholle et al., 1998). Contrary to the cycles found onshore and in the Campanian of the Eldfisk field, these cycles are made up of a laminated lower section containing escape burrows, capped by a bioturbated upper section. The bedding cycles are visible on porosity logs as well and can be correlated over long distances. The Dan field is located on a broad salt swell and the well correlation indicates that stratigraphic units are usually thinner on top of this structure than at the flanks. Since slumping has not been identified in this area and single erosional events would most likely remove entire bedding cycles instead of just thinning them, it is suggested that continuous winnowing modifies sedimentation throughout the area. The authors did not elaborate on the mode of astronomical forcing expressed in these cyclic beds, however.

Stage (1999; 2001b) performed a frequency analysis of magnetic susceptibility values on a 23 m long core of Maastrichtian chalk taken from the afore-mentioned Dan Field, as well as a gamma-ray and neutron porosity log of the same interval. All three datasets contain cycles of 2 m wavelength, as well as smaller 50 cm thick cycles. The author interpreted these to be the 100 ky eccentricity and 23 ky precession cycles respectively. The measured variations in bulk magnetic susceptibility were most likely caused by changes in the runoff from the hinterland into the basin (Stage, 2001a).

Niebuhr & Prokoph (1997) performed a spectral analysis of SP-logs of three wells in the North German Basin. Their study revealed that part of the Campanian interval of two these wells contained, among other periodicities, strong 27–29 m and 6–8 m cycles. Based on the characteristic wavelength ratio between both spectral peaks, these were interpreted to be the 412 ky eccentricity (E2) and 100 ky eccentricity (E1) cycles respectively. The Campanian in a third well contained strong 48 m and 12 m cyclicities, as well as several cyclicities with shorter frequencies. Based on the criteria used in the first two wells, these were interpreted to represent the 412 ky E2 and 100 ky E1 as well. Thus, the authors estimate net accumulation rates of 6 to 12

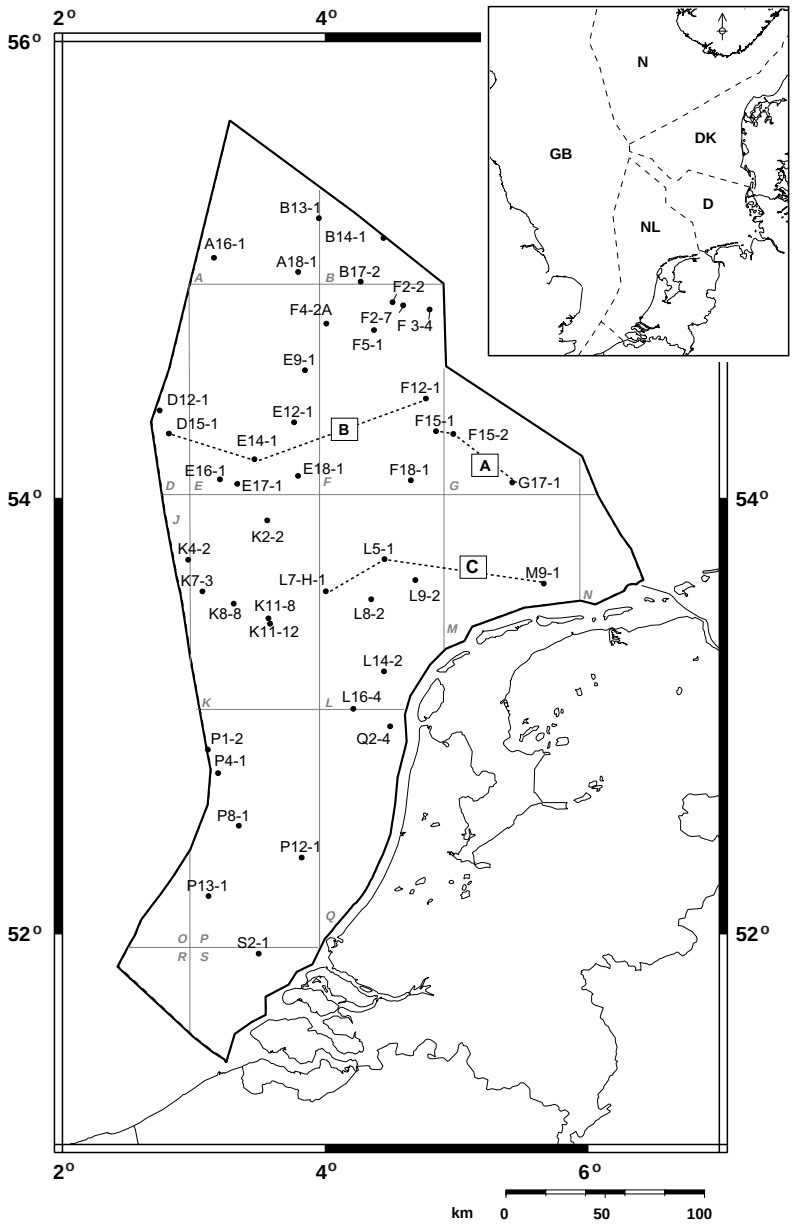

Figure 4.2: Map of the Netherlands offshore sector showing the location of the 43 boreholes used in the present study. Dotted lines represent location of profiles A, B and C. The small map indicates the position of the study area (NL) and the surrounding offshore sectors. GB = British, N = Norwegian, DK = Danish and D = German sectors.

cm/ky for part of the Campanian in the North German Basin. In the Lower Saxony Basin of northern Germany, strong 100 ky eccentricity cycles in the Cenomanian and Turonian (λ = 3.3–3.8 m) were found in the focussed resistivity log from the Konrad 101 borehole (Niebuhr et al., 2001).

When the studies discussed above are compared, a marked discrepancy in interpreted Milankovitch cycle modes becomes clear between cyclicities described in most outcrop and core studies and those found in well logs (Table 4.1). As a result, estimates of inferred sediment accumulation rates also vary highly. This discrepancy might suggests a bias in interpration caused by the difference in scale between outcrop or core studies and well log information.

4.3 Database & Methods

The dataset used in the present study consists of gamma-ray and sonic logs of 43 boreholes from the Netherlands offshore, supplemented with density and resistivity logs where available (Fig. 4.2; Table 4.3). Industrial biostratigraphy reports, predominantly based on benthic foraminifera from ditch cutting samples, were available for 14 of these wells (Fig. 2.20; Section 2.4 *Biostratigraphy*). The Chalk interval of each borehole was subdivided into units based on log response, with frequency content being the most important characteristic considered. Based on this subdivision, a well-log correlation was constructed between all boreholes.

A frequency analysis was carried out of all logs using the Maximum Entropy Spectral Analysis (MESA) routine of the Cyclolog© software package (Fig. 4.3). The MESA-routine calculates a frequency spectrum of a certain log interval using a matrix calculation, which the advantage over the established (Fast) Fourier Transformation (FFT) that boundary effects are less pronounced. The frequency spectrum of a larger interval is calculated by 'sliding' the calculation window along the log, after which the results are represented in a frequency spectrum scalogram. This frequency spectrum scalogram shows the frequency content (as wavelenght λ in m) of the log with depth. A sliding window length of 40 m was used in this study.

The frequency scalograms were initially used to appraise the overall cyclicity of the well log, enabling the characterisation of periodic intervals, most likely consisting of autochthonous chalk, and chaotic intervals that most likely indicate reworking, following the subdivision of Niebuhr & Prokoph (1997). Based on these results, an interval was assigned to one of the following spectral log facies types (Fig. 4.4).

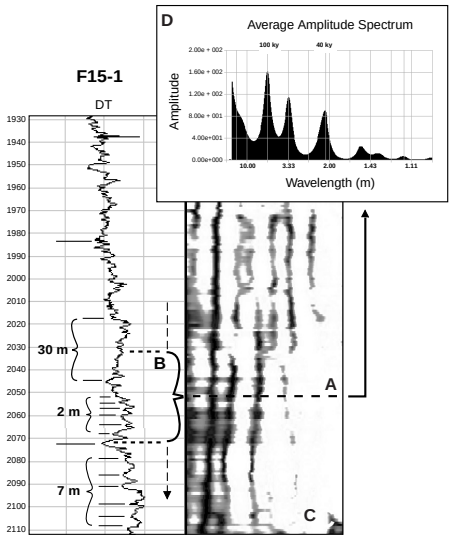

Figure 4.3: Frequency spectrum of the 1930–2110 m interval of the sonic log from borehole F15-1 (Fig. 4.7). At depth A, frequencies within 40 m sliding window B are determined and represented in a frequency scalogram (C) and/or spectrum (D). As is evident from the well-log, this interval contains well-developed 30 m, 7 m and 2 m cycles, which are interpreted to be 412 ky E2, 100 ky E1 and 40 ky O1 cycles based on the characteristic wavelength ratio. Frequency scalogram C also indicates the presence of a 3.3 m cyclicity from 2040 m to 2090 m, which is probably the 50 ky oscillation cycle. **See Fig. 4.3 (page 156) in Appendix - Colour plates for a colour version of this figure.**

Type 1 Containing well developed cycles that can be traced over several sliding window lengths, with associated weaker cyclicities.

Type 2 Containing cycles that can be traced over two to three sliding window lengths, with many associated cycles of variable strength.

Type 3 Not containing any cyclicity.

Based on the relative predominance of each facies type per log, an 'overall' spectral facies type was assigned to each individual well. The dominant cyclic wavelength (where present) and the log tool showing the most pronounced cyclicity were noted as well. This was done to allow regional comparisons to be made.

Of all logs with spectral facies type 1 or 2, the wavelength of the dominant cycles were noted. Following the procedure adopted in most studies of Milankovitch cyclicity in the Chalk (Section 4.2), cyclicity modes were assessed by looking for specific cyclicity wavelength ratios in the logs (Fig. 4.3) and comparing these to the known wavelength ratios between different Milankovitch cycles (Fig. 4.1). This was done under the assumption that periodic log responses are caused by Milankovitch-style climatic variations, and was attempted for all intervals showing log facies type 1 or 2. Where available, the biostratigraphical data (Fig. 2.20; Section 2.4 *Biostratigraphy*) was used to augment this analysis.

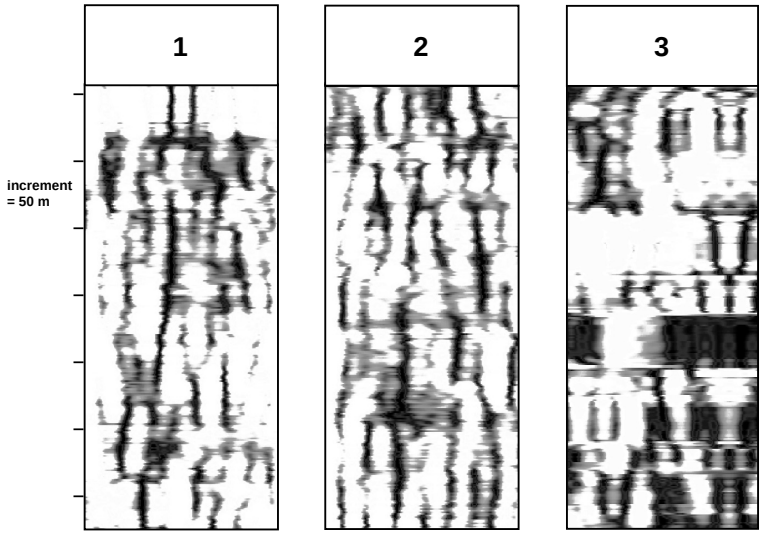

Figure 4.4: Examples of spectral log facies types appearing in frequency spectrum scalograms of the studied well-logs. See Section 4.3 for explanation. **See Fig. 4.4 (page 156) in Appendix - Colour plates for a colour version of this figure.**

4.4 Results

The results of the frequency analysis are summarised in Table 4.2 and Fig. 4.5. To discuss the frequency analysis and possible identification of orbitally forced (Milankovitch) cycles in more detail, profiles A, B and C are presented (Fig. 4.2). Profile A is oriented NW–SE and consists of wells F15-1 (Fig. 4.6), F15-2 (Fig. 4.7) and G17-1 (Fig. 4.8). These wells are located on the Schill Grund High and Ameland Block, where the Chalk is between 1000 and 1500 m thick (Fig. 1.8; Fig. 3.2). Profile B consists of wells D15-1 (Fig. 4.9), E14-1 (Fig. 4.10), and F12-1 (Fig. 4.11). The profile runs E–W across the Cleaver Bank High, connecting to the Schill Grund High, with an average Chalk interval thickness of about 500 m (Fig. 1.8; Fig. 3.2). Profile C is also oriented E–W, and includes wells L7-H-1 (Fig. 4.12), L5-1 (Fig. 4.13) and M9-1 (Fig. 4.14). The profile connects the southern part of the Cleaver Bank High with the Vlieland High and the southern part of the Ameland Block (Fig. 1.8) The Chalk is about 500 m thick along the profile (Fig. 3.2). Based on sonic log response, a seven-fold subdivision of the Chalk interval was made.

Well	Facies type	Avg. λ_{dom} (m)	Log tool	Well	Facies type	Avg. λ_{dom} (m)	Log tool
A16-1	2	4.7	DT	G17-1	2	5.2	DT
A18-1	1	*3.1*	DT	K2-2	3		
B13-1	2	*2.4*	GR	K4-2	3		
B14-1	2	3.5	DT	K7-3	3		
B17-2	3			K8-8	3		
D12-1	2	5.3	DT	K11-8	3		
D15-1	2	*2.4*	GR	K11-12	3		
E9-1	2	*2.9*	RESC	L5-1	2	*3.3*	RHOB
E12-1	1	4.8	DT	L7-2	2	5.2	DT
E14-1	2	7.3	DT	L8-2	3		
E16-1	3			L9-2	2	*2*	GR
E17-1	2	*2.5*	GR	L14-2	3		
E18-1	2	*2.4*	GR	L16-4	2	*2*	DT
F2-2	3			M9-1	1	*2.3*	GR
F2-7	3			P1-2	3		
F3-4	2	*1.9*	GR	P4-1	3		
F4-2A	2	*2.7*	DT	P8-1	2	*2.7*	GR
F5-1	2	*2.1*	GR	P12-1	3		
F12-1	1	*2.1*	GR	P13-1	2	*2.9*	GR
F15-1	1	5.9	DT	Q2-4	3		
F18-1	2	4.4	RESC	S2-1	3		

Table 4.2: Overview of the 'overall' spectral log facies type per well (Fig. 4.4), the average dominant cycle wavelength (avg. λ_{dom}) and log tool (DT: sonic, GR, gamma-ray, RESC: resistivity and RHOB: density logs) in which cyclicity is preserved. Two sets of dominant cycles were found in the studied well-logs, with average wavelengths of about 5 to 7 metres and 2 to 3 metres (in italics).

4.4.1 Well-log correlation

Based on log response characteristics of the sonic logs, the following seven-fold subdivision of the Chalk interval has been made (Figs. 4.6 to 4.14). The basal log unit 1 (Cenomanian) can characteristically be further subdivided into three subunits, and as a whole shows a fairly low amplitude and low frequency sonic response. A conspicuous spike, also visible on the density and gamma-ray logs, most likely representing the Plenus Marl Member (Van Adrichem Boogaert & Kouwe, 1994) tops this unit. Unit 2 (Turonian) shows a much more serrated log pattern (high amplitude and low

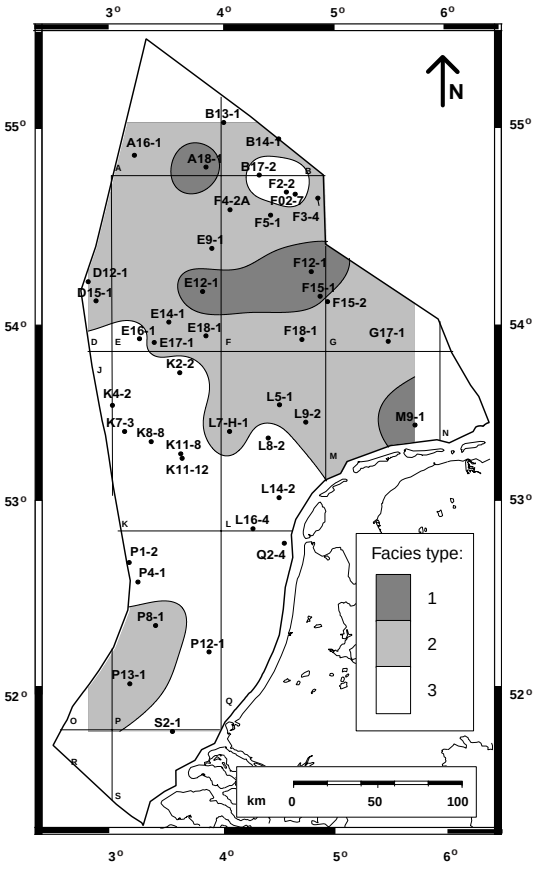

Figure 4.5: Regional distribution of 'overall' spectral log facies (fig. 4.4). The Chalk interval contains cyclic intervals of two to three sliding window lengths in the northern and eastern part of the study area. In contrast, a predominantly chaotic ('a-periodic') log response is encountered around the Dutch Central Graben and Broad Fourteens Basin (Fig. 1.8).

frequency sonic log character). Unit 3 (Coniacian) shows low amplitude and medium frequency sonic variations and is followed by an interval of medium amplitude and high frequency log response (Unit 4; Coniacian). A serrated (high amplitude and low frequency) log character, which is very similar to unit 2, is found in Unit 5 (Santonian). Unit 6 (Campanian to lower Maastrichtian) is the thickest, with low frequency variations of varying amplitude. The uppermost Unit 7 (Maastrichtian to Danian) shows very high amplitude log variations.

The sonic log subdivision described above is most obvious where the Chalk is thick, i.e. in F15-1 (Fig. 4.6), F15-2 (Fig. 4.7), G17-1 (Fig. 4.8) and E14-1 (Fig. 4.10). The characteristic ('serrated') log units 2 and 5 are visible in almost all of the logs, as is the spike in both gamma-ray and sonic reading that marks the upper boundary of unit 1. The close relation between sonic and density logs, which is evident from

the logs L5-1 (Fig. 4.13) and exists because both logs respond to porosity variations in chalk, means the well-log subdivision described for sonic logs can also be applied to density logs. Due to the generally low gamma-ray reading in chalk, the gamma-ray logs did not prove usable for a subdivision of the Chalk Group based purely on log response. Where the Chalk is thick, the log units correlate well with the seismic sequences described in Chapter 2 (Fig. 2.18 & Fig. 2.19). However, correlation of the lower and uppermost seismic sequences to the log correlation locally fails where the sequences are very thin.

4.4.2 Spectral log facies

Based on the 'overall' spectral log facies type per well, it is clear that the Chalk interval contains cyclic intervals of two to three sliding window lengths in the northern and eastern part of the study area (Fig. 4.5; Table 4.2). This is an area encompassing quadrants A through G, the northern part of quadrant L and quadrant M. A similar log facies is also encountered in wells P8-1 and P13-1, in the southern part of the study area. Cyclicity is most pronounced in boreholes A18-1, E12-1, F12-1, F15-1 and M9-1. A predominantly chaotic ('a-periodic') log response is encountered around the Broad Fourteens Basin (Fig. 1.8). This area encompasses most of quadrants K, southern L and the northern and eastern part of quadrant P. Wells B17-2, F2-2 and F2-7, all positioned in the Dutch Central Graben, show a similar chaotic log response.

4.4.3 Metre-scale cyclicity

An overview of the average wavelength of dominant cycles per well, as well as the log tool in which these are preserved, is given in Table 4.2. Two sets of dominant cycles were found in the studied well-logs, with average wavelengths of about 5 to 7 metres and 2 to 3 metres.

The well logs of profile A (Fig. 4.2), and in particular the sonic log of F15-1 (Fig. 4.6), provide the best examples of metre-scale cyclicities in the Chalk succession of the study area. In this profile, unit 1 does not show a convincing cyclicity, as the sub-units are thinner than the 40 m sliding window used for the frequency analysis.

Figure 4.6 ***(facing page)*****:** Sonic log of F15-1, with filtered (showing $\lambda > 2$ m) and unfiltered frequency spectrum scalograms. Frequency spectra at depths A–E show the Milankovitch cycles recognised in this log. Log interval 6 (2300–1750 m) shows well developed cyclicity, with a gradual upwards wavelength decrease. **See Fig. 4.6 (page 157) in Appendix - Colour plates for a colour version of this figure.**

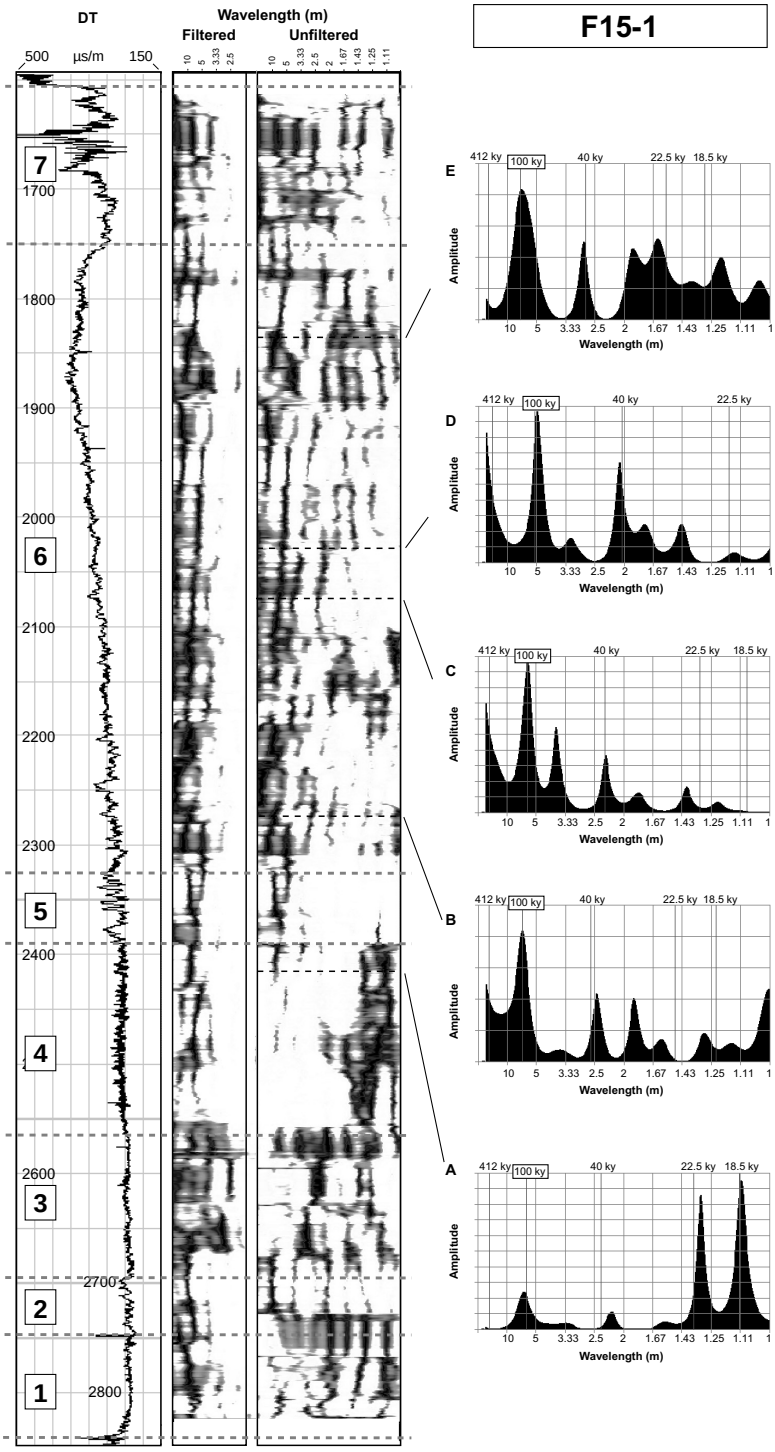
F15-1
DT
500 µs/m 150
Wavelength (m)
Filtered
Unfiltered
10 5 3.33 2.5 2 1.67 1.43 1.25 1.11
7
1700
1800
1900
2000
6
2100
2200
2300
5
2400
4
2600
3
2700
2
1
2800
E
D
C
B
A
412 ky
100 ky
40 ky
22.5 ky
18.5 ky
Amplitude
Wavelength (m)

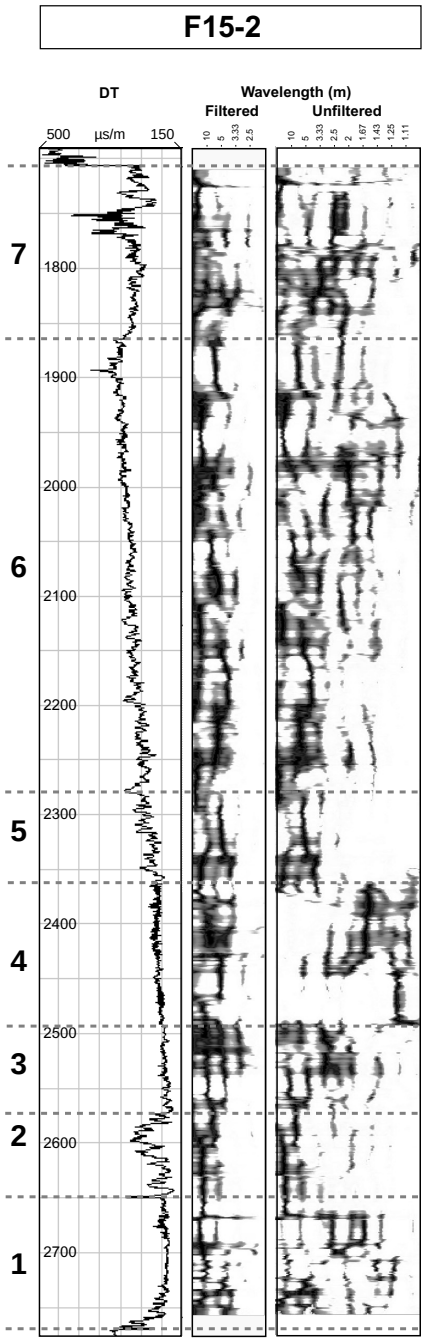

Figure 4.7: Sonic log of F15-2, with filtered (showing $\lambda > 2$ m) and unfiltered frequency spectrum scalograms. **See Fig. 4.7 (page 158) in Appendix - Colour plates for a colour version of this figure.**

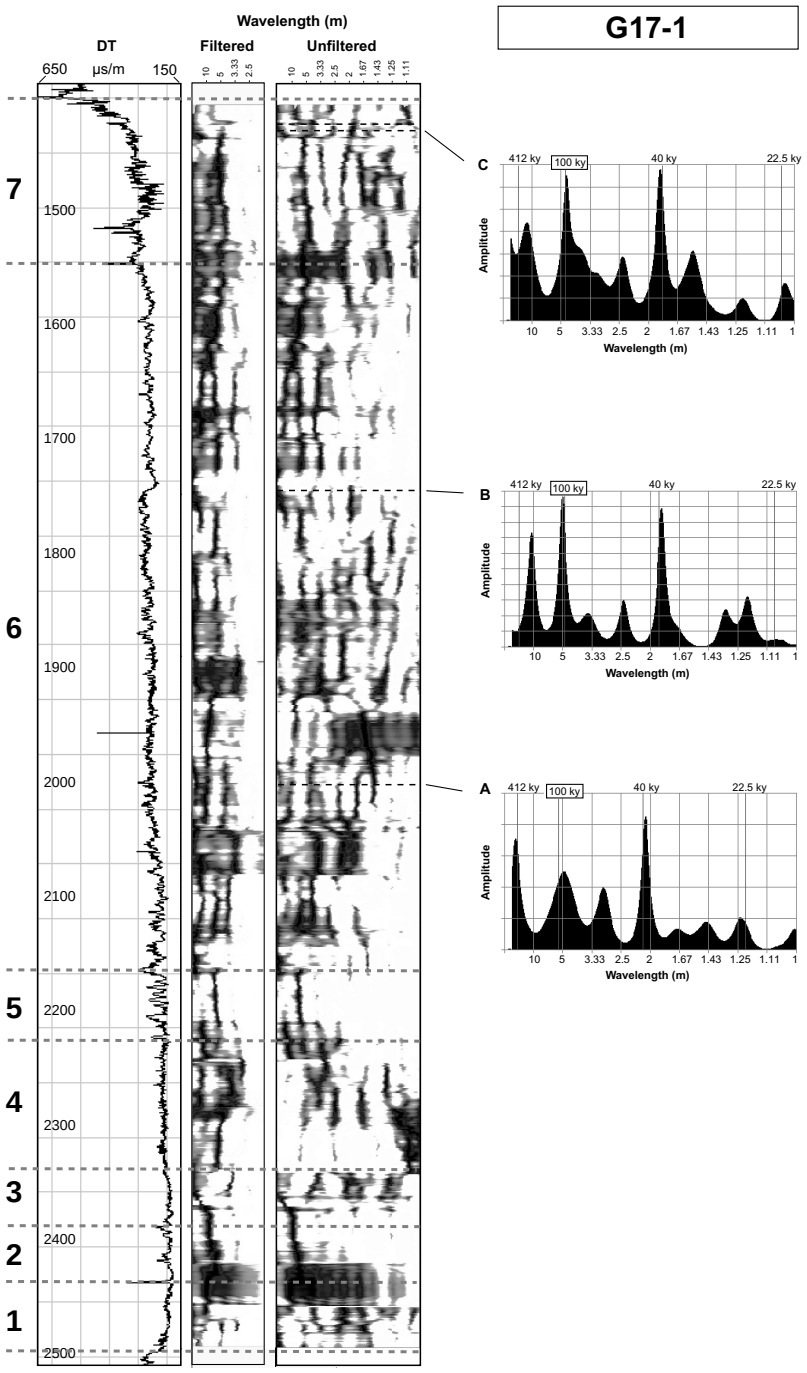

Figure 4.8: Sonic log of G17-1, with filtered (showing $\lambda > 2$ m) and unfiltered frequency spectrum scalograms. Frequency spectra at depths A–C show the the Milankovitch cycles recognised in this log. **See Fig. 4.8 (page 159) in Appendix - Colour plates for a colour version of this figure.**

Unit 2 does show a strongly cyclic character with a dominant wavelength (λ_{dom}) of 7–10 m. Unit 3 again shows a less well developed cyclicity, with a λ_{dom} of 2–3 m (unclear in G17-1; Fig. 4.8), which decreases stepwise towards the top (thinning upward). The dominant wavelength of unit 4 is below 1.5 m, with apparently not very pronounced cyclicity. In contrast, unit 5 shows a cyclicity similar in character and dominant wavelength (7–10 m) to unit 2.

In profile A, units 6 show the most striking cyclic features encountered in the studied well log dataset. Cyclicity is most pronounced in F15-1 (Fig. 4.6). Here, a major thinning upward trend is expressed by upwardly decreasing λ_{dom}-values, from 15 m to 3.5 m, with strong associated larger and smaller wavelength cyclicities. Although less pronounced, the dominant cyclicity alignment in unit 6 of G17-1 (Fig. 4.8) also shows a similar thinning upward trend, with wavelength decreasing from 10 m at 2060 m depth to 5.2 m at 1830 m, then subtly increasing to 5.5 m at 1615 m and again decreasing to 3.8 m at the lower portion of unit 7, at a depth of 1520 m. As in F15-1, strongly developed associated cyclicities are present throughout unit 6. Least clearly developed, a stepwise thinning upward trend is visible in unit 6 of F15-2 (Fig. 4.7), with λ_{dom} decreasing from 5.6 m to 1.9 m. With respect to cyclic frequency content, unit 7 in all wells of profile A appears to be a continuation of unit 6, with dominant wavelengths of about 2 m in high amplitude upper part of this unit.

The sonic log of E14-1 (Fig. 4.10) is the only well presented here in which all seven well log units have been recognised, outside of profile A. In all wells of profile B (Fig. 4.2), the basal log unit does not show convincing cyclicity. Unit 2 shows cyclicity with dominant wavelengths of about 10 m. Units 3 and 4 contains several smaller frequencies with wavelengths decreasing upwardly. Unit 5 (not present in D15-1; Fig. 4.9) shows a strongly developed 7 to 10 m cyclicity. The frequency content of units 2 to 5 in this profile, particularly in E14-1 (Fig. 4.10), resemble that of profile A. Finally, dominant wavelengths in units 6 and 7 show a steady upward decrease (thinning upward) trend, from $\lambda_{dom} = 15$ m at 1840 m to $\lambda_{dom} = 4$ m at 1610 m in E14-1 (Fig. 4.10).

The gamma-ray logs of profile B generally contain shorter wavelength cycles compared to sonic logs of the same stratigraphic interval. The frequency content of the gamma-ray log of D15-1 (Fig. 4.9) indicates for the largest part a single dominant cyclicity, with wavelengths of 2–2.5 m and 3.15 m. The gamma-ray logs of E14-1 (Fig. 4.10) and F12-1 (Fig. 4.11), on the other hand, contain several associated cycles. It is important to note that while several associated cycles are present in stratigraphic intervals that are several hundreds of metres thick, different cycles are dominant in different intervals. This is clear in E14-1 (Fig. 4.10), for instance, where between 1850 m and 1780 m a 1.15 m cycle is dominant, while the associated 1.75

m cycle 'takes over' as dominant cyclicity between 1775 m and 1690 m. Finally, the continuous thinning upward trend of Units 6 and 7 is clearly visible in the gamma-ray logs as well.

In the sonic logs of profile C (Fig. 4.2), the well log units described above are more difficult to recognise. Log unit 1 does not show a pervasive cyclicity, although of several well-defined 5 metre-scale cycles can be observed, particularly in L7-H-1 (Fig. 4.12) and L5-1 (Fig. 4.13). The overlying 'serrated' log unit 2 contains cycles with a wavelength of about 5 m. Unit 2 cannot be distinguished in well L5-1 (Fig. 4.13). The equivalent of units 3 and 4 contain numerous coinciding frequencies, with only L7-H-1 (Fig. 4.12) showing a dominant cyclicity of about 1.25 m wavelength. The serrated sonic log unit 5 is most strongly developed L7-H-1 (λ_{dom} = 3 m). The upper part of the Chalk succession (Units 5 and 6) in the sonic logs of profile C is less continuous than the stratigraphic equivalents in profiles A and B. In all wells of this profile, unit 5 includes several smaller intervals with variable cyclic characters. The thinning upward trend described earlier is, although less clear, discernible in L7-H-1 and M9-1 (Fig. 4.14). In the L7-H-1, this trend is visible as a stepwise to fairly continuous decrease of dominant wavelength from 2.3 m at 1700 m, to 1.5 m at 1477 m.

The wavelength ratio between the often-observed 5 to 10 metre dominant cyclicity and the roughly 2 to 3 metre associated cyclicity, the latter usually most clearly visible in the gamma-ray logs, is about 2.5 to 1 in most wells. This ratio resembles that of the 100 ky eccentricity and 40 ky obliquity cycle. This is particularly the case in F15-1 (Fig. 4.6), where these Milankovitch cycles best fit the frequency spectrum throughout unit 6 (spectra B to E).

4.4.4 Identification of Milankovitch cycles

As mentioned in Section 4.3, cyclicity modes were assessed by looking for specific cyclicity wavelength ratios in the logs and comparing these to the known wavelength ratios between different Milankovitch cycles (Fig. 4.1; Fig. 4.3). This was done assuming periodic log responses to be caused by Milankovitch-style climatic variations.

Associated cycles, including the 50 ky obliquity (spectra C and D) are present in smaller intervals as well. On the same grounds, the 5 m cycle in unit 6 and 7 of G17-1 (Fig. 4.8) is interpreted to be the 100 ky E1, with the strong peaks around 2 m wavelength being the 40 ky O1 (spectra A, B and C). The strong 10–20 m cyclicity observed throughout this log unit must then be the 412 ky eccentricity cycle, although the observed wavelength is usually shorter.

In the remaining sonic logs, a strong 100 ky E1 ($\lambda \sim 7$ m) with weaker associated

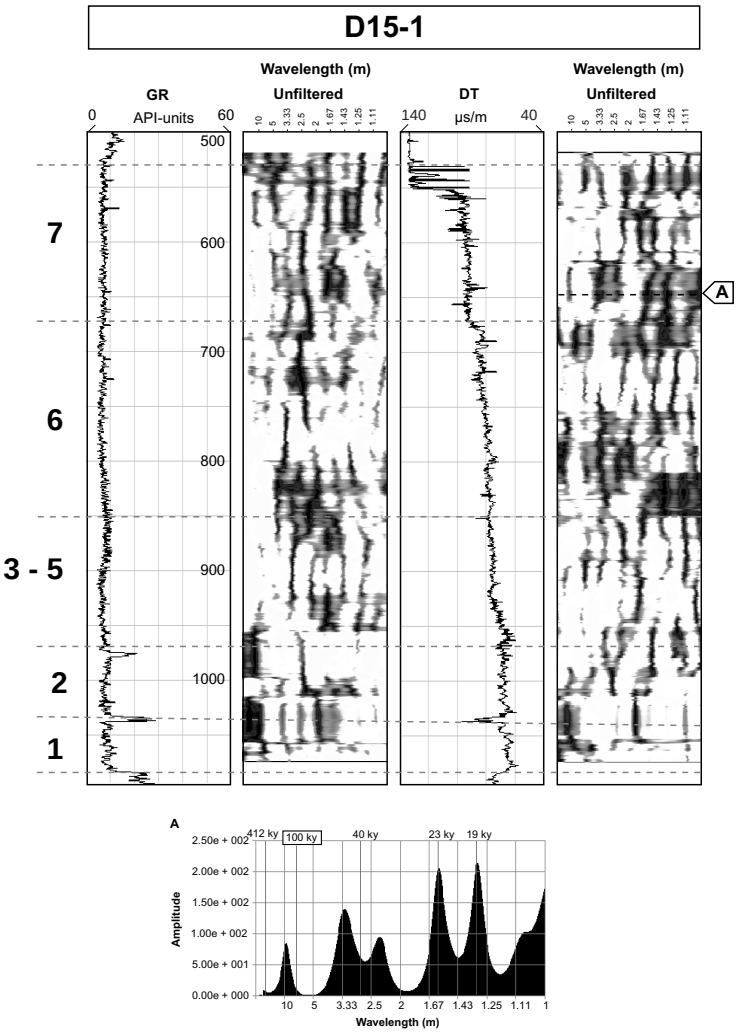

Figure 4.9: Gamma-ray and sonic log of D15-1 with frequency spectrum scalograms. Average frequency spectrum A shows Milankovitch cycles recognised in this log. **See Fig. 4.9 (page 160) in Appendix - Colour plates for a colour version of this figure.**

40 ky O1 ($\lambda \sim 2$) m cyclicity is interpreted in unit 6 and 7 of L5-1 (Fig. 4.13, spectrum B) and M9-1 (Fig. 4.14). In the unfiltered sonic log of L7-H-1 (Fig. 4.12), a good fit is observed between the 40 ky and 23 ky cycles, with alternating dominance of the

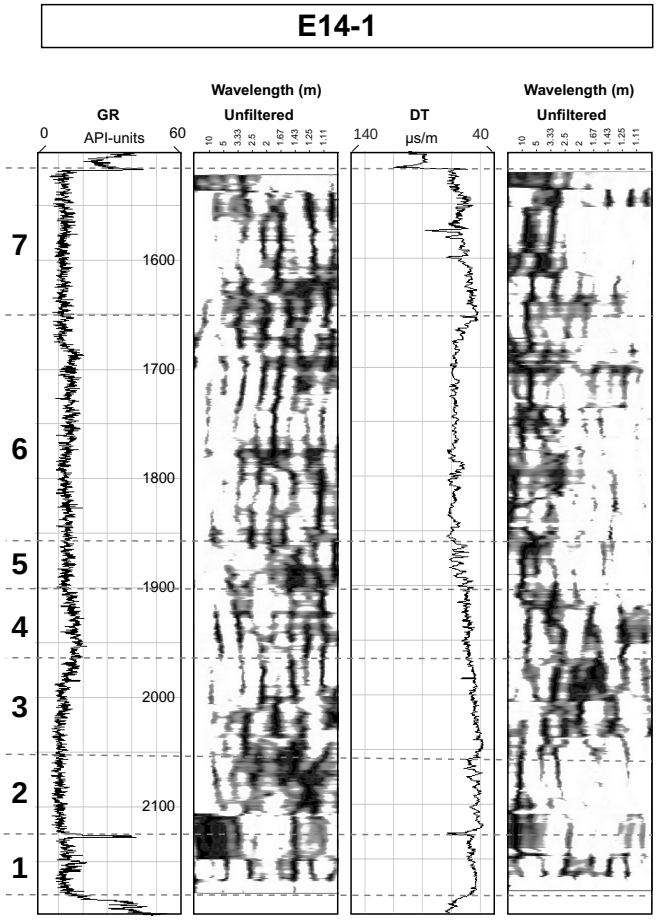

Figure 4.10: Gamma-ray and sonic log of E14-1 with frequency spectrum scalograms. **See Fig. 4.10 (page 161) in Appendix - Colour plates for a colour version of this figure.**

40 ky cycle (spectrum B) and the 23 ky cycle (spectra A and C). Here, the 100 ky cycle is observed more clearly in the filtered sonic log. In unit 6 and 7 of the sonic log of D15-1 (Fig. 4.9), two smaller spectral peaks with wavelengths of about 1.45 m are observed (spectrum A). These best fit the wavelength ratios of the 19 ky and 23 ky precessional cycles, with weaker 100 ky and 40 ky signals being present as well.

In the lower section of these sonic logs, the typical succession of high frequency/low amplitude (units 1, 3 and 4) and low frequency/high amplitude (units 2 and 5) log

responses has been recognised in the entire study area (Section 4.4) and is particularly well defined in profile A. This is well illustrated in F15-1 (Fig. 4.6) in units 4 and 5. In unit 4, two peaks are observed in the frequency spectrum that are most likely the 19 ky and 23 ky precessional cycles (spectrum A). Smaller peaks (better defined in the filtered log) are found fitting to the 100 ky E1 (λ = 7 m) and 40 ky O1 (λ = 2.25 m) cycles. Moving upward into unit 5, the 7 m long E1 cycle becomes dominant and the smaller frequencies disappear. Comparing the filtered and unfiltered logs, the 100 ky E1 is present in most of the lower log units of the Chalk, but it is in some instances overshadowed by strong high frequency cyclicity. As another example, the 100 ky E1 is visible in the filtered log in unit 1 and becomes dominant in unit 2, again leading to a strongly serrated, low frequency/high amplitude, log pattern. Moving into unit 3, the 40 ky O1 (λ = 2.7 m) becomes the strongest. Similar shifting cyclicity patterns are observed in all other sonic logs of the study area.

In gamma-ray logs, usually smaller cycle wavelengths are dominant compared to the same intervals in the sonic log. In certain interval of units 3–5 and 6 of the GR-log of M9-1 (Fig. 4.14), the 40 ky O1 forms a continuous spectral peak, with wavelengths varying from 3.3 m (spectrum A) to 2.25 m (spectrum B). This can be particularly well fitted with the 23 ky precession cycle and, to a lesser extent, the 19 ky cycle as well. In the gamma-ray logs of F12-1 (Fig. 4.11; spectra A and B), the double spectral peaks of both precessional cycles can also be seen.

4.5 Discussion

4.5.1 Spectral log facies

From the spectral log facies characterisation presented in Fig. 4.5, as well the frequency scalograms presented in Figs. 4.6 to 4.14, it is clear that marked variations exist between the frequency spectra of different log intervals in the Chalk. Several reasons have been presented for such variations. Niebuhr & Prokoph (1997) describe autochthonous chalk as characterised by periodic repetitions of log signals of one or more order. In contrast, chalk intervals formed by chaotic sedimentation contain aperiodic successions, high frequency non-cyclic changes, discontinuities and sudden breaks. Stage (1999) modelled the effect of hiatuses and variations in sedimentation rate on the frequency spectrum. In a time series consisting of cycles with a single frequency, sediment removal by hiatuses resulted in a shift of the main spectral peak towards a smaller wavelength, with increasing levels of noise. By increasing the variation in sedimentation rate, signal to noise ratios decrease progressively.

The spectral log facies of the Chalk in the Netherlands offshore partly reflects sed-

imentation conditions controlled by syn-depositional tectonic movements (Fig. 4.5). In the areas north and south of the Broad Fourteens Basin (Fig. 1.8), well logs generally have an aperiodic log response character with frequency spectra showing predominantly noise. This observation suggests chalk sedimentation to have been largely allochthonous here. Seismic interpretation showed these areas to be 'marginal throughs', developed alongside the inverted Broad Fourteens Basin (Section 3.2). Marginal throughs in other parts of NW Europe contain thick successions of mostly allochthonous sediment (i.e. slumps, slide sheets), derived from the central rising block (Kockel, 2003). Interestingly, the seismic facies of the Chalk around the Broad Fourteens Basin is very regular, indicating that the allochthonous chalk bodies that moved into the marginal throughs were too small to be resolved on seismic data, i.e. smaller than several tens of metres (Section 3.5). A number of wells in the Dutch Central Graben also show largely chaotic log responses. Here too, massive reworking of chalk occurred, as is described in Section 3.4. However, the influence of the uplifting Dutch Central Graben on chalk sedimentation in surrounding areas was less. This is because the inversion of the Dutch Central Graben was much less dramatic than that of the Broad Fourteens Basin, in both uplift and areal extent.

Cyclicity is best developed in areas that remained relatively stable during deposition of the chalks (Fig. 4.5; Section 3.3). Periodic intervals of up to a few hunderd metres are therefore encountered in the Schill Grund High (F12-1 and F15-1), Ameland Block (M9-1), Cleaver Bank High (E12-1) and the western part of the Step Graben (A18-1)

4.5.2 Metre-scale cyclicity

Rhythmic bedding in chalk is caused by cyclic variations in carbonate productivity, terrigenous dilution, redox conditions and bottom currents (R.O.C.C., 1986). In our well logs, periodicity is developed as cyclic variations in porosity ($\lambda_{dom} \sim$ 10–5 m) in sonic and density logs and clay content ($\lambda_{dom} \sim$ 3–2 m) in gamma-ray logs. Stage (2001a), based on analysis of the insoluble residue of Maastrichtian chalk, concludes that the cyclic variations in magnetic susceptibility, which is a measure of clay content, is due to changes in detrital runoff into the basin. Low sediment accumulation rates, often attributed to the winnowing effect of bottom currents, leads to the formation of tight zones, hard grounds and flint layers, which show up on sonic and density logs as porosity minima as well (Hancock, 1975; Scholle; 1977; Zijlstra, 1994, 1995). During compaction, initial porosity variations become more pronounced (Scholle, 1977; Herbert, 1993). The difference in dominant cyclic wavelength observed in the sonic log compared to the gamma-ray log indicates the sensitivity of clay sedimentation to smaller (40 ky O1) astronomical cycles, compared

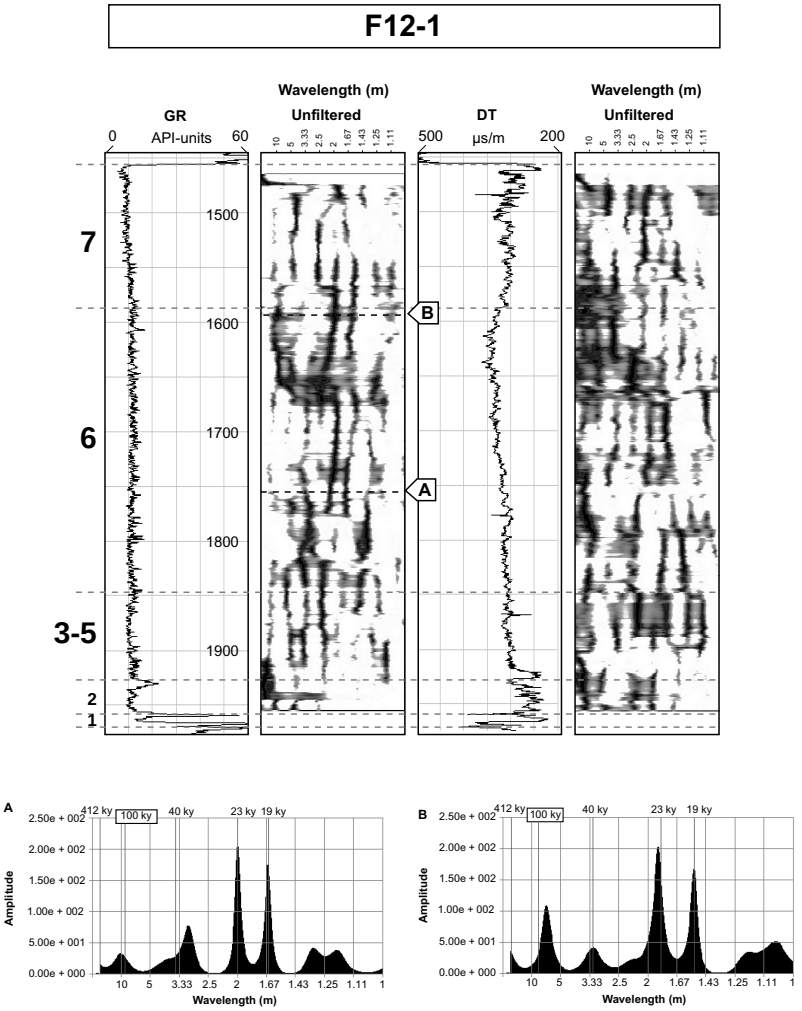

Figure 4.11: Gamma-ray and sonic log of F12-1 with frequency spectrum scalograms. Average frequency spectra A and B show Milankovitch cycles recognised in this log. **See Fig. 4.11 (page 162) in Appendix - Colour plates for a colour version of this figure.**

to the carbonate sedimentation rate.

An important feature of the sonic log response of the lower Chalk units throughout the study area are the high-frequency/low amplitude cyclic variations in units 3 and 4, while the log units above and below this level show a high-amplitude/low

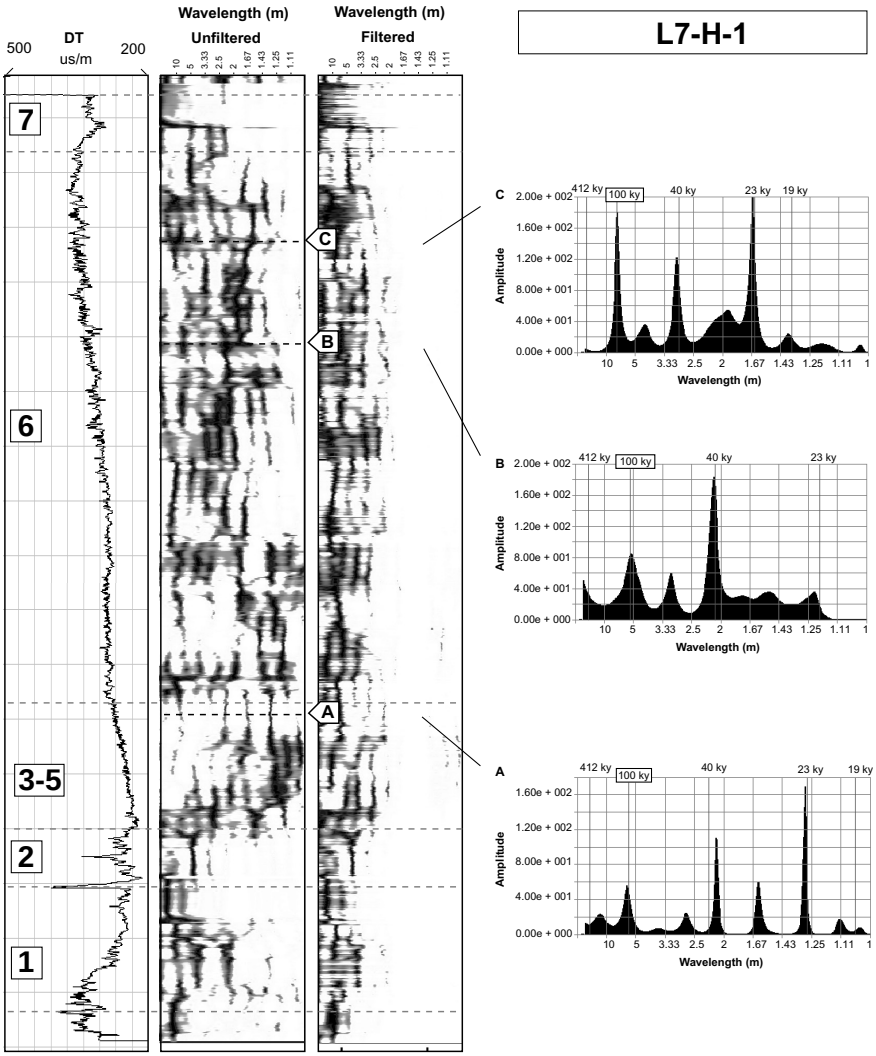

Figure 4.12: Sonic log of L7-H-1, with unfiltered and filtered (showing $\lambda > 2$ m) frequency spectrum scalograms. Average frequency spectra A–C show Milankovitch cycles recognised in this log. **See Fig. 4.12 (page 163) in Appendix - Colour plates for a colour version of this figure.**

frequency response. The wavelength ratio suggests a shift from dominance of the 100 ky eccentricity cycle to the 19/23 ky precession cycles which occurs moving

upward from unit 2 into unit 3 and 4, with the reverse happening at the boundary between unit 4 and 5. The regional character of these shifts indicates basinwide alterations of the Chalk sedimentation system, probably due to climatic shifts, took place during the Turonian to Santonian. The nature of these alternations remains unclear, however. The upwardly decreasing spectral wavelength trend in log unit 6 and 7, which is observed in most wells of profile A, B and C and is particularly well defined in F15-1 (Fig. 4.6), forms one of the most interesting features of the studied dataset. The trend indicates a gradual decrease in sedimentation rate throughout the Campanian to lower Maastrichtian that is even more pronounced than is immediately obvious because it is overprinted by a downward increasing compaction trend. Although local conditions clearly favoured the preservation of a continuous record at the location of well F15-1, the fact that upwardly decreasing wavelengths are found in most of the logs from the base of unit 6 upwards, points to a regional control. The most obvious cause for this trend is a gradual decrease in primary carbonate production during the Campanian and Maastrichtian. Interestingly, Jarvis et al. (2002) describe a gradual decrease of $d^{13}C$-values throughout the Campanian and Maastrichtian interval of the Trunch borehole in Norfolk (UK). The authors correlate this isotopic pattern to sections in SW France and Tunesia. Decreasing $d^{13}C$-values indicate decreasing productivity and/or decreased burial and preservation of marine phytoplankton (Scholle & Arthur, 1980; Jenkyns et al., 1994; Jarvis et al., 2002). The trend in upward cyclic wavelength decrease observed in the Campanian and Maastrichtian sections of the studied well logs is therefore most likely the result of a global decrease in carbonate productivity.

4.5.3 Identification of Milankovitch cyclicity and inferred net accumulation rates

The cycles described in the logs from the Dutch offshore are comparable to those found in SP-logs from the North German Basin in both wavelength and cycle mode (Section 4.2; Niebuhr & Prokoph, 1997). However, an important discrepancy exists between the interpretation of Milankovitch cycles presented in this study, and the majority of outcrop and core studies discussed in Section 4.2.

In the present study, the 5–7 m cycles have been interpreted to be the 100 ky eccentricity cycle. The best examples of these cycles are found in unit 6 of well F15-1 (Fig. 4.7). From Fig. 2.20 it follows that this log unit is of Campanian to early Maastrichtian age. Unit 6 represents about 9 My in time, assuming the 5–7 m cycle is indeed a 100 ky E1 cycle. This figure fits the known duration of the Campanian to early Maastrichtian (about 15 My), indicating that a substantial part of the succession is missing. However, if the 5–7 m cycles represent the 412 ky eccentricity

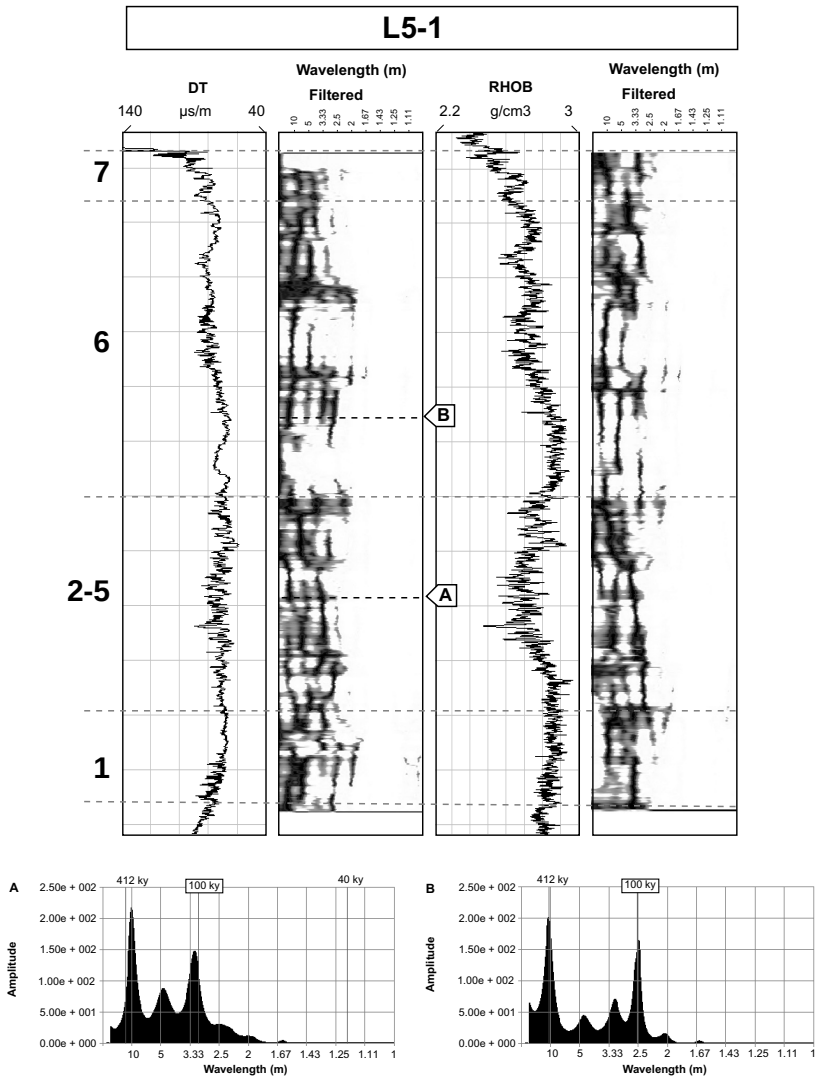

Figure 4.13: Sonic and density logs of L5-1 with frequency spectrum scalograms. Frequency spectra at depths A and B indicate Milankovitch cycles recognised in the logs. **See Fig. 4.13 (page 164) in Appendix - Colour plates for a colour version of this figure.**

cycle (E2), log unit 6 represents a time period of about 38 my. Such an assumption compares well with the cycle mode interpretations of most outcrop and core studies,

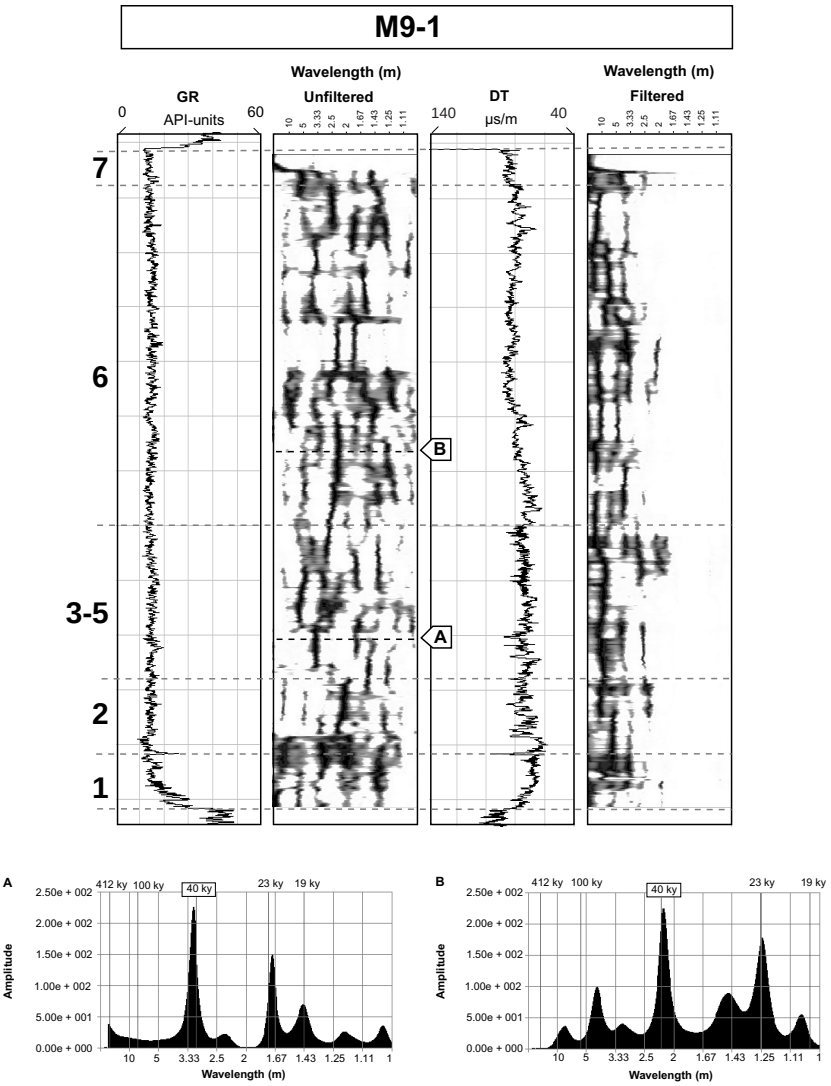

Figure 4.14: Gamma-ray log with unfiltered frequency spectrum scalogram and sonic log with filtered (showing $\lambda > 2$ m) frequency scalogram of M9-1. Frequency spectra at depths A and B indicate Milankovitch cycles recognised in the gamma-ray log. **See Fig. 4.14 (page 165) in Appendix - Colour plates for a colour version of this figure.**

e.g. the 8.25 m long E2 described by Cottle (1989), but the duration of 38 my is clearly far too long for this to be correct.

From the above follows that the average net accumulation rate, i.e. not corrected for compaction, is about 5 to 7 cm/ky, at least during the Campanian to early Maastrichtian. This estimate is similar to that of Niebuhr & Prokoph (1997), who describe net accumulation rates of 6 to 12 cm/ky in the North German Basin (Section 4.2). The accumulation rate of about 2.5 cm/ky estimated for the Turonian to Maastrichtian of the Dan field (Herrington et al., 1991; Stage, 1999, 2001b) concurs with sedimentation rates estimated from outcrop studies throughout Europe, which are backed up by extensive biostratigraphical data (Hart, 1987; Ditchfield & Marshall, 1989; Gale, 1989; Gale et al., 1999; Wendler et al., 2002). However, Scholle et al. (1998) proposed continuous sediment winnowing as a possible cause for thickness variations across the Dan Fields, and further into the basin. The wells from the Netherlands offshore presented in this study are all positioned away from salt diapirs. The higher net accumulation rates deduced here may therefore reflect pelagic sedimentation unaffected by winnowing, or even enhanced sedimentation through sediment supply by bottom currents.

In the aforementioned studies of outcrops in the UK and France, accumulation rates of about 2.5 cm/ky, with 2 m periodicity usually identified as the 100 ky E1, are typically determined for the Cenomanian and Turonian (Section 4.2). As is clear from paleogeographical maps of the Cenomanian, the outcrops were located near basin edges in the Cenomanian, where as the wells from the present study were located near the centre of the basin (Fig. 1.7). It is logical to assume that more accommodation space was available in the centre of the basin compared to the edges explaining the higher accumulation rates determined in the present study compared to outcrops.

4.6 Conclusions

- Where deposition of the Chalk took place under relatively stable syn-depositional tectonic conditions, well logs contain metre-scale cyclic intervals that are most likely the result of orbitally forced climate variations. In the study area, good examples are found in the Schill Grund High and Ameland Block.

- Well logs from areas that underwent intense syn-depositional tectonic activity show a predominantly non-cyclic log response, most likely representing reworked chalks. The chalk in the marginal through north of the Broad Fourteens Basin is thus shown to be mostly allochthonous, as is that of the Dutch Central Graben.

- In autochthonous chalk, cyclic log response variations of different frequencies occur simultaneously. These cyclic variations most commonly show wave-

lengths of about 5–7 m and 2–3 m.

- Regionally correlated shifts between low-frequency/high-amplitude and high-frequency/low-amplitude sonic and density log response indicate that alterations of the Chalk sedimentation system, probably due to climatic variations, took place during the Turonian to Santonian.

- The Campanian to lower Maastrichtian sections of autochthonous chalk interval show a gradual upward decrease in cycle wavelength that most likely reflects a global decrease in carbonate productivity.

- Based on the specific wavelength ratio between the 5–7 m and the 2–3 m cyclicity in most wells, these are interpreted to represent the 100 ky eccentricity (E1) and 40 ky obliquity (O1) cycles respectively. From this follows that average net accumulation rates of the Chalk are about 5 to 7 cm/ky.

Well	z_{TopCK}	z_{BaseCK}	Δ_{CK}	GR	DT	RHOB	RES	Bio
A16-1	1700	2031	331	•	•	•	•	•
A18-1	2126	2492	366	•	•	•	•	•
B13-1	1802	2302	500	•	•	•	•	
B14-1	1896	2199	304	•	•	•	•	•
B17-2	1818	2693	875	•	•	•	•	•
D12-1	948	1467	519	•	•		•	
D15-1	509	1084	575	•	•		•	•
E9-1	1718	2190	472	•	•	•	•	
E12-1	1582	2029	447	•	•		•	•
E14-1	1518	2184	666	•	•	•	•	
E16-1	1025	1632	607	•	•		•	
E17-1	968	1539	571	•	•		•	•
E18-1	1472	2032	561	•	•	•	•	•
F2-2	1888	2396	508	•	•			
F2-7	1933	2343	410	•	•			•
F3-4	1858	2277	419	•	•		•	

Table 4.3: Well database overview, indicating availability of gamma-ray (GR), sonic (DT), density (RHOB), and resistivity logs (RES), as well as biostratigraphical reports (Bio). See Fig. 4.2 for well locations. (Continued on facing page).

Well	z_{TopCK}	z_{BaseCK}	Δ_{CK}	GR	DT	RHOB	RES	Bio
F4-2A	1948	2525	577	•	•	•	•	
F5-1	1859	2254	395	•	•	•	•	•
F12-1	1456	1966	510	•	•	•	•	•
F15-1	1605	2838	1233	•	•		•	
F15-2	1704	2766	1062	•	•			
F18-1	1590	1870	280	•	•		•	
G17-1	1402	2546	1144	•	•		•	
K2-2	1585	3047	1462	•	•			
K4-2	1130	2120	990	•	•			
K7-3	988	1895	906	•	•	•		
K8-8	1110	2239	1129	•	•	•		
K11-8	1563	3378	1815	•	•	•		
K11-12	1370	2098	728	•		•		
L5-1	1682	2294	611	•	•	•		
L7-H-1	1439	2237	798	•	•	•		
L8-2	1675	3134	1459	•	•			
L9-2	1726	2473	747	•	•			
L14-2	1345	2705	1360	•	•			
L16-4	875	2531	1656	•	•			
M9-1	1155	1760	605	•	•	•		•
P1-2	837	1689	853	•	•	•		
P4-1	870	2173	1303	•	•	•		
P8-1	781	1579	798	•	•	•		•
P12-1	647	1362	715	•	•			•
P13-1	872	1288	416	•	•	•		
Q2-4	944	2331	1387	•	•			
S2-1	1057	1531	474	•	•			

Chapter 5

Acoustic velocity and burial history analysis of the Chalk Group, Netherlands North Sea area

The acoustic velocities of the sediments of the Chalk Group were determined to study its burial history. This was done by dividing true vertical depth thickness of the Chalk, derived from a well database, by its two-way travel time thickness, derived from the interpretation of 2D-seismics. By calculating the interval velocity where a well was within 500 m distance from a seismic line, 130 measurements could be made. Additionally, mean sonic velocity of the whole Chalk interval, as well as of newly established lower, middle and upper log units, were calculated from 43 sonic logs. Velocity gradient (k) and theoretical initial velocity (V_0) were calculated of both velocity datasets and individual sonic logs. The acoustic velocity of the Chalk is highly variable, with values ranging from 2200 to 5300 m/s. The primary control on acoustic velocity is burial depth, with regional variations in burial history forming a secondary control. Velocities are consistently lower than expected at present depth in the north of the study area, indicating undercompaction, probably as a result of rapid burial under impermeable clays. In contrast, high velocities are found throughout the south, indicating overcompaction, probably due to uplift. The velocity gradient in individual logs is usually greater than that derived from interval velocities of the whole area. This is probably due to the overlying low-permeable clays, causing escaping formation water to remain in the upper sections of the Chalk.

5.1 Introduction

Chalk consists for over 95% of low-magnesium calcite, with little or no lithological variations throughout the NW European region. Low-magnesium calcite is stable and therefore prohibits chemical alteration of chalk until great burial depths. (Hancock, 1975; Scholle, 1977; Jorgenson, 1986). As a result, compaction of chalk is largely mechanical during the first stages of burial, decreasing porosity from 70 % at the sea floor to about 35 % at one kilometre depth. Below this depth, the sediment is tight enough for grain contacts to become established. Increasing burial and subsequent grain-to-grain stresses lead to pressure solution and occlusion of pores by precipitation of calcite, thus rapidly reducing porosity (Scholle, 1977; Brasher & Vagle, 1996; Grützner & Mienert, 1999; Mallon & Swarbrick, 2002). Due to its monomineralic nature, the acoustic velocity of chalk is primarily controlled by its porosity (Campbell & Gravdal, 1995; Japsen, 1998; Anderson, 1999). Porosity reduction leads to an increase of acoustic velocity of a rock because the high-velocity rock matrix fraction (V_p of calcite: 6530 m/s) of the total rock volume increases at the expense of the low-velocity pore fraction (e.g. water: $V_p = 1500$ m/s; Wyllie et al., 1958; Gardner et al., 1974).

Several normal-compaction curves have been published that quantify the normal compaction of the Chalk in terms of decreasing porosity or increasing velocity (Scholle, 1977; Bulat & Stoker, 1987; Hillis, 1995; Japsen, 1998; Mallon & Swarbrick, 2002). Basin-wide variations in Chalk compaction are controlled by overpressuring and post-depositional vertical movements (Scholle, 1977; Brasher & Vagle, 1996). Normal velocities and porosities are encountered where pore fluid drainage rates were high enough to allow compaction after deposition. However, where pore drainage has been obstructed, higher porosities are retained in the buried rock than would normally be expected at a particular burial depth. Such undercompacted rock intervals have a lower than normal acoustic velocity. Furthermore, as the pore fluids bear a large part of the overburden stress, overpressures arise in these areas. Alternatively, sediment that was previously buried deeper and was therefore more compacted, has a lower porosity than expected at a particular burial depth after uplift. Such sediment is overcompacted and shows higher than normal acoustic velocities (Scholle, 1977; Bulat & Stoker, 1987; Hillis, 1995; Brasher & Vagle, 1996; Caillet et al., 1997; Japsen, 1998).

In addition to the regional controls discussed above, compaction of North Sea chalk is locally controlled by depositional mechanisms and hydrocarbon migration (Scholle, 1977; Brasher & Vagle, 1996). When initially compacted chalk is reworked as, for instance, a slump or debris flow deposit, the sedimentary fabric breaks up and the resulting allochthonous sediment body can remain less compacted than the

enveloping autochthonous chalk. Such structures traditionally formed important hydrocarbon targets in chalks (Hatton, 1986; Kennedy, 1987; Taylor & Lapré, 1987; Friedman, 1996). Furthermore, early entry of hydrocarbons into the sediment halts the chemical compaction otherwise active at burial depths below about one kilometre. This effect explains the anomalously high porosities of up to 30 % encountered in hydrocarbon-bearing chalks in the central North Sea area (Scholle, 1977; Kennedy, 1987). However, as Mallon & Swarbrick (2002) pointed out, such reservoirs form a minor part of the total North Sea Chalk volume and therefore cannot be expected to influence the regional velocity distribution of this interval considerably.

The study of acoustic velocities, as a measure of porosity, yields information on the post-depositional compaction history of the Chalk (Bulat & Stoker, 1987; Davis, 1987; Hillis, 1995). Furthermore, acoustic velocity information is needed for time-depth conversions of seismic sections through this interval.

In the present study, the interval velocity V_{int} (m/s) of the Chalk Group was determined by dividing travel time 'thickness', derived from seismics, by true vertical depth thickness derived from well data. This was done where a well was located on or very near (within 500 m) a 2D-seismic line. Velocity gradient $k_{V_{int}}$ (m/s/m) was calculated to study the influence of burial depth on the interval velocity. Furthermore, the regional distribution of interval velocities was studied as well, partly to determine the influence of post-depositional vertical movements, as expressed by theoretical initial velocity $V_{0\,V_{int}}$ (m/s).

Mean sonic velocity V_{μ} (m/s) of the whole Chalk interval and three separate log units was determined from sonic logs. Similar to the V_{int}-dataset, velocity gradient $k_{V_{\mu}}$ (m/s/m) and theoretical initial velocity $V_{0\,V_{\mu}}$ (m/s) were calculated from this mean sonic velocity dataset as well. The compaction of the Chalk was then studied in more detail by determining the velocity gradient k_{log} (m/s/m) and theoretical initial velocity $V_{0\,log}$ (m/s) for all log units of each individual well.

The interval velocity data were compared to the normal compaction trend of Japsen (1998) to quantify the undercompaction (i.e. overpressures) and overcompaction (i.e. uplift) of the Chalk throughout the Netherlands offshore area.

5.2 Published compaction trends for the Chalk

Japsen (1998) and Mallon & Swarbrick (2002) provided comprehensive overviews of published compaction trends for the Chalk. The trends described the compaction of chalk with increasing burial depth in terms of decreasing porosity or increasing acoustic velocity (Fig. 5.1). To enable direct comparison between these, velocity

values were converted to porosity values using the following equations (Japsen, 1998).

$$\phi = 1.15 - 2.83 \cdot 10^{-4} V \qquad (1600\ m/s < V < 2700\ m/s,\ \phi < 40\%) \tag{5.1}$$
$$\phi = 1 - (V/6403)^{0.57} \qquad (V > 2700\ m/s,\ \phi > 40\%)$$

Here, ϕ is porosity (in %) and V is velocity (in m/s). A discussion of the compaction trends considered in the present study is given below.

Scholle (1977) presented a compaction curve for southern North Sea chalk based on porosity measurements on well L16-1 from the Dutch offshore. According to this curve, the porosity of the Chalk decreases from about 30 % at a burial depth of 1200 m to about 10 % at 2200 m. The compaction at shallower depths was based on Deep Sea Drilling Project-data from the Atlantic and Pacific oceans and measurements from the Scotian Shelf of Canada. This data suggest that the porosity trend observed in L16-1 can be extended up to the sea floor, where initial porosity is 70 %. Scholle (1977) considered this a typical compaction trend for chalks, whereby the sediment was saturated with marine pore fluids and no uplift occurred.

Bulat & Stoker (1987) calculated interval velocities for the Chalk Group in 300 released wells in the British sector of the southern North Sea area. The authors considered the lowest observed velocities at a certain depth to represent (closest to) normal compaction. Thus, a linear velocity-depth trend was determined that estimated the velocity as follows:

$$V = 2145 + 0.75 \cdot z \tag{5.2}$$

whereby V (m/s) is velocity and z (m) is depth (Bulat & Stoker, 1987; Japsen, 1998).

Also in the British sector of the southern North Sea area, Hillis (1995) determined the normal compaction of the Chalk assuming a linear decrease of acoustic travel time Δt (μs/ft) with depth. The dataset consisted of Δt-values of the Chalk, excluding the Cenomanian, in 102 wells. Several trendlines were then drawn through wells with the lowest Δt-values at certain depths, i.e. representing maximum burial. From these, the trendline with a Δt-gradient closest to that of the entire dataset, and a surface Δt of 177.5 μs/ft, was chosen as the normal compaction trend:

$$\Delta t = 177.5 - 57.46 \cdot z \tag{5.3}$$

whereby z represents kilometres burial depth. The surface value of 177.5 μs/ft is slightly higher than that of seawater and is considered by the author to be a good approximation of the sea-floor conditions, where chalk has a porosity of 70 % (Scholle, 1977; Hillis, 1995). Equation 5.3 can be rewritten as a velocity trend:

$$V = 0.3048 \cdot 10^6 / 177.5 - (57.5 \cdot^{10-3}) \cdot z \tag{5.4}$$

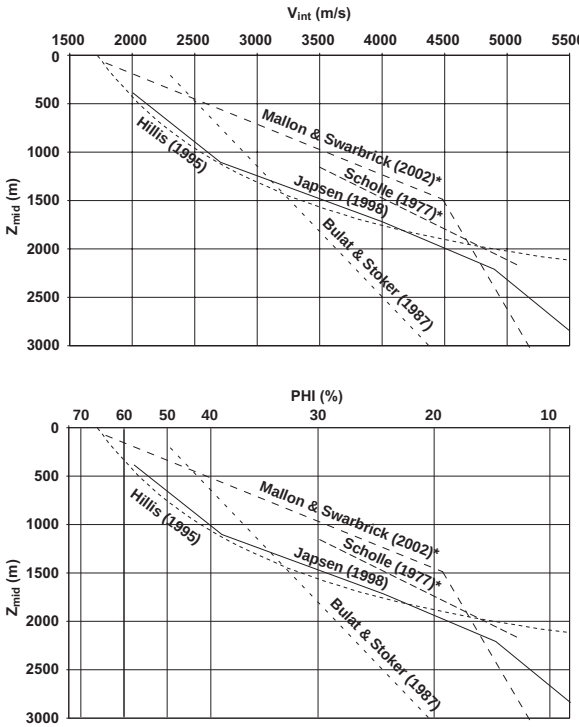

Figure 5.1: Overview of published compaction trends for the Chalk Group in the North Sea area. All trends describe the compaction of chalk with increasing burial depth in terms of decreasing porosity (*) or increasing acoustic velocity. To enable direct comparison between these, velocity values were converted to porosity values using the equations of Japsen (1998). See Section 5.3 for full discussion.

with V in m/s and z in m (Japsen, 1998). Japsen (1998) published a compaction trend for the Chalk in the whole North Sea area, which was compiled from sonic velocity data of a large number of wells where the Chalk is thought to be present at maximum burial depths. The V_n-trend consists of the following four linear segments, for different velocity intervals:

$$\begin{aligned} V_n &= 1600 + z && (V < 2700\ m/s) \\ V_n &= 500 + 2z && (2700\ m/s < V < 4000\ m/s) \\ V_n &= 937.5 + 1.75z && (4000\ m/s < V < 4875\ m/s) \\ V_n &= 2625 + z && (4875\ m/s < V < 5500\ m/s) \end{aligned} \tag{5.5}$$

whereby V (in m/s) is the acoustic velocity and z (in m) the depth below the sea floor.

Mallon & Swarbrick (2002) constructed a compaction trend for non-reservoir chalk to mitigate the porosity retaining effect of sediment reworking and early hydrocarbon entry (Scholle, 1977; Taylor & Lapré , 1987; Brasher & Vagle, 1996). The authors selected sonic and density log data of 59 wells from the British sector of the central North Sea area and determined interval (i.e. mean) sonic travel times (Δt) of the Ekofisk, Tor and Hod Formations (Fig. 1.5). The dataset was supplemented with DSDP-data to study compaction at shallow depths. Converted to porosity values, the data show a linear decrease from about 65% at the surface to about 18% at a depth of 1300–1500 m. Below this point, the rate of porosity loss increases and porosity drops to about 5% at 4500 m.

5.3 Database and Methods

5.3.1 Seismic horizons

The Base Chalk Group (Fig. 2.2) and Top Chalk Group (Fig. 2.13) seismic horizons provided the two-way traveltime (TWT in ms) data used in the present study. The traveltime statistics of these horizons are presented in Table 5.1. The horizons were interpreted on the *NOPEC* SNST83 (acquired in 1983) and SNST87 (acquired in 1987) 2D-seismic surveys (Fig. 5.2). See Section 2.2 *Seismic Reflection Data* for a detailed description of this dataset.

TWT (ms)	**min.**	**max.**	**mean**
Top CK	236	2822	1446
Base CK	406	3000	1838

Table 5.1: Two-way traveltime (TWT) statistics of the Top Chalk Group (Top CK) and Base Chalk Group (Base CK) reflectors.

5.3.2 Stratigraphic boundary depth data

The original stratigraphic boundary depth dataset consisted of the true vertical depths (TVD in m) of the lower and upper boundary of the Chalk Group, in all boreholes in the Netherlands offshore area that were completed before January 1st, 1992 (Table 5.2). This amounted to 860 well locations. From this dataset, all well locations on or within 500 m of a 2D-seismic line were selected, of which the TVD-data of the lower and upper boundary of the Chalk could be used (Fig. 5.2).

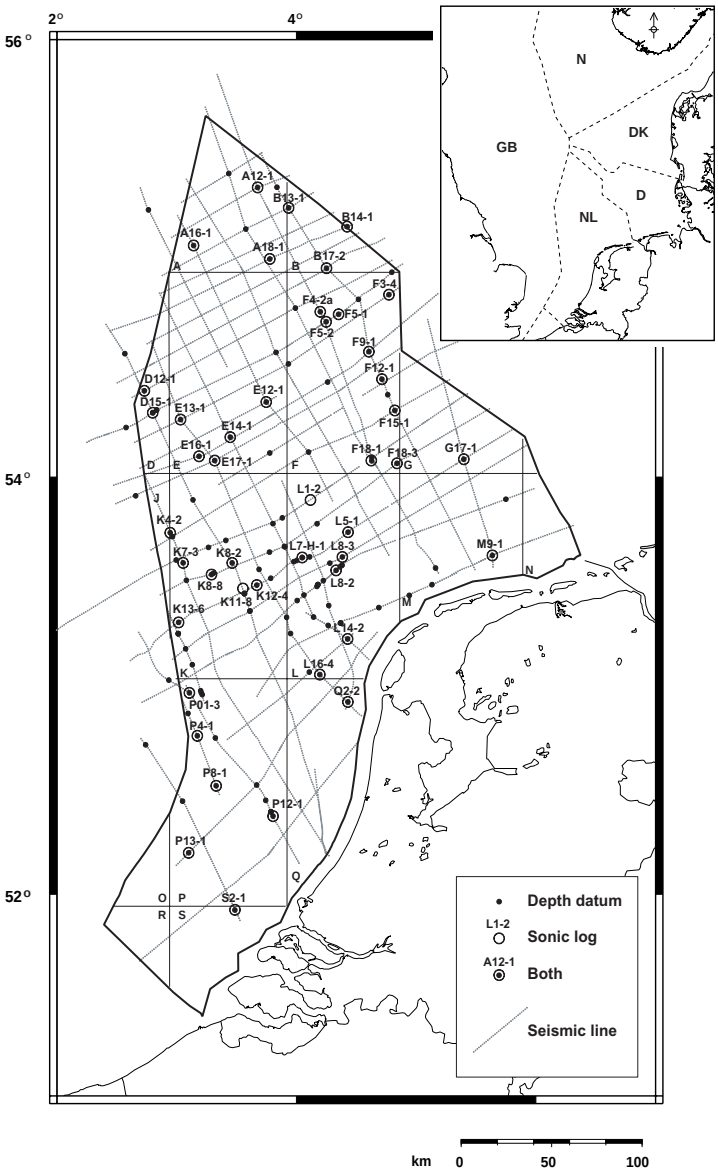

Figure 5.2: Map of the study area indicating the used data. Interval velocities were determined using a 2D-seismic grid and depth data of the lower and upper boundary of the Chalk Group at 139 well locations. Sonic logs of 43 wells were used to determine acoustic velocity and velocity gradient within the Chalk interval. The Netherlands North Sea area is subdivided into quadrants A–S. The small map indicates the position of the study area (NL) and the surrounding offshore sectors. GB = British, N = Norwegian, DK = Danish and D = German sectors.

To reduce possible complications due to seismic processing effects or interpretation errors, only those wells were used where the thickness of the Chalk is higher than 200 m, leaving a total of 130 well locations. This relatively high number can be explained by the fact that most wells date from the 1970s and the 2D-seismic surveys were acquired along trajectories designed to include the existing wells.

	min.	**max.**	**mean**
z Top CK (m)	509	2406	1306
z Base CK (m)	1079	3294	2103
Δz CK (m)	207	1772	797
z_{mid} CK (m)	796	2639	1704

Table 5.2: Depth (z in m), thickness (Δz in m) and mid-depth (z_{mid} in m) statistics of the stratigraphic boundary TVD dataset.

5.3.3 Sonics logs

Digital sonic logs through the Chalk Group interval were available of 45 wells in the Netherlands offshore (Fig. 5.2). Wells were selected with a minimum Chalk interval thickness of 250 m to make certain that representative velocities could be acquired. Furthermore, a selection of evenly distributed wells throughout the study area was realised. The sonic velocity data were treated as a separate velocity information source in this study, and no attempt was made to calibrate sonic logs with checkshot data, otherwise needed to reconcile sonic log and seismic data.

5.3.4 Interval velocity (V_{int}) from TVD-data and seismic horizons

The interval velocity (V_{int} in m/s) of the Chalk Group was determined by dividing the one-way traveltime (ΔT in ms) of the interval by its thickness (ΔZ in m), at each of the 130 well locations on or near a seismic line (Fig. 5.3), using the following equation:

$$V_{int} = (\Delta Z/\Delta T)^2 \tag{5.6}$$

ΔT was calculated by subtracting the two-way traveltime of the Base Chalk seismic reflector ($TWT_{Base\ CK}$) from the Top Chalk reflector traveltime (TWT $_{Top\ CK}$). The resulting two-way interval traveltime (ΔTWT) equals two times ΔT. Interval thickness ΔZ was calculated from the TVD's of the lower and upper boundary of the Chalk. Furthermore, the interval velocity of the overlying post-Danian siliciclas-

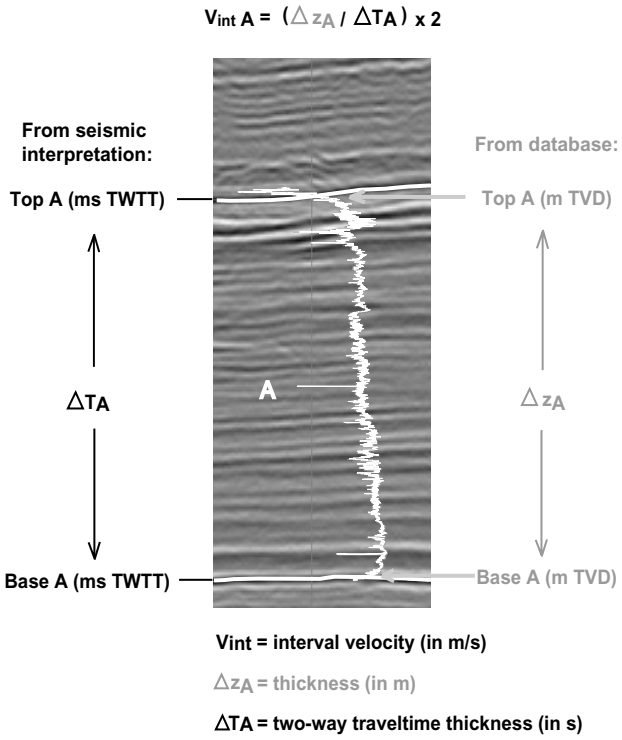

Figure 5.3: Interval velocity V_{int} (m/s) of the Chalk Group was calculated by dividing travel time interval thickness, derived from seismic interpretation, by the true vertical interval thickness, derived from a stratigraphic boundary depth dataset. This was done at each location where a borehole was on or within 500 m of a seismic line. No well-log data was used for this analysis.

tic cover (North Sea Super Group; Van Adrichem Boogaert & Kouwe, 1994), was determined following the same procedure, to allow comparison with the Chalk.

The regional distribution of interval velocities was studied to determine whether typical velocity ranges could be recognised for different parts of the study area. To estimate the velocity-depth relation, linear regression lines were fitted through the data that describe the increasing interval velocity with depth as:

$$V = V_0 + k \cdot z \tag{5.7}$$

where V (m/s) is the velocity (in this case V_{int}), z (m) is the burial depth, k (m/s/m) is the velocity-depth gradient (here $k_{\,V_{int}}$) and V_0 (m/s) is the theoretical initial velocity ($V_{0\,V_{int}}$). In all calculations presented in this study interval mid-depth

z_{mid} (m) is treated as the measure for burial depth. Correlation coefficient R^2 was calculated to quantify the accuracy of the linear regression.

5.3.5 Mean sonic velocity (V_μ), V_0 and k from sonic logs

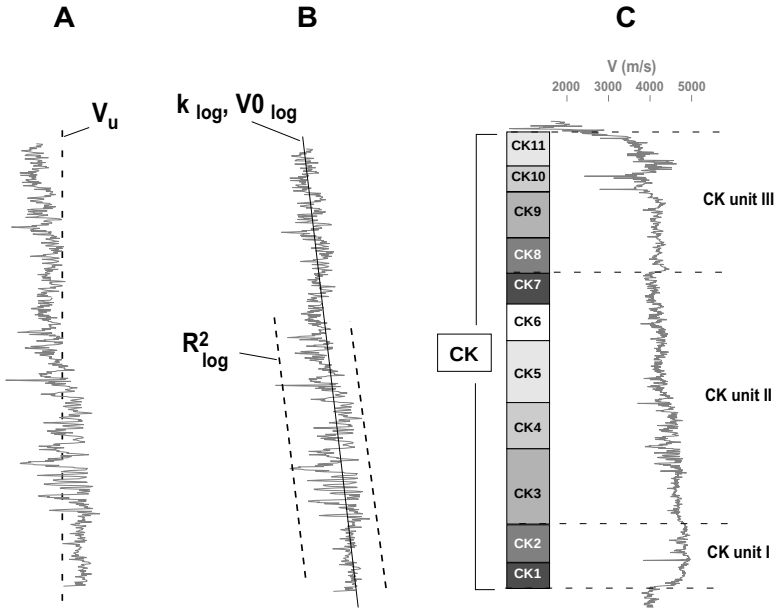

Figure 5.4: The sonic logs of 43 wells were converted to velocity logs, after which the mean velocity (V_μ) of each log was determined (A). V_μ represents the equivalent of interval velocity V_{int} at mid-depth z_{mid}. Then, a linear regression was fitted describing velocity (V) increase with depth (z) as $V = V_0 + k \cdot z$, whereby k_{log} is the velocity-depth gradient and $V_{0\,\log}$ the (theoretical) initial velocity (i.e. V at $z = 0\,m$). The $R^2{}_{\log}$ was also calculated to quantify the accuracy of the linear regression (B). These calculations were then repeated for log units I, II and III (C).

The sonic logs were first recalculated to velocity logs, after which the mean velocity V_μ (m/s) of the Chalk interval was determined (Fig. 5.4A). V_μ can be viewed as the sonic log equivalent of interval velocity V_{int}. Similar to the V_{int} dataset, the regional distribution of mean sonic velocities was studied and linear regression analyses were carried out to describe the relation between V_μ and burial depth in the form of equation 5.7, yielding values of 'bulk' velocity gradient k_{V_μ} (m/s/m) and initial velocity $V_{0\,V_\mu}$ (m/s).

The compaction of the Chalk was studied in more detail by fitting a linear regression to each sonic log interval, thus determining 'log' velocity gradient k_{log} (m/s/m) and theoretical initial velocity $V_{0\,log}$ (m/s), for each individual well (Fig. 5.4B). $R^2{}_{\log}$ was also calculated to quantify the accuracy of the linear regressions.

Furthermore, the Chalk interval was subdivided into log units I (encompassing sequences CK1 and CK2; Chapter 2), II (CK3 to CK7) and III (CK8–CK11) based on the sonic log response character. The previous calculations were then repeated for each log unit (Fig. 5.4C). The transition zones to the base and top of the Chalk, as well as those between log units, were excluded from the calculations to improve the fit of the linear depth trends.

5.3.6 Velocity and burial anomalies

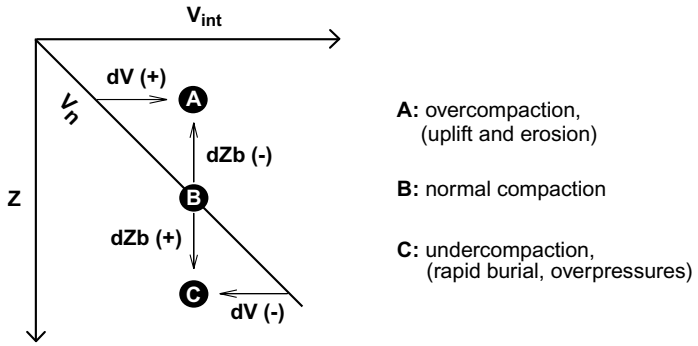

Figure 5.5: Interval velocities (V_{int}) were compared to a published normal-velocity curve (V_n) for North Sea Chalk (Japsen, 1998). Deviations from V_n are quantified as velocity deviation dV (m/s), which can be recalculated as burial anomaly dZ_b (m). This way, areas can be outlined where the Chalk is overcompacted, normally compacted or undercompacted with respect to present burial depth (z).

Following the method of Japsen (1998), the interval velocity data were compared to a normal velocity trend to quantify undercompaction and overcompaction of the Chalk in terms of velocity anomaly dV and burial anomaly dZ. Deviations from the normal velocity trend V_n (Equation 5.5; Japsen, 1998) are quantified by calculating the velocity anomaly dV (m/s):

$$dV = k\Delta z(e^{k\Delta T/2} - 1)^{-1} - V_0 - kz_t \tag{5.8}$$

where Δz (m) is layer thickness, ΔT (ms) the layer two-way travel time thickness, k (m/s/m) the velocity-depth gradient, V_0 (m/s) the acoustic velocity at zero depth

and z_t (m) depth to the top of the layer. The velocity anomaly values were also converted to burial anomaly dZ_b (m) values using the following equation:

$$dZ_b = -dV/k \tag{5.9}$$

Positive velocity anomalies (i.e. negative burial anomalies) point to overcompaction (Fig. 5.5A), suggesting that the sediment has been buried deeper before. The velocity of normally compacted sediment is expected to the V_n-trend (Fig. 5.5B). In contrast, undercompaction, such as resulting from overpressures, is indicated by negative velocity anomalies (i.e. positive burial anomalies; Fig. 5.5C).

5.4 Results

5.4.1 Interval velocity (V_{int}) from TVD-data and seismic horizons

The interval velocity of the Chalk Group ($V_{int\,CK}$) shows a large scatter, varying from 2200 m/s to 5300 m/s, with a general increase towards greater mid-depths (Fig. 5.6). The highest interval velocities are encountered in the central and eastern parts of the study area (Fig. 5.7). This includes the northern marginal through of the Broad Fourteens Basin and the Schill Grund High/Ameland Block (Section 3.2; quadrants K, L, M and G), as well as in the Elbow Split High/Outer Rough Basin (Section 3.2; quadrant A) in the north. Velocities are highest in quadrant L. Generally low velocities are found in the northern part of the Dutch offshore, in an area encompassing the northern Cleaver Bank High, Step Graben and Dutch Central Graben (Section 3.2; quadrants D, E, F and B). Furthermore, the area northwest of the Broad Fourteens Basin (southern K) also shows low interval velocities in the Chalk.

In the velocity data, four clusters could be recognised that, with the exception of cluster D, show roughly similar values for $k_{\,V_{int}}$ but vary with respect to $V_{0\,V_{int}}$ (Tablef 5.3). The clusters indicate that regional factors strongly control interval velocities. However, the areal distribution of these interval velocity clusters partly differs from that of the absolute interval velocities presented in Fig. 5.7. Generally low velocities relative to burial depth (cluster A) are encountered in the north of the Netherlands offshore, in the area of the Dutch Central Graben and Step Graben. Intermediate interval velocities relative to burial depth are found throughout the central and northeastern part of the study area (cluster B). In the south and east of the study area, high relative velocities are found at low mid-depths (cluster C). Relative interval velocities are highest in the northern marginal through of the Broad Fourteens Basin, particularly in quadrant L (cluster D). The variations of $V_{0\,V_{int}}$

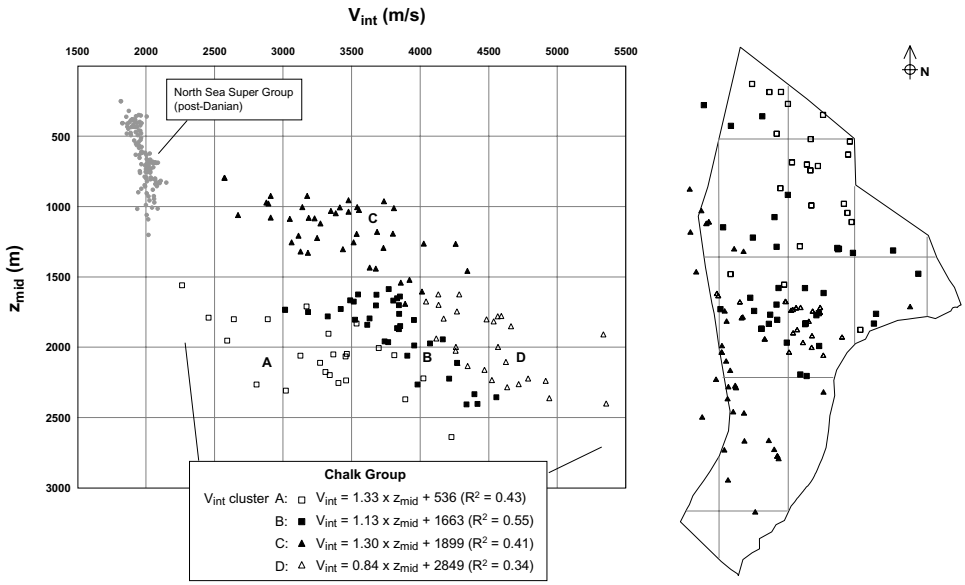

Figure 5.6: Interval velocity (V_{int}) vs. mid-depth (z_{mid}) of the Chalk Group (CK) and the overlying siliciclastics of the Tertiary North Sea Super Group (NS), as calculated from TWT and TVD-data.

indicate regional variations in post-depositional vertical movements, with cluster A being undercompacted and cluster C overcompacted, relative to clusters B and D. However, the accuracy of these values is limited as all clusters show marked scatter ($R^2 \approx 0.35$–0.55; Table 5.3). Contrary to the Chalk Group, the interval velocity of

Cluster	$k_{V_{int}}$	$V_{0\,V_{int}}$	R^2
A	1.33	536	0.43
B	1.13	1663	0.55
C	1.30	1899	0.41
D	0.84	2849	0.34

Table 5.3: Overview of $k_{V_{int}}$, $V_{0\,V_{int}}$ and R^2 determined in four clusters recognised in the interval velocity data of the Chalk

the overlying siliciclastic North Sea Super Group (NS) shows little scatter. The V_{int} NS increases linearly from about 1800 m/s at $Z_{mid} = 300$ m to a maximum of 2000 m/s at a mid-depth of about 600 m. Below 600 m mid-depth the interval velocity stays a constant 2000 m/s (Fig. 5.6).

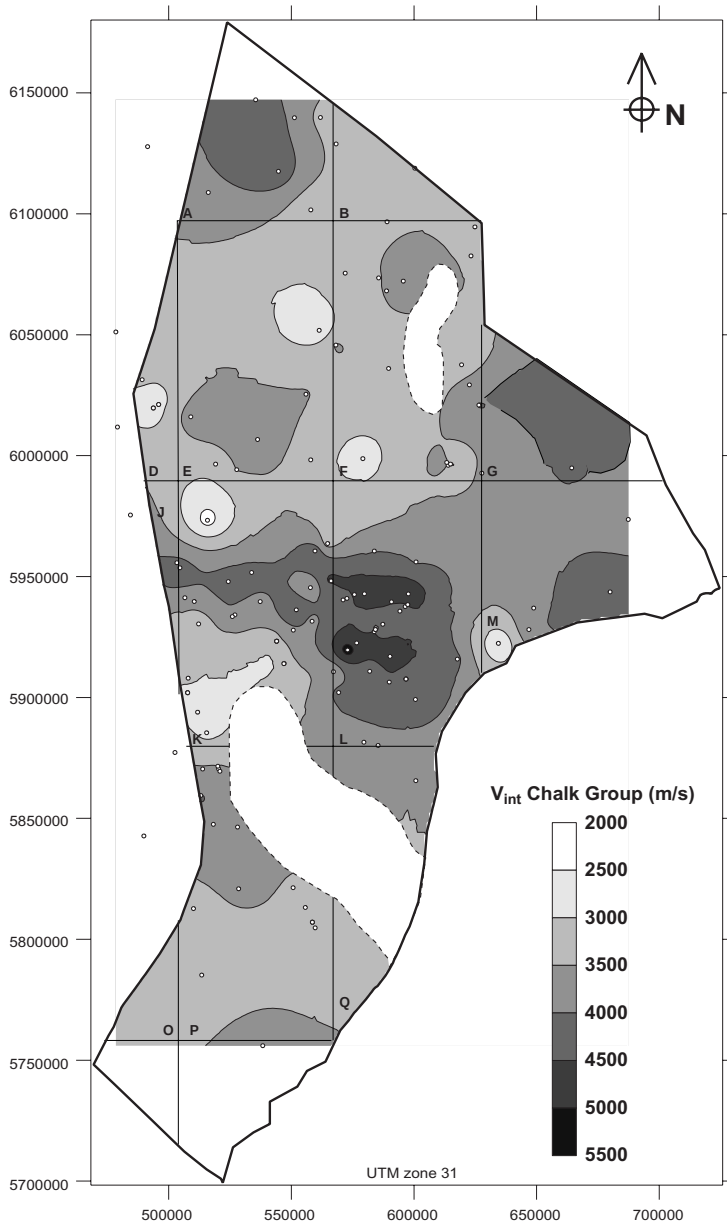

Figure 5.7: Interval velocity V_{int} (m/s) of the Chalk Group in the Netherlands offshore sector.

5.4.2 Mean velocity (V_μ) from sonic logs

The mean sonic velocity of the Chalk Group ($V_\mu CK$) shows slightly less scatter than $V_{int\,CK}$, with values between 2500 m/s and 4800 m/s over the same mid-depth range (Fig. 5.8A). Comparing the mean sonic velocities of the lower Chalk Group ($V_{\mu\,CK\,unit\,I}$; Fig. 5.8D), middle Chalk Group ($V_{\mu\,CK\,unit\,II}$; Fig. 5.8C) and upper Chalk Group ($V_{\mu\,CK\,unit\,III}$; Fig. 5.8B), a general increase with mid-depth is evident. V_μ increases from 2000 to 4250 m/s in the upper log unit III, from 2500 to 4800 m/s in unit II and from 3000 to 5600 m/s in basal log unit I.

The spatial distribution of $V_{\mu\,CK}$ (Fig. 5.9A) is similar to that of $V_{int\,CK}$ (Fig. 5.7), with highest velocities in the central and eastern part of the study area, i.e. from the southern Cleaver Bank High to the Ameland Block/Schill Grund High (quadrants K, L, M and G) and in the north, in the Elbow Split High/Outer Rough Basin area (part of quadrant A). Generally, low velocities are encountered in the north, particularly in parts of the Step Graben (B and F), western Cleaver Bank High (D), as well as west and south of the Broad Fourteens Basin (southwestern part of K, O, P and Q).

The general increase of V_μ with depth is also evident when Fig. 5.9B, C and D are compared. The spatial distribution of $V_{\mu\,CK\,unit\,I}$ (Fig. 5.9D), is similar to $V_{\mu\,CK}$ with regard to trends, but shows very high velocities (5000 to 5500 m/s) throughout the southern Cleaver Bank High and Vlieland Basin (quadrants K and L). $V_{\mu\,CK\,unit\,II}$ (Fig. 5.9C) is more or less equal to $V_{\mu\,CK}$. In contrast, low values of $V_{\mu\,CK\,unit\,III}$ (Fig. 5.9B) are found around the Dutch Central Graben (B and F) and in the eastern and southern part of the study area, i.e. in the eastern Cleaver Bank High and from the Broad Fourteens Basin southwards (D, E, J, southern parts of K and L, O, P and Q).

In the V_μ-data of the Chalk Group and the three log units, a clear relationship exists between velocity values and regions in the study area, which is very similar to that observed for V_{int} . Three clusters were thus identified (Fig. 5.8). Generally low relative velocities are found in the Dutch Central Graben and Step Graben (cluster A). Velocities in the central and northeastern part of the study area are intermediate with respect to burial (cluster B). Relatively high velocities are found throughout the south and east (cluster C). The k_{V_μ} and $V_{0\,V_\mu}$ estimates derived here are more reliable than those derived from the V_{int}-dataset as R^2 values are usually higher (Table 5.4). k_{V_μ} values vary from about 1.1 to 1.5 m/s/m, with cluster A mostly showing lower values. R^2 values are particularly high in log unit I (Fig. 5.8D). In log unit III (Fig. 5.8B), V_μ-values of cluster A show no trend at all. Moving down to unit II (Fig. 5.8C) and unit I (Fig. 5.8D), the depth trend of cluster A becomes more pronounced and V_μ-values approach those of cluster B. V_μ-values of Cluster C are

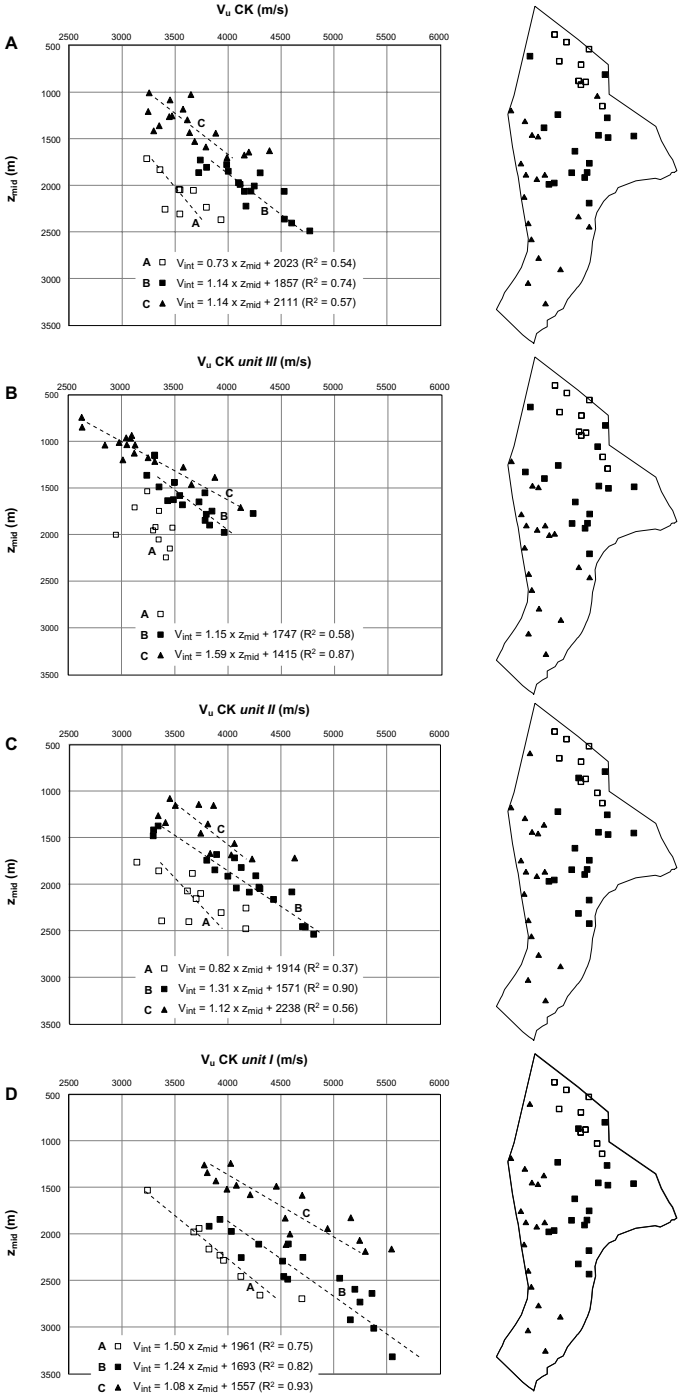

Figure 5.8: Mean sonic velocity V_μ (m/s) vs. mid-depth of the Chalk Group (A), upper Chalk Group (B), middle Chalk Group (C) and lower Chalk Group (D).

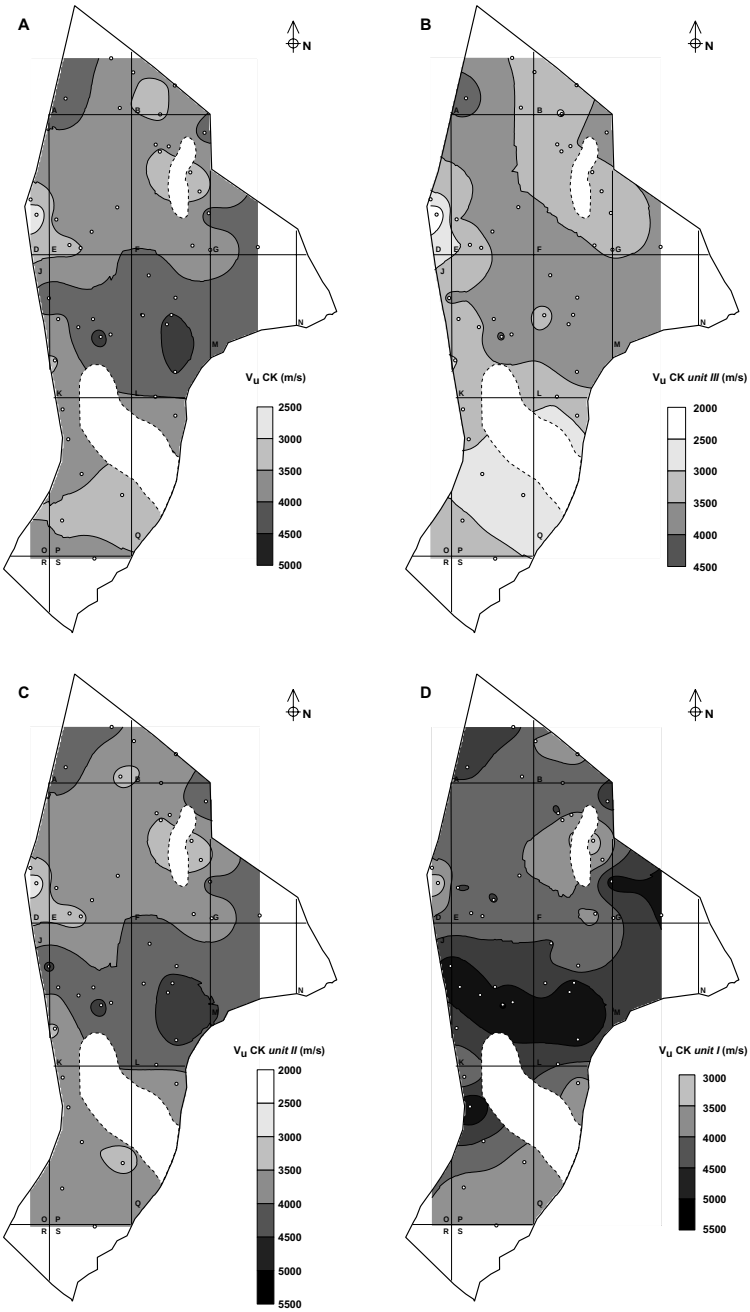

Figure 5.9: Mean sonic velocity V_μ (m/s) of the Chalk Group (A), upper Chalk Group (B), middle Chalk Group (C) and lower Chalk Group (D).

	k_{V_μ}			$V_{0\,V_\mu}$			R^2		
Cluster:	A	B	C	A	B	C	A	B	C
CK	0.73	1.14	1.14	2023	1857	2111	0.54	0.74	0.57
CK unit III		1.15	1.59		1747	1415		0.58	0.87
CK unit II	0.82	1.31	1.12	1914	1571	2238	0.37	0.9	0.56
CK unit I	1.5	1.24	1.08	1961	1693	1557	0.75	0.82	0.93

Table 5.4: Overview of k_{V_μ}, $V_{0\,V_\mu}$ and R^2 determined in three clusters recognised in the interval velocity data of the Chalk (CK) as well as log units I, II and III

relatively high in Unit 1 compared to clusters B and C. Values for k_{V_μ} are roughly similar in all data subsets although cluster A generally shows a slower increase of velocity with depth. As with V_{int}, the variations of $V_{0\,V_\mu}$ indicate regional variations in post-depositional vertical movements, with cluster A being undercompacted and cluster C overcompacted, relative to clusters B.

5.4.3 k_{log}, $V_{0\,log}$ and R^2_{log}

Based on the result of linear regressions fitted to sonic log intervals, k_{log}, $V_{0\,log}$ and R^2_{log} were determined for the whole Chalk Group (Fig. 5.10A, Fig. 5.11A & Fig. 5.12A), log unit II (Fig. 5.10B, Fig. 5.11B & Fig. 5.12B) and log unit III (Fig. 5.10C, Fig. 5.11C & Fig. 5.12C), in each well. Basal log unit I was not used for this analysis due to the generally irregular log response of this section of the Chalk, resulting in typical R^2_{log}-values being less then 0.4.

The degree to which sonic velocities change with depth varies markedly throughout the Netherlands offshore area. The velocity gradient of the whole Chalk Group ($k_{log\,CK}$; Fig. 5.10A) varies from about 1–1.5 m/s/m in the central part of the study area, i.e. the southeastern Cleaver Bank High–Vlieland Basin area (southeastern part of quadrant K; L and parts of M), to about 2–2.5 m/s/m in the western and southern part, i.e. the western Cleaver Bank High and south of the Broad Fourteens Basin (D, eastern E, J, eastern K, O, P and Q). However, individual wells are beyond the main cluster.

As sonic velocities stay within a certain range, values for theoretical initial sonic velocity $V_{0\,log}$ are predominantly influenced by k_{log}. In general, high positive k_{log}-values result in low or even negative $V_{0\,log}$-values, and vice versa. The regional distribution of $V_{0\,log\,CK}$ (Fig. 5.11A) therefore follows that of $k_{log\,CK}$, but with inversed values. The fit of the velocity trendline ($R^2_{log\,CK}$; Fig. 5.12A) is generally good in the study area, with $R^2_{log\,CK}$-values only falling below 0.5 in the north.

The complex internal structure of the Chalk is revealed when the k_{log}, $V_{0\,log}$

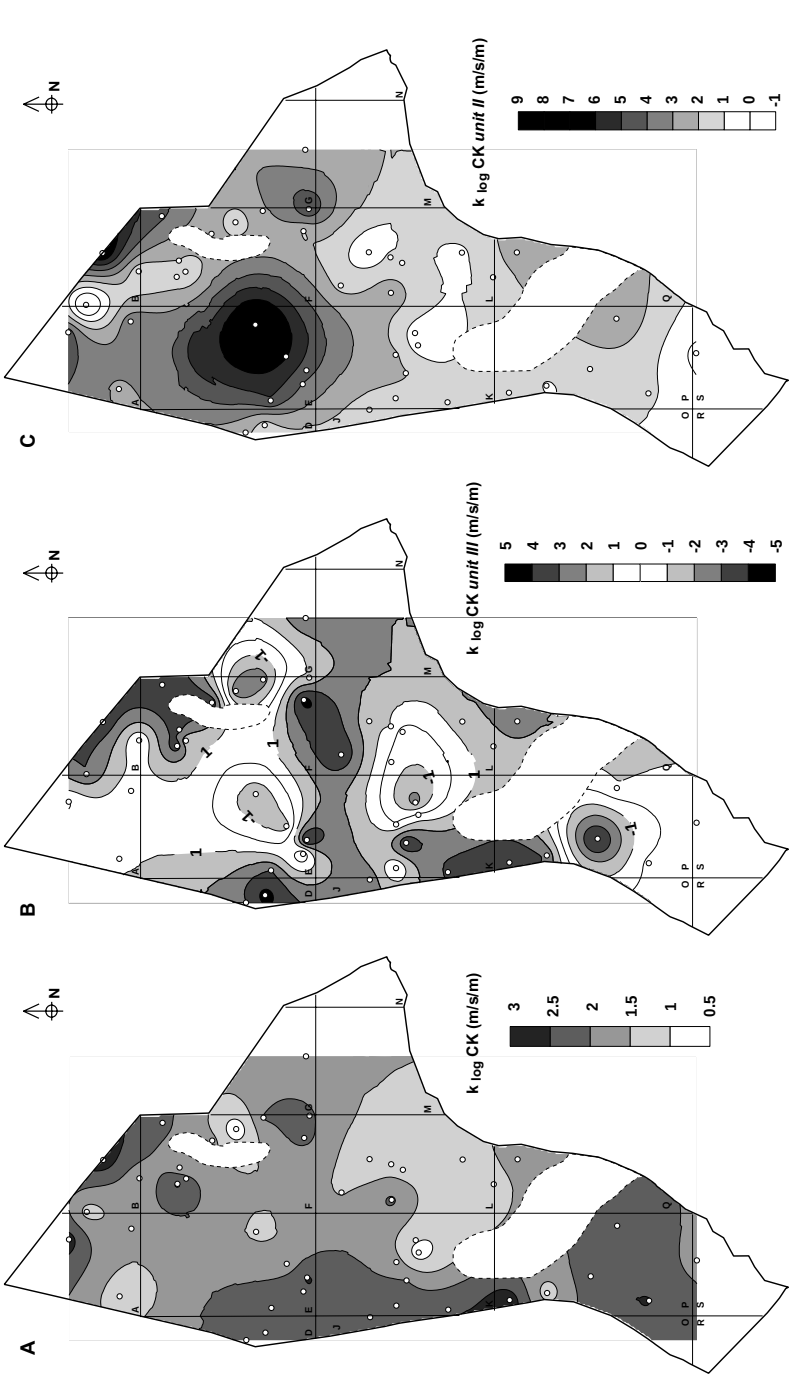

Figure 5.10: Velocity-depth gradient k_{log} (m/s/m) of the Chalk Group (A), upper Chalk Group (B), middle Chalk Group (C) and lower Chalk Group (D).

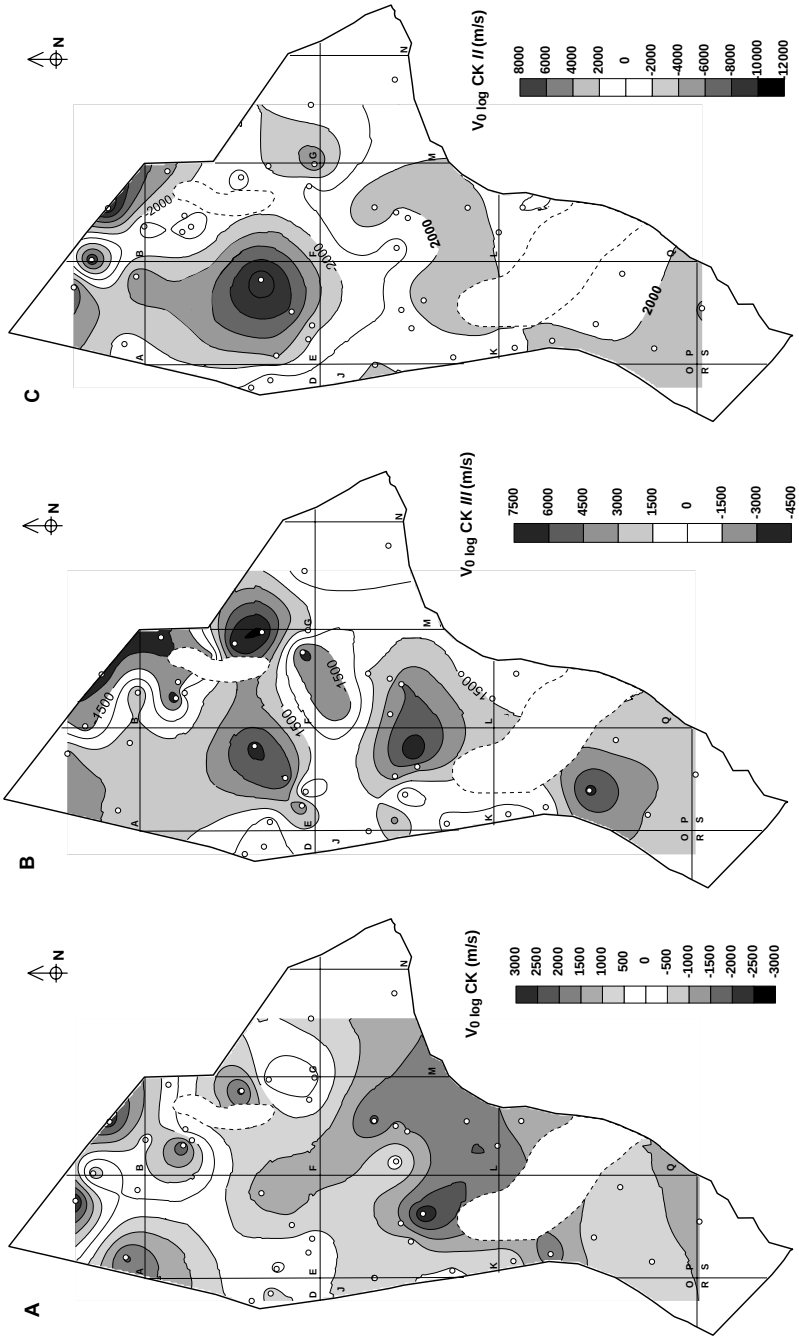

Figure 5.11: Theoretical initial velocity $V_{0\,log}$ (m/s) of the Chalk Group (A), upper Chalk Group (B), middle Chalk Group (C) and lower Chalk Group (D).

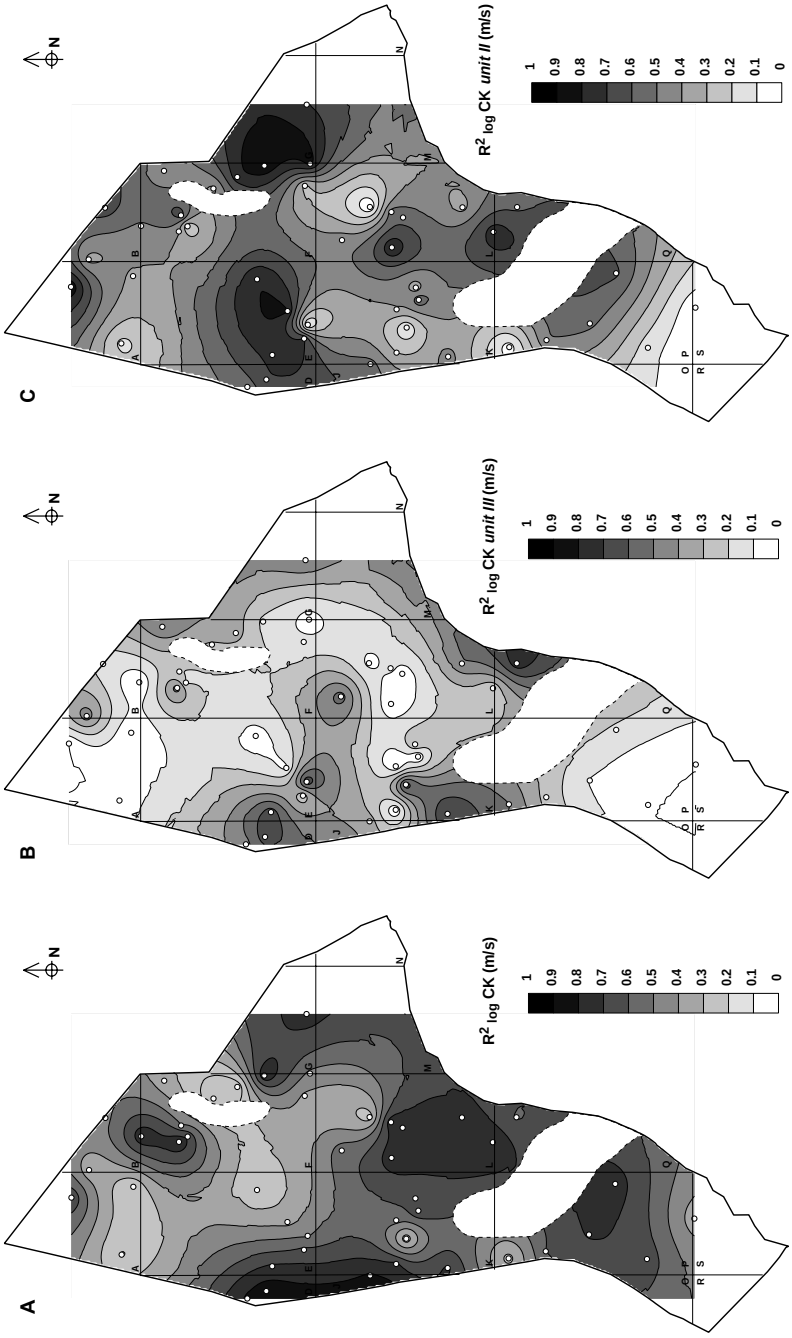

Figure 5.12: Correlation coefficient R^2_{log} of the linear regression through the calculated velocity log of the whole Chalk succession (A), as well as the lower (B), middle (C) and upper (D) sections of the Chalk Group (Fig. 5.3).

and $R^2{}_{log}$ values of the upper and middle Chalk sections are compared. Generally, $k_{log\,CK\,unit\,III}$ (Fig. 5.10B) is highly variable but positive throughout the western, central and eastern part of the Dutch offshore, i.e. from the western and southern Cleaver Bank High to the Schill Grund High (D, western E, J, K, L, M, northern P and Q), as well as in the northeast, in the central Graben and eastern Step Graben (northern F and B). In contrast, areas where sonic velocity remains equal or even decreases with depth, indicated by neutral or negative $k_{log\,CK\,unit\,III}$-figures, include the eastern Cleaver Bank High, Outer Rough Basin and northern Schill Grund High (A, E, southern F and G), the southeastern Cleaver Bank High (southeastern K, southwestern L) and the area south of the Broad Fourteens Basin. This distribution is mirrored by that of $V_{0\,log\,CK\,unit\,III}$ (Fig. 5.11B). The moderate spread of sonic log response in the upper Chalk section results in overall low values for $R^2{}_{log\,CK\,unit\,III}$ (Fig. 5.12B). It is important to note that the velocity fit is generally better where $k_{log\,CK\,unit\,III}$ is higher. However, this relation does not hold east and south of the southern Dutch Central Graben (southeast F and G).

The middle part of the Chalk shows constant to slowly increasing sonic velocity with depth throughout most of the study area, as indicated by neutral to low values for $k_{log\,CK\,unit\,II}$ (Fig. 5.10C). An exception to this is found in the central Cleaver Bank High (southern E), where $k_{log\,CK\,unit\,II}$ is much higher (up to 8 m/s/m). A similar value is also found in well B14-1. However, this contrast is not recognisable in the fit of the linear velocity trends. $R^2{}_{log\,CK\,unit\,II}$ (Fig. 5.12C) is moderate to high throughout the study area, with some exceptions. As described also in the previous paragraphs, the distribution of $V_{0\,log\,CK\,unit\,II}$ (Fig. 5.11C) follows that of $k_{log\,CK\,unit\,II}$.

5.4.4 Velocity and burial anomalies

Following the method of Japsen (1998), the interval velocity data were compared to a normal velocity trend to quantify undercompaction and overcompaction of the Chalk in terms of velocity anomaly dV and burial anomaly dZ. $V_{int\,CK}$ (Fig. 5.7) is lower than expected at present burial depth in the northern part of the study area (Fig. 5.13). This indicates undercompaction, and is expressed as negative values for velocity anomaly dV_{CK} (Fig. 5.13A), and positive values for burial anomaly $dZ_{b\,CK}$ (Fig. 5.13B). Undercompaction is most prominent in the northern Step Graben (eastern part of quadrant A; B, northeastern E and northern F), and in the southern Step Graben and southeastern Cleaver Bank High (around southwestern F), where dV_{CK} is down to -2250 m/s ($dZ_{b\,CK}$ up to 1000 m). The Chalk is near normal compaction in the western and central part of the Netherlands offshore, in the area from the western (western A, D, western E, J, K) and southern (central and southern L)

Cleaver Bank High to the Ameland Block/southern Schill Grund High (M, south-eastern G). However, local variations are found throughout this area. The Chalk is overcompacted in the south, particularly south of the Broad Fourteens Basin (O, P and Q), with dV_{CK} up to 1250 m/s and dZ_b down to -600 m.

A revision of the normal velocity trend used here predicts higher velocities at shallower depths (Japsen, 2000). This results in a reduction in uplift and erosion estimates and an increase in undercompaction estimates(i.e. dZ_b-values increase with 150–200 m).

5.5 Discussion

5.5.1 Acoustic velocity of the Chalk

Contrary to the overlying Tertiary succession, the sediments of the Chalk Group show a great variation in interval velocities throughout the Netherlands offshore. This range in interval velocity $V_{int\,CK}$ (Fig. 5.6 & 5.7) and mean sonic velocity $V_{\mu\,CK}$ (Fig. 5.8 & 5.9) is comparable to previously published results. Bulat & Stoker (1987) measured velocities between 2150 and 3970 m/s at mid-depths ranging from 100 to 2500 m in the British sector of the southern North Sea. However, much higher velocities, i.e. 2400 to 4700 m/s at mid-depths of 100 to 2000 m, are reported by Hillis (1995) in the same area. In the Netherlands offshore, velocities at such mid-depths generally lie between these two extremes. Interval velocities between 2300 m/s and 5400 m/s are encountered in the whole North Sea area (Japsen, 1998), but since the mid-depth range of this area is much larger than that of the Netherlands offshore (z_{mid}: 100–3900 m), a slower increase of velocity with depth is indicated by this data. Mallon & Swarbrick (2002) provide porosity data that can be converted to velocity data using equation 5.1. Their data show an increase of velocity from 2600 m/s at 500 m to 4500 m/s at 1500 m. Below this depth, velocity increases at a much slower rate to 5900 m/s at 4500 m. Such a sudden decrease is not observed in the present dataset.

To investigate the significance of the velocities determined in the present study, possible complications arising from the used methods need to be discussed. In the case of $V_{int\,CK}$, the velocity estimations required during several stages of seismic processing form the primary control. The accuracy of these procedures generally declines in areas where the structure of the underground is complex. Dipping reflections, particularly when several reflections with different dips are present, and large lateral acoustic velocity contrasts bring about such a deterioration (Yilmaz, 1987). Furthermore, as the maximum distance of a well location to a seismic line is 500 m, an error in the estimate of ΔT (Section 5.3) at a well location may occur where

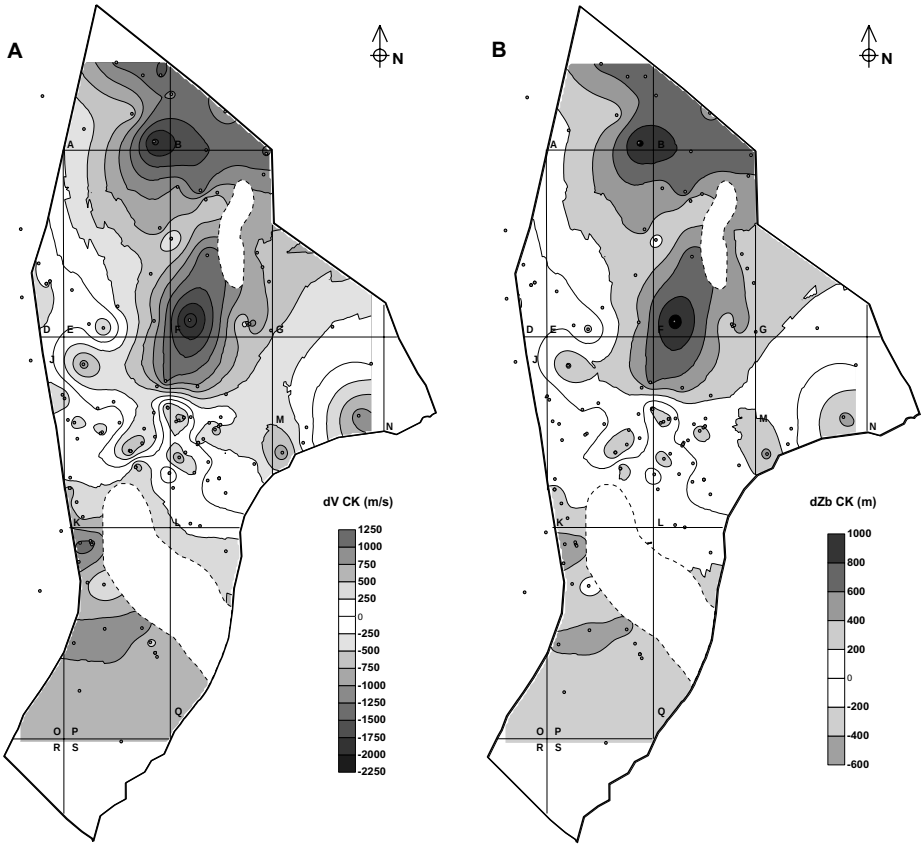

Figure 5.13: Velocity anomaly (A) and burial anomaly (B) of the Chalk Group. Neutral dV ($250\ m/s < dV < -250\ m/s$) and dZ_b ($200\ m < dZ_b < -200\ m$) values represent Chalk that is normally compacted with respect to burial depth. The Chalk is undercompacted in the north of the Dutch offshore, indicated by negative dV-values and positive dZ_b-values. In the south of the Dutch offshore, the Chalk is overcompacted. Overcompaction is indicated by positive dV-values and negative dZ_b-values. **See Fig. 5.13 (page 166) in Appendix - Colour plates for a colour version of this figure.**

the Top Chalk and Base Chalk reflections dip at different angles. In the present dataset, however, dip angles are generally very low (Table 5.5). This is predominantly because well locations with a minimum interval thickness of 200 m were used, thereby removing locations too close to salt diapirs. Therefore, dip related errors

in V_{int}-estimates can only be expected in the Dutch Central Graben or along the boundaries of the Broad Fourteens Basin, were reflections often show steeper dips (Section 3.2).

	Top CK	**Base CK**	**Difference**
mean	1.9°	2.8°	0.9°
min.	0°	0°	1.3°
max.	10.9°	11.5°	7.5°
std.	1.9°	2.2°	1.4°

Table 5.5: Overview of dip angles of the Top Chalk and Base Chalk reflectors

The sonic logs used to determine $V_{\mu\,CK}$ are generated by sending a high frequency (typically 20–40 kHz; Rider, 1996) signal into the rock and measuring the traveltime from source to receiver. Only non-deviated wells were used in the present study, so only the vertical velocity component is measured in horizontally bedded chalks. However, small velocity divergences may occur where sediment beds are dipping, again due to the acoustic anisotropy of chalk. The complicating effect of drilling mud invasion into pore space is regarded minimal due to the low permeability of 'non-reservoir' chalk, i.e. not reworked as slumps, slide sheets or debris flow deposit, or extensively fractured (Mallon & Swarbrick, 2002). Moreover, evidently erroneous sonic logs, as caused by disintegration of the borehole wall by drilling mud ('wash-out') or the presence of faults, were excluded from the database.

Throughout most of the study area, $V_{\mu\,CK}$-values are within 10 % of $V_{int\,CK}$-values, at well locations were both parameters have been measured (Fig. 5.14). This reasonable similarity confirms the applicability of both methods to determine the acoustic velocity of the Chalk. Interestingly, the variations observed in Fig. 5.14 outline the 'stretch' factor needed to tie the sonic logs to the seismics, which is normally derived from checkshot data when synthetic seismograms are constructed (Section 2.2 Dataset and methods, Integration of the seismic and well database). Apart from the possible complications discussed in the previous paragraph, the much higher signal frequency of a sonic log (typically 20–40 kHz; Rider, 1996) compared to seismics (about 35 Hz) accounts for much of the difference between $V_{int\,CK}$ and $V_{\mu\,CK}$. The 16 % difference observed in well F3-4 is most likely the result of the strong lateral velocity contrast caused by the nearby presence of large salt diapirs (Fig. 3.7).

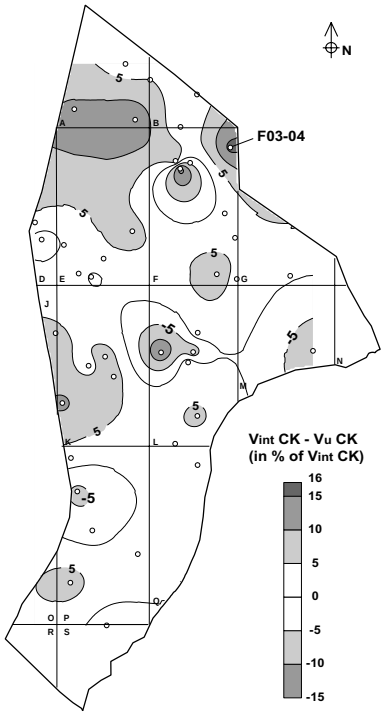

Figure 5.14: The difference between $V_{int\,CK}$ and $V_{\mu\,CK}$, expressed as percentage of $V_{int\,CK}$.

5.5.2 Compaction of the Chalk

The primary factor controlling compaction, and thus velocity, of the Chalk is burial depth (Fig. 5.6 & Fig. 5.8), although the scatter of velocities indicate the presence of several other factors as well. In Fig. 5.15, all velocity data compiled in this study is presented in one graph, accepting the inherent differences between $V_{int\,CK}$ and $V_{\mu\,CK}$. The dataset was separated into the clusters described before, assuming clusters B and D to represent normally compacted chalk, cluster A to be overcompacted and cluster C undercompacted. From the figure it becomes clear that the jointed linear velocity trend of Japsen (1998) best fit the velocity data of normally compacted chalk from the Netherlands. The data also show a slower increase of velocity below a depth of about 2200 m, much like the gradient described by the last section of the velocity trend of Japsen (1998). The higher velocities predicted by Mallon & Swarbrick (2002), even in spite of the overall lesser compaction in their study area, might be explained by the fact that only non-reservoir chalk was used to compile this trend. This then would indicate a significant volume of reservoir chalk to be present in the Netherlands offshore area. However, such an explanation is not supported

by the present research. In contrast, the velocity trend of Bulat & Stoker (1987) bounds the bulk of the normally compacted chalk velocity data towards the least compaction.

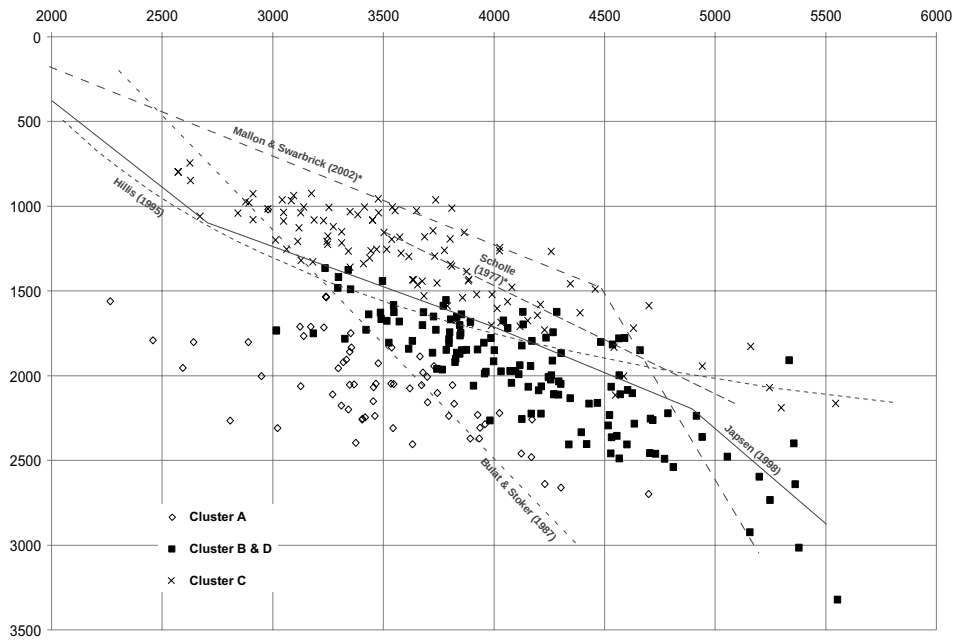

Figure 5.15: Combined plot of the interval and mean sonic velocity of the Chalk Group, log unit I, log unit II and log unit III compared to various normal-compaction trends of the Chalk.

A reasonable consistency in velocity-depth gradients exists between the trends of Hillis (1995), Japsen (1988), Mallon & Swarbrick (2002) and Scholle (1977), at least for the medium burial depths. However, these velocity-depth gradients are somewhat steeper (k $\approx$ 2 m/s/m) than those observed in the present dataset (k $\approx$ 1.15–1.3 m/s/m). The marked differences between V_0 estimates show that determining which part of a dataset represents 'normally' compacted sediment, i.e. not undercompacted by reworking, hydrocarbon entry or overpressuring and not overcompacted due to uplift, remains the most uncertain task when a normal compaction trend is constructed.

5.5.3 Variation in chalk compaction

Apart from burial depth, compaction of the Chalk is regionally controlled by overpressures and vertical movements (Bulat & Stoker, 1987; Hillis, 1995; Brasher & Vagle, 1996; Japsen, 1998). Interval velocities in the southern Dutch Central Graben and Step Graben (eastern parts of quadrants A and E; B and F) are anomalously low with respect to burial depth. When interval velocities are compared to the normal-velocity trend of Japsen (1998), this is demonstrated by the marked negative velocity anomalies (dV), and consequently: positive burial anomalies (dZ_b), found in this area (Fig. 5.13). Japsen (1998) describes increasing negative dV-values, indicating increasing undercompaction of the Chalk, towards the Tertiary depocenter of the North Sea Basin. This trend furthermore coincides with overpressures in the Chalk and lower sections of the Tertiary succession. Rapid burial of the Chalk under impermeable clays during the Tertiary most likely resulted in the retention of pore water in the sediment. This pore water partly carried the overburden during burial and subsequently impeded compaction of the Chalk (Scholle, 1977; Brasher & Vagle, 1996; Japsen, 1998). Velocity variations observed in this study are larger than those reported by Doornenbal (2001) from the same area.

Generally higher velocities than expected at present burial depth are encountered in the southern part of the Netherlands offshore. These are expressed as positive velocity anomalies (and negative burial anomalies; Fig. 5.13) and indicate uplift post-dating deposition and burial of the Chalk (Bulat & Stoker, 1987; Hillis, 1995; Japsen, 1998).

Interestingly, the rates of velocity increase observed in individual well sections (i.e. k_{log}; Fig. 5.10) are generally higher than those derived from the bulk of the velocity dataset, i.e. $k_{V_{int}}$ and $k\,V_{\mu}$ (Table 5.3 & 5.4). This indicates that chalk compaction at a certain location does not follow the trend observed in the whole area. High k_{log} values may be explained by the presence of low-permeable clays overlying the Chalk. The post-Danian clay cover impaired or blocked the pore water release of the compacting chalk, leading to overpressures in the Chalk in the central part of the North Sea area (Japsen, 1998). The presence of such a pressure barrier over a rock sequence with an initial downwardly decreasing porosity gradient will most likely result in the intensification of this gradient with ongoing burial. This is because the remaining pore water will be pushed upwards to be trapped under the pressure barrier, increasing the porosity contrast between overpressured chalks above and tightly compacted chalk below.

However, the eventual results of the overpressure mechanism discussed above are highly variable, as is suggested by the marked lateral variation of k_{log} throughout the study area, particularly in upper log unit III (Fig. 5.10). Furthermore, log unit

III of those wells that are part of cluster A, where overpressure is most pronounced, show highly varying sonic velocities, with no apparent depth trend (Fig. 5.8).

Local factors thought to influence compaction of North Sea chalk are depositional mechanism and hydrocarbon migration (Scholle, 1977; Watts et al., 1980; Kennedy, 1987; Brasher & Vagle, 1996). However, porosity retention in reworked chalks cannot be proven in the present dataset. A large portion of the chalk of the northern Broad Fourteens Basin marginal through is made up of reworked chalk, as is suggested by the absence of significant cyclic log intervals (Fig. 4.5; Section 4.5). However, this area shows very high interval velocities (e.g. cluster D in Fig. 5.6). Early hydrocarbon entry is described to explain the anomalously high porosities of up to 30 % encountered in reservoir chalks in the central North Sea area. (Scholle, 1977; Brasher & Vagle, 1996). Oil is currently produced from chalk in the Dutch Central Graben, therefore the low velocities encountered in this area might thus be partly explained, but specific data is presently lacking to confirm such a hypothesis.

5.6 Conclusions

- Interval velocity V_{int} of the Chalk Group ranges from 2200 to 5300 m/s, at mid-depth of 800 to 2600 m
- Sonic velocity V_{μ} of the Chalk Group ranges from 2500 to 4800 m/s, at similar mid-depths. V_{μ} increases from 2000 to 4250 m/s in the upper log unit III, from 2500 to 4800 m/s in unit II and from 3000 to 5600 m/s in basal log unit I.
- Burial depth is the primary control of the acoustic velocity of the Chalk, with velocity increasing at a rate of 1.15–1.3 m/s with each metre of burial.
- Regional variations in post-depositional history form the secondary control. Velocities are consistently lower than expected at present burial depth in the north of the study area, indicating undercompaction. This is probably caused by rapid burial under impermeable siliciclastics during post-Danian times. In contrast, higher velocities than expected are found throughout the south, indicating overcompaction, due to uplift.
- As a result of undercompaction, interval velocities are down to 2250 m/s lower than normal in the north of the study area. In the south, a maximum of 600 m of uplift is indicated by interval velocities being up to 1250 m/s higher than normal.
- The velocity gradient in individual logs is usually greater than that derived from interval velocities of the whole area. This is probably because of the

presence of overlying low-permeable clays, causing escaping formation water to remain in the upper part of the Chalk.

- The interval velocity maps can be used to improve time-depth conversions through the Chalk interval. The difference between V_{int} and V_{μ} is equivalent to the 'stretch' factor needed to tie the sonic logs to the seismics, which is normally derived from checkshot data when synthetic seismograms are constructed.

Chapter 6

Synthesis

This thesis discusses the sedimentary development, (seismic) stratigraphy and burial compaction of the Upper Cretacous to lower Paleocene Chalk Group in the Dutch section of the southern North Sea. These sediments represent a period in the Earth's history during which intense volcanic activity at oceanic sea-floor spreading ridges coincided with globally high sea-levels and high sea surface temperatures (Fig. 1.1). The high sea-level led to the inundation of large areas of land, reducing the influx of erosional detritus into the basin (Fig. 1.6 & 1.7). The ensuing clear water conditions led to the proliferation of calcitic algae (coccolithophorids), which, in turn, resulted in the accumulation of chalk. Presently, the knowledge of the Chalk in the Netherlands offshore is hampered by the hitherto restricted significance of the interval as a hydrocarbon reservoir. This situation is in contrast to that in the Norwegian and Danian sectors of the North Sea, where the Chalk does form an important reservoir, particularly in the Central Graben (Fig. 1.4). Therefore, the bulk of the scientific literature focussed on the Chalk Group stems from this area, as well as from the outcrops around the North Sea. The present thesis augments the literature database by describing the regional development of the Chalk in the Dutch sector of the southern North Sea.

The primary sedimentation mechanism of the Chalk is the settlement of calcitic algae tests from suspension in the water column. Net sediment accumulation rates varied periodically, as is indicated by periodic variations in sonic velocity, density and clay content (e.g. Fig. 4.7). Cyclic bedding is a widely recognised characteristic of the Chalk, most commonly credited to climatic variations resulting from periodic variations of the Earth's distance to the sun. A wide range of orbital cycles, as represented by various petrophysical and lithological parameters, have been recognised in Chalk outcrops and cores from north-western Europe (Section 4.2). In the well-logs

presented in this thesis, periodic variations occur with different frequencies simultaneously, most commonly with wavelengths of about 5–7 metre and 2–3 metre. The specific wavelength ratio between these cyclicities suggests that these represent the 94 ky eccentricity and 40 ky obliquity cycle. Such an interpretation suggests very high sediment accumulation rates, 5 to 7 cm/ky including compaction, for sections of the Chalk.

The degree to which Chalk deposition was mediated by basin-wide controls is made evident by the regionally correlated alternations between low-frequency/high-amplitude and high-frequency/low-amplitude sonic and density log responses, in sediments of Turonian to Santonian age (Section 4.4.3 *Metre-scale cyclicity*). Furthermore, gradual long-term climatic variations also influenced the deposition of the Chalk. The gradual decrease in net sedimentation rate occurring throughout the Campanian and Maastrichtian (e.g. Fig. 4.7; log unit 6) is an example of this.

The seismic facies of the Chalk Group is characterised by parallel and continuous reflections in most of the study area (Fig. 2.2–2.12). Reflection strength varies, but is primarily controlled by the magnitude of decametre-scale porosity variations, such as the low-frequency/high-amplitude variations that occur in the Turonian and Santonian, mentioned in the previous paragraph (Fig. 2.16, log intervals 'A').

Parallel and continuous seismic reflections represent pelagic chalk, as well as chalk reworked on a sub-seismic scale, i.e. as allochthonous bodies less than a few tens of metres thick. This is shown by the well-log facies (Fig. 4.5). Truly cyclic chalk intervals are only encountered in areas that underwent gradual subsidence during deposition, such as the Schill Grund High and parts of the Cleaver Bank High (Fig. 3.1). In contrast, the wells around the uplifted Broad Fourteens Basin show an aperiodic log response that is indicative of reworking, although a regular seismic facies is encountered here as well. Most likely, sediment from the inverting Broad Fourteens Basin accumulated into these areas as slumps, turbidites or debris-flow deposits.

Large scale reworking, as expressed by a chaotic seismic reflection configuration, is evident in areas that underwent intense syn-depositional tectonic movement. At least two kilometre-scale allochthonous sediment bodies are visible along the flanks of the Dutch Central Graben inversion dome (Fig. 3.9, Fig. 3.10 & Fig. 3.11). As a unique feature in the study area, a large N-S trending channel system was active in the eastern part of the Ameland Block during the Late Maastrichtian and possibly also the Danian. This system consists of at least two separate channels, or possibly several stacked channels. The often-chaotic seismic reflection configuration within these structures suggests extensive slumping of the channel levees (Fig. 3.5).

An important goal of this study was to improve the subdivision of the Chalk interval in the Netherlands offshore area. The existing subdivision comprises of the

Cenomanian Texel Formation, the Turonian to Maastrichtian Ommelanden Formation and the Danian Ekofisk Formation (Fig. 1.5). By mapping unconformities in 2D and 3D seismic sections covering the whole study area, a subdivision into eleven seismic sequences was made. These represent the Cenomanian (CK1), Turonian (CK2), Coniacian (CK3), Santonian (CK4), lower Campanian (CK5; CK6), middle to upper Campanian (CK7), lower Maastrichtian (CK8), lower to upper Maastrichtian (CK9), upper Maastrichtian to lower Danian (CK10) and Danian (CK11). The sequences were dated by correlation with micropaleontological data (Fig. 2.20). This subdivision served as a framework for the remaining analyses presented in this thesis. More unconformities than those defining the eleven seismic sequences are visible in the seismic sections, particularly where the Chalk interval is thick. This means that more phases of chalk deposition must have occurred than the eleven phases recognised in the study area. Furthermore, closer examination of well-logs reveals the existence of even more unconformities that indicate that locally frequent breaks in sedimentation occurred.

The sedimentary-tectonic development of the Chalk in the study area was strongly influenced by several phases of inversion tectonics during the Late Cretaceous and Early Tertiary. As a result, a regional subdivision into nine, roughly NW–SE trending, Chalk 'provinces' can be made that each are made up of one or more early Mesozoic structural elements (Fig. 3.1).

The Chalk is thinnest on former intra-basinal lows, such as the Vlieland Basin and Terschelling Basin, which were uplifted during the Turonian to Santonian. Uplift of the Dutch Central Graben and Broad Fourteens Basin, from the middle Campanian onwards, resulted in the removal of the entire Chalk sequence (Fig. 3.4 & 3.6). Inversion of the Broad Fourteens Basin resulted in the formation of deep marginal throughs, particularly to the north, which probably filled up with material derived from the uplifted structure. As already mentioned, the likely allochthonous origin of the Chalk in the northern marginal through is suggested by the predominantly chaotic log response character observed here.

Early Mesozoic intra-basinal highs underwent predominantly gradual subsidence during the Late Cretaceous and Early Tertiary, leading to the accumulation of thick sequences of Chalk. The Schill Grund High–Ameland Block province is a good example of such an area, where up to 1250 m of mostly pelagic chalk is present. In north-western Europe, the period of chalk deposition ended with the surfacing of landmasses during the Alpine continental convergence, at the beginning of the Tertiary, because influx of erosional detritus effectively ended the clear water conditions that had favoured the coccolithoporids, and deposition of siliciclastic sediments took over (Section 1.1). The Chalk became compacted as it was buried under increasingly thicker layers of clay. As a result, the interval velocity of the Chalk increased

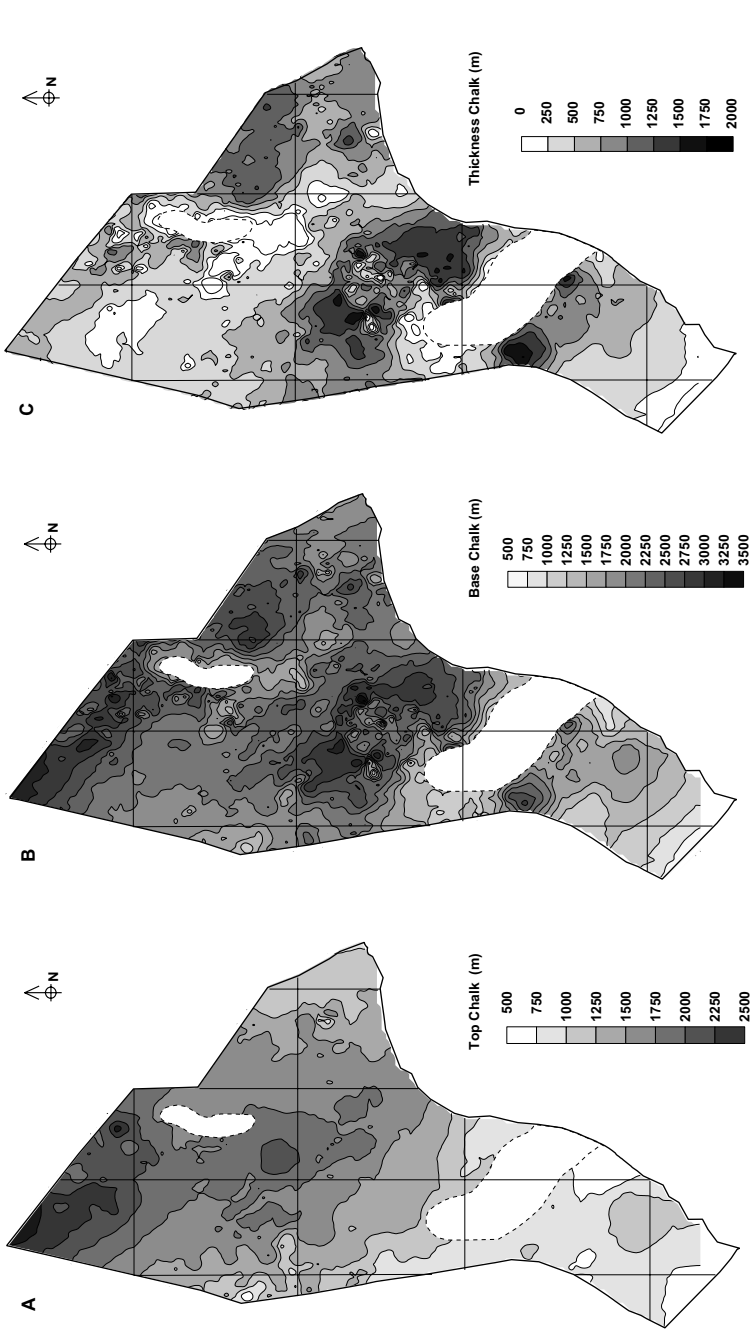

Figure 6.1: Upper boundary (A) and lower boundary (B) depth, and thickness (C) of the Chalk Group in the Netherlands offshore area

at a rate of 1.15 to 1.3 m/s below one kilometre burial depth. This equals to a 1% porosity loss per 70–80 m (Section 5.4). The Tertiary clays acted as pressure barrier for the compacting chalk, resulting in pore fluids to be trapped in the upper part of the Chalk interval (Fig. 5.10). In the northern part of the Netherlands offshore area, where burial rates where highest, interval velocities are up to 2250 m/s lower than would normally be expected at the present burial depth because the trapped pore fluids carry part of the lithostatic pressure. Post-Danian uplift of the southern part of the study area was probably as much as 600 m, as is indicated by high interval velocities here (Fig. 5.13).

A practical application of the interval velocities used to study the burial compaction of the Chalk is that these allow for a more accurate time-depth conversion through this interval. The Top Chalk (Fig. 2.12) and Base Chalk (Fig. 2.2) seismic traveltime maps have been converted to a Top Chalk (Fig. 6.1A) and Base Chalk (Fig. 6.1B) depth map, using the the interval velocities of the Chalk Group and North Sea Super Group (Fig. 5.6). Fig. 6.1C shows the thickness of the Chalk.

References

Alvarez, L.W., Alvarez, W., Asaro, F. & Michel, H.V., 1980. Extraterrestrial cause for the Cretaceous–Tertiary extinction, Science, v. 208, n. 4448, p. 1095–1108.

Andersen, C., Clausen, C.K., Möller, C., Nygaard, E., Stouge, S., 1990. Intra-chalk Study, EFP-87: A Multidisciplinary Breakdown, Geological Survey of Denmark, 30 p.

Anderson, J.K., 1999. The capabilities and challenges of the seismic method in chalk exploration, *in:* Fleet, A.J. & Boldy, S.A.R. (eds.), Petroleum Geology of Northwest Europe: proceedings of the 5th Conference, The Geological Society, London, p. 939–949.

Barron, E.J., Arthur, M.A. & Kauffman, E.G., 1985. Cretaceous rhythmic bedding sequences: a plausible link between orbital variations and climate, Earth & Planetary Science Letters, v. 72, p. 327–340.

Bergen, J.A. & Sikora, P. J., 1999. Microfossil diachronism in southern Norwegian North Sea chalks; Valhall and Hod fields, *in:* Jones, R.W. & Simmons, M.D. (eds.), Biostratigraphy in production and development geology, Geological Society Special Publications, Geological Society of London. London, United Kingdom, v. 152, p. 85–111.

Box, R. & Lowrey, P., 2003. Reconciling sonic logs with check-shot surveys: Stretching synthetic seismograms, The Leading Edge, v. 6, p. 510–516.

Bramwell, N.P., Caillet, G., Meciani, L., Judge, N., Green, A. & Adam, P., 1999. Chalk exploration, the search for a subtle trap, *in:* Fleet, A.J. & Boldy, S.A.R. (eds.), Petroleum Geology of Northwest Europe: proceedings of the 5th Conference, The Geological Society, London, p. 911–937.

Brasher, J.E. & Vagle, K.R., 1996. Influence of lithofacies and diagenesis on Norwegian North Sea chalk reservoirs, AAPG Bulletin, v. 80, n. 5, p. 746–769.

Britze, P., Nielsen, E.B., Dahl, N. & Haug, S., 2003. North Sea chalk porosity resolved by integration of seismic reflectivity and well log data, Abstract P100, 64th EAGE conference & exhibition, Florence, 4 p.

Bromley, R.G. & Ekdale, A.A., 1987. Mass transport in European Cretaceous chalk; fabric criteria for its recognition, Sedimentology, v. 34, n. 6, p. 1079–1092.

Brown, A.R., 1991. Interpretation of Three-Dimensional Seismic Data, 3rd edition, AAPG Memoir 42, 341 p.

Buchanan, P. G., Bishop, D.J. & Hood, D.N., 1996. Development of salt-related structures in the Central North Sea: results from section balancing, *in:* Alsop, G.I., Blundell, D.J. & Davison, I. (eds.), Salt Tectonics, Geological Society Special Publications No. 100, p. 111–128.

Bulat, J. & Stoker, S.J., 1987. Uplift determination from interval velocity studies, UK southern North Sea, *in:* Brooks, J. & Glennie, K. (eds.), Petroleum geology of North West Europe, p. 293–305.

Caillet, G., Judge, N. C., Bramwell, N. P., Meciani, L., Green, M. & Adam, P., 1997. Overpressure and hydrocarbon trapping in the Chalk of the Norwegian Central Graben, Petroleum Geoscience, v. 3, p. 33–42.

Campbell, S.J.D. & Gravdal, N., 1995. The prediction of high porosity chalks in the East Hod Field, Petroleum Geoscience, v. 1, p. 57–69.

Clarke, R.H., 1973. Cainozoic subsidence in the North Sea, Earth & Planetary Science Letters, v. 18, p. 329–332.

Clausen, O.R. & Hansen, J.P. V., 2000. Late Cretaceous and Cenozoic inversion tectonics in the North Sea basin, *in:* Cenozoic development of the eastern North Sea Basin, Observation and Modelling.Abstract volume Basin Workshop Aarhus 2–3 November 2000, p. 8–9.

Clausen, O.R. & Huuse, M., 1999. Topography of the Top Chalk surface on- and offshore Denmark, Marine and Petroleum Geology, v. 16, p. 677–691.

Cloetingh, S., 1986. Intraplate stresses: A new tectonic mechanism for fluctuations of relative sea level, Geology, v. 14, p. 617–620.

Cloetingh, S., McQueen, H. & Lambeck, K., 1985. On a tectonic mechanism for regional sealevel variations, Earth & Planetary Science Letters, v. 75, p. 157–166.

Cottle, R.A., 1989. Orbitally mediated cycles from the Turonian of southern England: their potential for high-resolution stratigraphic correlation, Terra Nova, v. 1, p. 426–431.

Davis, B.K., 1987. Velocity changes and burial diagenesis in the Chalk of the southern North Sea Basin, *in:* Brooks, J. & Glennie, K. (eds.), Petroleum Geology of North West Europe, p. 307–313.

Davison, I., Alsop, G.I., Evans, N. G., Safaricz, M., 2000. Geometry and late-stage structural evolution of Central Graben salt diapirs, North Sea, Marine and Petroleum Geology, v. 17, p. 499–522.

Davison, I., Alsop, I, Birch, P., Elders, C., Evans, N., Nicholson, N., Rorison, P., Wade, D., Woodward, J., & Young, M., 2000. Overburden deformation patterns and mechanisms of salt diapir penetration in the Central Graben, North Sea, Marine and Petroleum Geology, v. 17, p. 601–618.

De Boer, P. L., 1991. Astronomical cycles reflected in sediments, Zbl. Geol. Palaeont. Teil I, v. 8, p. 911–930.

De Jager, J., 2003. Inverted basins in the Netherlands, similarities and differences, Netherlands Journal of Geosciences, v. 82, n. 4, p. 355–366.

De Lugt, I.R., van Wees, J.D. & Wong, T.E., 2003. The tectonic evolution of the southern Dutch North Sea during the Palaeogene: basin inversion in distinct pulses, Tectonophysics, v. 373, p. 141–159.

Ditchfield, P. & Marshall, J.D., 1989. Isotopic variation in rhythmically bedded chalks: Paleotemperature variation in the Upper Cretaceous, Geology, v. 17, p. 842–845.

Doornenbal, J.C., 2001. Regional velocity models of the Netherlands Territory, Abstract A-08, 63rd EAGE conference & exhibition, Amsterdam, 4 p.

Dronkers, A.J. & Mrozek, F.J., 1991. Inverted basins of The Netherlands, First Break, v. 9, n. 9, p. 409–425.

Emery, D. & Myers, K.J., 1996. Sequence Stratigraphy, Blackwell Science, 291 p.

Farmer, C.L. & Barkved, O.I., 1999. Influence of syn-depositional faulting on thickness variations in chalk reservoirs—Valhall and Hod fields, *in:* Fleet, A.J. & Boldy, S.A.R. (eds.), Petroleum Geology of Northwest Europe: proceedings of the 5th Conference, The Geological Society, London, p. 949–957.

Fontaine, J.M., Cussey, R., Lacaze, J., Lanaud, R. & Yapaudjian, L., 1987. Seismic interpretation of carbonate depositional environments, AAPG Bulletin, v. 71, n. 3, p. 281–297.

Friedman, G., 1996. Chalk Reservoirs, *in:* Chilingarian, G.V., Mazzullo, S.J. & Rieke, H.H. (eds.), Carbonate Reservoir Characterization: A Geologic-Engineering Analysis, Part II, p. 773–796.

Gale, A.S, Young, J.R., Shackleton, N. J., Crowhurst, S.J. & Wray, D.S., 1999. Orbital tuning of Cenomanian marly chalk successions: towards a Milankovitch time-scale for the Late Cretaceous, Philosophical Transactions of the Royal Society of London, p. 1815–1829.

Gale, A.S., 1989. A Milankovitch scale for Cenomanian time, Terra Nova, v. 1, p. 420–425.

Gardner, G.H.F., Gardner, L.W. & Gregory, A.R., 1974. Formation velocity and density—the diagnostic basics for stratigraphic traps, Geophysics, v. 39, n. 6, p. 770–780.

Gilbert, G.K., 1895. Sedimentary measurement of Cretaceous time, Journal of Geology, v. III, n. 2, p. 121–127.

Glennie, K.W., 1992. Some geological advances resulting from North Sea exploration, First Break, v. 10, n. 5, p. 161–173.

Grützner, J. & Mienert, J., 1999. Physical property changes as a monitor of pelagic carbonate diagenesis; an empirically derived diagenetic model for Atlantic Ocean basins, AAPG Bulletin, v. 83, n. 9, p. 1485–1501.

Gras, R., 1995. Late Cretaceous sedimentation and tectonic inversion, southern Netherlands, Geologie en Mijnbouw, v. 74, p. 117–127.

Gras, R. & Geluk, M., 1999. Late Cretaceous–Early Tertiary sedimentation and tectonic inversion in the southern Netherlands, Geologie en Mijnbouw, v. 78, n. 1, p. 1–19.

Håkansson, E., Bromley, R. & Perch-Nielsen, K., 1974. Maastrichtian chalk of north-west Europe—a pelagic shelf sediment, *in:* Hsü, K.J. & Jenkyns, H.C. (eds.), Pelagic Sediments: on Land and under the Sea, Blackwell Scientific Publications, p. 211–235.

Hancock, J.M, 1990. The formation and diagenesis of chalk, *in:* Downing, R.A., Price, M. & Jones, G.P. (eds.), The Hydrogeology of the Chalk of North-West Europe, p. 14–35.

Hancock, J.M. & Scholle, P. A., 1975. Chalk of the North Sea, *in:* Woodland, A.W.(ed.), Petroleum and the continental shelf of North-West Europe, John Wiley & Sons, New York.

Hancock, J.M., 1975. The petrology of the Chalk, Proceedings of the Geological Association, v. 86, n. 4, p. 499–535.

Hardenbol, J., Thierry, J., Farley, M.B., Jacquin, T., De Graciansky, P.-C. & Vail, P.R., 1998. Mesozoic and Cenozoic sequence chronostratigraphic framework of European basins *and* Chart 1: Mesozoic and Cenozoic Sequence Chronostratigraphic Chart, *in:* De Graciansky, P.-C., Hardenbol, J., Jacquin, T. & Vail, P.R. (eds.), Mesozoic and Cenozoic Sequence Stratigraphy of European Basins, SEPM Special Publication 60, p. 100–150.

Hardenbol, J., Thierry, J., Farley, M.B., Jacquin, T., De Graciansky, P.-C. & Vail, P.R., 1998. Chart 3: Cenozoic Biochronostratigraphy *and* Chart 5: Cretaceous Biochronostratigraphy, *in:* De Graciansky, P.-C., Hardenbol, J., Jacquin, T. & Vail, P.R. (eds.), Mesozoic and Cenozoic Sequence Stratigraphy of European Basins, SEPM Special Publication n. 60.

Hart, M.B., 1987. Orbitally induced cycles in the Chalk facies of the United Kingdom, Cretaceous Research, v. 8, p. 335–348.

Hatton, I.R., 1986. Geometry of allochthonous Chalk Group members, Central Through, North Sea, Marine and Petroleum Geology, v. 3, p. 79–98.

Hays, J.D. & Pitman, W.C., 1973. Lithospheric Plate Motion, Sea Level Changes and Climatic and Ecological Consequences, Nature, v. 246, p. 18–22.

Henry, S., 2000, Pitfalls in synthetics, The Leading Edge, v. 6, p. 604–606.

Herbert, T.D. & Fischer, A.G., 1986, Milankovitch climatic origin of mid-Cretaceous black shale rhytms in central Italy, Nature, v. 321, p. 739–743.

Herbert, T.D., 1993. Differential compaction in lithified deep-sea sediments is not evidence for 'diagenetic unmixing', Sedimentary Geology, v. 84, n. 1-4, p. 115–122.

Herbert, T.D. & D'Hondt, S.L., 1990. Precessional climate cyclicity in Late Cretaceous–Early Tertiary marine sediments: a high resolution chronometre of Cretaceous–Tertiary boundary events, Earth & Planetary Science Letters, v. 99, p. 263–275.

Herngreen, G.F.W., Eillebrecht, A.T.J.M., Gortemaker, R.E., Remmelts, G., Schuurman, H.A.H.M. & Verbeek, J.W., 1996. Upper Cretaceous Chalk Group stratigraphy near the isle of Texel, the Netherlands (a multidisciplinary approach), Medelingen Rijks Geologische dienst, v. 56, 63 p.

Herngreen, G.F.W., Smit, R. & Wong, Th.E., 1991. Stratigraphy and tectonics of the Vlieland Basin, The Netherlands, *in:* Spencer, A.M.(ed.), Generation, accumulation, and production of Europe's hydrocarbons, Special Publication of the European Association of Petroleum Geoscientists, n. 1, p. 175–192.

Herrington, P. M., Pederstad, K. & Dickson, J.A.D., 1991. Sedimentology and diagenesis of resedimented and rhythmically bedded chalks from the Eldfisk Field, North Sea Central Graben, AAPG Bulletin, v. 75, n. 11, p. 1661–1674.

Heybroek, P. 1974. Explanation to tectonic maps of the Netherlands, Geologie en Mijnbouw, v. 53, p. 43–50.

Heybroek, P., 1975. On the structure of the Dutch part of the Central North Sea Graben, *in:* Woodland, A.W. (ed.), Petroleum and the continental shelf of north-west Europe, p. 339–349.

Hillis, R.R., 1995. Quantification of tertiary exhumation in the United Kingdom southern North Sea using sonic velocity data, AAPG Bulletin, v. 79, n. 1, p. 130–152.

Hofmann, A.P., Price, A.,Kaffenberger, G., Godderij, R. & Simpson, M., 2002. Hanze chalk oil field—the chalk pearl in the Dutch North Sea, Abstract P211, 64th EAGE conference & exhibition, Florence, 4 p.

Hooper, R.J, Goh, L.S. & Dewey, F., 1995. The inversion history of the northeastern margin of the Broad Fourteens Basin, *in:* Buchanan, J.G. & Buchanan, P. G. (eds.), Basin Inversion, Geological Society Special Publication, n. 88, p. 307–317.

Huber, B.T., Norris, R.D. & MacLeod, K.G., 2002. Deep-sea paleotemperature record of extreme warmth during the Cretaceous, Geology, v. 30, n. 2, p. 123–126.

Huuse, M., 1999. Detailed morphology of the Top Chalk surface in the eastern Danish North Sea, Petroleum Geoscience, v. 5, p. 303–314.

Huyghe, P. & Mugnier, J.L., 1994. Intra-Plate Stresses and Basin Inversion: A Case from the Southern North Sea, *in:* Roure, F. (ed.), Peri-Thetyan Platforms, p. 211–226.

Japsen, P., 1998. Regional velocity-depth anomalies, North Sea Chalk: a record of overpressure and Neogene uplift and erosion, AAPG Bulletin, v. 82, n. 11, p. 2031–2074.

Japsen, P., 1999. Overpressured Cenozoic shale mapped from velocity anomalies relative to a baseline for marine shale, North Sea, Petroleum Geoscience, v. 5, n. 4, p. 321–336.

Japsen, P., 2000. Investigation of multi-phase erosion using reconstructed shale trends based on sonic data.Sole Pit axis, North Sea, Global and Planetary Change, v. 24, p. 189–210.

Jarvis, I., Mabrouk, A, Moody, R.T.J. & De Cabrera, S., 2002. Late Cretaceous (Campanian) carbon isotope events, sea-level change and correlation of the Tethyan and Boreal realms, Palaeogeography, Palaeoclimatology, Palaeoecology, v. 188, p. 215–248.

Jenkyns, H.C., 1980. Cretaceous anoxic events: from continents to oceans, Journal of the Geological Society London, v. 137, p. 171–188.

Jenkyns, H.C., Gale, A.S. & Corfield, R.M, 1994. Carbon- and oxygen-isotope stratigraphy of the English Chalk and Italian Scaglia and its palaeoclimatic significance, Geological Magazine, v. 131, n. 1, p. 1–34.

Johnson, H., 1987. Seismic expression of major chalk reworking events in the Palaeocene of the central North Sea, *in:* Brooks, J. & Glennie, K. (eds.), Petroleum Geology of North West Europe, p. 591–598.

Jorgensen, N. O., 1986. Geochemistry, diagenesis and nannofacies of chalk in the North Sea Central Graben, Sedimentary Geology, v. 48, p. 267–294.

Kearey, P. & Brooks, M., 1991. An introduction to geophysical exploration, Blackwell Science, 254 p.

Kennedy, W.J., 1987. Sedimentology of Late Cretaceous–Palaeogene chalk reservoirs, North Sea Central Graben, *in:* Brooks, J. & Glennie, K. (eds.), Petroleum Geology of North West Europe, p. 469–481.

King, C., 1989. Cenozoic of the North Sea, *in:* Jenkins, D.G. & Murray, J.W. (eds.), Stratigraphic atlas of fossil foraminifera., p. 418–490.

King, C., Bailey, H.W., Burton, C. & King, A.D., 1989. Cretaceous of the North Sea, *in:* Jenkins, D.G. & Murray, J.W. (eds.), Stratigraphic atlas of fossil foraminifera., p. 372–418.

Koch, W., 1977. Biostratigraphie in der Oberkreide und Taxonomie von Foraminiferen, *in:* Lang, H.D.(ed.), Stratigraphie der Oberkreide in Nordwestdeutschland (Pompeckjsche Scholle)—Teil 2, Geologisches Jahrbuch, Reihe A, v. 38, p. 11–123.

Kockel, F., 2003. Inversion structures in Central Europe—Expressions and reasons, an open discussion, Netherlands Journal of Geosciences, v. 82, n. 4, p. 355–366.

Koyi, H. & Petersen, K., 1993. Influence of basement faults on the development of salt structures in the Danish Basin, Marine and Petroleum Geology, v. 10, p. 82–94.

Kristensen, L., Dons, T., Gunn Maver, K. & Schiøler, P., 1995. A Multidisciplinary Approach to Reservoir Subdivision of the Maastrichtian Chalk in the Dan Field, Danish North Sea, AAPG Bulletin, v. 79, n. 11, p. 1650–1659.

Larson, R.L., 1991. Geological consequences of superplumes, Geology, v. 19, p. 963–966.

Larson, R.L., 1991. Latest pulse of Earth: evidence for a mid-Cretaceous superplume, Geology, v. 19, p. 547–550.

Li, L. & Keller, G., 1999. Variability in Late Cretaceous climate and deep waters: evidence from stable isotopes, Marine Geology, v. 161, p. 171–190.

Macurda, B.D., 1997. Carbonate Seismic Facies Analysis, *in:* Palaz, I & Marfurt, K.J. (eds.), Carbonate Seismology, Geophysical Developments No.6, Society of Exploration Geophysicists, pp. 95–119.

Maliva, R.G. & Dickson, J.A.D, 1992. Microfacies and diagenetic controls of porosity in Cretaceous–Tertiary chalks, Eldfisk Field, Norwegian North Sea, AAPG Bulletin, v. 76, n. 11, p. 1825–1838.

Mallon, A.J. & Swarbrick, R.E., 2002. A compaction trend for non-reservoir North Sea Chalk, Marine and Petroleum Geology, v. 19, p. 527–539.

Megson, J,B., 1992. The North Sea Chalk play: examples from the Danish Central Graben, *in:* Hardman, R.F.P. (ed.), Exploration Britain: geological insights for the next decade, Geological Society Special Publication 67, p. 247–282.

Megson, J. & Hardman, R., 2001. Exploration for and development of hydrocarbons in the Chalk of the North Sea: a low permeability system, Petroleum Geoscience, v. 7, p. 3–12.

Mettraux, M., Homewood, P., Schwab, A. & Guillocheau, F., 1999. Sedimentology and accomodation cycles of Paris Basin Campanian chalk; the key to high-resolution stratigraphy and seismic signature, *in:* Harris, P. H., Saller, A.H. & Simo, J.A. (eds.), Advances in carbonate sequence stratigraphy; application to reservoirs, outcrops and models, SEPM Special Publication No. 63, Society for Sedimentary Geology, p. 317–334.

Mitchum, jr., R.M, Vail, P. R., Sangree, J.B., 1977. Seismic stratigraphy and Global Changes of Sea Level, Part 6: Stratigraphic Interpretation of Seismic Reflection Patterns in Depositional Sequences, *in:* Payton, C.E. (ed.), Seismic Stratigraphy—applications to hydrocarbon exploration, AAPG Memoir 26, p. 117–135.

Mitchum, jr., R.M., Vail, P. R., 1977. Seismic stratigraphy and Global Changes of Sea Level, Part 7: Seismic Stratigraphic Interpretation Procedure, *in:* Payton, C.E. (ed.), Seismic Stratigraphy—applications to hydrocarbon exploration, AAPG Memoir 26, p. 135–145.

Molenaar, N. & Zijlstra, J.J.P., 1997. Differential early diagenetic low-Mg calcite cementation and rhythmic hardground development in Campanian–Maastrichtian chalk, Sedimentary Geology, v. 109, n. 3–4, p. 261–281.

Niebuhr, B. & Prokoph, A., 1997. Periodic-cyclic and chaotic successions of the Upper Cretaceous (Cenomanian to Campanian) pelagic sediments in the North German Basin, Cretaceous Research, v. 18, n. 5, p. 731–750.

Niebuhr, B., Wiese, F. & Wilmsen, F., 2001. The cored Konrad 101 borehole (Cenomanian–Lower Coniacian, Lower Saxony): calibration of surface and subsurface log data for the lower Upper Cretaceous of northern Germany, Cretaceous Research, v. 22, n. 5, p. 643–676.

Norris, R.D., Bice, K.L., Magno, E.A. & Wilson, P. A., 2002. Jiggling the tropical thermostat in the Cretaceous hothouse, Geology, v. 30, n. 4, p. 299–302.

Nygaard, E., Andersen, C, Möller, Clausen, C.K. & Stouge, S., 1989. Integrated multidisciplinary stratigraphy of the Chalk Group: an example from the Danish Central Through, *in:* Chalk: proceedings of the International Chalk Symposium held at Brighton Polytechnic on 4–7 September 1989, p. 195–201.

Oakman, C.D. & Partington, M.A., 1998. Cretaceous, *in:* Glennie, K.W. (ed.), Petroleum geology of the North Sea, Blackwell Science, Oxford, p. 294–349.

Olsen, J.C., 1987. Tectonic evolution of the North Sea region, *in:* Brooks, J. & Glennie, K. (eds.), Petroleum Geology of North West Europe, p. 389–401.

Oudmayer, B.C. & De Jager, J., 1993. Fault reactivation and oblique-slip in the Southern North sea, *in:* Parker, J.R. (ed.), Petroleum Geology of Northwest Europe: Proceedings of the 4th Conference, The Geological Society, London, p. 1281–1290.

Paul, C.R.C., Lamolda, M.A., Mitchell, S.F, Vaziri, M.R., Gorostidi, A. & Marshall J.D., 1999. The Cenomanian–Turonian boundary at Eastbourne (Sussex, UK): a proposed European reference section, Palaeogeography, Palaeoclimatology, Palaeooecology, v. 150, p. 83–121.

Prokoph, A., Villeneuve, M., Agterberg, F.P. & Rachold, V., 2001. Geochronology and calibration of global Milankovitch cyclicity at the Cenomanian–Turonian boundary, Geology, v. 29, n. 6, p. 523–526.

R.O.C.C. Group, 1986. Rhythmic bedding in Upper Cretaceous pelagic carbonate sequences: Varying sedimentary response to climatic forcing, Geology, v. 14, p. 153–156.

Remmelts, G., 1995. Fault-related salt tectonics in the southern North Sea, The Netherlands, *in;* Jackson, M.P. A., Roberts, D.G. & Snelson, S. (eds.), Salt tectonics: a global perspective, AAPG Memoir 65, p. 261–272.

Rider, M.H., 1996. The geological interpretation of well logs, Whittles Publishing, London, 245 p.

Schatzinger, R.A., Feazel, C.T. & Henry, W.E., 1985. Evidence of resedimentation in Chalk from the Central Graben, North Sea, SEPM Core Workshop No. 6, 'Deep-water Carbonates', 261 p.

Scheck, M., Bayer, U. & Lewerenz, B., 2003. Salt movements in the Northeast German Basin and its relation to major post-Permian tectonic phases—results from 3D structural modelling, backstripping and reflection seismic data, Tectonophysics, v. 361, p. 277–299.

Scholle, P.A. & Arthur, M.A., 1980. Carbon Isotope Fluctuations in Cretaceous Pelagic Limestones: Potential Stratigraphic and Petroleum Exploration Tool, AAPG Bulletin, v. 64, n. 1, p. 67–87.

Scholle, P.A., 1974. Diagenesis of Upper Cretaceous chalks from England, Northern Ireland, and the North Sea, *in:* Hsü, K.J. & Jenkyns, H.C. (eds.), Pelagic Sediments: on Land and under the Sea, Blackwell Scientific Publications, p. 177–211.

Scholle, P.A., 1977. Chalk diagenesis and its relation to petroleum exploration; oil from chalks, a modern miracle?, AAPG Bulletin, v. 61, n. 7, p. 982–1009.

Scholle, P.A., 1998. Formation and diagenesis of bedding cycles in uppermost Cretaceous chalks of the Dan Field, Danish North Sea, Sedimentology, v. 45, n. 2, p. 223–243.

Skirius, C., Nissen, S., Haskell, N., Marfurt, K., Hadley, S., Ternes, D., Michel, K., Reglar, I., D'Amico, D., Deliencourt, F., Romero, T., D'Angelo, R. & Brown, B., 1999. 3-D seismic attributes applied to carbonates, The Leading Edge, v. 3, p. 384–393.

Smit, J. & Hertogen, J., 1980. An extraterrestrial event at the Cretaceous–Tertiary boundary, Nature, v. 285, p. 198–200.

Smit, J., 1990. Meteorite impact, extinctions and the Cretaceous–Tertiary boundary, Geologie en Mijnbouw, v. 69, p. 187–204.

Stage, M., 1999. Signal analysis of cyclicity in Maastrichtian pelagic chalks from the Danish North Sea, Earth & Planetary Science Letters, v. 173, p. 75–90.

Stage, M., 2001. Magnetic susceptibility as carrier of a climatic signal in chalk, Earth & Planetary Science Letters, v. 188, p. 17–27.

Stage, M., 2001. Recognition of cyclicity in the petrophysical properties of a Maastrichtian pelagic chalk oil field reservoir from the Danish North Sea, AAPG Bulletin, v. 85, n. 11, p. 2003–2015.

Stewart, S.A., 2003. How will we recognize buried impact craters in terrestrial sedimentary basins?, Geology, v. 31, n. 11, p. 929–932.

Stewart, S.A. & Allen, P. A, 2002. A 20-km-diameter multi-ringed impact structure in the North Sea, Nature, v. 418, p. 520–523.

Surlyk, F., 1997. A cool-water carbonate ramp with bryozoan mounds: Late Cretaceous–Danian of the Danish Basin, *in:* James, N.P. & Clarke, J.D.A. (eds.), Cool-water carbonates, SEPM Special Publication No. 56, p. 293–307.

Surlyk, F., Dons, T., Clausen, C.K., & Highham, J., 2003. Upper Cretaceous, *in:* Evans, D., Graham, C., Armour, A. & Bathurst, P. (eds.), The Millenium Atlas, Petroleum Geology of the Central and Northern North Sea, Chapter 13, p. 213–233.

Taylor, S.R. & Lapré, J.F., 1987. North Sea chalk diagenesis: its effect on reservoir location and properties, *in:* Brooks, J. & Glennie, K. (eds.), Petroleum Geology of North West Europe, p. 483–495.

Tucker, M.E. & Wright, P. V., 1990. The Chalk, *in:* Carbonate Sedimentology, Blackwell Science, Oxford, p. 245–254.

Underhill, J.R., 2004. An alternative origin for the 'Silverpit crater', Nature, v. 418, p. 520–523.

Vail, P. R., Mitchum, jr., R.M. & Thomson III, S., 1977. Seismic stratigraphy and Global Changes of Sea Level Part 3: Relative Changes of Sea Level from Coastal Onlap, *in:* Payton, C.E (ed.), Seismic Stratigraphy—applications to hydrocarbon exploration, AAPG Memoir 26, p. 99–117.

Vail, P. R., Todd, R.G. & Sangree, J.B., 1977. Seismic stratigraphy and Global Changes of Sea Level, Part 5: Chronostratigraphic Significance of Seismic Reflections, *in:* Payton, C.E (ed.), Seismic Stratigraphy—applications to hydrocarbon exploration, AAPG Memoir 26, p. 99–117.

Van Adrichem Boogaert, H.A. & Kouwe, W.F.P. (eds.), 1994, Stratigraphic nomenclature: section H—Upper Cretaceous and Danian (Chalk Group), Mededelingen Rijks Geologische Dienst, n. 50.

Van Hoorn, B., 1987. Structural evolution, timing and tectonic style of the Sole Pit inversion, Tectonophysics, v. 137, p. 239–284.

Van Wijhe, D.H., 1987. Structural evolution of inverted basins in the Dutch offshore, Tectonophysics, v. 137, p. 171–219.

Vejbæk, O.V. & Andersen, C., 1987. Cretaceous–Early Tertiary inversion tectonism in the Danish Central Trough, Tectonophysics, v. 137, p. 221–238.

Vejbæk, O.V. & Andersen, C., 2003. Post mid-Cretaceous inversion tectonics in the Danish Central Graben—regionally synchronous tectonic events?, Bulletin of the Geological Society of Denmark, v. 49, p. 129–144.

Voigt, E., 1962. Über Randtröge vor Schollenrändern und ihre Bedeutung im Gebiet det Mitteleuropäische Senke und angrenzender Gebiete, Zeitschrift der deutschen geologischen Gesellschaft, v. 114, p. 378–418.

Watts, N. L., Lapré, J.F., Van Schijndel-Goester, F.S. & Ford, A., 1980. Upper Cretaceous and Lower Tertiary chalks of the Albuskjell area, North Sea: deposition in a base-of-slope environment, Geology, v. 8, p. 217–221.

Wendler, J., Gräfe, K.-U., Willems, H., 2002. Reconstruction of mid-Cenomanian orbitally forced palaeoenvironmental changes based on calcareous dinoflagellate cysts, Palaeogeography, Palaeoclimatology, Palaeoecology, v. 179, p. 19–41.

Wyllie, M.R.J., Gregory, A.R. & Gardner, G.H.F., 1958. An experimental investigation of factors affecting elastic wave velocities in porous media, Geophysics, v. 3, p. 459–493.

Yilmaz, O., 1987. Seismic data processing, Society of Exploration Geophysicists, 450 p.

Ziegler, P. A., 1990. Geological atlas of western and central Europe, Shell Internationale Petroleum Maatschappij, The Hague, 237 p.

Zijlstra, J.J.P., 1994. Sedimentology of the Late Cretaceous and Early Tertiary (tuffaceous) chalk of northwest Europe, Geologica Ultraiectina, v. 119, 192 p.

Zijlstra, J.J.P., 1995. The sedimentology of chalk, *in:* Bhattacharji, S. (ed.), Lecture notes in earth sciences, v. 54, Springer Verlag, 194 p.

Appendix - Colour plates

Fig. 3.1 (page 154) Base Chalk surface flattened at Top Chalk level (i.e. TWT isopach of the Chalk Group), viewed from the south. Indicated by white dashed lines are the locations of profiles A–A' to G–G' of Fig. 3.4. The geometry of this surface outlines the vertical movement that occurred during deposition of the Chalk Group. Compression during the Late Cretaceous and Paleogene inverted the older structures, leading to uplift of former basins such as the Central Graben (CG) and Broad Fourteens Basin (BFB), and subsidence of former highs such as the southern Cleaver Bank High (CBH), Texel-IJsselmeer High (TIJH), North Holland Platform (NHP) and Schill Grund High (SGH). Other structural elements include the London-Brabant Massif (LBM), Winterton High (WH), West Netherlands Basin (WNB), Vlieland Basin (VB), Vlieland High (VH), Terschelling Basin (TB), Ameland Block (AB), Rynkøbing-Fyn High (RFH), Step Graben (SG), Outer Rough Basin (ORB), Elbow Split High (ESH), and Mid North Sea High (MNH). The small map indicates the position of the study area (NL) and the surrounding offshore sectors. GB = British, N = Norwegian, DK = Danish and D = German sectors.

Fig. 3.7 (page 155) Base Chalk two-way travel time map of the Dutch Central Graben survey, with the Top Chalk horizon outlined in red. The geometry of the Base Chalk Horizon clearly illustrates the dramatic tectonic events that shaped the Chalk in this area. During the Late Cretaceous and Paleogene, the Dutch Central Graben was inverted, whereby movement along existing boundary faults (F) was reversed. As a result, the Chalk Group is thickest outside the inverted graben, decreasing to zero in the southernmost part of the inversion zone. Reactivated NS (A) and WSW-ENE (B) trending normal fault systems accommodated the uplift of the inversion zone. The upward movement of Zechstein salt, usually along the graben boundary faults, formed salt diapirs (SD). These salt diapirs have deformed the Chalk into highly fractured 4-way structural closures that are important hydrocarbon exploration targets in the Chalk in the North Sea (Oakman & Partington, 1998; Bramwell et al., 1999; Davison et al., 2000b). The 'Hanze' field is presently the only example of such a field in the Dutch offshore (Hofmann et al., 2002).

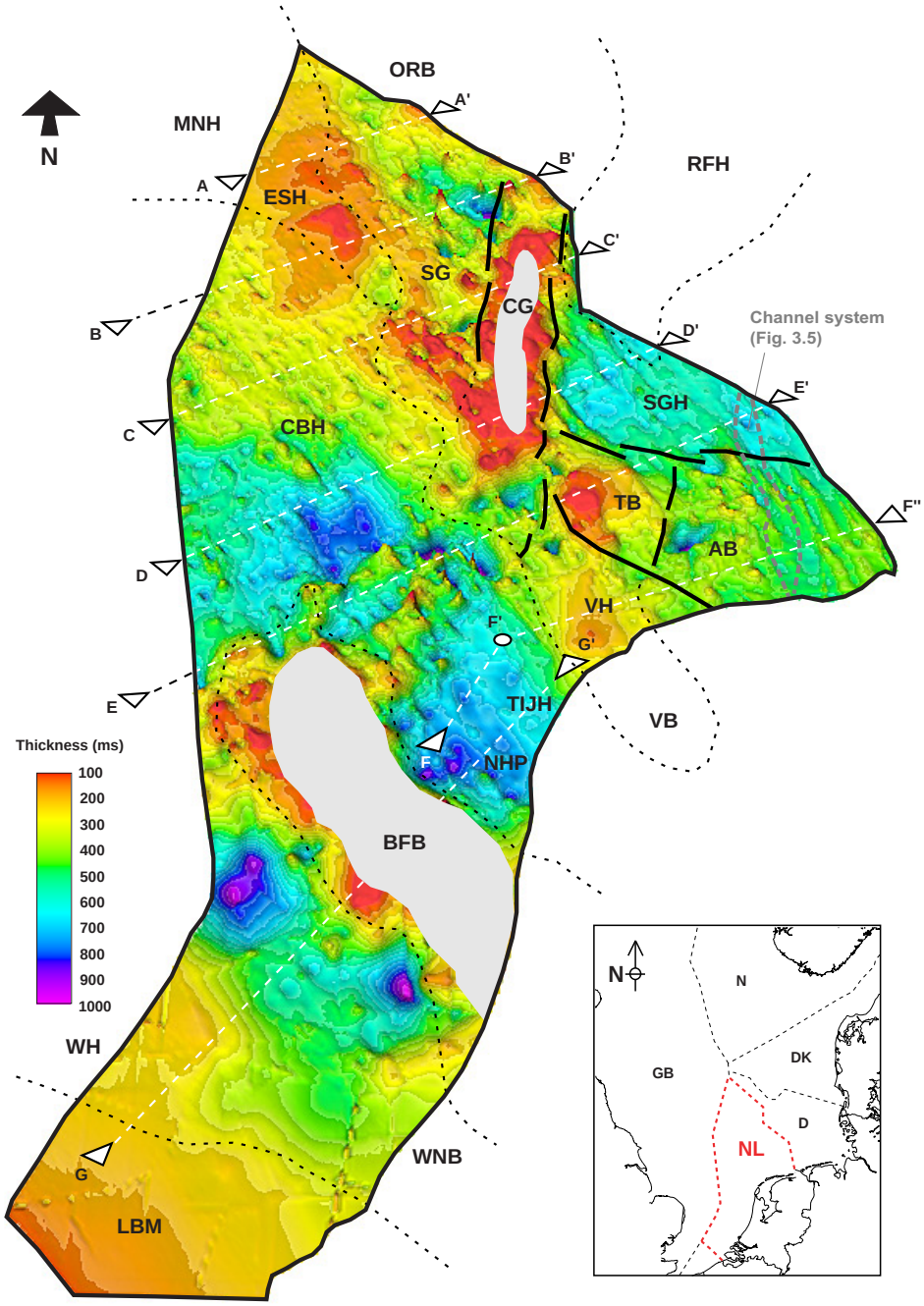
N
ORB
MNH
RFH
ESH
SG
CG
CBH
SGH
TB
AB
VH
TIJH
VB
NHP
BFB
WH
WNB
LBM
Channel system
(Fig. 3.5)
A
A'
B
B'
C
C'
D
D'
E
E'
F
F'
F''
G
G'
Thickness (ms)
100
200
300
400
500
600
700
800
900
1000
N
N
GB
DK
D
NL

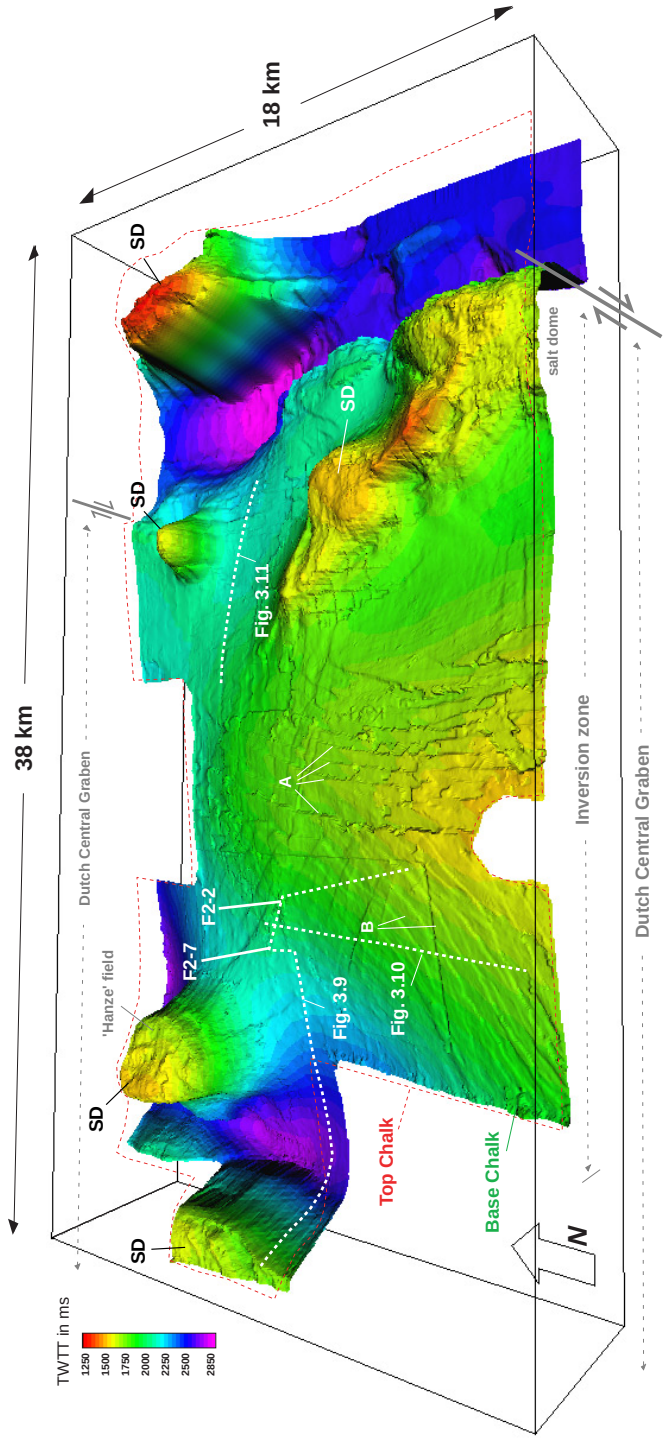
18 km
38 km
SD
SD
SD
SD
SD
Fig. 3.11
A
B
F2-2
F2-7
Fig. 3.9
Fig. 3.10
Top Chalk
Base Chalk
salt dome
Inversion zone
Dutch Central Graben
Dutch Central Graben
'Hanze' field
N
TWTT in ms
1250
1500
1750
2000
2250
2500
2850

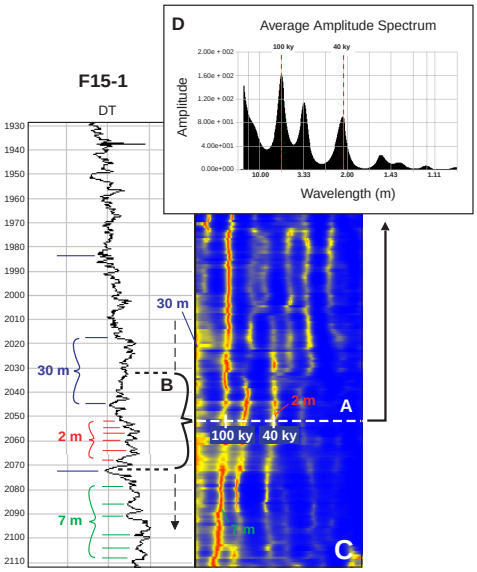

Fig. 4.3 Frequency spectrum of the 1930 to 2110 m interval of the sonic log from borehole F15-1 (Fig. 4.7). At depth A, frequencies within 40 m sliding window B are determined using the MESA routine in Cyclolog and represented in a frequency scalogram (C) and/or spectrum (D). As is evident from the well-log, this interval contains well-developed 30 m, 7 m and 2 m cycles, which are interpreted to be 412 ky E2, 100 ky E1 and 40 ky O1 cycles based on the characteristic wavelength ratio. Frequency scalogram C also indicates the presence of a 3.3 m cyclicity from 2040 m to 2090 m, which is probably the 50 ky oscillation cycle.

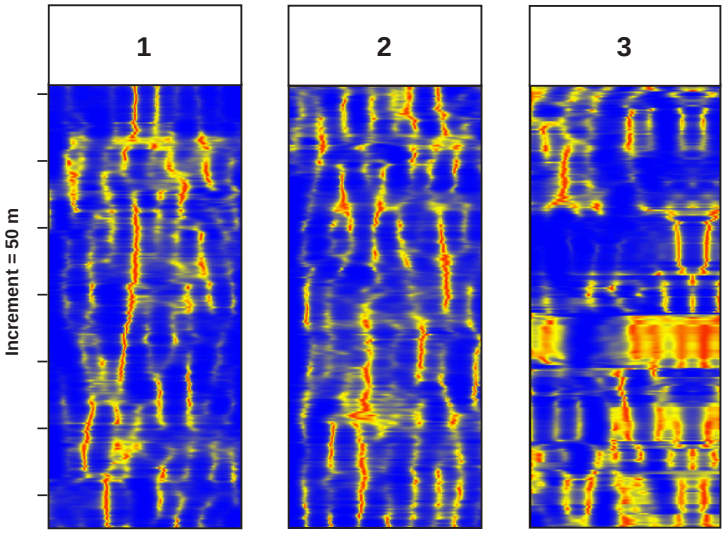

Fig. 4.4 Examples of spectral log facies types appearing in frequency spectrum scalograms of the studied well-logs. See paragraph 4.3 for explanation.

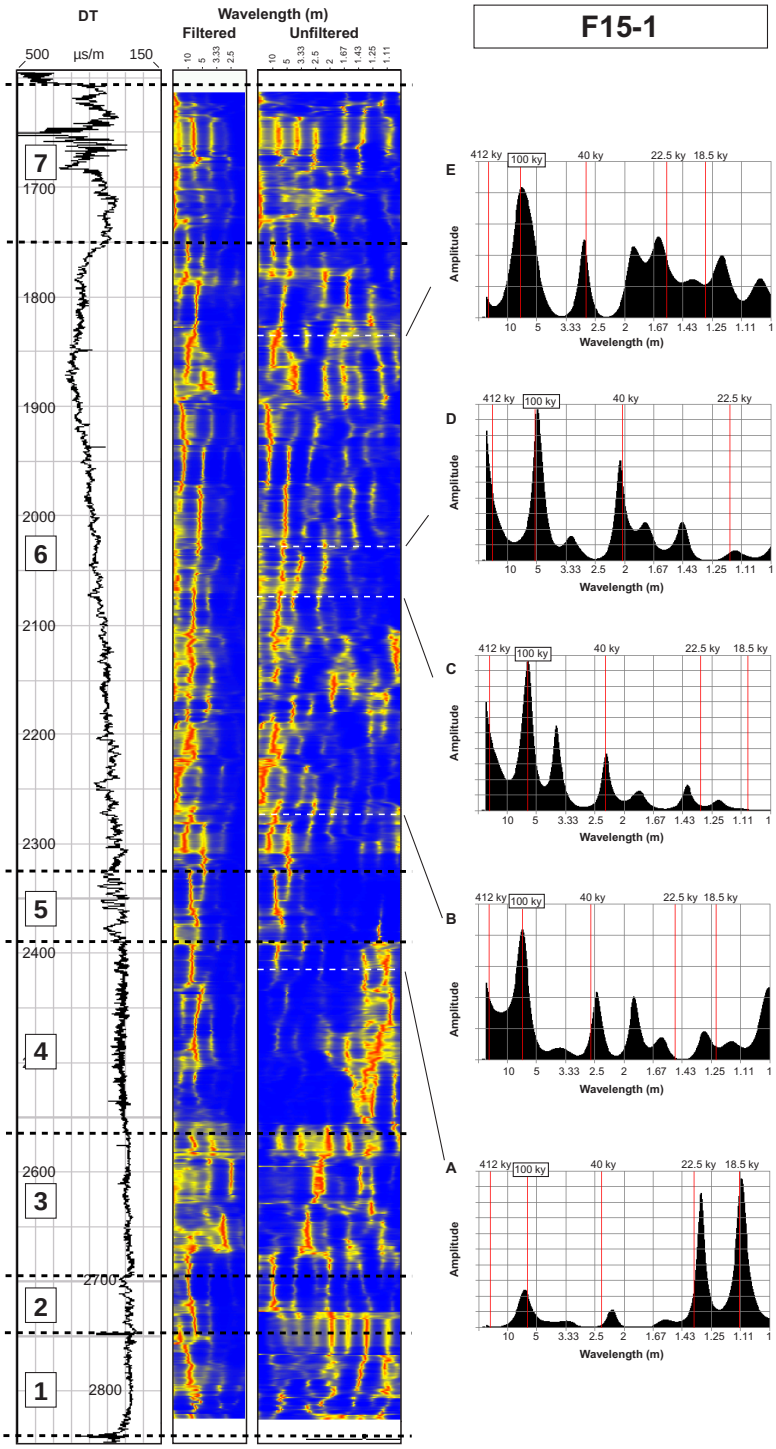

Fig. 4.6 Sonic log of F15-1, with filtered (showing wavelengths larger than 2 m) and unfiltered frequency spectrum scalograms. Frequency spectra at depths A - E indicate Milankovitch cycles recognised in this log. Log interval 6 (2300 - 1750 m) shows well developed cyclicity, with a gradual upwards wavelength decrease.

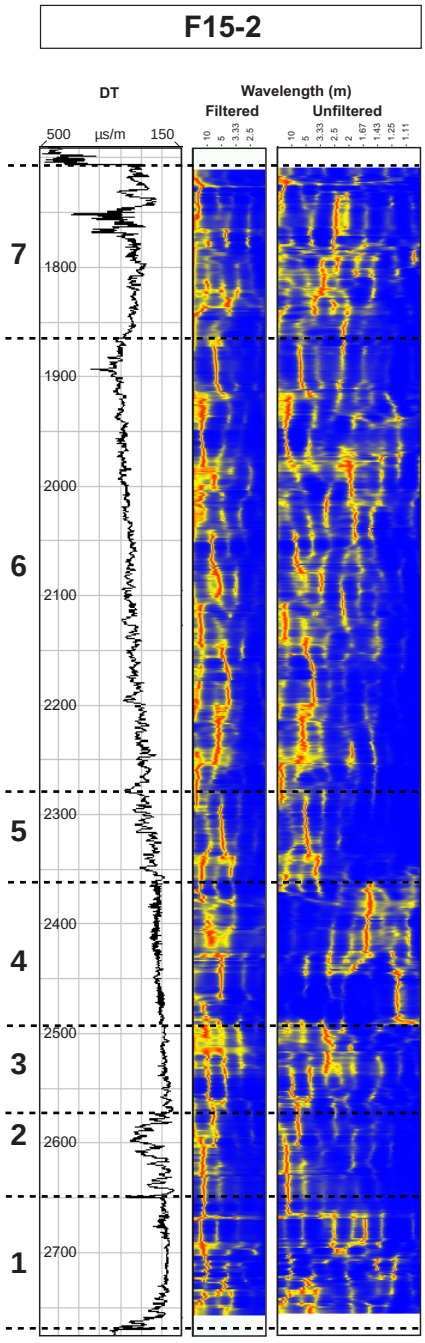

Fig. 4.7 Sonic log of F15-2, with filtered (showing wavelengths > 2 m) and unfiltered frequency spectrum scalograms.

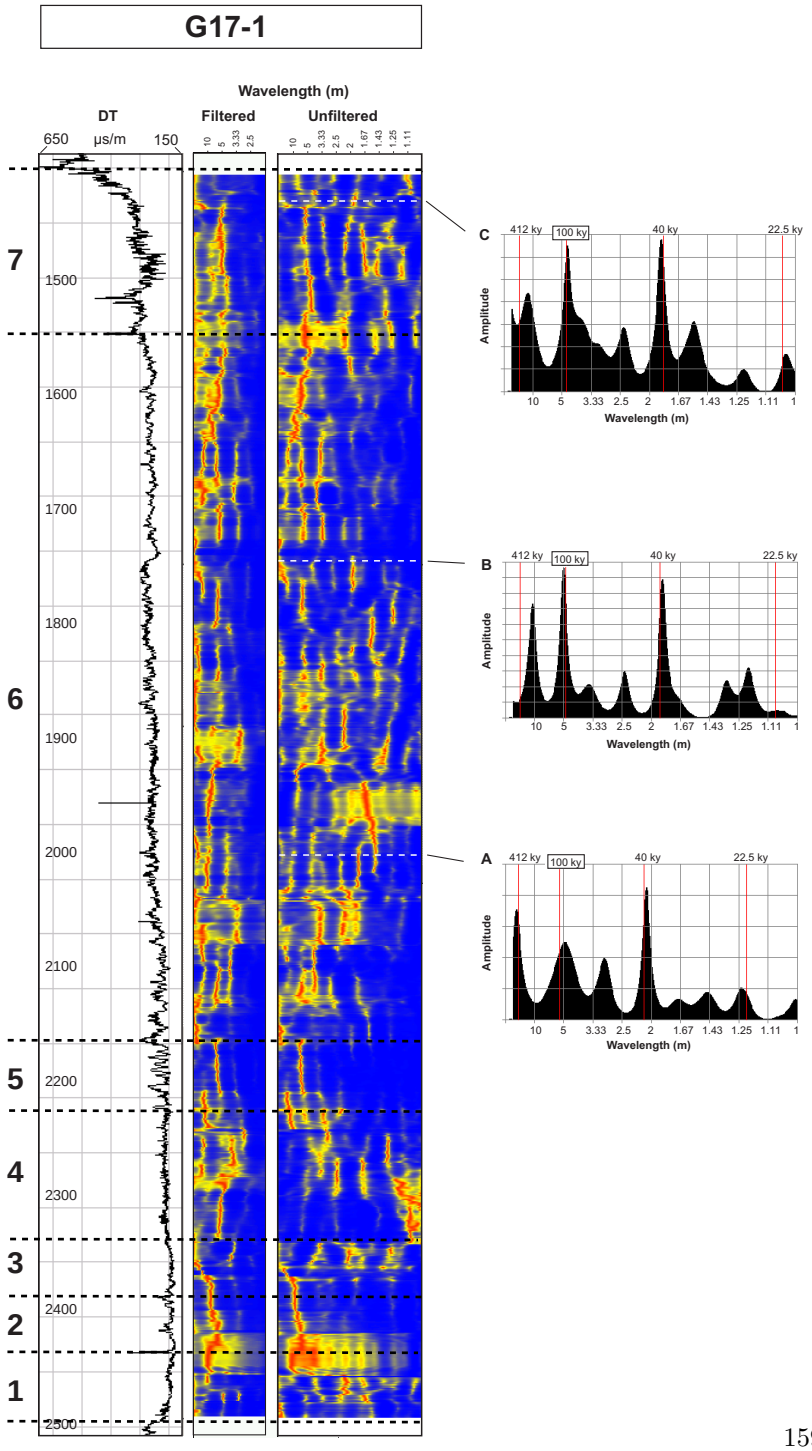

Fig. 4.8 Sonic log of G17-1, with filtered (showing wavelengths > 2 m) and unfiltered frequency spectrum scalograms. Frequency spectra at depths A - C show Milankovitch cycles recognised in this log.

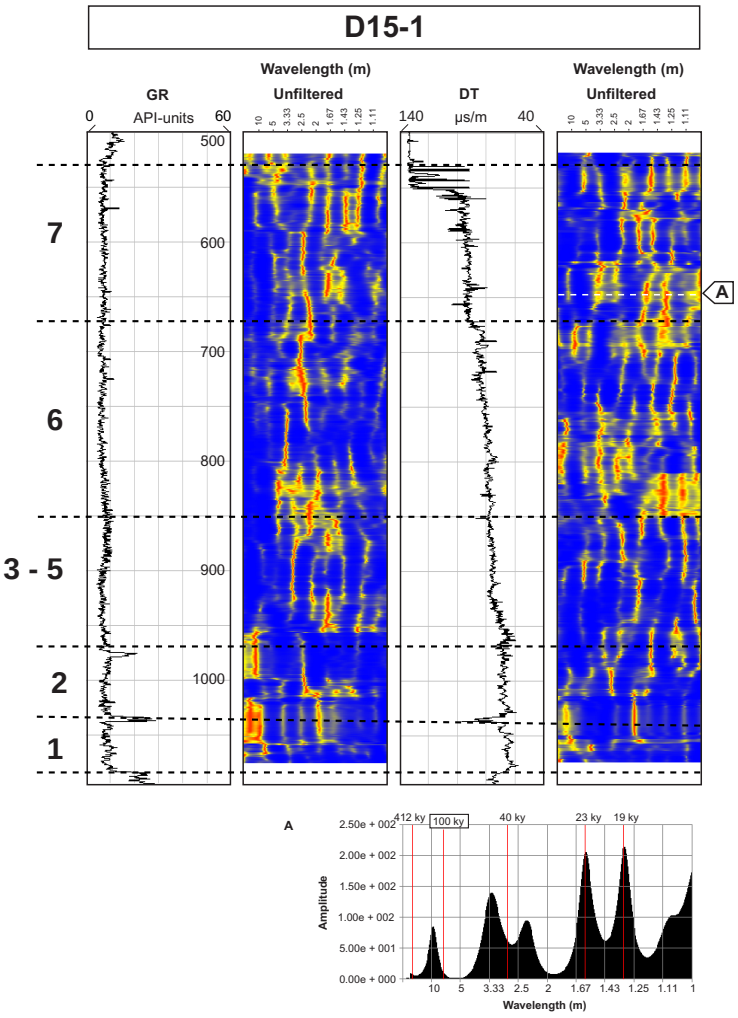

Fig. 4.9 Gamma-ray and sonic log of D15-1 with frequency spectrum scalograms. Average frequency spectrum A shows Milankovitch cycles recognised in this log.

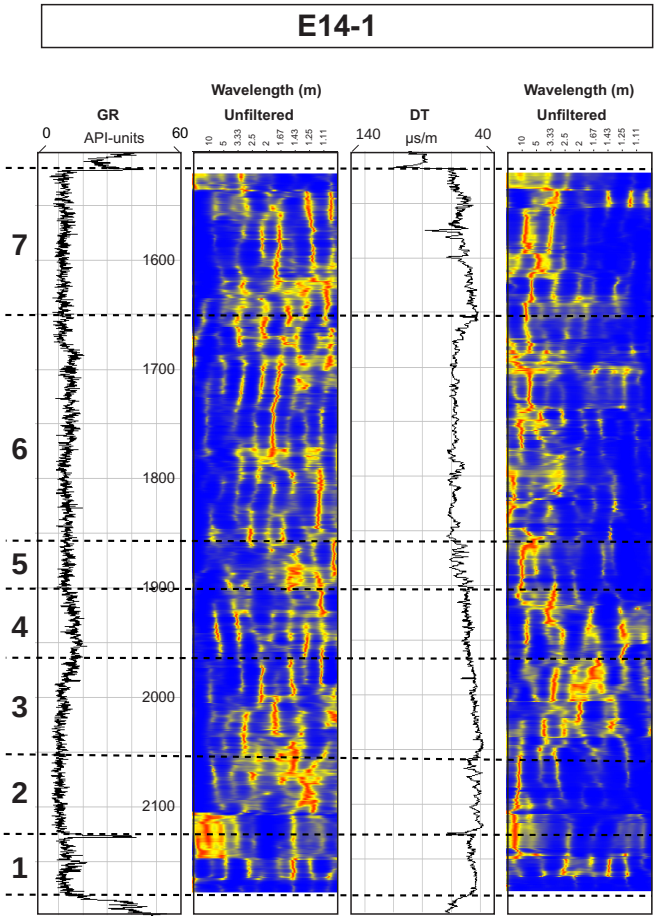

Fig. 4.10 Gamma-ray and sonic log of E14-1 with frequency spectrum scalograms.

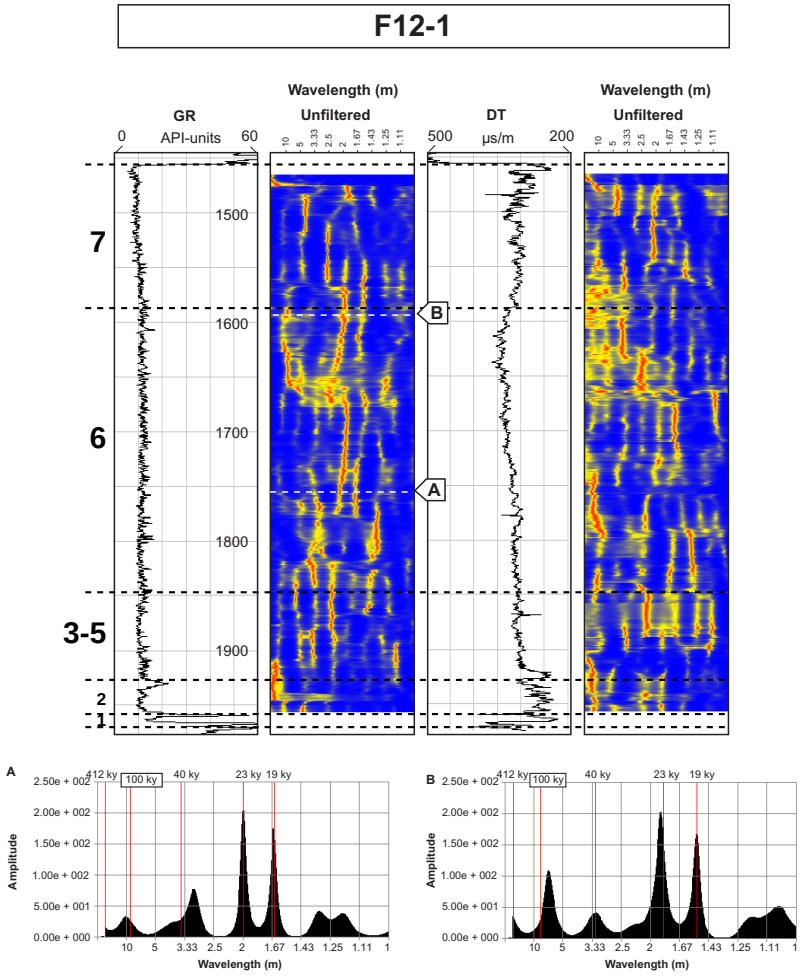

Fig. 4.11 Gamma-ray and sonic log of F12-1 with frequency spectrum scalograms. Average frequency spectra at depths A and B show Milankovitch cycles recognised in this log.

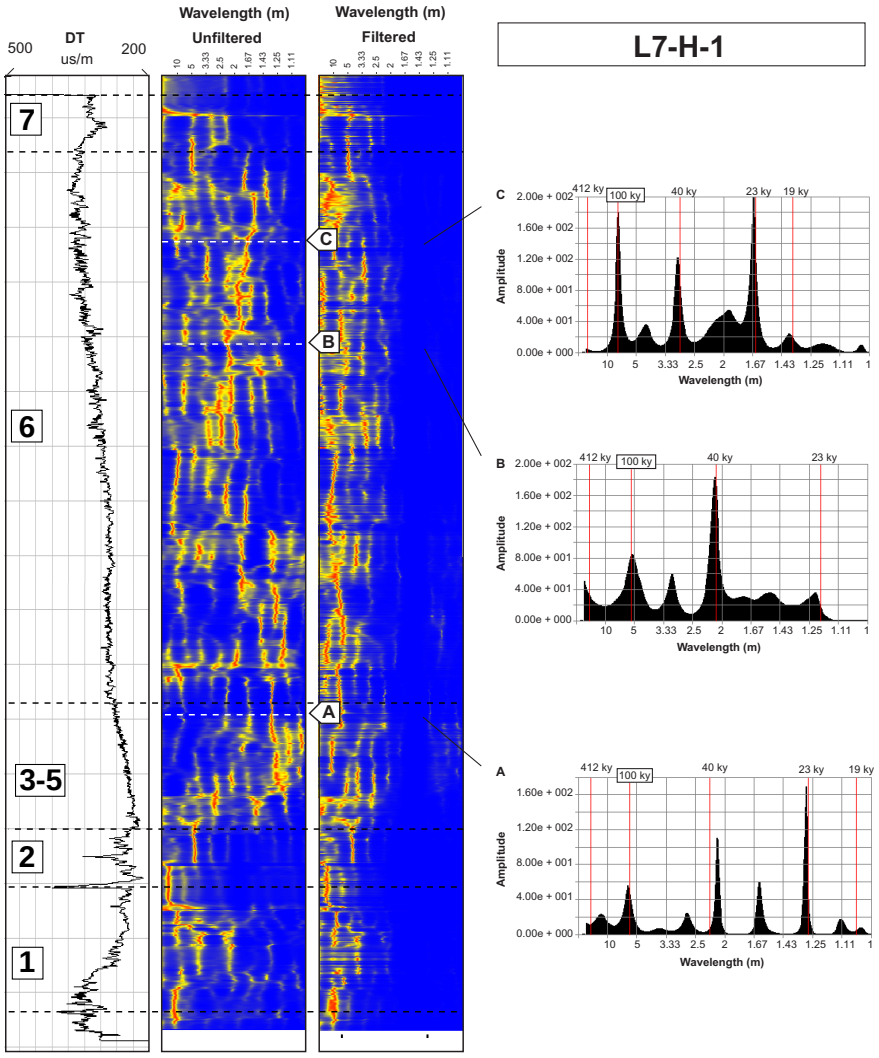

Fig. 4.12 Sonic log of L7-H-1, with unfiltered and filtered (showing $\lambda > 2$ m) frequency spectrum scalograms. Average frequency spectra A–C show Milankovitch cycles recognised in this log.

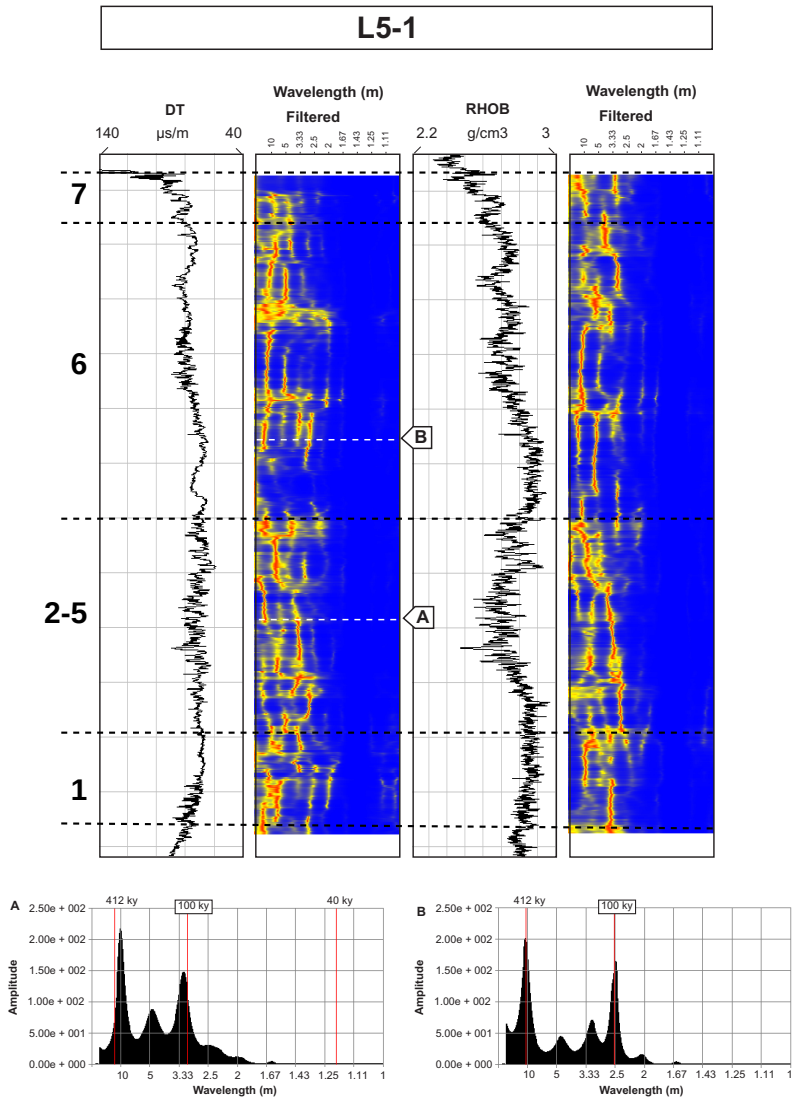

Fig. 4.13 Sonic and density logs of L5-1 with frequency spectrum scalograms. Frequency spectra at depths A and B indicate Milankovitch cycles recognised in the logs.

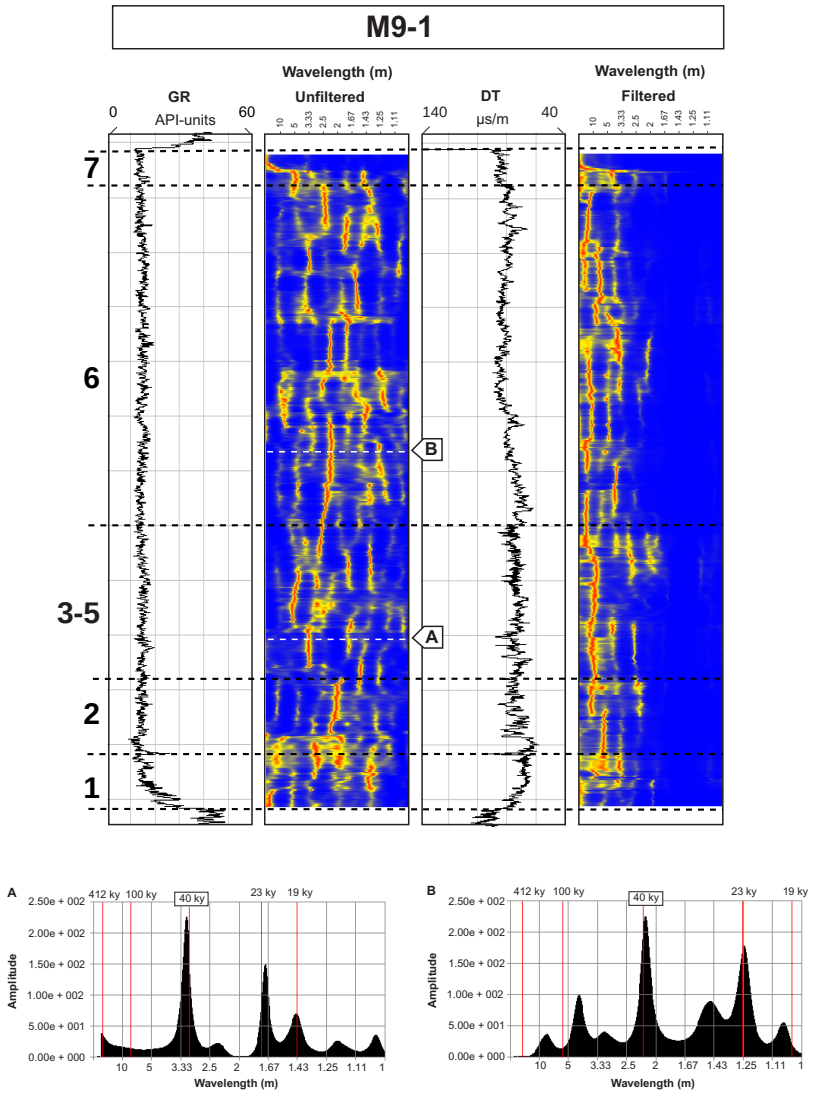

Fig. 4.14 Gamma-ray log with unfiltered frequency spectrum scalogram and sonic log with filtered (showing $\lambda > 2$ m) frequency scalogram of M9-1. Frequency spectra at depths A and B indicate Milankovitch cycles recognised in the gamma-ray log.

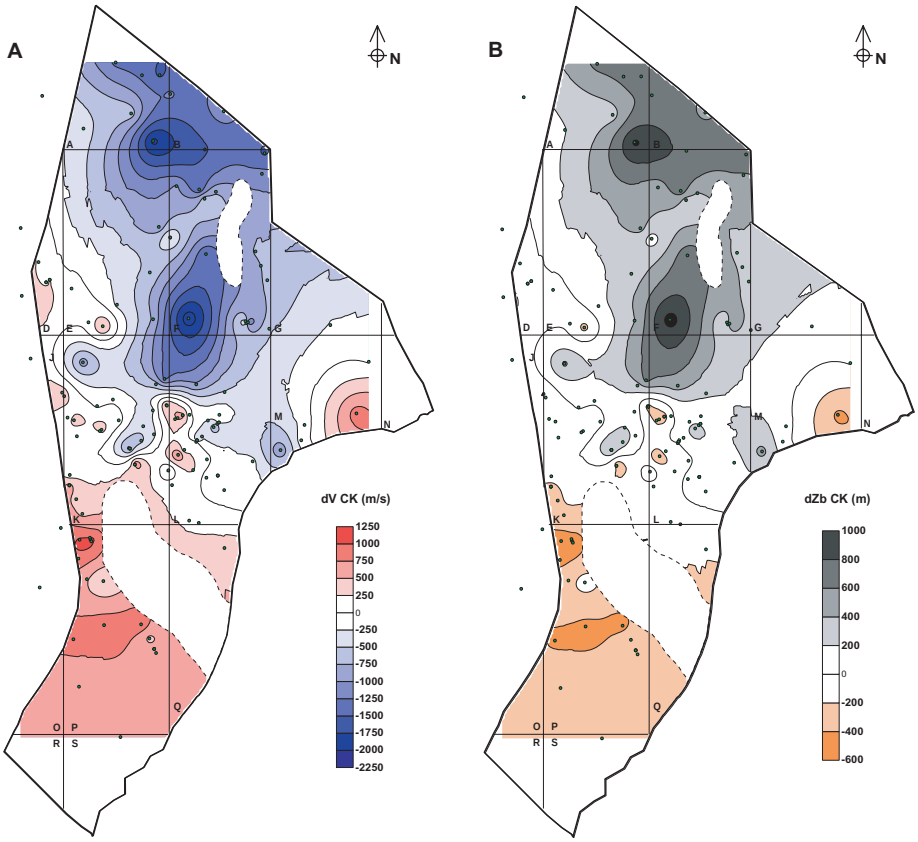

Fig. 5.13 Velocity anomaly (A) and burial anomaly (B) of the Chalk Group. Neutral dV ($250\ m/s < dV < -250\ m/s$) and dZ_b ($200\ m < dZ_b < -200\ m$) values represent Chalk that is normally compacted with respect to burial depth. The Chalk is undercompacted in the north of the Dutch offshore, indicated by negative dV-values and positive dZ_b-values. In the south of the Dutch offshore, the Chalk is overcompacted. Overcompaction is indicated by positive dV-values and negative dZ_b-values.

Samenvatting

Sedimentaire ontwikkeling, seismische stratigrafie en begravingscompactie van de Chalk Groep in het Nederlandse Noordzeegebied

Dit proefschrift behandelt verschillende aspecten van de sedimentaire ontwikkeling, seismische stratigrafie en begravingscompactie van de gesteenten van de Chalk (*krijt*) Groep in de Nederlandse sector van de Noordzee (Fig. 1.2). Deze sedimenten zijn afgezet gedurende het Laat Krijt en vroegste Tertiair, ongeveer 99 tot 61 miljoen jaar geleden. Gedurende deze periode zorgde verhoogde vulkanische activiteit van oceanische spreidingsruggen direct en indirect voor een hoge zeespiegel. Hierdoor raakte een zeer groot deel van noordwest Europa overstroomd, hetgeen onder andere tot gevolg had dat de aanvoer van erosiemateriaal naar zee sterk verminderde. Deze omstandigheden bleken zeer gunstig voor de groei van kalkalgen zodat de zeebodem bedekt raakte met de fossiele resten hiervan. In de loop van miljoenen jaren werd zo een dik pakket krijtkalk afgezet. Deze periode kwam ten einde toen, als gevolg van het dalen van de zeespiegel en het vormen van de Alpiene gebergtegordel, wederom grote hoeveelheden erosiemateriaal in zee stroomden. Sindsdien is de krijtkalklaag in het Noordzeegebied tot meer dan drie kilometer diep onder erosiemateriaal begraven (Fig. 1.3).

Geologische kennis van de samenstelling en structuur van gesteentelagen in de diepe ondergrond is voor een groot deel afhankelijk van het economische belang van dergelijke gesteentelagen, bijvoorbeeld voor de winning van olie of gas. Daar de Chalk Groep in de Nederlandse sector van de Noordzee pas recentelijk als reservoirgesteente is herkend, is de kennis hiervan in dit gebied nog betrekkelijk gering. Er zijn vooral goede beschrijvingen voorhanden van gebieden waar krijtkalk aan de oppervlakte ontsloten is, zoals in delen van zuidwest Engeland, noordoost Frankrijk, noord Duitsland en Denemarken. Daarnaast is een groot deel van de studies afkom-

stig uit de Deense en Noorse sectoren van de Noordzee, waar de Chalk Groep wel een belangrijk reservoirgesteente vormt (Fig. 1.4). Dit proefschrift nu beoogt de lacune die in de kennis van het Nederlandse Noordzeegebied bestaat voor een deel op te vullen.

Een korte uiteenzetting van de tektonische en paleogeografische ontwikkeling van noordwest Europa gedurende het Laat Krijt en vroegste Tertiair, alsmede van de samenstelling, sedimentatie en diagenese ("verstening") van krijt, wordt gegeven in hoofdstuk 1 *Introduction*.

De kartering en beschrijving van de verschillende sedimentpakketten waaruit de Chalk Groep bestaat is het onderwerp van hoofdstuk 2 *Improved subdivision of the Chalk Group in the Netherlands North Sea area through mapping and facies analysis of seismic sequences*. Voor deze kartering is gebruikt gemaakt van gegevens afkomstig van verschillende geofysische opsporingsmethoden, zoals deze in de loop der tijd bij de exploratie naar olie en gas zijn verkregen. De belangrijkste hiervan zijn seismische secties (bijvoorbeeld Fig. 2.14) en boorgatmetingen (bijvoorbeeld Fig. 2.18). Op basis van het seismische reflectiepatroon kon de aanwezigheid van hiaten in de stratigrafische opeenvolging, en daarmee de aanwezigheid van verschillende gesteentepakketten, worden vastgesteld. In totaal zijn er aldus elf seismisch stratigrafische eenheden herkend en beschreven (paragraaf 2.3). Deze eenheden worden doorgaans gekenmerkt door een parallel en continu patroon van seismische reflecties (aangeduid als $=$ in figuren 2.2 tot 2.12). Echter, plaatselijk wijst een chaotisch reflectiepatroon op de aanwezigheid van aardverschuivingen (aangeduid als $\approx$ in figuren 2.2 tot 2.12). De ouderdom van de verschillende seismisch stratigrafische eenheden is bepaald met behulp van micropaleontologische dateringen van gesteentemateriaal afkomstig van boringen. De onderscheiden eenheden vormen de basis voor een verbeterde stratigrafische indeling van de Chalk Groep in dit gebied, en worden zo ook toegepast in de rest van dit proefschrift.

In hoofdstuk 3 *Cenomanian to Danian tectono-sedimentary evolution of the Netherlands North Sea area* wordt de tektonische en sedimentaire evolutie van het Nederlandse Noordzeegebied gedurende het Laat Krijt tot vroegste Tertiair gereconstrueerd. Dit gebeurt aan de hand van de resultaten uit hoofdstuk 2. In verspreiding en diktekaarten van de Chalk Groep (o.a. Fig. 3.1) is een duidelijke onderverdeling in verschillende gebieden te ontdekken, die hier 'provinces' worden genoemd (paragraaf 3.2). Deze "provinces" zijn oudere, meerendeels vroeg-Mesozoische, strukturele elementen van het Noordzeebekken (Fig. 1.8). Deze zijn gedurende de afzetting van de krijtkalk in meer of mindere mate zijn gedaald of opgeheven, met grote dikteverschillen in het krijtkalkpakket tot gevolg. Een belangrijk aspect van de ontwikkeling van het Noordzeebekken is dat gedurende deze periode een aantal grote compressiefases optraden. Deze hielden verband met de zich op dat moment ope-

nende noordelijke Atlantische Oceaan, alsmede de nadering van het Afrikaanse tot het Eurasische continent. Als gevolg van deze compressiefasen werden gebieden die tot dusver waren gedaald, en waarin zich dientengevolge grote hoeveelheden sediment hadden afgezet, opgeheven. Dit proces wordt inversietektoniek genoemd. De Centrale Noordzeeslenk (Central Graben, CG in Fig. 3.1 en Fig. 3.7) en het Breeveertien Bekken (BFB in Fig. 3.1) zijn hiervan in het Nederlandse Noordzeegebied de belangrijkste voorbeelden. Als gevolg van die opheffing ontbreken krijtkalkafzettingen in deze gebieden. Veel gebieden welke voordien stabiele hogen vormden daalden gedurende het Laat Krijt tot vroeg Tertiair, met de afzetting van dikke pakketten krijtkalk tot gevolg. De gebieden aan weerszijden van het Breeveertien Bekken en het Schill Grund Hoog (SGH in Fig. 3.1) zijn daarvan de belangrijkste voorbeelden.

De eerder beschreven compressieve tektonische krachten hebben op veel plaatsen geresulteerd in de opstuwing (*diapirisme*) van dieperliggende zoutlagen tot zoutkoepels, zoals deze te zien zijn op Fig. 3.7. De koepelvormige deformatie van de krijtkalklagen en het daardoor veroorzaakte breken van het gesteente, alsmede de aanwezigheid van overliggende vloeistofondoorlatende Tertiaire kleien, maken deze structuren tot interessante doelen voor de exploratie van olie en gas in de gehele Noordzee regio. Het zgn. "Hanze"-veld vormt echter het enige Chalk olieveld in de Nederlandse sector tot nu toe (Fig. 3.7).

Uit nauwkeurige bestudering van (3D-) seismische secties van een deel van de Centrale Noordzeeslenk blijkt dat opheffing naast erosie van sediment ook in grote aardverschuivingen heeft geresulteerd. Voorbeelden hiervan zijn te zien in de figuren 3.10 en 3.11. Kleinschaliger sedimentbewegingen dan op seismische secties is waar te nemen kwamen waarschijnlijk ook veel voor, en vormen deels het onderwerp van het volgende hoofdstuk.

Hoofdstuk 4 *Metre-scale cyclicity in well logs of the Chalk Group, Netherlands North Sea area* behandelt de resultaten van een frequentieanalyse uitgevoerd op boorgatmetingen door het Chalk interval. Het doel van een frequentieanalyse is periodieke herhalingen in een meetreeks op te sporen. In dit hoofdstuk betreft dat vooral metingen van de voortplantingsnelheid van geluid door het gesteente (*sonic logs*), hier te gebruiken als maat voor de dichtheid, en metingen van natuurlijke radioactiviteit (*gamma-ray logs*). Hierbij wordt ervan uitgegaan dat periodieke herhalingen (cycli) van de gemeten petrofysische eigenschappen de weergave zijn van klimaatschommelingen tijdens de afzetting van het gesteente. Deze klimaatschommelingen zijn op hun beurt het gevolg van de periodieke variatie in de baan van de aarde en de daardoor ontstane variatie in de afstand van de aarde tot de zon (Fig. 4.1).

De resultaten van een frequentieanalyse worden hier weergegeven door middel van een frequentiespectrum welke op elk punt de golflengte van periodieke variaties

weergeeft die aanwezig zijn binnen een interval van 40 meter. Dikkere gesteenteintervallen waarin een continu cyclisch signaal aanwezig is worden zichtbaar gemaakt door oplijning van de frequentiepieken tot de rode lijnen zoals die in interval 6 van boring F15-1 (Fig. 4.6). Uit de analyses blijkt de veelvuldige aanwezigheid van een cyclische dichtheidsvariatie met een golflengte van 5 tot 10 meter, alsmede minder vaak voorkomende kortere cycli. De aldus aangetoonde cycliciteit wijst erop dat dit gesteente bewaard is gebleven zoals het destijds door neerslag van kalkdeeltjes uit het zeewater gevormd is, al dan niet na verplaatsing door stromingen. De afwezigheid van cycliciteit wijst daarentegen op de werking van chaotische sedimentatieprocessen zoals de aardverschuivingen van figuren 3.10 en 3.11. Het voornamelijk chaotische logpatroon van boringen in de Centrale Noordzeeslenk en aan weerszijden van het Breeveertien Bekken geeft dan ook aan dat de Chalk hier voornamelijk uit verschoven sedimentpakketten bestaat, waarschijnlijk afkomstig van de naastgelegen opgeheven gebieden (Fig. 4.5).

Een in meerdere boringen teruggevonden graduele afname in cyclusdikte naar boven, dus naar jonger sediment, toe wijst op een regionale afname van de productie van kalkmateriaal die zich over een zeer lange periode moet hebben afgespeeld. Deze afname is wederom het best te zien in interval 6 van boring F15-1 als het naar rechts (richting kortere golflengtes) opschuiven van de frequentiepiek (Fig. 4.6).

Omdat de verhoudingen tussen de periodes van verschillende astronomische cycli bekend zijn kunnen de golflengteverhoudingen tussen in het gesteente aangetroffen cycli gebruikt worden voor de identificatie van een astronomisch geïnduceerd klimaatsignaal. Deze verhoudingen en correlatie met ouderdomsgegevens doen vermoeden dat de 5 tot 10 meter lange cyclische dichtheidsvariaties de geologische weergave zijn van een 100.000 jaar durende excentriciteitcyclus (Fig. 4.1).

In hoofdstuk 5 *Acoustic velocity and burial history analysis of the Chalk Group, Netherlands North Sea area* wordt de akoestische of geluidsnelheid en begravingscompactie van de Chalk sedimenten behandelt. Sediment raakt bij begraving door de toenemende (lithostatische) druk samengeperst, waarbij de hoeveelheid grondwater geleidelijk minder wordt (Figuren 1.11 en 1.12). De aldus toenemende dichtheid van het sediment zorgt voor een evenredige toename in voortplantingsnelheid van geluid. Deze geluidsnelheid, zoals gemeten met sonic logs of bepaald met behulp van seismische secties, vormt dus een graadmeter voor de begravingsdiepte. Het vaststellen van de normale mate van compactie met diepte is voor de Chalk geen eenvoudige zaak, zoals blijkt uit de veelheid aan compactiecurves die tijdens eerdere studies zijn vastgesteld (Fig. 5.1).

In deze studie is de dichtheid van de Chalk op een groot aantal plaatsen door het gehele Nederlandse Noordzeegebied vastgesteld als de geluidsnelheid (hier V_{int} in m/s). Uitgezet tegen begravingsdiepte laten deze een duidelijke toename zien,

hoewel met een aanzienlijke verspreiding (Figuren 5.6 en 5.8). Er blijkt naast diepte echter ook een duidelijke relatie te bestaan tussen akoestische snelheid en geografische positie van de meting zodat een aantal clusters in de data kan worden herkend (vier in Fig. 5.6 en drie in Fig. 5.8).

De relatief lage snelheden in het noorden van het studiegebied wijzen erop dat het sediment hier minder is gecompacteerd dan op basis van de begravingsdiepte zou mogen worden verwacht. Dit is waarschijnlijk een gevolg van de relatief snelle begraving onder waterondoorlatende kleien gedurende het Tertiair. Dit zorgde ervoor dat grondwater in de krijtkalklagen werd vastgehouden, en de porositeit van het gesteente aldus naar verhouding hoog bleef. De relatief hoge intervalsnelheden in het zuiden van het studiegebied wijzen erop dat het sediment in deze regio is opgeheven na eerst op grotere diepte begraven te zijn geweest. Hierdoor is het meer gecompacteerd dan op de aangetroffen diepte zou zijn verwacht.

Dankwoord

Nu mijn proefschrift klaar is wil ik alle mensen bedanken die bij de totstandkoming ervan een belangrijke rol hebben gespeeld. Hierbij begin ik graag bij het begin: mijn promotor Theo Wong. Theo, heel erg bedankt voor je initiatief om dit onderzoek op te zetten en voor de onmisbare rol die je daarin als begeleider en "facilitator" hebt gespeeld. De door jouw geïnitieerde samenwerking tussen TNO-NITG en de Faculteit Geowetenschappen was een vruchtbare, en volgens mij is er nog meer dan genoeg interessante data over voor nog een paar promovendi. Mijn tweede promotor, Johan Meulenkamp, bedank ik in de eerste plaats voor het feit dat hij mij tot tweemaal toe heeft laten deelnemen aan de begeleiding van de derdejaarsexcursie naar Griekenland. Deze trips behoren in veel opzichten tot de meest leerzame episodes van mijn promotietijd. Ook ben ik veel wijzer geworden van onze wetenschappelijke discussies en hoop dat dat in het voorgaande is terug te vinden.

Ik wil graag de leden van de leescommissie, t.w. prof. Poppe de Boer (UU), prof. Cees van der Zwan (UU), prof. Jan Smit (VU) en prof. Finn Surlyk (University of Copenhagen) bedanken voor alle tijd en moeite die zij in de beoordeling van dit proefschrift hebben gestoken en voor alle waardevolle commentaren en suggesties die het heeft opgeleverd. Poppe natuurlijk ook erg bedankt voor al je eerdere lees en corrigeerwerk.

Heel, heel belangrijk waren kamergenoten en mede-AIO's Iwan en Gesa. We hebben een enorm lange tijd samengewerkt en het was goed om lief en leed te kunnen delen. Het is een vreemd idee dat we nu ineens over de halve wereld verspreid zijn. Ik hoop maar dat we elkaar blijven zien in de toekomst.

Ik dank TNO-NITG van harte voor de financiering van dit promotieonderzoek. Alle mensen van de afdeling Geo-Energie van dit instituut hebben altijd gezorgd voor een hele plezierige werksfeer en ik ben velen van hen dank verschuldigd. Rob Arts en Pascal Winthaegen hebben heel vaak geholpen met allerlei geofysische problemen. Hans Doornenbal heeft veel vragen over akoestische snelheden beantwoord. Harald de Haan heeft me het maken synthetische seismogrammen bijgebracht. Aan Oscar Abbink en Dirk Munsterman heb ik de biostratigrafische data te danken. Ik heb Ed Duijn, Erik Simmelink, Barthold Schroot, Robert-Jan van Leeuwen, Cees Geel, Erik Bloem, Manuel Nepveu, Harmen Mijnlieff e.v.a. vaak lastig gevallen over van alles en nog wat. Ik heb Nora Witmans-Parker echt heel erg vaak lastig gevallen over van alles en nog wat. Ik heb in de beginfase veel gehad aan de discussies met de zgn. "klankbordcommissie". Hierin zaten, naast enkele eerderge-

noemden, o.a. Henk Pagnier, Berend Scheffers, René Giessen, Kees de Leeuw (inmiddels werkzaam bij Total), Mark Geluk (inmiddels werkzaam bij NAM, nogmaals bedankt voor het corrigeren van hoofdstukken 2 en 3) en Waldemar Herngreen. Aan de heren van de computergroep vooral dank voor alle hulp met de "Metz". Jan-Diederik van Wees dank voor o.a. het doorlezen van hoofdstukken 2 en 3. Jan Brouwer heel erg bedankt voor Cyclolog en alle uitleg. Frank, veel succes met je promotie. Henk, veel plezier op mijn oude werkplek en veel succes de komende vier jaar.

Van mijn universiteitscollega's wil ik vooral Douwe bedanken voor twee zeer gedenkwaardige trips naar Griekenland. Tzatziki zal nooit meer hetzelfde smaken. Voor de rest groet ik Andor, Erik, Jan-Willem, Julia, Kim, Marjolein, Quintijn, Rink, Sjoukje en Suus (van Douwe) van harte. Mijn eerste en enige afstudeerstudent Heelco wens ik vooral veel succes met zijn vervolgstudie.

Petro-Canada B.V. in Den Haag en haar medewerkers hebben een cruciale rol gespeeld in de totstandkoming van dit proefschrift. Ik heb van dit bedrijf een hoop nuttige gegevens gekregen en erg geprofiteerd van hun kennis als exploitant van het "Hanze"-veld (Fig. 3.7). Daarnaast heb ik een zeer welkome financiële ondersteuning van hen mogen ontvangen. Rob Smit dank ik voor het mogelijk maken van het contact, het realiseren van de financiële steun en de toestemming van alle gegevens gebruik te maken. Thank you Gerd Kaffenberger, Rob Lidster, Matthias Schöbel, Bernard Kaufmann, Eveline Rosendaal and others for so many good discussions. My very personal thanks to Andreas Hofmann for all your time and sharing of knowledge. I wish you all the best in Syria.

A short visit to Denmark also proved very benificial for this research. Mr. Poul-Henrik Larsen and a number of his colleagues of Mærsk Olie og Gas AS in Copenhagen were kind enough to let me present my results and provided many useful comments and suggestions. Many thanks to Ole Valdemar Vejbæk for inviting me to give a talk at the GEUS office, where I had many fruitful discussions, and for proof reading chapters 2 and 3. Ole Rønø Clausen is warmly thanked for his invitation to the University of Aarhus and for spending time at the photocopier for the huge "Andersen"-report.

Daarnaast wil ik nog graag Ton Romein (NAM), Marco van der Meulen (Wintershall) en Huibert van den Brink (Gaz de France) bedanken voor hun in dit onderzoek getoonde interesse en uitnodigingen voor presentaties en discussies.

Van fundamenteel belang bij het welslagen van elke promotie is de steun van familie en vrienden. Daarom Heit, Mem, Mare, Peter en Jildou bij deze als eerste genoemd! Jurgen, ik kan zonder meer stellen dat zonder jou dit proefschrift er niet had gelegen. En dat niet eens alleen vanwege de door mij zo schandelijk verspeelde fles Balvenie. Roeland, ik zal je niet langer lastigvallen met gezeur over promoveren. Maar niet getreurd, ik heb binnenkort weer een geheel nieuw (geel) gespreksonderwerp paraat! Annemarie, heel erg bedankt voor al je steun gedurende een belangrijke periode. Elout, 'I'm so damn happy'. Oh, en Bart, Bas, Branko, Gertjan, Ilona, Ingrid, Ivet, Joost, Laura, Lisette, Margot, Marijke, Max, Nick, Nienke, Nynke, Onno, Paul, Paul, Sander, Twan en Valentina..., ik ben weer aanspreekbaar. En tot slot: lieve Paulien, dank je wel voor al je liefde in dit al te hektische afgelopen jaar.

Curriculum vitae

Allard Sytse van der Molen

12 November 1972	Born in Drachten, the Netherlands.
1985–1991	Higher general secondary education (HAVO), *Het Drachtster Lyceum*, Drachten., the Netherlands.
1991–1992	Higher professional education (HBO), propeadeutic exam Environmental Studies, *Van Hall Instituut*, Groningen, the Netherlands.
1992–1998	M.Sc. Geology (Sedimentology and Stratigraphy), *Free University of Amsterdam*, the Netherlands.
1998–1999	Employed in an offshore engineering project in Leidschendam and Delft, and an information systems project in Amsterdam.
2000–2004	Ph.D-student, Faculty of Geosciences, *Utrecht University* and *Netherlands Institute of Applied Geoscience TNO - National Geological Survey*, Utrecht, the Netherlands.